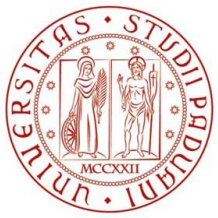

UNIVERSITÀ
DEGLI STUDI
DI PADOVA

Sede Amministrativa:

UNIVERSITÀ DEGLI STUDI DI PADOVA

DIPARTIMENTO DI INGEGNERIA INDUSTRIALE

CORSO DI DOTTORATO DI RICERCA IN: Ingegneria Industriale

CURRICOLO: Ingegneria Chimica, dei Materiali e Meccanica

CICLO: XXIX

INDUSTRIAL PRODUCTION OF MICROALGAE BY AN ECO-SUSTAINABLE PROCESS: LIGHT UTILIZATION EFFICIENCY AND NUTRIENT RECYCLING

Direttore della Scuola: Ch.mo Prof. Paolo Colombo

Coordinatore di indirizzo: Ch.mo Prof. Giovanni Meneghetti

Supervisore: Ch.mo Prof. Alberto Bertucco

Dottoranda: Elena Barbera

Contents

Abstract

This Ph. D. project is aimed to improve the efficiency and the sustainability of microalgal cultivation in view of large-scale biofuels production. Experiments as well as modeling and process simulation were used to investigate: i) the light utilization efficiency in algal photobioreactors and ii) different strategies for the recovery and recycling of nutrients.

First of all, microalgal growth in continuous photobioreactors is modeled in order to identify optimum working conditions that allow maximum productivity, accounting for light intensity and regime, as well as for axial dispersion. Then, the integration of photovoltaic (PV) technologies with photobioreactors is studied as a possible technical solution to improve the photons utilization per surface area. In this regard, experiments applying either standard, low-cost silicon solar cells or a novel organic dye-sensitized semi-transparent photovoltaic module on the reactor surface are reported. An energetic and economic analysis of microalgal cultivation in a photovoltaic greenhouse, with the roof partially covered by PV panels is also presented.

Two different strategies for nutrients recovery and recycling are investigated, namely flash hydrolysis (FH) of whole algal biomass and anaerobic digestion (AD) of lipid-extracted residues. The nutrients-rich aqueous phases produced by FH of two different algal species (*Scenedesmus* sp. and *Nannochloropsis gaditana*) are used to assess the growth performances of the respective algae in this medium. As an alternative to the direct recycling of the aqueous hydrolysate, the possibility of precipitating the nutrients in stable fertilizers is also reported. The biogas production from AD of lipid-extracted microalgae is evaluated, and the subsequent growth rate in the liquid digestate was compared to that obtained in standard synthetic medium. Finally, the experimental data gained from FH and AD are used to implement process simulations with the aim of evaluating the material and energy balances and to assess the feasibility on a large-scale.

Foreword

This research project was developed at the Department of Industrial Engineering (DII) of the University of Padova, under the supervision of Prof. Alberto Bertucco.

Part of the work reported in this Thesis (Chapter 6) has been carried out at the Biomass Research Lab of Old Dominion University (Norfolk, Virginia, USA), under the supervision of Dr. Sandeep Kumar.

As a tangible result of the work completed during the Ph. D. school, a number of publications and presentations to conferences has been produced, as listed below.

Publications in Refereed Journals

1. Sforza E., **Barbera E**., Bertucco A. (2015). Improving the photoconversion efficiency: an integrated photovoltaic - photobioreactor system for microalgal cultivation. *Algal Research*, vol. 10, p. 202-209, ISSN: 2211-9264, doi: 10.1016/j.algal.2015.05.005

2. **Barbera E.**, Sforza E., Bertucco A. (2015). Maximizing the production of *Scenedesmus obliquus* in photobioreactors under different irradiation regimes: experiments and modeling. *Bioprocess and Biosystems Engineering*, vol. 38, p. 2177-2188, ISSN: 1615-7591, doi: 10.1007/s00449-015-1457-9

3. **Barbera E**., Sforza E., Kumar S., Morosinotto T., Bertucco A. (2016). Cultivation of *Scenedesmus obliquus* in liquid hydrolysate from flash hydrolysis for nutrient recycling. *Bioresource Technology*, vol. 207; p. 59-66, ISSN: 0960-8524, doi: 10.1016/j.biortech.2016.01.103

4. Teymouri A., **Barbera E**., Sforza E., Morosinotto T., Bertucco A., Kumar S. (2016). Integration of Biofuels Intermediates Production and Nutrients Recycling in the Processing of a Marine Algae. *AIChE Journal*, doi: 10.1002/aic.15537

5. **Barbera E**., Teymouri A., Bertucco A., Stuart B., Kumar S. (2017). Recycling minerals in microalgae cultivation through a combined flash hydrolysis-precipitation process. *ACS Sustainable Chemistry & Engineering*, vol. 5; p. 929-935, doi: 10.1021/acssuschemeng.6b02260

Papers submitted for publication in Refereed Journals

1. **Barbera E.**, Sforza E., Guidobaldi A., Di Carlo A., Bertucco A. Integration of dye-sensitized solar cells (DSC) on photobioreactors for improved photoconversion efficiency in microalgal cultivation. Submitted to: *Renewable Energy*
2. **Barbera E**., Sforza E., Vecchiato L., Bertucco A. Energy and economic analysis of microalgae cultivation in Algreenhouse (a photovoltaic-assisted greenhouse). Submitted to: *Energy*
3. Sforza E., **Barbera E.**, Girotto F., Cossu R., Bertucco A. Anaerobic digestion of lipid-extracted microalgae: enhancing nutrient recovery towards a closed loop recycling. Submitted to: *Biochemical Engineering Journal*

Papers or abstracts in conference proceedings

1. **Barbera E**., Sforza E., Gris B., Bertucco A. (2014). Improving light absorption and energy conversion in Photobioreactors for microalgae production, Algae Biomass Summit 2014, Sept. 29 – Oct. 2, 2014, San Diego, California. Poster presentation.
2. Bertucco A., **Barbera E**., Sforza E., Morosinotto T., Kumar S., (2015) Nutrient recycling for sustainable microalgal cultivation: a comparison between anaerobic digestate and flash hydrolysate as nutrient sources, Algae Biomass Summit 2015, Sept. 29 – Oct 2, 2015, Washington, DC. Poster presentation.
3. Kumar S., Teymouri A., Obeid W., Hatcher P.G., Sforza E., **Barbera E**., Bertucco A., Morosinotto T., (2015). Flash hydrolysis of *Nannochloropsis spp*. for nutrient recycling and biofuels production, Algae Biomass Summit 2015, Sept- 29 – Oct 2. 2015, Washington DC. Oral presentation.
4. Talbot C., Teymouri A., **Barbera E**., Bertucco A., Kumar S., Stuart B., (2016). Phosphorus recycling for sustainable algae to biofuels production, DOE Bioenergy 2016, July 12-14, 2016, Washington, DC. Poster presentation.
5. **Barbera E**., Sforza E., Kumar S., Bertucco A., (2016). Nutrient recycling strategies in view of sustainable biofuels production from microalgae, Convegno GRICU 2016, Sept. 12-14, 2016, Anacapri, NA. Oral presentation

6. **Barbera E**., Teymouri A., Bertucco A., Stuart B., Kumar S., (2016). Microalgal cultivation using minerals recycled through hydrothermal mineralization, Algae Biomass Summit 2016, Oct 23-26, 2016, Phoenix, Arizona. Oral presentation.

Riassunto

Nel contesto internazionale è ormai emersa chiaramente la necessità di sviluppare fonti alternative e rinnovabili di energia, per contrastare il progressivo esaurimento delle riserve fossili, e i cambiamenti climatici legati alle emissioni di anidride carbonica derivanti dal loro utilizzo. Sebbene lo sviluppo di tecnologie per la produzione di elettricità da fonti rinnovabili (quali l'eolico, l'idroelettrico o il fotovoltaico) sia molto promettente, e abbia raggiunto una certa maturità anche a livello commerciale, alcuni settori quali l'aviazione e il trasporto su lunga distanza sono tuttavia ancora fortemente dipendenti dalla disponibilità di combustibili liquidi (Ringsmuth et al., 2016). In questo contesto le biomasse, e in particolare le microalghe, rappresentano una promettente materia prima per la produzione di diversi tipi di biocarburanti: principalmente bioetanolo e biodiesel, come sostituti della benzina e del diesel convenzionali, ma anche biogas e biometano, syn-gas, o combustibili solidi dalle proprietà simili a quelle del carbone.

Le microalghe sono microorganismi aquatici in grado di convertire acqua, anidride carbonica e nutrienti semplici (principalmente nitrati e fosfati, e piccole quantità di micronutrienti a base metallica) in molecole ad alto contenuto energetico, mediante le reazioni di fotosintesi. Rispetto alle piante superiori terrestri, l'utilizzo di microalghe per la produzione di carburanti liquidi ha suscitato un vivo interesse a livello internazionale grazie alla loro elevata velocità di riproduzione ed efficienza di conversione dell'energia luminosa: ciò le rende maggiormente adatte alla coltivazione su larga scala, in quanto si riflette in minori estensioni superficiali necessarie per la loro produzione. Ulteriori vantaggi di questi microorganismi sono l'elevato contenuto di olio, una buona capacità di cattura della CO_2, la potenzialità di crescere anche in acque reflue depurandole dagli elevati contenuti di azoto e fosforo, nonché la possibilità di sfruttare la biomassa residua per l'estrazione di biomolecole di interesse commerciale, per la produzione di biogas o per scopi energetici (Chisti, 2007; Mata et al., 2010). Inoltre, le microalghe non necessitano di terreni coltivabili per la loro produzione eliminando, di conseguenza, il problema della competizione con risorse agricole destinate all'uso alimentare.

Ad oggi, la produzione di biocombustibili da biomassa microalgale è stata dimostrata a livello di impianti pilota, ma nonostante le buone premesse la prospettiva di raggiungere l'applicazione su scala industriale appare ancora lontana. Le poche aziende che hanno investito nella commercializzazione di carburanti microalgali, scontrandosi con gli elevati costi operativi e di produzione, resi ancora meno favorevoli dal calo dei prezzi del petrolio degli ultimi tre anni, hanno recentemente convertito la produzione verso composti ad alto valore aggiunto, il cui mercato è più solido e redditizio.

Tra le principali limitazioni allo *scale-up* di questa tecnologia vi sono ragioni di tipo economico, dovute ai costi di produzione della biomassa e della successiva conversione in carburanti, e di tipo ambientale, legate alla disponibilità di risorse quali superficie, acqua, anidride carbonica e nutrienti che, nel caso dei volumi di produzione considerati, sollevano problematiche in merito alla sostenibilità (Chisti, 2013; Pate et al., 2011).

Nel primo caso, un fattore fondamentale su cui agire per ottenere una riduzione dei costi dell'intero processo è senza dubbio un sostanziale incremento della produttività nel sistema di coltura rispetto ai valori attualmente raggiunti: difatti, ciò che più influisce sul costo finale dei biocarburanti è la produzione stessa della biomassa (intesa come sistema di coltivazione e successiva riduzione del contenuto d'acqua), mentre le tecnologie di conversione hanno un contributo minore (Davis et al., 2016; U.S. DOE, 2016). Attualmente, i valori di produttività ottenuti sono di molto inferiori a quello che è il massimo limite teorico di efficienza di conversione della luce solare tramite fotosintesi (pari a circa l'11% della radiazione incidente). Ciò è legato a vari fattori, primo tra i quali l'inefficiente utilizzo dell'energia luminosa, dovuto alla concomitanza di una scarsa penetrazione della stessa negli strati più profondi della coltura algale e di fenomeni di saturazione e inibizione dei fotosistemi negli strati superiori, sottoposti invece a intensità di luce troppo elevate (Carvalho et al., 2011). Risulta evidente dunque la necessità di operare il sistema di coltivazione in condizioni tali da massimizzare l'efficienza di utilizzo della luce incidente.

In merito alla disponibilità di risorse necessarie per la produzione di microalghe su larga scala, i grossi quantitativi di nutrienti coinvolti rappresentano una delle sfide più significative: in base alla composizione elementare della biomassa infatti, per produrre 1 tonnellata di microalghe sono necessari 60-90 kg di azoto e 3-15 kg di fosforo (Canter et al., 2015; Pate et al., 2011). Tali quantità non solo entrerebbero in competizione con il settore agricolo per il fabbisogno di

fertilizzanti, con verosimili ripercussioni sui prezzi degli stessi, ma non sarebbero nemmeno disponibili in maniera sostenibile sfruttando le risorse da cui sono attualmente prodotte. Tuttavia, considerando che N e P sono presenti solo in piccole quantità nei combustibili finali, essi possono potenzialmente essere recuperati dalla biomassa residua e riciclati, sotto forma di composti assimilabili dalle microalghe, al sistema di coltivazione, riducendo così il contributo di fertilizzanti richiesti (Chisti, 2013).
Questa tesi di dottorato è focalizzata sull'individuazione di strategie atte a migliorare l'efficienza e la sostenibilità della produzione di microalghe, sia da un punto di vista energetico (utilizzo dell'energia luminosa) che ambientale (riciclo di nutrienti), in prospettiva di uno *scale-up* di processo a livello industriale.

A tal scopo, la crescita microalgale in fotobioreattori a pannello sottile operati in continuo è stata studiata dettagliatamente da un punto di vista sperimentale e modellistico, con l'obiettivo di comprendere l'effetto delle principali variabili (tempo di residenza, grado di mescolamento e soprattutto della luce) sulle prestazioni, in termini di produttività ed efficienza fotosintetica. Per tutti i casi considerati, è stato possibile identificare un tempo di residenza ottimale che consente di massimizzare la produttività, il quale è strettamente correlato con il profilo di estinzione della luce lungo lo spessore del reattore. Pertanto emerge come sia fondamentale operare il sistema di coltivazione in uno stretto intervallo di tempi di residenza che consenta di ottenere le migliori prestazioni, a seconda del regime luminoso considerato.
Al fine di sfruttare al meglio l'energia luminosa incidente per unità di area superficiale, è stata inoltre valutata la possibilità di integrare la produzione di microalghe con diverse tecnologie fotovoltaiche. In questo modo, in aggiunta alla produzione di energia sotto forma di biomassa mediante fotosintesi, parte della radiazione viene convertita in energia elettrica, utilizzabile direttamente all'interno del processo, per integrarne i consumi e migliorarne l'efficienza. In particolare, l'effetto dell'applicazione di due diverse tecnologie fotovoltaiche (rispettivamente celle solari convenzionali al silicio, e un emergente modulo fotovoltaico organico semitrasparente basato sulla tecnologia *dye-sensitized solar cells*) sulla superficie del fotobioreattore è stato valutato sperimentalmente utilizzando sistemi in continuo. I risultati ottenuti mostrano che l'ombreggiamento della coltura microalgale, causato dalla presenza del pannello fotovoltaico, ha un effetto sulla produttività di biomassa. Tuttavia, se da un lato quando la luce incidente è limitante ciò si riflette in un calo della produttività, quando

l'irraggiamento raggiunge valori fotosaturanti o fotoinibenti l'attenuazione dell'intensità luminosa ha invece un effetto positivo sulla produzione di biomassa. In un regime di illuminazione diurno inoltre, con valori di irradianza che spaziano da limitanti ad altamente inibenti, la produttività è risultata invariata rispetto al caso di un fotobioreattore trasparente, mentre l'efficienza globale di conversione dell'energia è invece al contempo significativamente migliorata.

Su larga scala, questo concetto può essere applicato collocando il sistema di coltivazione all'interno di una serra, i cui tetti siano parzialmente coperti con pannelli fotovoltaici commerciali al silicio. Da un'analisi energetica ed economica condotta su due possibili località italiane (il Veneto nel Nord, e la Sicilia nel Sud), come casi studio, è emerso che, nonostante i costi di investimento significativamente superiori per l'installazione dei pannelli fotovoltaici, il prezzo di *break-even* della biomassa prodotta risulta inferiore rispetto al caso di una serra trasparente (senza fotovoltaico), per entrambe le zone considerate. Inoltre, l'efficienza di utilizzo e conversione dell'energia solare è notevolmente maggiore, e l'elettricità prodotta per via fotovoltaica può essere utilizzata per rendere il processo energeticamente auto-sostenibile. L'area meridionale risulta essere in generale l'opzione più conveniente, in quanto le temperature ed irradianze mediamente più elevate consentono di ottenere produzioni annuali migliori, e un conseguente prezzo di mercato inferiore di circa il 38% rispetto alla località settentrionale.

In merito al recupero e riciclo dei nutrienti, in questa tesi sono state studiate approfonditamente due possibili alternative di processo: la *flash hydrolysis*, un trattamento condotto utilizzando acqua ad alte temperature e pressioni (ma comunque in condizioni sub-critiche) sulla biomassa direttamente a valle del sistema di coltivazione, previa concentrazione del contenuto di solidi (Garcia-Moscoso et al., 2013); e la digestione anaerobica della biomassa residua in seguito all'estrazione della frazione lipidica, destinata alla produzione di combustibili liquidi (Ward et al., 2014).

La *flash hydrolysis* consente di estrarre più del 60% di N e l'80% di P e i vari micronutrienti dalla biomassa iniziale nella fase acquosa, o idrolizzato, mentre i lipidi vengono preservati in un prodotto solido. In particolare, l'idrolizzato è risultato essere generalmente un buon substrato per la coltivazione di microalghe, consentendo di ottenere velocità di crescita e produttività anche più elevate rispetto a quelle ottenute in terreni standard, grazie ad una

crescita di tipo mixotrofo, in cui il carbonio organico disciolto nel mezzo viene utilizzato come ulteriore fonte di energia. Tuttavia, la capacità di assimilare tale carbonio ed azoto in forma organica dipende dalla specie microalgale considerata: mentre l'alga di acqua dolce *Scenedesmus obliquus* ha dimostrato buone prestazioni di crescita nell'idrolizzato, sia in sistemi batch che in continuo, la specie marina *Nannochloropsis gaditana*, essendo in grado di utilizzare solamente l'azoto inorganico presente nel mezzo, non raggiunge velocità di crescita pari a quelle ottenute in terreno di coltura standard.

In aggiunta al riciclo diretto dell'idrolizzato, è stata valutata anche la possibilità di recuperare i nutrienti inorganici disciolti nel mezzo tramite precipitazione sotto forma di fertilizzanti, per il successivo riciclo nel sistema di coltivazione, permettendo così il recupero di altre molecole ad alto valore aggiunto preservate nella fase acquosa. In particolare, ammonio e fosfati sono stati recuperati come struvite ($MgNH_4PO_4$), la quale è risultata essere una buona fonte di N e P per la crescita microalgale, sebbene in questo caso sia necessario fornire un supplemento di azoto per rispettare il rapporto stechiometrico necessario alla biomassa (circa 16:1 su base molare) (Redfield, 1934).

Per quanto riguarda la seconda alternativa di processo considerata, dalla digestione anaerobica di microalghe in seguito all'estrazione dei lipidi si è ottenuta una produzione soddisfacente di biogas, come ulteriore output energetico del processo. L'effluente acquoso (digestato), riciclato come substrato per la successiva coltivazione microalgale, è risultato avere un buon contenuto di ammonio come fonte di azoto, ma una scarsa o quasi nulla quantità di fosfati e solfati, entrambi necessari per la crescita, e persi nei residui solidi per precipitazione e nella fase gassosa rispettivamente. Poiché il P è un nutriente determinante, e la sua scarsa disponibilità genera non poche perplessità in termini di sostenibilità ambientale, diversi trattamenti per aumentarne il recupero e la solubilizzazione nella fase liquida sono stati presi in considerazione. Tra questi, il più efficiente è risultato l'impiego di bicarbonato di sodio, il quale riduce l'attività dei cationi metallici coinvolti nella precipitazione dei relativi sali.

Nell'ultima parte di questa tesi, viene fatta una valutazione quantitativa delle due alternative di processo considerate, in termini di bilanci di materia e di energia, mediante simulazioni con il software Aspen Plus™ e utilizzando i dati sperimentali ottenuti. A tal scopo, per simulare la produzione microalgale nel fotobioreattore si è implementata una cinetica che tenga conto delle

limitazioni dei vari nutrienti (N, P e C), e un modello termodinamico che consideri l'equilibrio chimico tra le specie ioniche in fase acquosa.

In sintesi, i risultati ottenuti in questa tesi offrono spunti interessanti per migliorare l'efficienza della produzione di biomassa microalgale, in vista di un auspicabile *scale-up* su scala industriale per l'ottenimento di combustibili. Sebbene ulteriore lavoro debba essere svolto in questo senso per raggiungere la sostenibilità economica, e le aziende si stiano momentaneamente orientando verso applicazioni delle microalghe in mercati ad alto valore aggiunto, c'è un ampio potenziale di miglioramento e svolte dal punto di vista tecnologico nel campo dei biocarburanti. Indubbiamente, ciò richiede un impegno mirato e focalizzato, a livello globale, da parte di governo, istituzioni accademiche e private affinché le microalghe possano diventare una nuova fonte alternativa e rinnovabile di energia, per fronteggiare il problema del cambiamento climatico e l'esaurimento delle fonti convenzionali.

Introduction

Currently, about 88% of the global primary energy supply is produced exploiting fossil fuels sources. The constantly increasing trend of the energy demand has forced the world population to confront with the irreversible depletion of traditional sources of fossil fuels. Even though the development of new extraction technologies allowed the exploitation of new, unconventional crude oil reserves, this can only be considered a contingency.

In addition, extensive utilization of fossil fuels generates huge amounts of GHG (greenhouse gases) emissions, with serious repercussions on the ecosystems (e.g., oceans acidification), environmental pollution and global climate change (Bauer et al., 2016). The growing awareness towards these indisputable environmental issues has raised concerns globally, so that many countries agreed, in the Paris Agreement of 2015 (COP21), that measures have to be taken rapidly to reduce GHG emissions.

The development of renewable and sustainable energy sources plays a significant contribution in dealing with these issues. Although various renewable technologies, such as photovoltaics, wind or hydropower, show great potential and can have a significant impact by producing clean electrical energy, some sectors (e.g., transportation, aviation) are still highly dependent on carbon-based liquid fuels (Ringsmuth et al., 2016). In this regard, biomass can provide a wide variety of fuels that can be integrated in existing technologies, such as biodiesel and bioethanol, which would require little or no engine modifications and could be supplied through the available distribution system. In particular, microalgae have become the focus of much academic and commercial research, due to their great potential as a high yield source of biofuels. Microalgae are photosynthetic organisms able to convert solar energy into chemical energy using only water, CO_2 and nutrients.

The interest in microalgal biomass as a feedstock for biofuels was raised by the several advantages that they present compared to terrestrial crops. Among the most important ones are their significantly higher productivities and growth rates, as algae are able to double their biomass as much as many times a day when in exponential growth, together with high oil yields (Chisti, 2007). In addition, once harvested the algal biomass is closer to a finished fuel product

compared to terrestrial plants, as less downstream processing is required to convert it into biofuels. Ultimately, a highly valued advantage of microalgae is that their production does not compromise food supplies, and does not compete with agriculture for arable land as they can be grown almost everywhere, including possibly offshore locations.

So far, the production of microalgae biofuels has been demonstrated at pilot scale levels but, despite the enthusiastic boost towards commercialization registered at the beginning of this decade, there are no large-scale facilities operating to date. In fact, several issues related to microalgae cultivation and subsequent conversion to fuel products are to be solved yet, from either the energetic, environmental and economical points of view (Chisti, 2013).

Certainly, economic constraints are the major constraint to scalability of algal biofuels. In order to cut down the production costs it is fundamental to optimize the biomass productivity in the cultivation system, which needs to be significantly improved compared to values currently obtained in outdoor facilities: the final cost of algal biofuels is indeed highly sensitive to the one of algal biomass (cultivation and dewatering), while relatively little influence is given by the conversion process (Davis et al., 2016; U.S. DOE, 2016). Despite the higher productivity of microalgae compared to terrestrial biomass, the efficiency of solar light conversion presently reached is still much lower than the maximum theoretical value achievable through photosynthesis. A lower productivity reflects in increased costs associated with the higher surface area required, as well as with the dewatering step. This inefficiency in light energy utilization is due to a number of factors, mostly a scarce penetration of light in the deeper layers of the microagal culture, together with photosystems saturation and inhibition under high light intensities such as those commonly reached throughout the day. As algal productivity is inherently connected to light conversion efficiency, clearly the cultivation system needs to be operated so to maximize the light utilization.

In addition to interrelated energetic and economic constraints, mass production of microalgal biofuels aiming at displacing petroleum-derived ones has raised concerns in terms of environmental sustainability (Pate et al., 2011). Land and water are the primary resources needed to grow algae. Land requirements however are likely to be the most manageable of the resource demands involved (Pate et al., 2011; Ringsmuth et al., 2016). On the other hand, water demands represent a challenge, especially in open cultivation systems with evaporative losses, which require significant fresh-water make-up supplies. In this regard, closed cultivation

facilities and water recycling in the process could help reducing the fresh-water consumption. Alternatively, cultivation could be performed in seawater. In both cases, nutrients (especially nitrogen and phosphorus) represent a significant challenge for algae biofuels production scale-up. The amounts required to sustain algal growth on a large-scale would seriously compete with agriculture for commercial fertilizers use, potentially raising their market price (Canter et al., 2015). Actually, the high demands involved would be unsustainable to entirely meet by commercial fertilizers sources, especially for phosphorus. However, considering that little amounts of N and P end up in the desired fuels products, they could be effectively recovered from the spent biomass and recycled in the cultivation system, reducing the amount of fresh fertilizers required.

With regard to the open issues recalled above, the aim of this research project has been to study how to improve the efficiency of microalgal cultivation towards large-scale biofuels production, both from the energetic (light utilization) and the environmental (nutrients recycling) sustainability point of view. The topics addressed by this thesis are organized and subdivided in chapters as follows.

Chapter 1 is an introductory discussion on the microalgae world situation, highlighting the major constraints to algal fuels commercialization, together with most recent investigations regarding this technology and the current industrial scenario.

Chapter 2 reports the modeling of microalgal growth in continuous flat-plate photobioreactors (PBRs), keeping into account the effect of light intensity and regime, together with that of axial dispersion on the production performances, in order to identify the optimum operating residence time.

Chapter 3 presents the experimental work carried out integrating photovoltaic (PV) cells on the photobioreactor surface, with the aim of increasing the impinging light utilization efficiency. Two different PV technologies are tested, namely standard silicon panels covering a portion of the PBR, and organic semi-transparent orange dye-sensitized solar cells applied on the entire reactor irradiated surface. Different constant light intensities together with day-night irradiation were investigated to ascertain the effect of PV on both microalgal productivity and overall light conversion efficiency.

In **Chapter 4**, an energetic and economic analysis of microalgal cultivation in a photovoltaic greenhouse (with the roof partially covered by silicon PV panels) is discussed, as a potential

large-scale application, for two different Italian latitudes (Veneto, North and Sicily, South). The performances are compared to those obtained with a transparent greenhouse (without photovoltaic panels).

Chapter 5 is focused on the direct recycling of the aqueous, nutrients-rich hydrolysate produced by flash hydrolysis (FH) of algal biomass. The hydrolysates obtained from FH of two different microalgal species (the freshwater *Scenedesmus* sp. and the marine alga *Nannochloropsis gaditana*) were used to cultivate the corresponding algae, and to compare the growth to that obtained in standard synthetic media. To this purpose, both batch and continuous cultivation experiments were carried out, with the aim of optimizing the nutrients consumption and utilization.

In **Chapter 6**, the possibility of precipitating the nutrients from the hydrolysate in the form of stable, mineral fertilizers to be recycled for algal cultivation (while allowing the recovery of high-value molecules from the remaining medium) is investigated.

Chapter 7 reports the experimentation performed on anaerobic digestion of microalgae to enhance nutrients recovery. The biogas production of lipid-extracted microalgae is first evaluated, and subsequently the liquid digestate collected is used to test microalgal growth in this substrate. Various treatments were carried out on the raw digestate prior to separation, in order to increase the phosphorus solubilization in the liquid and reduce the amount of fresh fertilizer to be supplied.

In **Chapter 8**, the results gained through the experimental work are used to implement process simulations of both the flash hydrolysis and anaerobic digestion pathways. Aspen Plus^{TM} was used to evaluate material and energy balances, in order to compare the processes investigated and assess their feasibility for possible large-scale applications.

I would like to thank Dr. Sandeep Kumar for his valuable supervision during my time spent at the Biomass Research Lab in Old Dominion University, and for his help throughout the development of many important results achieved in this thesis.

Chapter 1

Biofuels from microalgae: state of the art

1.1. The global energy situation

The worldwide demand and consumption of primary energy have been increasing consistently in the last 50 years, and this trend is expected to continue in the future. This comes as a direct consequence of the demographic pattern (the world's population is estimated to grow by 0.9% per year on average, from 7.1 billions in 2013 to 9 billions in 2040), together with the economic development of emerging countries, with a foreseen world gross domestic product (GDP) in 2040 equal to twice its current size (IEA, 2015).

1.1.1. Fossil fuels

The current world primary energy supply relies on non-renewable fossil fuels sources (petroleum, coal and natural gas), which account for about 88% of the total consumption (IEA, 2015). In particular, liquid fuels represent the most utilized form of energy at the present time, with global crude oil consumption accounting for 33.6% of the total energy supply, mainly used in the transport sector (Ringsmuth et al., 2016). At present, the low price of crude oil which, after a period of relatively high stable prices around 115 $/barrel in the years 2010-2014, fell by more than 50%, ranging now between 40-60$/barrel (Figure 1.1), together with the development of new extraction technologies to exploit "unconventional" oil sources (e.g. shale oil), have somehow buffered the concern related to the indispensable use of this non-renewable source. However, this is clearly a contingency, considering that the burning of fossil fuels is the major cause of greenhouse gas emissions: the growing awareness towards environmental pollution and related climate change has led to extensive efforts aiming at promoting the transition from fossil fuels to renewable energy sources (Milano et al., 2016).

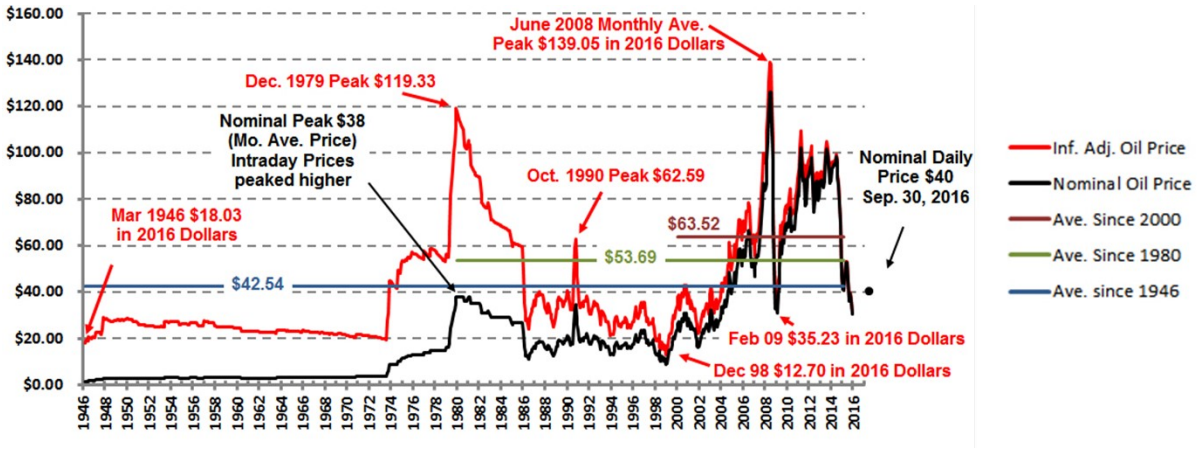

Figure 1.1 *Inflation adjusted monthly average of crude oil prices (1946-present) in August 2016 dollars, modified from* (InflationData, 2016)

In this context, it is important to consider that shale oil extraction is more expensive, resource intensive and environmentally damaging compared to conventional oil drilling. Therefore, although precise trajectories for future global oil production are still uncertain, it is clear that new, sustainable substitutes to crude oil are required soon.

1.1.2. Biofuels

In the last 20 years, many countries in the world have made efforts in developing renewable energy sources to reduce the demand of traditional fossil fuels and achieve at least a partial replacement. At present, renewable energy is estimated to account for about 19% of the world consumption, among which hydropower and wind energy for power generation (Milano et al., 2016). However, although electricity is certainly a good energy carrier, which can be efficiently converted to mechanical work, about 60% of the primary energy is actually consumed in the form of carbon-based fuels. It is difficult to foresee that chemical fuels can be replaced by electricity in certain sectors, such as aviation and long-distance road transportation. Moreover, due to the time constraints that urge the transition from fossil fuels to cleaner and sustainable sources, focusing on the development of renewable carbon-based fuels compatible with the existing technologies appears more suitable, until other options harder to implement are available (Mata et al., 2010; Ringsmuth et al., 2016).

Biomass can indeed provide biofuels in either gaseous (biogas, syngas), solid (biochar) and liquid forms. The latter are mainly constituted by biodiesel, produced by transesterification of vegetable oil, and bioethanol, obtained from sugar (starch, cellulose) fermentation: nowadays these two, which are substitutes for diesel and gasoline respectively, account for almost the entire global solar fuel sector, even though the biogas demand is growing.

Based on the type of biomass feedstock, biofuels are divided into categories, or "generations". First generation biofuels are derived from food and oil crops, such as corn or sugar cane. They have reached commercial level and are well established in the US and Brazil, but their impact in the transportation sector is questioned and they are criticized for directly competing with the food production and supply (Milano et al., 2016; Ullah et al., 2015). Second generation biofuels have been developed to overcome this relevant issue, and are derived from non-food sources such as agricultural residues, switchgrass, etc., or in general lignocellulosic materials. In this case, the main issues are related to cellulose extraction and degradation, together with the spread and diversity of the feedstock material.

Third generation biofuels, like the previous ones, are derived from non-edible biomass sources, but present much higher areal production yields compared to the former. Microalgae, belonging to this last category, have received wide attention as a promising feedstock for the production of liquid biofuels. Their characteristics are summarized hereafter.

1.2. Overview of microalgae as feedstock for biofuels production

Microalgae are a large and diverse group of simple aquatic photosynthetic microorganisms, which lack differentiation of thallus into roots, leaves and stem (Lee, 1989). They can be organized in either unicellular, colonial or filamentous arrangement. Cyanobacteria (or blue-green algae) are included in this definition even though they are prokaryotic organisms. It is estimated that more than 50,000 species exist (Mata et al., 2010).

Like other photosynthetic organisms, microalgae have the ability of converting solar light energy and inorganic compounds (CO_2, water and nutrients) into energy-rich organic molecules: the main constituents of microalgal biomass are lipids, proteins and carbohydrates. Depending on the target, microalgae can potentially provide energy in several forms: biodiesel via transesterification of the lipid fraction, bioethanol through carbohydrates fermentation, but

also biogas through anaerobic digestion, syngas by gasification, bio-oil via hydrothermal liquefaction or pyrolysis, char by hydrothermal carbonization (Elliott, 2016), and ultimately also electricity by direct combustion. With respect to molecules exploitable for the production of liquid fuels, the lipid fraction is of essential importance: depending on the cultivation conditions, microalgae can reach oil contents ranging between 20% to 70% of their dry weight (Chisti, 2007; Milano et al., 2016), mainly in the form of simple fatty acids and triglycerides, while membrane walls are constituted by phospholipids and glycolipids. The amount of lipids accumulated is strongly dependent on the species considered. Clearly, also aspects related to the growth rate and productivity, as well as the robustness and resistance to changes in environmental conditions have to be considered. Between the most promising in this regard are the freshwater species *Scenedesmus*, *Chlorella*, *Neochloris oleoabundans* and *Botryococcus braunii*, and the marine species *Tetraselmis*, *Dunaliella*, *Nannochloropsis* and *Phaeodactylum tricornutum* (Bonvincini et al., 2015).

The main advantages of using microalgae biomass for the production of renewable fuels, compared to other available feedstocks, are the following:

- differently from with terrestrial plants, microalgae are able to achieve higher values of photosynthetic efficiency (PE, i.e., the portion of sunlight energy that is converted into chemical energy stored in the biomass): while the first ones only reach PE between 0.5-1%, for microalgae values up to 8%, and normally ranging between 4-5% are reported (Chisti, 2013; X.-G. Zhu et al., 2008). This is a crucial point since, as can be seen from Figure 1.2, it is directly correlated to land requirements: between 1 and 3% of the total US cropping area would be required to satisfy 50% of the transport fuel needs with microalgae, compared to 24% needed for oil palm, and even 326% if soybean were to be used (Chisti, 2007);
- they can be grown almost everywhere (including on the ocean surface), not requiring arable land and hence avoiding also indirect competition with food production. Microalgae indeed have the capability of adapting to different environmental conditions, and can grow in fresh, brackish and saline water. In addition, different algal species can be found that are most suitable for particularly hostile temperatures or irradiance conditions;

- microalgae and cyanobacteria have good potential for environmental applications such as CO_2 mitigation and wastewaters treatment, which raise major concerns worldwide (Milano et al., 2016; Sforza et al., 2014b). In fact, they are able to fix CO_2 from flue-gases as a carbon source and to assimilate phosphorus and nitrogen from wastewaters, reducing the concentration of these pollutants from the corresponding streams.

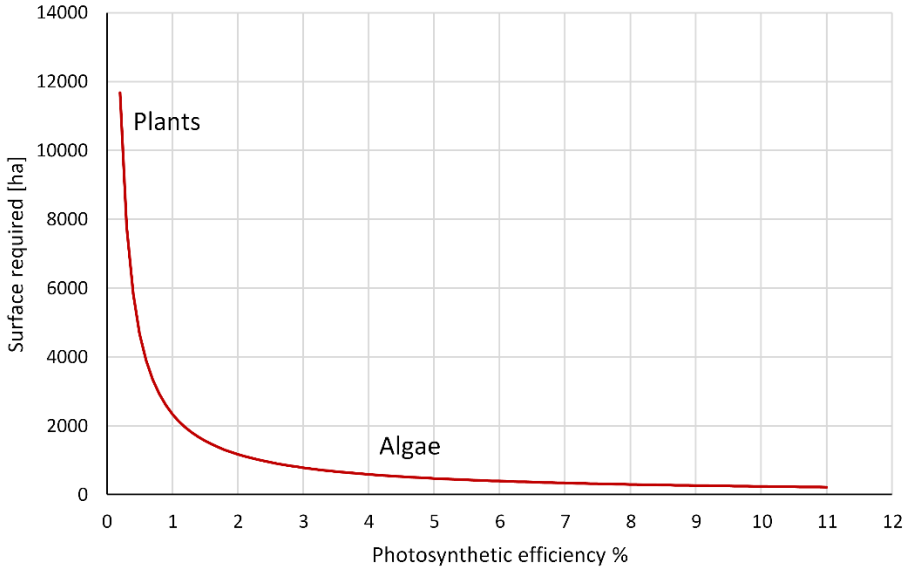

Figure 1.2 *Surface land requirements as a function of the photosynthetic efficiency, for a production of 1 ton h^{-1} of oil, at middle latitudes*

Additionally, microalgal biodiesel contains no (or very low amounts) of sulfur, so that emissions of SO_x would be reduced compared to traditional diesel, together with particulate matter, CO and hydrocarbons, even though NO_x emissions might be slightly higher (Mata et al., 2010). Furthermore, depending on the species, other compounds besides oil can be extracted from microalgae, such as pigments, dyes, or sugars, which can be valuable ì in a large number of biotechnology applications.

1.3. Cultivation systems for microalgae

The entire algae-to-fuels process is composed of several steps, starting from the production of biomass, its harvesting, and the subsequent conversion to the desired fuel product. Regardless

the conversion route chosen, the cultivation system is the core step of the process, as in most cases it ultimately determines its economic viability.

Microalgae can grow using different metabolic pathways: photoautotrophic growth exploits light as the sole energy source that is converted to chemical energy through photosynthetic reactions; heterotrophy takes advantage of only organic compounds (i.e., no light) as both carbon and energy source; some organism are able to grow mixotrophically, assimilating both organic and inorganic (CO_2) carbon sources, with photosynthesis being the main energy source (Mata et al., 2010). Clearly, if the long-term objective is to achieve production of biofuels in a sustainable way, the only viable alternative is to rely on freely available solar energy rather than "transferring" the issue on the availability of other raw materials (e.g. glucose) to be converted by microalgae. Therefore, although heterotrophic cultivation might be profitable when the target is to produce high-value compounds, it is unlikely to represent a viable solution for large-scale fuel production (Bonvincini et al., 2015).

The cultivation unit can be operated in either batch or continuous mode, even though from an industrial point of view the latter, with fresh medium constantly fed and the corresponding amount of biomass withdrawn continuously, appears preferable (Sforza et al., 2014a).

Factors that are determinant in autotrophic microalgal productivity are light intensity and distribution, temperature, pH, nutrients (N and P) and carbon availability, together with operative parameters such as mixing, dilution rate (or residence time) and culture depth.

At present, no sound technology has been identified for industrial microalgal production yet, so that a wide variety of cultivation systems has been proposed. However, within the multitude of technical solutions, they can be classified into open ponds (OP) and closed photo-bioreactors (PBR).

Open ponds (mostly with *Raceway ponds* configuration, Figure 1.3) is the most commonly used artificial system (Chisti, 2007). OP are the cheapest method of large-scale algal biomass production, because of their simple construction, operation, durability and low installation costs. In addition, cooling is achieved simply by evaporation, resulting in lower energy requirements (but in higher water consumption).

Figure 1.3 *Open Pond reactor (Photo: Aban Infrastructure Ltd)*

Normally, the culture depth ranges between 0.2-0.5 m, and biomass productivity reaches 60-100 mg L^{-1} d^{-1} (i.e. 10-25 g m^{-2} d^{-1}) (Bonvincini et al., 2015). However, major drawbacks are related to a poor control of the environmental conditions: evaporative water loss can be significant, affecting also the salinity of the cultivation medium; CO_2 is used with a much lower efficiency compared to closed system, because of significant losses to the atmosphere; the performances in terms of biomass productivity are sensibly lower as a consequence of poor mixing and related light utilization; finally, contamination by external microorganisms such as unwanted algae or zooplankton who feed on algae represents the main limitation of this technology, as some microalgae species tend to collapse due to predation.

Closed photobioreactors allow having an accurate regulation of the most important variables that influence microalgal growth. The tight control of environmental conditions prevents to some extent contamination by undesired microorganisms and grazers, so that single-species microalgae cultures can be sustained for prolonged periods (Posten, 2009). A closed system has also the advantages of better CO_2 utilization and reduced water footprints as evaporation losses are prevented. Because of all of these factors, PBRs are characterized by significantly higher areal and volumetric productivities (more than 13-fold) so that biomass concentration is nearly 30 times higher compared to open ponds. This has a great impact in terms of both surface required and harvesting costs (Chisti, 2007).

Although different geometries have been developed, the most commonly employed designs include flat-plate and tubular photobioreactors (Figure 1.4), in either vertical or horizontal configurations.

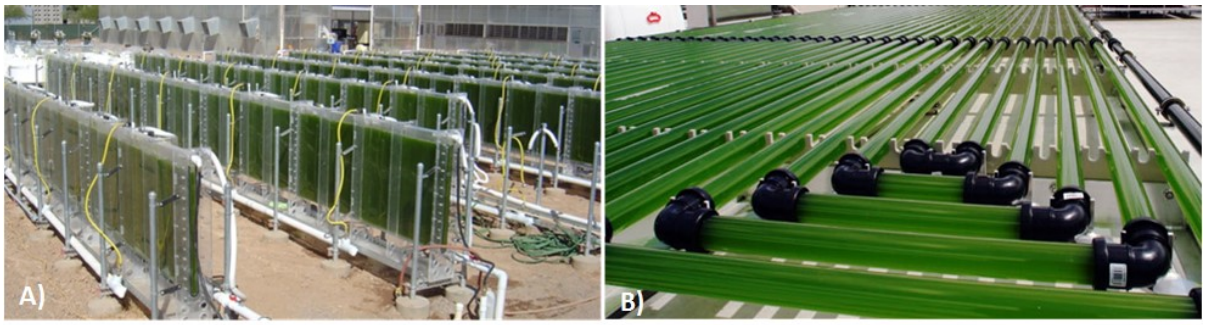

Figure 1.4 *Flat-plate (A) and tubular (B) photobioreactors*
(Photos: NanoVoltaics, Inc. and AlgaePARC, Wageningen)

Flat-panel PBRs allow good light path and utilization, due to a large surface-to-volume ratio, on the other hand they are more difficult to scale up.

The main disadvantage of closed PBRs is related to economic and energetic constraints: in fact, cooling represents a huge energetic input and the major operation cost of these systems, in which temperatures inside the reactor might otherwise reach values up to 55°C (Mata et al., 2010).

1.4. Downstream processes and biomass conversion routes

Prior to subsequent processing for biofuels production, the microalgal suspension from the cultivation system needs to be concentrated through mechanical water removal, so to obtain a thick algae paste. This harvesting step is currently accounted for 20-30% of the total biofuels production costs, even though this is still an active area for research. It can be divided into two process steps: bulk harvesting, where the biomass is separated from the bulk culture through methods such as flocculation or sedimentation, and a thickening step in which the algae slurry is concentrated with techniques like centrifugation or filtration (Milano et al., 2016). For low value products such as biofuels, gravity sedimentation is the most common pre-concentration method, and especially for microalgae with high density like *Chlorella* and *Scenedesmus* sp. Centrifugation or filtration allow then to concentrate the slurry up to 15-20% solids content. The former is more energy demanding and costly, while on the other hand conventional and vacuum filtration might be relatively slow for some application and suitable only for microalgae with size larger than 70 µm.

Once concentrated, microalgal biomass can be converted into biofuels through a number of ways. They can be mainly classified in four groups (Figure 1.5): chemical conversion, biochemical conversion, thermochemical conversion and hydrothermal conversion.

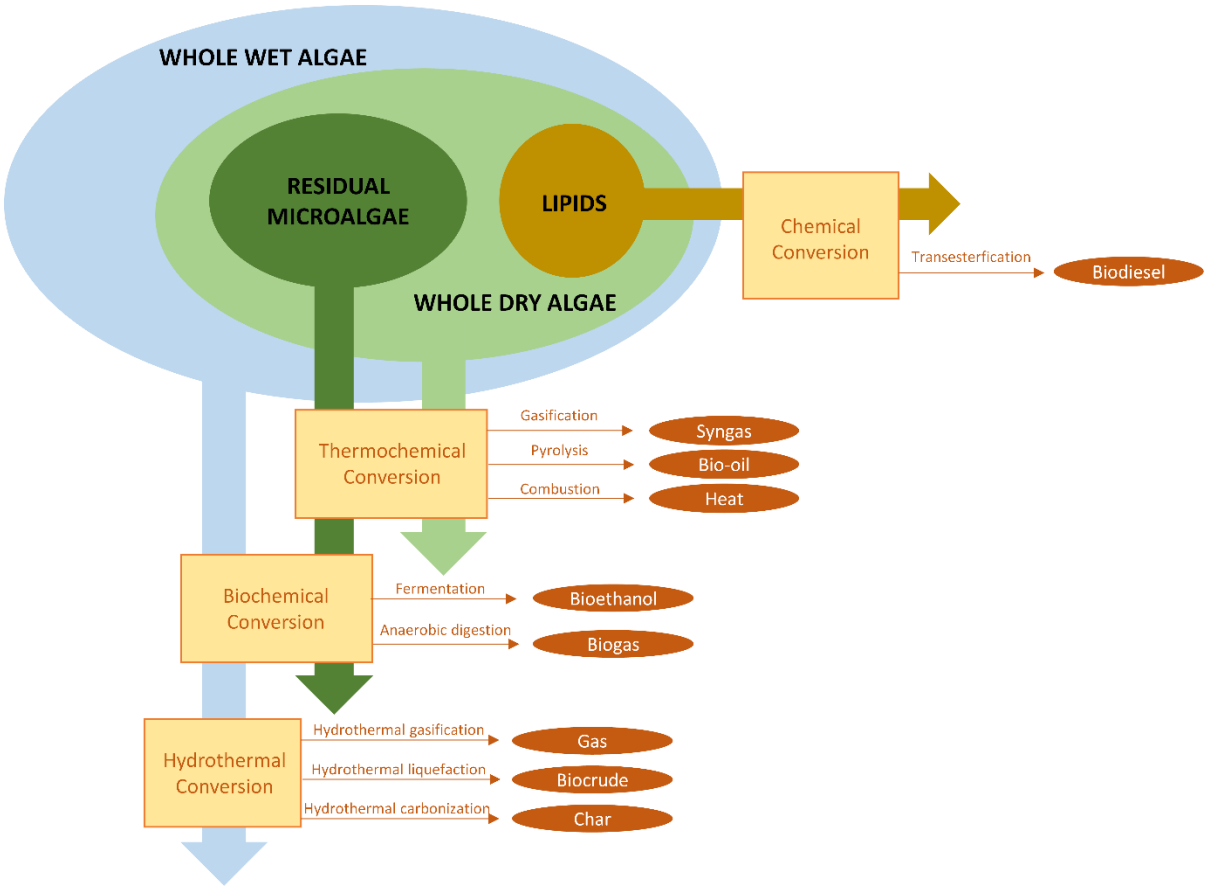

Figure 1.5 *Microalgae-to-biofuels conversion routes*

1.4.1. Chemical conversion

The traditional route for conversion of microalgae into liquid fuels is the production of biodiesel via transesterification of the lipid fraction contained in the biomass. This process requires the extraction and recovery of lipids from the algal cell, and subsequent reaction with methanol to form Fatty Acid Methyl Esters (FAME). Glycerol is a massive byproduct of this process.

Conventional extraction methods involve the use of organic solvents, which penetrate the cell membrane and solubilize neutral lipids. Efficient solvents employed to this purpose are hexane, chloroform (alone or in a mixture with methanol), isopropanol (Halim et al., 2012). However,

there are many drawbacks: first, the process requires the algal biomass to be dried up to a moisture content of 10% or less, which demands huge energy inputs and associated costs (much higher than those of previous mechanical dewatering) (Mata et al., 2010). In addition, the large solvent requirement is related to additional disadvantages in terms of sizing of the equipment for both extraction and solvent recovery, as well as associated fire, explosion and toxicity risks (Ghasemi Naghdi et al., 2016).

A possible alternative to the use of organic solvents could be supercritical CO_2 ($SCCO_2$). This fluid shows great potential due to tunable solvent properties, which can be adjusted based on extraction pressure and temperature, in order to make it more selective towards biodiesel-desirable neutral lipids rather than phospholipids. In addition, the extraction is rapid, non-toxic, and produces solvent-free crude lipids (Halim et al., 2012). Nevertheless, $SCCO_2$ extraction has considerable economic and energetic costs associated with fluid compression and the high pressures involved (P_c = 72.9 atm), which make it unfavorable for process scale-up in biofuels production.

Currently, in order to mitigate the costs associated with biomass drying, wet lipid extraction techniques are being proposed. This can be achieved by increasing the polarity of the solvent mixture: the polar solvent can in fact penetrate the water layer and make the lipids available for non-polar lipid extraction. Sathish and Sims (2012) developed a wet lipid extraction procedure capable of extracting 79% of transesterifiable lipids from algal biomass with 84% moisture via acid and base hydrolysis.

1.4.2. Biochemical conversion

Biochemical processes involve the use of microorganisms for the conversion of microalgae biomass into fuels.

Through alcoholic fermentation the carbohydrates contained in the biomass (mainly starch and cellulose) can be converted to bioethanol: after some pre-treatment mechanical steps, carbohydrates undergo enzymatic hydrolysis, then yeast fermentation, and finally subsequent distillation to remove water and impurities from the ethanol product (Milano et al., 2016). Among promising microalgae species able to accumulate large amounts of carbohydrates are the genera *Scenedesmus*, *Chlorella*, *Chlorococcum* and *Tetraselmis*, along with the

cyanobacterium *Synechococcus*, which can reach contents up to 50% (de Farias Silva and Bertucco, 2015).

On the other hand, anaerobic digestion (AD) is a well-known and developed technology that involves the conversion of complex organic matter into biogas (i.e. a mixture of CH_4 and CO_2) through suitable activated sludge. This process includes four biological steps, namely hydrolysis of proteins, carbohydrates and lipids into amino acids, sugars and long chain fatty acids, which are further degraded into volatile fatty acids, hydrogen, acetate and CO_2 during acidogenesis and acetogenesis; finally, methanogenesis carried out by methanogenic bacteria results in the production of methane and CO_2 (Gonzalez-Fernandez et al., 2015). Anaerobic digestion of microalgae has been proven feasible, using both whole biomass and the residue remaining after lipids extraction, with methane yields ranging from 100 to 600 mL g^{-1} VS (Ward et al., 2014). This could be potentially used for the production of electricity or heat to be exploited within the process itself. Compared to other types of biomass however, AD of algal biomass is associated with some intrinsic challenges, namely the low degradability of the cell wall, which acts as a protection of the intracellular organic matter from bacteria, and the low C/N ratio due to the high protein content, which might lead to excessive production of ammonia, resulting in toxicity effects. In this regard, anaerobic digestion carried out on microalgae residues appears favorable: in addition to exploiting the lipid fraction for the production of liquid fuels, the extraction process allows the disruption of cell walls and increases the solubilization of the organic matter, resulting in higher methane yields (Ramos-Suárez and Carreras, 2014). Moreover, the glycerol obtained as a by-product of the transesterification process could be used as co-digestion substrate to increase the C/N ratio in the digester (Ehimen et al., 2009).

1.4.3. Thermochemical conversion

Thermochemical conversion is the thermal decomposition of biomass into biofuels products. The main characteristic is that they can be applied on whole algae, not just on lipid-extracted ones, and that the feedstock composition is not so critical to the process, so that various feedstocks and blends can be handled (Elliott, 2016). Depending on the process conditions, different fuel products can be obtained. Specifically:

- pyrolysis is a process carried out in the absence of oxygen/air at temperatures between 350°C and 550°C (Milano et al., 2016). The main products are bio-oil, charcoal and a gaseous phase. In order to maximize the production of bio-oil, fast pyrolysis (i.e., few seconds of residence time) is used. The liquid bio-oil product needs to be subsequently upgraded (hydrodeoxygenation) in order to have properties comparable to those of crude oil;
- gasification involves partial combustion of algal biomass, with oxygen concentration ranging between 0.2-0.4 of the stoichiometric value required for complete combustion, at very high temperature (800°C – 1000°C). Under these conditions, syngas (a mixture of CO and H_2) constitutes the main product, which could be directly used as fuel for engines and turbines, or for liquid fuels production via Fischer-Tropsch reactions;
- dried microalgal biomass can also undergo direct combustion, under the presence of excess air/oxygen and temperatures ranging between 800°C and 1000°C, producing direct heat/electricity. Even though direct combustion of biomass presents advantages over conventional coal-fired plants (Milano et al., 2016), it does not lead to the production of any liquid fuel. Therefore, in this case, it would be more suitable to perform the combustion on microalgae lipid-extracted residues.

Even though thermochemical processes have been tested on microalgal biomass with success, they require the feedstock to be dried: this leads inevitably to strongly negative energy balances so that, while probably being more feasible for other types of feedstocks, e.g. lignocellulosic biomass, little hope is given for industrial application for microalgae.

1.4.4. Hydrothermal conversion

Although commonly considered as part of the thermochemical conversion processes, hydrothermal treatments differ from the previous ones as they are carried out on wet algal biomass, with significant energy savings as the drying step is avoided. Furthermore, these processes exploit the properties of water under sub/supercritical conditions: in fact, under high temperatures and pressures several chemical and physical properties of the water change, so that non-polar organic compounds become increasingly miscible with it, because of decreased dielectric constant. These tunable physiochemical properties allow to target the reaction toward

the production of solid, liquid or gaseous fuels by simply varying the temperature and pressure, together with the residence time (Patel et al., 2016). Different operating conditions can be used:

- under low to moderate temperatures (120°C-250°C), pressures around 20 bars and long residence times (~1 h), a solid product with coal/char properties is produced, in a process referred to as Hydrothermal Carbonization (HTC). Solid yields of up to 60% are reported, with a HHV of approximately 30 MJ kg^{-1} and characteristics similar to coal. In addition, most of the lipids are retained in this hydrochar, and can be later recovered by a simple solvent extraction (Heilmann et al., 2011).
- moving forward on the temperature scale, Hydrothermal Liquefaction (HTL) occurs in the range of 250°C up to the supercritical point of water (i.e. 374°C) and P < 220 bar. The typical residence times vary between 10 to 30 min. HTL is considered the most promising treatment option for algal biomass, and extensive research work has been carried out in this field. The main product of HTL is a liquid biofuel precursor (biocrude, with HHV between 30 – 40 MJ kg^{-1}), together with a gas phase, a solid residue and an aqueous phase rich in soluble organics. The key parameters influencing the biocrude yield are temperature and residence time, which are intrinsically correlated (López Barreiro et al., 2013). Generally, the highest biocrude yield was found at T > 300°C and residence time < 20 min, as longer residence times result in higher N content in the oil (Elliott, 2016). Some issues connected with HTL are related to the separation of the organic liquid product from the aqueous phase, together with the fact that, despite the high heating value, the biocrude produced through HTL needs significant upgrading before it can be used as a transportation fuel because of high oxygen, nitrogen and sulfur contents, together with acidity and viscosity issues. Finally, the complexity of the process in terms of reaction involved makes it difficult to identify the kinetic pathways so to target specific products while avoiding the formation of undesirable ones.

  Recently, a novel process called Flash Hydrolysis (FH) was developed and proposed (Garcia-Moscoso et al., 2013). FH is very rapid HTL characterized by short residence times (< 10 s), resulting in the production of an aqueous phase in which proteins and carbohydrates are hydrolyzed, together with a lipid-rich solid product.
- when the operating temperature is higher than 374°C, Supercritical Water Gasification (SCWG), also known as Hydrothermal Gasification occurs (López Barreiro et al., 2013).

This process converts the algal feed into gaseous products such as CH_4, CO, CO_2, H_2 and C_2-C_4 gases. Compared to neat gasification, the use of water allows having lower tar generation and higher carbon efficiency. Temperatures generally range between 400°C – 700°C and corresponding saturation pressures. Moderate temperatures (around 500°C) enhance methane production, while harsher conditions increase H_2 yields, even though the use of a catalyst is often required (Patel et al., 2016).

1.5. Constraints to scale-up and commercialization of algal fuels

Of the different types of biofuels that microalgae can provide, the production of liquid fuels for transportation has undoubtedly gained most attention, including commercialization efforts by many companies. Lipids from algal biomass have been successfully transformed into diesel, which gave good results in terms of performances, showing that algal fuels production for transportation is indeed a proven technology. However, at present, serious impediments still exist to the implementation of biofuels production from microalgal biomass on a large-scale (Chisti, 2013).

The main burden is the fact that algal fuels are currently significantly more expensive compared to petroleum derived ones, with this gap being even larger after the drop of crude oil prices at the end of 2014. In addition, oil price fluctuations introduce further uncertainties for potential investment commitments in biofuels commercialization. Regarding production costs, inexpensive harvesting and oil product recovery are certainly required, but ultimately the major costs drivers are related to the biomass production performances of the cultivation system, which should be maximized. For instance, Tredici et al. (2016) report a production cost of 12.4 € kg^{-1} (dry weight) of algal paste in a 1-ha production facility in Tuscany, potentially reduced down to 3.2 € kg^{-1} for a 100-ha facility in a more suitable location, with major cost contributions due to capital expenses and labor. Clearly, these numbers show commercial potential for high-value (e.g., cosmetics, aquaculture) and medium/low-value products (such as nutritional foods), but biofuels appears to be out of reach. In fact, Ramos Tercero et al. (2014) found a sale price of 21 $ gal^{-1} for algal biodiesel, definitely not competitive with that of conventional diesel. Similar conclusions are drawn by Ruiz et al. (2016), who report a cost per unit of dry biomass of 3.4 € kg^{-1} for microalgae cultivation in a

100-ha facility in Spain. In order for algal biofuels to become economically attractive, improvements in productivity are essential, having pronounced effects on the downstream and market price. In particular, the same authors pinpoint photosynthetic efficiency as the most influential parameter on production cost, with a potential reduction of 1.6 € kg^{-1} (Ruiz et al., 2016).

In autotrophic microalgal cultivation a key role is played by sunlight availability and utilization. Theoretically, the efficiency of sunlight conversion into energy-rich biomass through photosynthesis is limited by thermodynamic constraints to a maximum value of about 12% (Blankenship et al., 2011): this results as not all the solar spectrum can be absorbed by photosynthetic pigments, but only 43% of the irradiance is a Photosynthetically Active Radiation (PAR, 400-700 nm). Moreover, only the blue and red ranges are effectively absorbed, while the other wavelengths are reflected and possibly wasted into heat. Thermodynamics furthermore dictates that not all the energy in absorbed photons is captured for productive use, but some of it is lost for inefficient energy transfer within the photosystems as well as for cellular respiration and maintenance (Ringsmuth et al., 2016).

However, existing cultivation systems do not come close to the theoretical limit, and one of the main reasons contributing to this inefficiency is the concurrence of light limitation (due to mutual shading of cells in the deeper culture layers) and photoinhibition phenomena. The latter takes place at irradiance levels of only 10% of the peak midday sunlight in a tropical region: under these super-saturated light conditions in fact, photosystems absorb the light energy flux at a faster rate compared to what can be processed, resulting in significant losses through heat and fluorescence dissipation. It is commonly recognized that, in order to obtain higher photosynthetic efficiencies and productivities of microalgal biomass, and consequently cut down overall production costs, light utilization needs to be improved. Besides genetic engineering (Ringsmuth et al., 2016), turbulence induced high-frequency light-dark cycles of algal cells resulted in increased productivity; however, attaining the required level of turbulence is impractical at large scale because of intense energy requirement, together with high risks of cell damage by shear stress (Chisti, 2013).

In addition to biomass productivity, severe limitations to scale-up of algal biofuels production are related to the necessary resources demand, not only from the economic point of view but also, and especially, from an environmental sustainability perspective.

Carbon dioxide supply appears as one of the most significant challenges in this regard. This compound is essential for photosynthetic microalgal growth. Based on the elemental composition of microalgae (which contain about 50% of C on mass basis), roughly 1.8-2 kg of CO_2 are required for each kg of algal biomass produced. Unfortunately, the atmospheric carbon dioxide concentration is strongly limiting for algal growth, so that CO_2-enriched air needs to be employed, resulting in significantly enhanced growth rate. At commercial scale, algal fuels production can only be feasible if CO_2 is available at low or no cost, and this could be possible by exploiting concentrated flue-gas emissions from power plants or the cement industry (Chisti, 2013). However, Pate et al., (2011) estimated that, depending on the oil production target and the location, between half and the totality of stationary emission sources in the US would be required, and this is clearly a major drawback to algal fuels production at a meaningful scale. In addition, relying on flue-gas derived from fossil sources for the production of renewable fuels is an evident controversy. The possibility of concentrating CO_2 from the atmosphere would avoid at the same time the need of relying on fossil fuels and the necessity of point emission sources, but at present available technologies are too expensive (Chisti, 2013), even though recently the use of carbonation membranes for efficient CO_2 supply are under investigation (Bilad et al., 2014). Alternatively, CO_2 may be supplied in the form of soluble bicarbonate, reducing also equipment costs related to its insufflation in the cultivation system (Gris et al., 2014), but this possibility depends on the algal species considered.

In addition to carbon, nutrients (nitrogen and phosphorus) are required for algal growth (between 6-9% of N and 0.3-1.5% of P of the total dry weight). Fulfilling the necessary nutrients requirement on a scale that aims at displacing a significant amount of petroleum fuels by using N and P fertilizers is clearly unfeasible and unsustainable. Various authors estimated that algal biofuels would inevitably compete with agriculture and food crops production for fertilizers availability, and this would potentially result in significant increase in fertilizers market prices (Canter et al., 2015; Pate et al., 2011). In addition to affecting the agricultural sector, the high nutrients demand raises serious sustainability concerns: phosphorus supply derives from finite phosphate rocks reserves, which are expected to be depleted in the short-term future (Cordell et al., 2009); nitrogen supply, on the other hand, is less critical, but the production of inorganic nitrogen compounds requires tremendous amounts of energy and relies on fossil fuel sources (i.e. natural gas), which increase the environmental burden of N-derived

fertilizers. Wastewaters represent a good source of nutrients to grow algae for low value products such as fuels (Sforza et al., 2014b). However, they can only contribute to a minimal amount of the total needs. It is estimated that roughly up to 3% of the transport fuel requirements of a big city could be provided using microalgae grown on wastewaters produced by the city. Considering that little or no nutrients are contained in the oil, it is clear that the only way an industrial production of algal fuels can be feasible is by recovering N and P from the spent biomass and, somehow, by recycling them for further growth (Chisti, 2013).

These and other problems need to be addressed and solved before microalgae-derived biofuels commercialization can become a concrete reality.

1.5.1. Nutrients recycling in microalgal cultivation

Despite the importance of nutrients in the production of algal fuels has been frequently overlooked or neglected in the early stages, the awareness towards this crucial environmental aspect has grown significantly in the latest years, and several research efforts are directed to finding nutrients recovery and recycling solutions. Among the biomass-to-fuels conversion pathways discussed in §1.4, anaerobic digestion and hydrothermal treatments result in the production of an aqueous phase containing good amounts of nutrients recovered from the biomass.

Nutrients values in digestate obtained from AD of algal biomass have been reported between 500-850 mg L^{-1} of ammonium-nitrogen and up to 150 mg L^{-1} of phosphate (Ras et al., 2011; Ward et al., 2014). The capability of microalgae to grow on liquid digestates originated from AD of municipal wastewaters or dairy manure was proven successful (Cai et al., 2013; Wang et al., 2010), even though considerable dilutions (around 20x) of these effluents were necessary, due to the otherwise too high concentration of toxic ammonia and for turbidity issues. Prajapati et al. (2014) investigated a closed-loop process involving AD of the cyanobacterium *Chroococcus* sp. and subsequent recycling of the liquid digestate, showing that diluting the medium with rural wastewaters helped providing all the required macro and micronutrients, ensuring growths comparable to control medium. An additional synergistic benefit of integrating AD with algal biofuels production is the possibility of using the biogas as a source of CO_2 (typical contents range between 30-50% v/v), with the double goal of purifying the methane content (Ward et al., 2014).

On the other hand, various studies have examined the possibility of recycling nutrients in the aqueous phase (AP) produced by hydrothermal processing of microalgal biomass, assessing the growth in such substrate. General results show that most microalgae are able to grow in the AP from HTL, but in this case very heavy dilutions are required (from 100x to 400x), to avoid inhibition by high concentrations of toxic compounds, i.e. phenols, heterocyclic compounds or nickel originated from corrosion of reactor walls (Biller et al., 2012). Jena et al., (2011) indicated that *Chlorella minutissima* was not able to grow in the diluted AP from HTL as good as in control medium, while Garcia Alba et al., (2013) reported that up to 50% of nutrients could be effectively replaced by the aqueous phase, provided that the other micronutrients from standard medium are supplied as well. López Barreiro et al., (2015) investigated the possibility of employing supercritical water gasification to purify the AP after HTL, thus reducing the load of inhibitory organic compounds. They conclude that SCWG did not bring any advantage in terms of algal growth, with *Chlorella vulgaris* and *Nannochloropsis gaditana* growing just as well as in the standard medium when 75% of the nutrients were provided by HTL aqueous phase. Finally, Du et al. (Du et al., 2012) and Levine et al. (Levine et al., 2013) both reported higher microalgal growth rates and biomass production compared to those achieved in standard media when recycling the aqueous byproducts of hydrothermal carbonization, likely due to mixotrophic growth.

1.6. The current industrial scenario

In the last decade, the urgent need to find alternative solutions to fossil fuels together with the very optimistic and promising prospects brought by microalgae as an ideal feedstock to this purpose, led to huge investment in this field and to the development of a number of startup companies, attempting to commercialize algal fuels. Unfortunately, to date, many of these companies have been struggling to retain a high productivity at larger scale, and the drop of crude oil prices made it even worse to comply with already difficult economics.

A few companies are however still active in the biofuels sector, even though the general trend has shown that many pivoted into the production of high value compounds, e.g. for nutraceutical applications.

Algenol (www.algenol.com) has been one of the leading companies in the production of biofuels. They have been using a proprietary strain of engineered cyanobacteria to produce

bioethanol directly from the algae, which is thus recovered from the photobioreactors, while the spent biomass is subsequently converted into green crude using hydrothermal liquefaction. Algenol has a 2-acre production site in Florida, operational since 2014, and claims that its process produces around 8000 gal of liquid fuels per year on one wet acre of algal cultivation (Elliott, 2016). The majority of the product is ethanol, but also diesel (500 gal), gasoline (380 gal) and jet fuel (315) gal are obtained from the HTL process. Overall 85% of the CO_2 feedstock is converted in biofuels. Very recently, after the departure of former CEO and founder Paul Woods, they have added natural food colorants and bio-fertilizers to their commercial products, and maintained a more low-key profile.

Sapphire Energy (www.sapphireenergy.com) started developing their green crude oil production from algae since 2007. In 2010, the company began constructing the world's first commercial demonstration plant, with 100 acres of ponds, which was completed in 2012. They have a patented process for liquefaction, which includes a hydrothermal step with biocrude recovery and treatment. Sapphire biocrude has been tested in partnership with petroleum refiners, to be co-processed with crude oil streams in refineries. As of January 2015, however, Sapphire has announced a shift in the targeted market, for the production of nutraceutical products and animal/aquaculture feed (Elliott, 2016), but since then no further communications have appeared.

Muradel (www.muradel.com) developed an integrated algae production and hydrothermal liquefaction demonstration plant, opened at the end of 2014 in Australia., which can produce 300,000 L $year^{-1}$of biocrude. They use their Green2Black^{TM} process, with a sub-critical water reactor for the conversion of the feedstock into hydrocarbons, which are extracted and upgraded to drop-in fuels. In addition to algae, they are now focusing on other biosolids as feedstock for the process.

Cellana (www.cellana.com) has operated its demonstration facility based in Kona, Hawaii, since 2009, and is in the process of evaluating multiple commercial algae facility locations with a modular scale-up approach. Their patented process, ALDUO^{TM}, couples closed-culture photobioreactors with open ponds. Cellana has a three-products biorefinery approach, which comprises the production of Omega-3 nutritional oils, animal feed and biofuels.

Reliance Industries Ltd. (www.ril.com), one of the leading Indian companies in the oil&gas sector, has recently partnered with the Pacific Northwest National Laboratory (PNNL) and

others in the National Association for Advanced Biofuels and Bioproducts (NAABB) in the research of algal fuels pathways. They have developed and constructed a pilot plant for rapid hydrothermal processing of algal biomass to liquid and gaseous fuels (Elliott, 2016).

The evident trend shows that, at present, microalgae-derived biofuels cannot compete with their fossil counterpart at an industrial level. However, due to the diversity of products that can be obtained from this type of biomass (especially high-value biomolecules for the nutraceutical and cosmetic sector), the general approach of many companies is currently that of temporarily diverting the production from fuels to such high-value products. This behavior emerged clearly also in the last edition of the Algae Biomass Summit (the most important annual scientific congress on this field, held in Phoenix, AZ, October 23-26, 2016) with a major focus on algae-derived high-value products and a few environmental applications, while very little space was taken by biofuels.

However, despite this temporary diversion due to financial reasons, algal fuels have not been given up on. The US Department of Energy in the 2016 Billion-Ton Report (U.S. DOE, 2016) considered for the first time the potential supply of biomass from microalgae, in addition to conventional terrestrial feedstocks. In particular, the report concludes that the United States have the future potential to produce 1 billion tons of overall biomass resources per year, which could be used to generate enough biofuels, bioenergy and bioproducts to displace approximately 30% of the 2005 US petroleum consumption. Of these, up to 130 million tons could be derived from microalgal biomass (both freshwater and saline), even though it is acknowledged that the use in algal biofuels pathways is not economically sustainable yet (with more than 90% of global algae production currently used for nutritional products). Therefore, even though coproducts are currently required for the commercial viability of most algal systems, R&D efforts are still going on (including the industry) in the energy sector until this technology becomes sufficiently convenient.

Chapter 2

Maximizing the production of *Scenedesmus obliquus* in photobioreactors under different irradiation regimes: experiments and modeling

Maximizing biomass productivity and photosynthetic efficiency are key factors to develop large-scale microalgae cultivation for biodiesel production. If the photobioreactor is not operated under proper conditions, productivity and efficiency values drop considerably. In this chapter, the growth of the freshwater microalga *Scenedesmus obliquus* in continuous horizontal flat-panel photobioreactors (PBR) is considered. Experimental data and simulations are used with the aim of determining suitable working conditions to achieve maximum productivity. Microalgae concentration and productivity have been measured in a continuous 250 mL flat-panel PBR as a function of the residence time τ. Simulations were performed at both low and high irradiance values, and with different light regimes (constant light and day-night profiles). Model parameters were optimized based on laboratory-scale experimental data. The effect of different extent of axial mixing on PBR performances was investigated. Results obtained show how to determine optimum working conditions and how they could be used in the design of a large-scale photobioreactor to achieve maximum microalgal productivity.

[0]Part of this chapter was published in Bioprocess and Biosystems Engineering (Barbera E., Sforza E., Bertucco A., 2015, 38:2177–2188)

2.1. Introduction

Microalgae have recently received wide interest as an alternative source for the production of biofuels, aiming at potentially replacing traditional fossil fuels in the medium-long term. These microorganisms are able to convert light energy into high heating value and lipid-rich biomass through photosynthesis. They offer many advantages compared to terrestrial crops, among which much higher growth rate, areal productivity and efficiency in converting sunlight into biochemical energy (Chisti, 2013; Stephenson et al., 2011; Ullah et al., 2015; X. G. Zhu et al., 2008). Nonetheless, despite these promising aspects, there are still many limitations to the development of microalgae-derived biodiesel production processes at commercial scale, which affect transformation of light energy into biomass and decrease overall productivity, leading to negative process energy balance, i.e. to unsatisfactory EROEI (Energy return on Energy Investment) values (Ramos Tercero et al., 2013).

The core of the whole process is the microalgal cultivation system, which needs to be optimized in order to achieve the best performances in terms of productivity and light energy conversion efficiency. However, the complexity of the phenomena involved in microalgal growth make the optimization of such a system a difficult task. This explains the wide variety of cultivation systems that, as reviewed in Chapter 1, can be found in the literature, ranging from open ponds (Chiaramonti et al., 2013; Muñoz-Tamayo et al., 2013) to different geometries and design varieties of closed photobioreactors (PBRs) (Fernandes et al., 2014; Posten, 2009; Pruvost et al., 2011a; Takache et al., 2010), all of which have both advantages and disadvantages. For instance, closed PBRs have the main disadvantage of requiring higher construction and operation costs, but their advantage is the possibility of maintaining a strict control of operating variables, and to preserve the system from external contamination, therefore reaching generally higher productivities (Borowitzka and Moheimani, 2012; Pandey et al., 2014). On the other hand, Open Ponds (OP) productivity is heavily affected by contamination (Posten, 2009). In both PBRs and OPs already widely used at the industrial scale, the cost-benefit analysis is still far from being attractive for industrial applications.

Clearly, when considering photoautotrophic microalgal cultivation, a key role is played by light availability and utilization (Carvalho et al., 2011), hence PBRs need to have a wide light-exposed surface, and a thin depth to avoid the presence of dark zones inside the culture. In this

view, a flat-panel PBR appears to be the best configuration to maximize light utilization. Moreover, despite batch studies are fundamental to assess growth parameters, a continuous operation is preferable when considering industrial scale plants, allowing to reach remarkable steady-state productions (Sforza et al., 2014a).

Being able to predict the behavior of a PBR is crucial for the design and operation of a large-scale facility. Many factors affect the performances of the cultivation system, namely nutrient availability, temperature and pH, but assuming that these parameters can be controlled and that nutrients are supplied in non-limiting amounts, light is the most important variable. Main efforts about design and operation of PBRs have to be focused in order to increase the portion of light energy transformed into biomass.

Continuous PBRs under constant artificial light have been widely studied (Cuaresma et al., 2009; Kim et al., 2014; Pruvost et al., 2011b; Sforza et al., 2014c) as they allow to assess how the performances are affected by operating variables (i.e. residence time of biomass inside the reactor and incident light intensity) as well as to gain information on light distribution and utilization inside the culture, and to analyze the biological response (e.g. pigment content, biochemical composition, maintenance requirements) in different stable conditions.

However, for an industrial scale microalgal production to be economically and energetically sustainable, the PBR needs to efficiently exploit the radiation coming from the sun. Outdoor PBRs are much more complex to characterize, due to the dynamic nature of the system. Microalgal cells are not only subjected to day-night cycles, but irradiation values are extremely variable throughout the year, depending on location and orientation, as well as other climatic factors. In addition, the angle of incidence of the radiation is never perpendicular to the PBR surface, but it also changes during the day and the year. Despite an accurate prediction of the behavior of an outdoor PBR cannot be obtained, it is possible to estimate average performances based on mean solar irradiation data for a specific location. Eventually, most of the works found in the literature refer to perfectly mixed PBRs, hence assuming a homogeneous biomass concentration in the culture volume (Bertucco et al., 2014; Muñoz-Tamayo et al., 2013; Pruvost et al., 2011b). However, this condition is hard to be achieved in large-scale applications, where wide surface areas are involved. Rather, an axial dispersion-flow PBR has to be considered: in this case, an increasing microalgae concentration profile develops along the reactor length.

In this chapter the growth of *Scenedesmus obliquus* in continuous flat-panel PBRs was investigated, with the aim of defining proper operating conditions in order to optimize the performances in terms of biomass productivity and photosynthetic efficiency. *S. obliquus* appears to be a very interesting species from the industrial point of view (Kaewkannetra et al., 2012; Tang et al., 2011), showing higher specific growth rates (0.8-0.9 d^{-1} at 150 μmol m^{-2} s^{-1}) and efficiencies compared to other species, as well as an acceptable amount of lipids (around 30-40%) even in the absence of stressing conditions (Sforza et al., 2014a), together with the capability of growing in wastewaters and non-sterile media (Gris et al., 2013). Experimental laboratory data were first used to adjust model parameters, then to verify the model results under different irradiation intensities and regimes, with both constant and day-night light profiles. In addition, the effect of different axial mixing extent, ranging from a completely stirred tank reactor (CSTR), to a plug flow reactor (PFR), was evaluated.

2.2. Experimental setup

Experimental data used in this chapter refer to continuous cultures of *Scenedesmus obliquus*. Growth experiments were carried out in vertical flat-panel polycarbonate PBRs, having a depth of 1.2 cm to maximize light utilization, and a working volume of 250 mL (Sforza et al., 2014c). *S. obliquus* was cultured in modified BG11 medium buffered with 10 mM HEPES pH 8, with non-limiting nutrient concentrations, and a CO_2-air mixture (5% v/v) was sparged from the bottom. The reactor was kept in a refrigerated incubator at a temperature of 23 ± 1°C. This way, light was the only variable to be investigated.

Experiments were conducted under different continuous constant light intensities (150 μmol m^{-2} s^{-1} and 650 μmol m^{-2} s^{-1} respectively), as well as under light-dark cycles that reproduce natural solar conditions at the latitude of Padova, Italy. In particular, typical winter and summer days are chosen as reference (in the latter case peak irradiances reach values of around 1700 μmol m^{-2} s^{-1}). Light was provided by a LED lamp (Photon System Instruments, SN-SL 3500-22) both for continuous and alternated day-night cycles. Photon Flux Density (PFD) was measured at both the front and back surface of the PBR with a photoradiometer (HD 2101.1 from Delta OHM), provided with a quantum-radiometric probe for measuring the photons flow in the PAR (Photosynthetically Active Radiation, 400-700 nm).

The system considered can be approximated to a CSTR (Sforza et al., 2014a, 2014c). For each light condition, different values of residence time (τ) were tested. The culture volume was kept constant by an overflow tube, and τ was modified adjusting the flow-rate by means of a peristaltic pump (Watson-Marlow sci400, flow rate range: 25-250 mL d^{-1}). For each value of τ, once steady state was reached, biomass concentration in terms of dry weight (DW) in g L^{-1} was measured daily, by filtering 5 mL of previously harvested cells with a 0.22 μm filter, and then drying for 4 h at 80 °C in a laboratory oven. Steady state concentrations were averaged on three to seven experimental points. Irradiance values at the back of the reactor were also measured. Biomass concentration and back irradiance measurements were then used to calculate productivity and photosynthetic efficiency for each experimental condition investigated.

2.3. Modeling

The models summarized below apply to both vertical (as in the lab) and horizontal (as in field application) flat-plate PBRs.

2.3.1. PBR material balances

2.3.1.1 CSTR

For a completely stirred PBR with no recycle (CSTR), the material balance is expressed by:

$$\frac{dc_x}{dt} = \dot{V}c_{x,e} - \dot{V}c_x + r_x V_R \qquad \text{(Eq. 2.1)}$$

where $\dot{V}$ is the volumetric flow rate, V_R the reactor volume, $c_{x,e}$ and c_x the biomass concentration at the inlet and outlet respectively, and r_x the net biomass growth rate. Assuming that the feed contains nutrients only (i.e. $c_{x,e} = 0$), at steady state Eq. 2.1 can be rewritten as:

$$\frac{c_x}{\tau} = r_x \qquad \text{(Eq. 2.2)}$$

where τ is the residence time of biomass inside the PBR, $\tau = V_R/\dot{V}$, hence the time that is necessary to process one volume of culture. Alternatively, the space-velocity (or dilution rate, $D = 1/\tau$) could be used as well.

The volumetric productivity is defined as:

$$P_x = \frac{\dot{V} c_x}{V_R} = \frac{\dot{V} r_x \tau}{V_R} = r_x \qquad \text{(Eq. 2.3)}$$

therefore it reaches its maximum when the net growth rate is maximized.
The photosynthetic efficiency (i.e. the fraction of light energy converted into biomass through photosynthesis) is determined according to the energy balance, and can be calculated as:

$$\eta_{PAR} = \frac{c_x \cdot \dot{V} \cdot LHV}{PFD_{abs} \cdot E_p \cdot A_{PBR}} = \frac{c_x \cdot H \cdot LHV}{PFD_{abs} \cdot E_p \cdot \tau} \qquad \text{(Eq. 2.4)}$$

$$\eta_{TOT} = 0.43 \cdot \eta_{PAR} \qquad \text{(Eq. 2.5)}$$

In Eq. (2.4) and (2.5) η_{PAR} and η_{TOT} are the conversions referred to photosynthetic active radiation (PAR) and total radiation, respectively. *LHV* is the lower heating value (assumed equal to 22 kJ g^{-1} for *S. obliquus* (Sforza et al., 2014c)), PFD_{abs} the PAR photon flux density absorbed by the culture (given by the difference between the irradiance value at the front and at the bottom surface of the PBR) [µmol m^{-2} s^{-1}], E_p the energy of photons [kJ µmol^{-1}], A_{PBR} is the irradiated surface of the reactor [m^2], and *H* is the PBR depth.

2.3.1.2 PBR with axial dispersion

In large installations, it is quite difficult to achieve complete stirring within the reactor volume, where the biomass concentration changes along the axial coordinate (*y*). The simplest way to account for axial mixing is to model the actual reactor by a Plug-Flow Reactor with partial recycle of the products (Levenspiel, 1996). The material balance in this case is expressed by:

$$\frac{dc_x}{dt} = r_x - \frac{R+1}{\tau}\frac{dc_x}{dy'} \qquad \text{(Eq. 2.6)}$$

where R is the recycle ratio ($R = \dot{V}_{recycle}/\dot{V}$), and y' is the dimensionless axial coordinate ($y'=y/L$), ranging from 0 to 1.
At steady state, Eq. 2.6 becomes:

$$\frac{dc_x}{dy'} = r_x \frac{\tau}{1+R} \qquad \text{(Eq. 2.7)}$$

with boundary condition at $y'=0$:

$$c_x = c_{x,e} = \frac{Rc_{x,out}}{1+R} \qquad \text{(Eq. 2.8)}$$

$c_{x,out}$ being the biomass concentration at the outlet. The volumetric productivity is defined as in (Eq. 2.3), but as the material balance is different, it is not equal to the net growth rate r_x at the outlet, and is calculated as:

$$P_x = \frac{c_{x,out}}{\tau} \qquad \text{(Eq. 2.9)}$$

The photosynthetic efficiency is calculated by averaging values along the length of the PBR, as the biomass concentration and hence the PFD absorbed are not constant with y, according to:

$$\langle \eta_{PAR} \rangle = \int_0^1 \frac{c_x(y') \cdot H \cdot LHV}{PFD_{abs}(y') \cdot E_p \cdot \tau} dy' \qquad \text{(Eq. 2.10)}$$

Note that, in both the cases of complete and incomplete axial mixing, perfect mixing is assumed along the reactor depth. This condition is not difficult to achieve in reality, as the microalgae growth kinetics is quite slow compared to mixing time scales, and, in horizontal PBRs, also thanks to the CO_2 bubbling from the bottom.

2.3.2. Growth model

For the prediction of the net biomass growth rate r_x, the model proposed by Cornet and Dussap (Dussap, 2009) was used, as modified by Pruvost et al. (Pruvost et al., 2011b) for eukaryotic

microalgae. According to this model, the value of r_x depends on the local light intensity. In a flat-panel PBR, it can be assumed that the variations in light intensity only occur along the depth of the reactor (z).

The light attenuation profile is determined by the following equations:

$$I(z) = I_{dir}(z) + I_{diff}(z) \quad \text{(Eq. 2.11)}$$

where $I_{dir}(z)$ and $I_{diff}(z)$ are the direct and diffuse contributions at distance z from the PBR surface. According to the two-flux model (Pottier et al., 2005; Pruvost et al., 2011a), they are expressed as follows:

$$\frac{I_{dir}(z)}{I_{dir}(0)} = \frac{2}{\cos\theta} \frac{(1+\alpha)\exp[(-\delta_{dir}(z-H)] - (1-\alpha)\exp[(\delta_{dir}(z-H)]}{(1+\alpha)^2 \exp[\delta_{dir}H] - (1-\alpha)^2 \exp[-\delta_{dir}H]} \quad \text{(Eq. 2.12)}$$

$$\frac{I_{diff}(z)}{I_{diff}(0)} = 4\frac{(1+\alpha)\exp[(-\delta_{diff}(z-H)] - (1-\alpha)\exp[(\delta_{diff}(z-H)]}{(1+\alpha)^2 \exp[\delta_{diff}H] - (1-\alpha)^2 \exp[-\delta_{diff}H]} \quad \text{(Eq. 2.13)}$$

where:

$$\delta_{dir} = \frac{\alpha c_x}{\cos\theta}(E_a + 2bE_s) \quad \text{(Eq. 2.14)}$$

$$\delta_{diff} = 2\alpha c_x (E_a + 2bE_s) \quad \text{(Eq. 2.15)}$$

$$\alpha = \sqrt{\frac{E_a}{E_a + 2bE_s}} \quad \text{(Eq. 2.16)}$$

In the above equations, θ is the light incident angle with respect to the normal to the PBR surface, E_a is the light absorption mass coefficient, E_s the light scattering mass coefficient, and b the backscattering fraction.

The local biomass growth rate is expressed as follows:

$$r_x(z) = \rho_m \frac{K}{K + I(z)} \Phi E_a I(z) c_x - \mu_e c_x \quad \text{(Eq. 2.17)}$$

where ρ_m is the maximum energetic yield for photon conversion, K the half saturation constant for photosynthesis, Φ the mass quantum yield for the Z-scheme of photosynthesis, and μ_e the maintenance coefficient. The net average biomass growth rate is then obtained integrating the local growth rate along the reactor depth:

$$r_x = \frac{1}{H}\int_0^H r_x(z)dz \qquad \text{(Eq. 2.18)}$$

If axial mixing is not complete, r_x changes along with *y'*, due to the corresponding change in concentration.

In Eq. 2.17 it can be noticed that the growth rate is composed by two terms: the positive one accounts for photosynthesis, while the other term takes into account the negative contribution due to respiration. Also, the effect of temperature is not kept into consideration in this chapter, and all the results herein presented are referred to 23°C. Eq. 2.11-2.18 have been solved using Matlab® codes.

2.3.3. Model parameters

In order to apply the model described above a number of parameters must be known. Some of them have been retrieved from the literature, while others have been determined from our experimental data, as detailed below.

The maximum energy yield for photon dissipation, ρ_m, can be considered as a species-independent parameter, whose value is equal to 0.8 (Dussap, 2009; Pruvost et al., 2011b; Sforza et al., 2014a).

The mass quantum yield for the Z-scheme of photosynthesis, Φ, represents the amount of biomass produced per mole of photons. The stoichiometric composition of *Scenedesmus obliquus* is $CH_{1.642}N_{0.098}O_{0.484}$, (Zelibor et al., 1988) hence the molecular weight per mole of carbon is equal to M_x = 22.76 g mol_C^{-1}. Considering that in photosynthesis 8 moles of photons are required for producing one mole of carbon, Φ results to be:

kg μmol^{-1}.

$$\Phi = \frac{M_x \cdot 1 mol_C}{8 photons} = 2.84 \cdot 10^{-9} \text{ kg } \mu mol^{-1} \qquad \text{(Eq. 2.19)}$$

The optical properties of the species considered (E_a and bE_s) can be evaluated using the theoretical approach proposed by Pottier et al. (Pottier et al., 2005), applying the generalized Lorenz-Mie theory. In this chapter, their values were determined from experimental data. In particular, the scattering coefficient E_s was retrieved from OD_{750} measurements, correlated to biomass concentration. Following the Lambert-Beer law:

$$OD = K_a c_x L \qquad \text{(Eq. 2.20)}$$

the optical density (i.e. absorbance) was found proportional to the biomass concentration [kg m^{-3}] and to the optical path (which in our case was equal to 0.01 m^{-1}) through the extinction coefficient K_a [m^2 kg^{-1}]. Since OD measurements were performed at 750 nm, which is outside the microalgae pigments absorption range, light extinction is due to scattering only, and $K_a = E_s$.

As it can be seen in Figure 2.1, from the correlations an average value of E_s = 532 m^2 kg^{-1} was obtained, quite independently of the light intensity. Assuming a back-scattered fraction b equal to 0.008 (Takache et al., 2012), bE_s results to be 4.25 m^2 kg^{-1}.

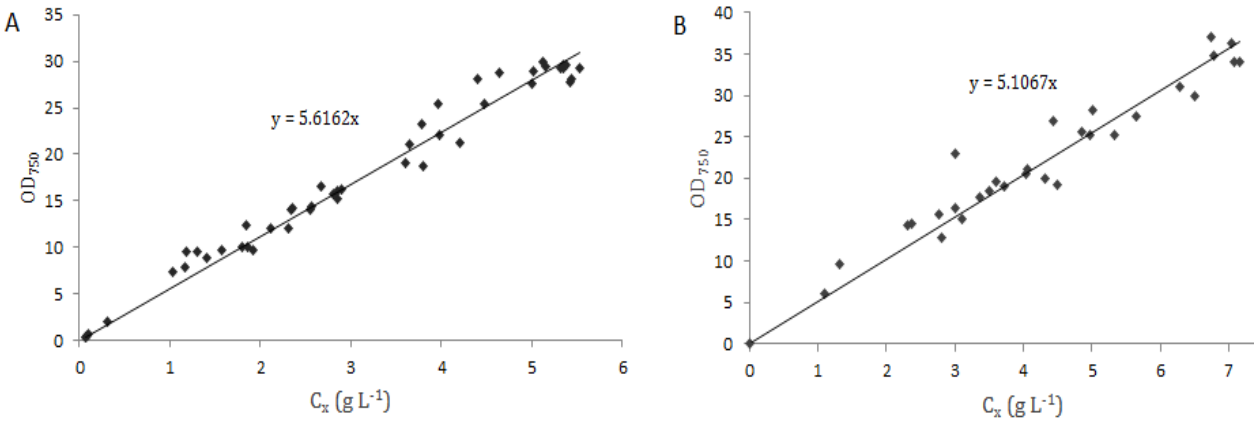

Figure 2.1 *Optical density at 750 nm as a function of the biomass concentration at a light intensity of 150 µmol m^{-2} s^{-1} (A) and 650 µmol m^{-2} s^{-1} (B)*

To obtain the value of the absorption coefficient E_a, experimental measurements of back irradiance (i.e. the irradiance at the back of the PBR) as a function of concentration c_x were fitted using Eq. 11, 13 and 15, for different incident light intensities. Results gave a value of

E_a = 206 m^2 kg^{-1} at 150 µmol $m^{-2}s^{-1}$ (used also for winter conditions) and of 85 m^2 kg^{-1} at 650 µmol $m^{-2}s^{-1}$ (used also for summer irradiation).

A parameter of crucial importance is the maintenance coefficient μ_e, which represents the negative contribution to the net growth rate, taking into account the energy required for all non-growth pathways involved in respiration, cell turnover and repair and homeostatic maintenance. Sforza et al. (Sforza et al., 2014c) studied the maintenance energy requirement of *S. obliquus* under different light intensities and regimes, and the values there reported as a function of operating conditions were used in this work.

The half-saturation constant *K* parameter is normally estimated through oxygen evolution rate or fluorescence measurements as a function of light intensity (the so-called PI curve) (Takache et al., 2012), or alternatively by measuring the specific growth rate (d^{-1}) at different light intensities (Posten, 2009). The values found in the literature usually range between 70 and 200 µmol $m^{-2}s^{-1}$ (Muñoz-Tamayo et al., 2013; Pruvost et al., 2011a, 2011b; Takache et al., 2012). Nonetheless, these measurements are often conducted on cells grown in batch cultures. However, from the physiological point of view, working in batch mode does not allow to take into account the possible effect of long-term acclimation to light conditions. On the other hand, when considering continuous cultures at steady-state, where microalgal cells are actively acclimated to the environmental conditions, it would probably be more appropriate to plot the "maximum specific growth rate", obtained following the wash-out method as described by Molin (Molin, 1983), as a function of light intensity. In this chapter, the value of *K* was fitted in order to reproduce the productivity profiles measured experimentally, and it resulted to be 325 µmol $m^{-2}s^{-1}$. This value is also in agreement with productivity values obtained from continuous experiments carried out with *S. obliquus* at different light intensities (τ = 0.9 d), and shown in Figure 2.2: it can be clearly seen that photosaturation and inhibition occur at irradiances higher than 650 µmol $m^{-2}s^{-1}$. This is compatible with the hypothesis of an acclimated culture, even though it appears higher compared to the ones found in the current literature. All the parameter values specified above are summarized in Table 2.1.

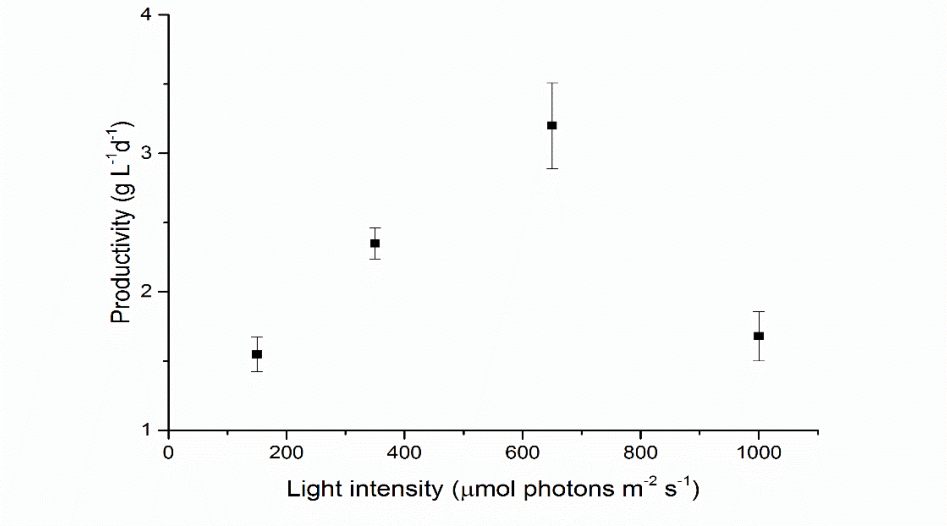

Figure 2.2 *Productivity of S. obliquus as a function of the light intensity*

Table 2.1 *Summary of parameters values in the model (S.obliquus)*

Parameter	Unit of measure	Value
K	μmol $m^{-2}s^{-1}$	325
ρ_m	-	0.8
Φ	kg μmol^{-1}	$2.84 \cdot 10^{-9}$
bE_s	m^2 kg^{-1}	4.25
E_a	m^2 kg^{-1}	206 (150 μmol $m^{-2}s^{-1}$, winter)
		85 (650 μmol $m^{-2}s^{-1}$, summer)
μ_e	d^{-1}	0.181 (150 μmol $m^{-2}s^{-1}$)
		0.517 (650 μmol $m^{-2}s^{-1}$)
		0.185 (winter)
		0.673 ummer)

2.4. Results and discussion

2.4.1. Constant light intensity

First of all, a CSTR photobioreactor with a depth of 1.2 cm, corresponding to that of the experimental apparatus, at two constant light intensities of 150 μmol $m^{-2}s^{-1}$ and 650 μmol $m^{-2}s^{-1}$ (PAR) is considered. The first irradiance value was chosen as it is the one at which growth rate is maximum (Gris et al., 2013), while the second one is representative for high

illuminations. To reproduce experimental measurements conditions, θ was set equal to zero, and only the direct irradiance contribution was taken into account. Fig. 2.3 A and B show the measured biomass concentration and productivity as a function of the space-time, while in Fig. 2.4 productivity is plotted versus concentration. Increasing the residence time the concentration increases as well, but the increase results to be less than linear. When considering the productivity, an optimum condition at which its value is maximum is clearly identified. In fact, when a constant illumination is provided to the PBR surface, the following theoretical criterion has been proposed to ensure maximum productivity: the irradiance value at the bottom of the reactor ($z = H$) should be equal to the compensation point for photosynthesis (G_c) of the microorganism considered. G_c is defined as the irradiance above which there is a positive net growth rate (Takache et al., 2012, 2010). There is only one concentration c_x that allows $I(H) = G_c$, and this corresponds to the optimal biomass concentration $c_{x,opt}$ which maximizes productivity. In fact, at concentrations lower than $c_{x,opt}$ part of the photons are not absorbed and are not used for photosynthesis, leading to a loss of efficiency; on the other hand, concentration values higher than $c_{x,opt}$ mean that a dark zone is present in the PBR, where respiration becomes more relevant than photosynthesis, leading to productivity losses as well (Grobbelaar, 2006; Vonshak et al., 1982). This results in the existence of an optimum value of τ at which the PBR should be operated to satisfy the compensation condition.

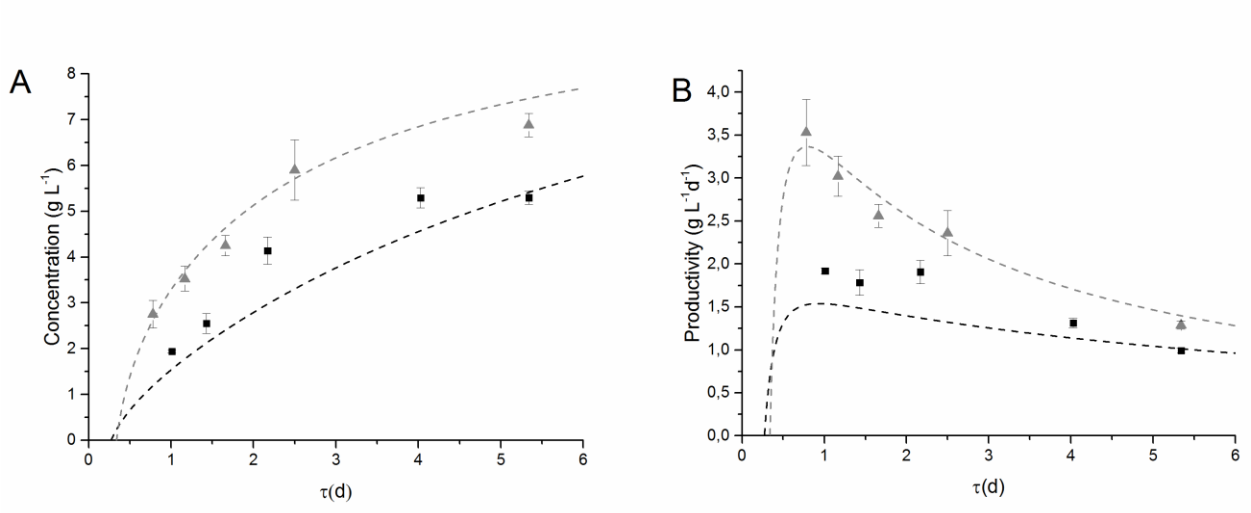

Figure 2.3 *Biomass concentration (A) and productivity (B) as a function of residence time τ for a CSTR-PBR with constant light intensity of 150 µmol $m^{-2}s^{-1}$ (black) and 650 µmol $m^{-2}s^{-1}$(grey). Dots correspond to experimental data, while lines are the output of the simulations.*

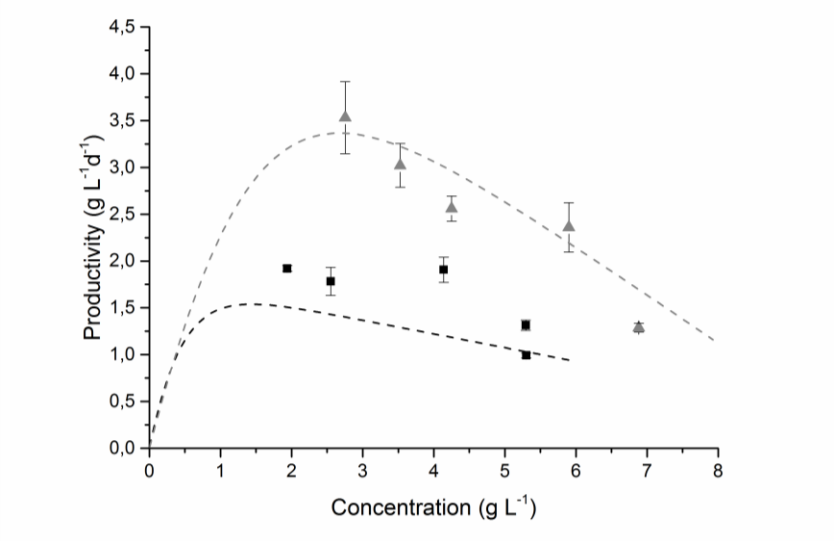

Figure 2.4 *Biomass productivity as a function of concentration for a constant light intensity of 150 µmol $m^{-2}s^{-1}$(black) and 650 µmol $m^{-2}s^{-1}$(grey). Dots correspond to experimental data, while lines are the output of the simulations*

Clearly, the optimum operating conditions depend on the PBR depth. Table 2.2 summarizes the results obtained computationally setting different values of *H*, ranging from 1 cm to 10 cm, for both of the irradiances considered: for each condition investigated, the optimal concentration can be determined, the compensation criterion verified, and the optimum photoconversion efficiency calculated accordingly. When the reactor depth increases, the optimal biomass concentration gets lower, so as to allow the light to be properly absorbed throughout the whole thickness. The optimal residence time that allows to have $c_{x,opt}$, however, does not change with *H*, and is equal to 0.93 d at 150 µmol $m^{-2}s^{-1}$ and to 0.79 d at 650 µmol $m^{-2}s^{-1}$. It is worth noting that at z = *H* the net biomass growth rate results to be around zero (i.e. the photosynthetic production rate is equal to the maintenance rate), meaning that at optimum conditions the compensation criterion is satisfied. In particular, the irradiance value at the PBR bottom was found to be equal to 3.63 ± 0.083 µmol $m^{-2}s^{-1}$ for an incident *PFD* of 150 µmol $m^{-2}s^{-1}$, and 33.2 ± 0.17 µmol $m^{-2}s^{-1}$ at 650 µmol $m^{-2}s^{-1}$. The irradiance of compensation G_c is different in the two cases, as the maintenance rate changes as well. Interestingly, even though biomass concentration and volumetric productivity depend on the reactor depth, the optimum photosynthetic efficiency results to be independent of it.

Table 2.2 *Optimum working conditions at different reactor depth values*

I [μmol m^{-2} s^{-1}]	H [cm]	P_x [g L^{-1} d^{-1}]	$C_{x,opt}$ [g L^{-1}]	$r_{x,growth}$ (H) [g L^{-1} d^{-1}]	$r_{x,main}$(H) [g L^{-1} d^{-1}]	r_x (H) [g L^{-1} d^{-1}]	Irr (H) [μmol m^{-2} s^{-1}]	η_{opt} [%]
150	**1**	1.85	1.720	0.247	-0.2526	-0.0056	3.59	16.09
150	**1.2**	1.54	1.430	0.2071	-0.21	-0.0029	3.62	16.10
150	**5**	0.37	0.345	0.049	-0.0507	-0.0017	3.55	16.09
150	**10**	0.18	0.170	0.0255	-0.025	0.0005	3.75	16.11
650	**1**	4.04	3.21	1.607	-1.6596	-0.0526	33.06	8.38
650	**1.2**	3.37	2.675	1.3392	-1.383	-0.0438	33.06	8.38
650	**5**	0.81	0.64	0.323	-0.3309	-0.0079	33.35	8.39
650	**10**	0.405	0.32	0.1615	-0.1654	-0.0039	33.35	8.39

In particular, its value is found equal to 16.10 ± 0.01 % and 8.38 ± 0.003 % of PAR at 150 and 650 μmol $m^{-2}s^{-1}$ respectively, corresponding to 6.92% and 3.60% of total incoming radiation. From Table 2.2 it can also be noticed that at high intensities, even if the biomass concentration and productivity increase, the photosynthetic efficiency drops considerably, due to photosaturation and photoinhibition phenomena. In addition, although the volumetric productivity P_x decreases with an increase in H, the areal productivity:

$$P_{x,A} = P_x \cdot H \qquad \text{(Eq. 2.21)}$$

is constant. Therefore, changing the reactor depth does not affect the PBR optimal performances in terms of efficiency, areal productivity, and optimum τ, even though the reactor outlet biomass concentration is different: however, this last variable is relevant for downstream operations (separation and drying).

When considering large-scale applications, a perfectly mixed system with a homogeneous concentration would be quite difficult to achieve. An axial dispersion reactor with intermediate axial mixing seems more appropriate, so that a variation in biomass concentration along the length of the reactor is found (assuming perfect mixing in the cross-section due to CO_2 bubbling). By modeling this reactor with a Plug-Flow Reactor plus recycle system, simulations have been performed and compared to the CSTR ones, considering a reactor depth of 1.2 cm. The results summarized in Fig. 2.5 show that the volumetric productivity has a similar trend as in the case of the perfectly mixed system, and optimum operating conditions can be

identified for each extent of mixing, even though the compensation criterion cannot be matched in this case, as the biomass concentration increases along the PBR length. However, the lower the axial mixing (i.e. the recycle ratio), the lower is the maximum productivity that can be achieved, and therefore the PBR performances. In addition, the PBR needs to be operated at higher values of τ to avoid wash-out of microalgal biomass from the cultivation system. Nonetheless, when using a recycle ratio equal to 3, the performances become highly comparable to those of the CSTR (reported in Table 2.2), with a maximum productivity of 1.54 g L^{-1} d^{-1} at τ = 1d under an incident irradiance of 150 µmol $m^{-2}s^{-1}$ and 3.352 g L^{-1} d^{-1} at τ = 0.88 d under 650 µmol $m^{-2}s^{-1}$. Therefore, choosing a proper value of *R*, any extent of axial mixing can be reproduced, from completely mixed to fully segregated.

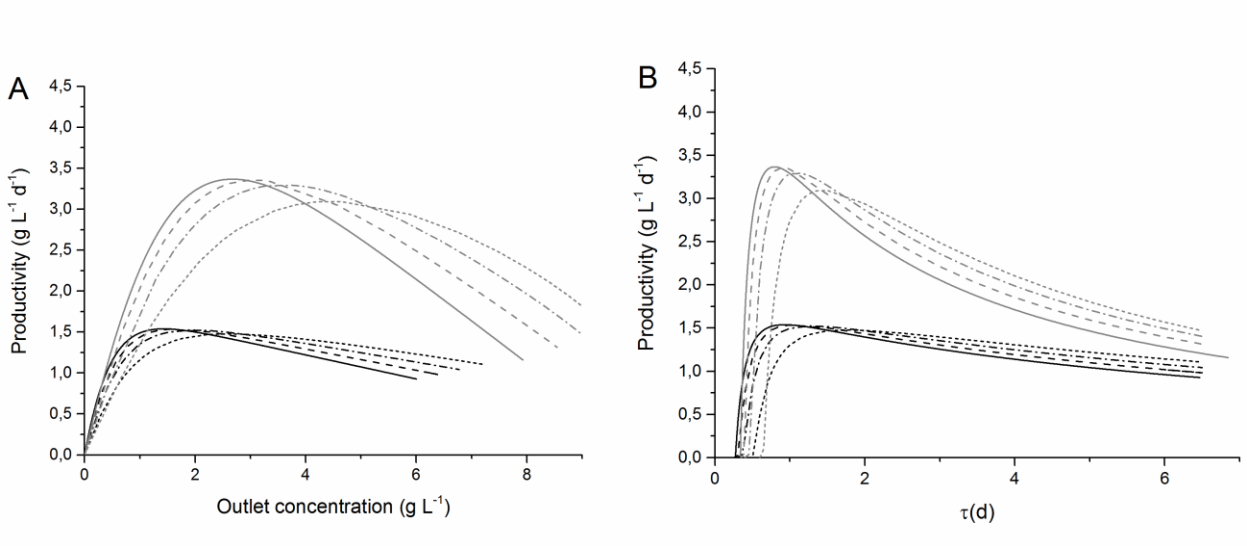

Figure 2.5 *Volumetric productivity as a function of outlet concentration (A) and residence time (B) at different mixing conditions and light intensities (black for 150 µmol $m^{-2}s^{-1}$ and grey for 650 µmol $m^{-2}s^{-1}$). Continuous lines represent CSTR, dashed lines the PFR with R = 3, dash dot lines PFR with R = 1, and dotted lines PFR with R = 0.3*

When considering the photosynthetic efficiency, a maximum value is reached in correspondence of the optimal space-time (Fig.2.6). It appears that axial mixing conditions affect this parameter in a more severe way compared to productivity: the optimum values drop from 16.1% to 14.4% of PAR for a recycle ratio equal to 3, and to 9.77% when R = 0.3 at 150 µmol $m^{-2}s^{-1}$, and the same trend is observed at 650 µmol $m^{-2}s^{-1}$. This is likely due to the fact that in this case the photoconversion efficiency is averaged, as the occurrence of a

concentration profile along the PBR length does not allow full light absorption throughout the whole system, and part of the inlet radiation energy is wasted. Interestingly, the residence time affects not only the efficiency of exploitation of light, as calculated in Eq. 2.4, but also the efficiency of light capture, obtained by calculating the ratio of biomass produced on incident light provided. The efficiency of light capture as a function of residence time is reported in Fig. 2.7 for the case of CSTR, as an example. It appears that, at higher values of τ, when the biomass concentration increases, all the light is absorbed, and the efficiency of light exploitation is equal to that of light capture. At low values of τ instead there is a loss of light through the culture, due to the lower biomass concentration, and the efficiency of light capture is lower.

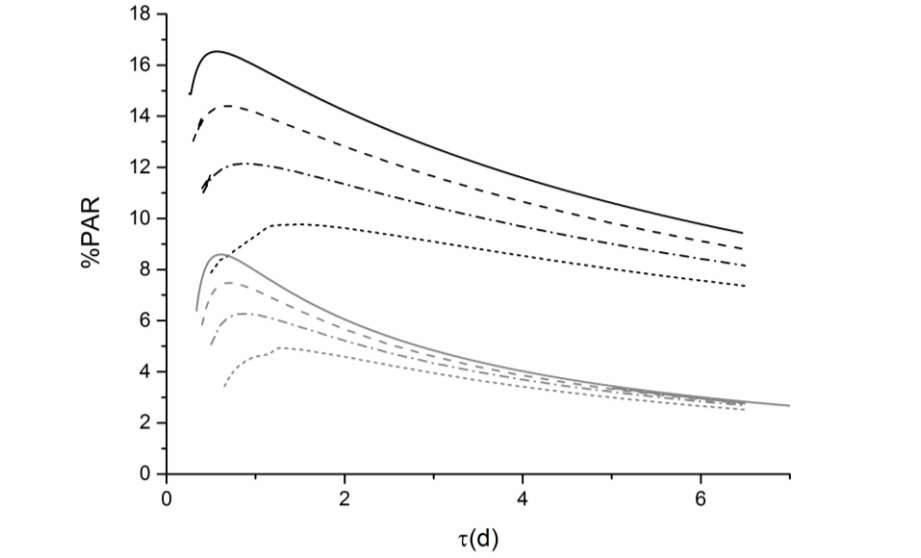

Figure 2.6 *Photosynthetic efficiency referred to PAR as a function of τ at different mixing conditions and light intensities (black for 150 µmol $m^{-2}s^{-1}$ and grey for 650 µmol $m^{-2}s^{-1}$). Continuous lines represent CSTR, dashed lines the PFR with R = 3, dash dot lines PFR with R = 1, and dotted lines PFR with R = 0.3*

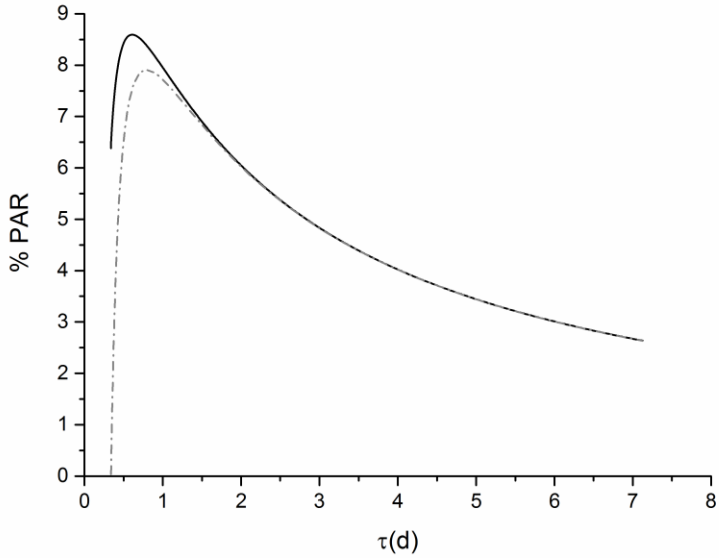

Figure 2.7 *Comparison between photosynthetic efficiency calculated on absorbed light (black continuous light) and on incident light (grey dashed line), for a CSTR photobioreactor at 650 µmol* m^{-2} s^{-1}

At the optimum, the efficiency referred to the irradiated light is slightly lower, but not significantly, since the compensation irradiance is not high.

Most importantly, it is clear that in order to achieve the maximum volumetric productivity and photoconversion efficiency possible, the cultivation system has to be operated in quite a narrow range of residence times close to the optimum, otherwise the performances drop consistently from both points of view.

2.4.2. Day-night irradiation

Investigating the behavior of PBRs under constant artificial light is helpful to understand the effect of operating parameters on the performances, and it provides useful information. Clearly, when considering an industrial application, the only feasible possibility is exploiting the radiation coming from the sun, hence with a variable light intensity profile during the day and at different times of the year. Defining a criterion for optimizing the PBR performances is not straightforward, due to the dynamic behavior of the system: even when considering a CSTR, the compensation condition cannot be achieved throughout the day, as it would require

microalgal dynamics to immediately adapt to the change in light intensity (Cuaresma et al., 2011). However, Munoz-Tamayo et al. (Muñoz-Tamayo et al., 2013) showed that operating the PBR at a suitable and constant flow-rate (i.e. as a chemostat) it is possible to obtain high productivities. Obviously, the value of the flow-rate needs to be optimized, as a wrong choice would lead to a severe drop in the performances.

In this chapter a horizontal flat-panel PBR located in Padova, Italy was simulated. Irradiation data for a typical day of January and July, representative of winter and summer respectively, at this specific location were retrieved from PVGIS Solar Irradiation Data (http://re.jrc.ec.europa.eu/pvgis/). The profile of total, diffuse and beam radiation is shown in Fig. 2.8 A and B for the two seasons. As it can be seen, the diffuse contribution plays a significant role during the winter season. Data reported are referred to the entire solar spectrum, but since only the PAR (400-700 nm), which accounts for about 43% of the total range, can be used by algae for photosynthesis, irradiance values used in Eq. 2.12 and Eq. 2.13 were corrected accordingly. According to Table 2.1, model parameters, except for the maintenance one, are the same as for the constant light simulations, which refer to 23°C.

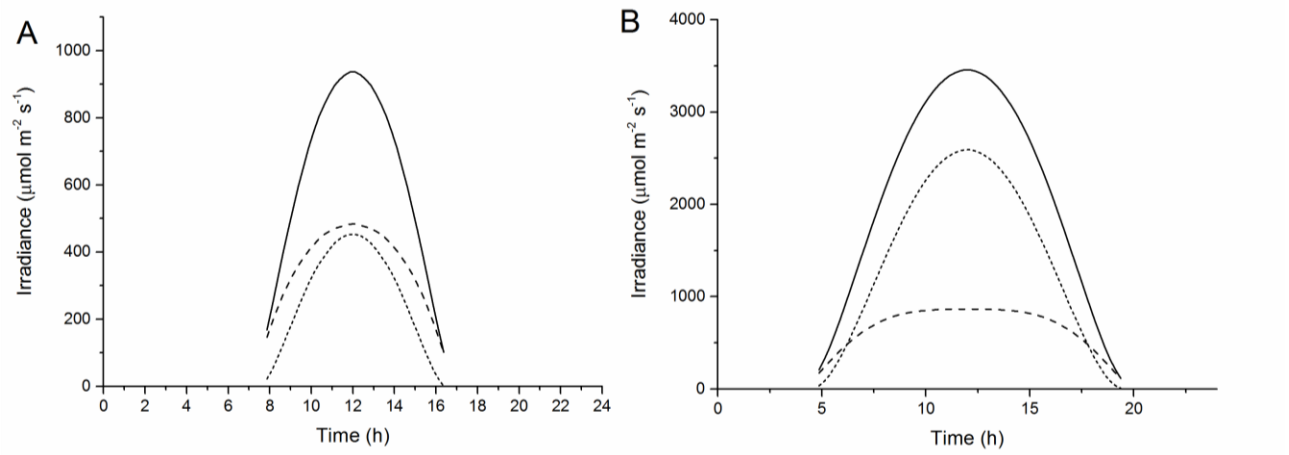

Figure 2.8 *Irradiance profiles of beam (dotted line), diffuse (dashed line) and total (continuous line) radiation for a typical winter (A) and summer (B) day on a horizontal surface in Padova, Italy*

So, both for winter and summer conditions, the reactor temperature was kept equal to 23°C, assuming that the PBR is equipped with a suitable temperature control system.

Fig. 2.9 shows the outlet concentration profile during time obtained for a CSTR PBR, operating at a residence time of τ = 1 d, for the winter and summer season, respectively.

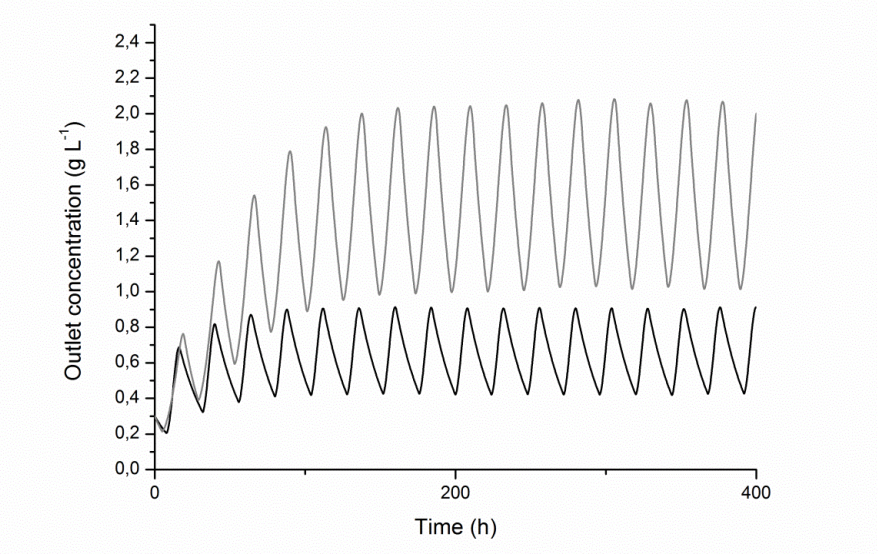

Figure 2.9 *Biomass concentration as a function of time for a CSTR-PBR at τ = 1d, grey for summer and black for winter*

These profiles reproduce the oscillatory trend of the irradiance, and achieve a cyclic steady state. The variations are significantly more relevant during summer (>1 g L^{-1}), mainly due to the much higher maintenance rate exhibited in this condition, but the average value is more than double with respect to winter. Anyway, in the latter case, the light period is shorter and the average daily irradiance is lower with respect to summer, as well as the angle of incidence of the beam radiation, which is less favorable. Simulations were performed at different values of τ, with the aim of determining which is the optimum value to achieve the maximum average productivity and photosynthetic efficiency. Also in the case of day-night light, the effect of recycle ratio values were simulated and compared to the CSTR situation (Fig. 2.10). Here, the trend of the average volumetric productivity in the two seasons and for the different mixing conditions is shown. These plots are similar to the case of constant light intensity, highlighting the existence of an optimum value of residence time. Again, a decrease of axial mixing worsens the PBR performances, but operating with a recycle ratio equal to 3 is sufficiently close to a perfectly mixed system. In this case, τ_{opt} results to be about 1.25 d in summer, and 1 d in winter.

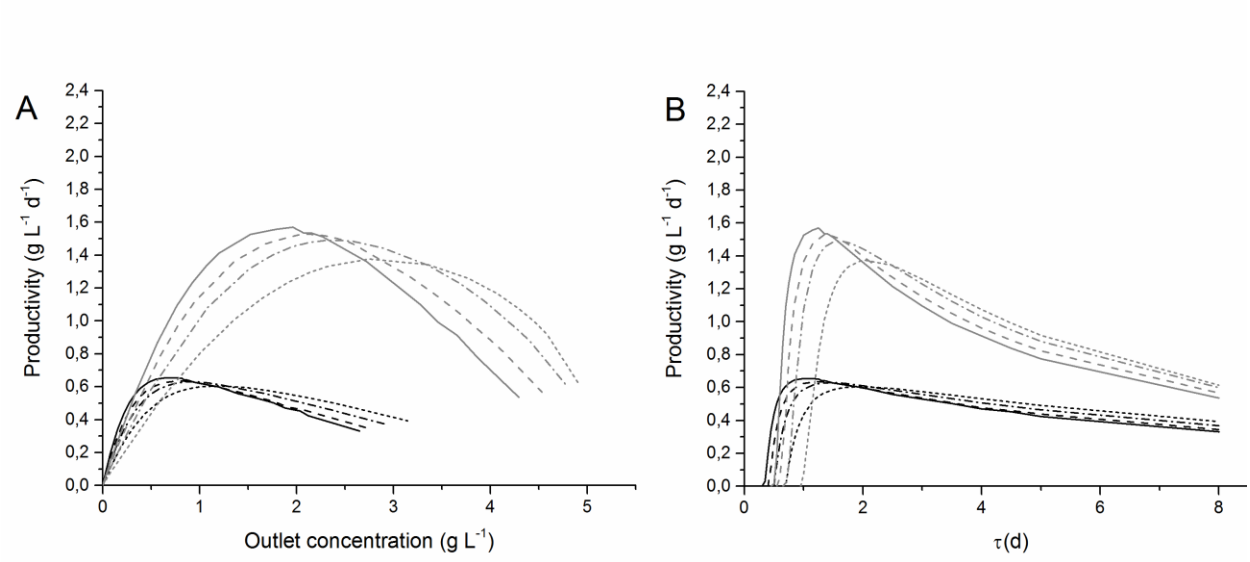

Figure 2.10 *Average biomass productivity as a function of outlet concentration (A) and residence time τ (B) for different mixing conditions and different seasons (black for winter and grey for summer). Continuous lines represent CSTR, dashed lines the PFR with R = 3, dash dot lines PFR with R = 1, and dotted lines PFR with R = 0.3*

Apparently, the optimum operating conditions change along the year, due to the seasonal variation in sunlight, so that the PBR should be operated accordingly.

It is worth noticing that, even if the amount of photons per day is comparable to the constant light intensities investigated (560 μmol m^{-2} s^{-1} in summer versus constant 650 μmol m^{-2} s^{-1} and 100 μmol m^{-2} s^{-1} in winter versus constant 150 μmol m^{-2} s^{-1}), the maximum productivity is considerably lower in outdoor irradiation conditions, with values of 1.57 g L^{-1} d^{-1} in summer and 0.66 g $L^{-1}d^{-1}$ in winter, compared to 3.37 g $L^{-1}d^{-1}$ and 1.54 g $L^{-1}d^{-1}$ at constant 650 and 150 μmol m^{-2} s^{-1} respectively (CSTR). In fact, in the first case the irradiance value is averaged between very high light intensities during the day, with values up to 1500 μmol m^{-2} s^{-1} in summer, and long dark periods, both of which affect the growth negatively. Also the fact that radiation is divided into a direct and a diffuse component, and that the angle of incidence of the former is generally not normal to the PBR surface have a negative impact on the performances.

Figure 2.11 shows the comparison between experimental data and the volumetric productivities simulated under summer and winter light conditions in the laboratory (where the whole radiation can be considered as beam radiation, and $\theta = 0$), for a CSTR configuration.

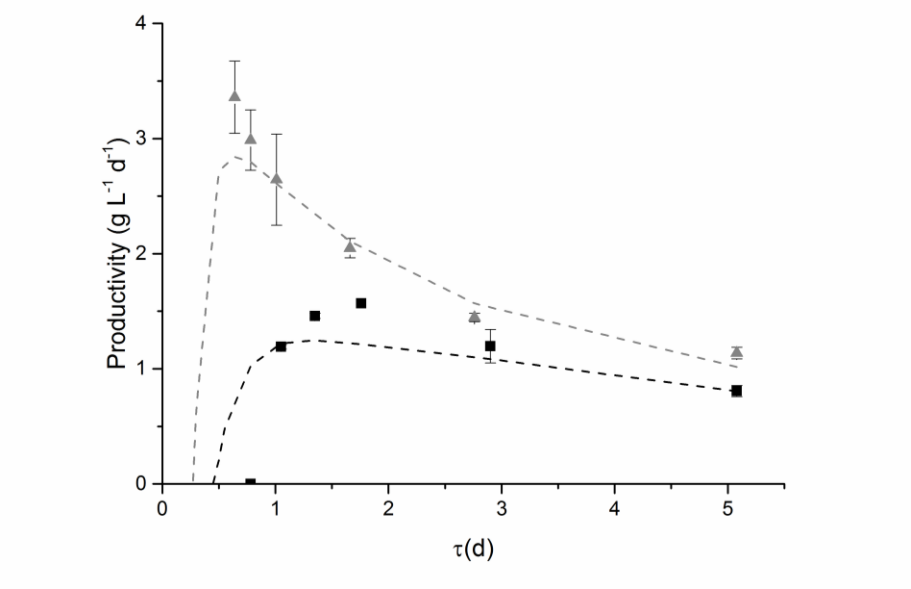

Figure 2.11 *Volumetric productivity as a function of τ for the summer (grey) and winter (black) seasons. Dots and triangles represent experimental data, and dashed line simulations under laboratory conditions (beam radiation and θ=0)*

Finally, it is interesting to consider also the average photosynthetic efficiency of the system. In the case of outdoor irradiation conditions it results to be quite lower with respect to that obtained at constant light intensities (Fig. 2.12).

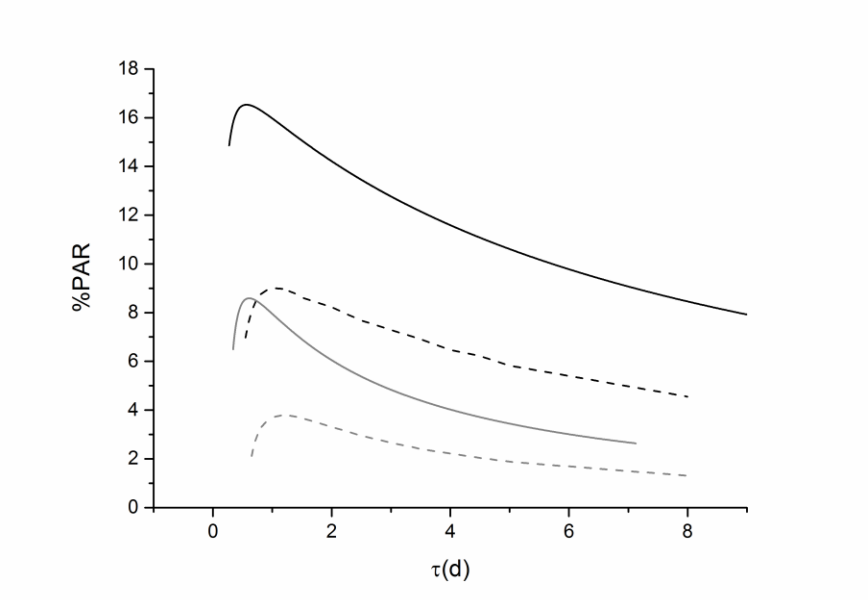

Figure 2.12 *Photosynthetic efficiency of CSTR photobioreactor operated under constant light intensities (continuos lines, black for 150 μmol m^{-2} s^{-1} and grey for 650 μmol m^{-2} s^{-1}) or outdoor day-night conditions (dashed lines, black for winter and grey for summer)*

This stresses the importance of operating the PBR under proper values of τ, to reach the maximum performances allowed, and avoid further losses. The discussion presented in this chapter highlights how the design and operation of an outdoor PBR is quite a complicated task. The approach developed provides useful hints for the design of industrial flat-plate PBRs for large-scale microalgae production, as far as the residence time and the effect of axial mixing are concerned.

2.5. Final remarks

In this chapter the growth of *Scenedesmus obliquus* in a continuous flat-panel PBR was considered, both from experimental and modeling point of view, with the attempt of defining suitable operating conditions to achieve the maximum performances in terms of biomass productivity and photosynthetic efficiency. Both low and high irradiance values were investigated, with constant illumination as well as day-night cycles, according to actual solar irradiation conditions.

A simple simulation model was developed, and experimental data were used to evaluate model parameters. The extent of axial mixing was also taken into consideration, by changing the recycle ratio in a plug flow reactor plus recycle model.

Results obtained show that laboratory data can be reproduced satisfactorily by the model. An optimum value of the residence time to obtain maximum productivity and photosynthetic efficiency was evidenced. Simulation showed that the PBR needs to be operated in a narrow range of τ close to the optimum, otherwise the performances drop considerably, especially close to washout. A reduction in axial mixing was found to worsen the performances, requiring higher residence times and achieving lower productivities, but a recycle ratio $R = 3$ allows to be sufficiently close to a CSTR condition.

The model was able to predict experimental data also when the outdoor irradiation conditions were investigated. In this case, the overall performances of the PBR are severely affected, since an efficient light utilization is made difficult by the dynamic nature of solar radiation, the presence of long dark periods, and non-optimal light incidence angles. The results obtained in this chapter can provide useful hints for the design of industrial flat-plate PBR s for large-scale microalgae production.

Chapter 3

Improving light utilization and photoconversion efficiency: integrated photovoltaic-photobioreactors for microalgal cultivation

One of the main limitations to outdoor large-scale production of biofuels derived from microalgae is the low efficiency of sunlight energy conversion. The maximum theoretical value for photosynthetic efficiency is hardly achieved in real outdoor cultivation systems, mainly due to inefficient light utilization, in addition to photosaturation and photoinhibition phenomena that take place at high irradiances. This chapter is focused on testing different possibilities aimed at improving the overall photoconversion efficiency of microalgal production in photobioreactors. Two strategies were followed: the first one increases the portion of spectrum available for photosynthesis employing luminescent spectral-converter filters on the photobioreactor surface, the second one integrates microalgae reactors with photovoltaic panels, producing electrical energy together with biomass. In the latter case, different photovoltaic technologies (standard Si modules and novel organic dye-sensitized solar cells) were tested. Experiments were carried out both in batch and continuous laboratory scale flat-plate photobioreactors, at different light intensities and regimes, with two different species (*Nannochloropsis salina* and *Scenedesmus obliquus*), measuring the growth rate, pigment content, biomass concentration and photosynthetic efficiency. Results show that spectral-converters do not substantially improve the growth rate, while an integrated PV and PBR system could be a valid way to improve energy conversion performances.

[0]Part of this chapter was published in Algal Research (Sforza E., Barbera E., Bertucco A., 2015. 10:202-209)

3.1. Introduction

The growing demand for liquid fuels, which is expected to increase quite fast in the next decades, has driven research efforts into the development of numerous biofuels production technologies. Even though the oil price is recently dropped, due to the exploitation of shale oil and shale gas (Maugeri, 2013), this is a contingent occurrence which cannot face the long term demand for renewable energy sources to produce liquid fuels, and does not solve environmental issues. Among renewable sources, biofuels derived from the cultivation of microalgal biomass are worldwide recognized as a very promising sustainable alternative energy source that aims at replacing traditional fossil fuels (Driver et al., 2014). Nonetheless, despite the many advantages that microalgae offer compared to terrestrial crops, many factors still limit the feasibility of a competitive large-scale production facility, so that a sustainable algal biofuel industry is considered at least one or two decades away from maturity (Chisti, 2013). One of the main limits is the low photosynthetic efficiency (PE), which results also in a negative net energy balance of the process.

A key factor concerning autotrophic microalgal cultivation is played by light availability and utilization (Carvalho et al., 2011). In fact, in view of an outdoor cultivation system, the main constraint to microalgae productivity is sunlight availability, which depends on location and other climatic factors (Quinn et al., 2011). It is evident that, in order to achieve massive algal productions, an autotrophic photobioreactor needs to have a large light-exposed surface. However, even if increasing surface results in a greater overall production, the energetic and economic costs can only be reduced by improving light use efficiency. For sunlight it has been estimated that the maximum theoretical efficiency of energy conversion (i.e. the fraction of light energy that is converted into biomass through photosynthesis) is about 11-12% (Blankenship et al., 2011). Nonetheless, microalgae are in fact not able to absorb all the incoming energy and to convert all the harvested radiation into biomass, and actual photoconversion efficiencies drop to values which are usually about 3% of the total light received (Chisti, 2013).

Photosynthesis depends on the absorption of light by pigments, the most important of which is Chlorophyll-A (Chl-A), but several accessory pigments contribute to increase the spectral range absorbed as well. However, one of the main critical factors lowering the photosynthetic

efficiency is the limited absorption of the incident sunlight: of the whole solar radiation spectrum, only about 43% is Photosynthetically Active Radiation (PAR, ranging from 400 to 700 nm) (McCree, 1972) that can be utilized by algae for photosynthesis. Moreover, only the blue and red wavelengths of the visible range (which constitutes the PAR) are generally absorbed and utilized for photosynthesis, while the green and yellow wavelengths are reflected. To overcome this issue, luminescent PBR design for improved algal growth and photosynthetic pigment production through spectral conversion of light was recently proposed, where luminescent acrylic PBRs in blue, green, yellow, orange, and red colors capable of spectral conversion of light are used (Mohsenpour and Willoughby, 2013). However, it is not clear yet if the exploitation of these filters may result in an overall increase of biomass productivity, in particular when light intensity is varying along with time as it occurs for sunlight.

In a second place, while a low irradiation is limiting, its excess leads to the formation of reactive oxygen species (ROS) that have an inhibitory effect on growth (the so-called photosaturation and photoinhibition phenomena). Therefore, when exposed to the high irradiances of sunlight, photosystems are not able to process the high flow rate of photons received. If photosynthesis is inefficient, the excess of light energy is dissipated as heat or as chlorophyll fluorescence to avoid damaging the photosynthetic apparatus, resulting again in an additional reduction of photoconversion efficiency.

In this chapter, two strategies are investigated to improve the light energy conversion in photobioreactors: i) increasing the portion of spectrum available for photosynthesis, ii) integrating microalgae photobioreactor (PBR) with photovoltaic (PV) technology. In the first case, focus was given to the possibility of increasing light capture by employing a commercially available red spectral-converter filter on the PBR surface. Such a filter is able to absorb the green wavelengths and shift this radiation to the red range, potentially enhancing the total amount of photons that algae are able to utilize, which could result in increased productivity in the case of light-limited conditions.

On the other hand, an integrated photovoltaic-photobioreactor (PV-PBR) approach might increase the overall photoconversion efficiency of the whole cultivation system, by producing directly available electrical energy together with microalgal biomass. The idea of combining photovoltaics with microalgal growth in order to better exploit incoming photons has received much attention in the last years, as also proposed by Bernard et al. (Bernard et al., 2015), and

a number of applications have recently been studied also by other authors. For instance, Parlevliet and Moheimani (Parlevliet and Moheimani, 2014) proposed to apply a particular filter above the algal culture which transmits only certain wavebands, while the others are redirected to a solar cell for electricity production. Detweiler et al. (Detweiler et al., 2015) tested the effect of wavelength selective luminescent solar concentrators (LSC), applied to greenhouse roofs, on microalgal growth. These systems are able to absorb certain wavelengths and to re-emit them as longer ones, part of which are then guided within the panel and concentrated onto solar cells for electricity production, while the remaining are transmitted to the culture, reducing photoinhibition phenomena. However, in the open literature, preliminary experimental results only are available, and more efforts are required to ascertain the actual possibility to grow microalgae in such a combined system, from both an experimental and economical point of view.

Two different photovoltaic technologies are tested in this chapter: in the first case, the front surface of a flat PBR is partially covered with standard and low-cost silicon photovoltaic cells: if the PV cells are placed with a proper geometry, this could be beneficial to avoid or reduce photoihibition phenomena, exploiting the positive effect of high frequencies light-dark cycles (Gutierrez-Wing et al., 2012; Liao et al., 2014; Vejrazka et al., 2012). Secondly, a novel semi-transparent “orange”-dye sensitized solar cells module (DSC) is directly placed onto the whole irradiated surface of the PBR: such a PV module absorbs a limited range of wavelengths, allowing to produce electricity, while the rest of the light is transmitted through the PBR walls and is used by algal cells for photosynthesis.

Two microalgal species, *Nannochloropsis salina* (marine species) and *Scenedesmus obliquus* (freshwater species) were cultivated in both batch and continuous laboratory scale flat-panel PBRs, to test the performances of the solutions proposed in terms of biomass productivity and energy conversion efficiency.

3.2. Materials and methods

3.2.1. Algae strains and culture media

Nannochloropsis salina, strain no. 40.85 (obtained from SAG-Goettingen, Germany) was maintained and cultivated in f/2 medium, with 33 g L^{-1} sea salts (Sigma-Aldrich), buffered with 40 mM TRIS HCl pH 8, modified with a non-limiting nitrogen concentration (1.5 g L^{-1} $NaNO_3$). *Scenedesmus obliquus* 276.7 (SAG) was cultivated in BG11 medium, buffered with 10 mM HEPES pH 8. For continuous experiments, BG11 and f/2 media were modified to guarantee non-limiting nutrient conditions (3 g L^{-1} $NaNO_3$ and 500 mg L^{-1} K_2HPO_4 in the case of BG11, 1.5 g L^{-1} $NaNO_3$ and 25 mg L^{-1} of $Na_2HPO_4 \cdot H_2O$ in f/2), and focus on the effect of light only.

Pre-inoculum of both species were grown at 100-120 µmol of photons m^{-2} s^{-1}, provided by fluorescence lamps. The culture media and all the materials were sterilized in an autoclave at 121°C for 20 min in order to prevent any contamination.

3.2.2. Experimental set-up

The experiments were conducted both in batch and continuous mode, in flat-panel polycarbonate (PC) PBRs to maximize light utilization (Sforza et al., 2014a). Reactors were exposed to different constant light intensities, ranging from 50 to 1000 µmol m^{-2} s^{-1} of PAR, and to alternated dark-light cycles to mimic outdoor irradiation conditions. Light was provided by a LED lamp (Photon System Instruments, SN-SL 3500-22, warm white color, with a spectral emission range from 400 to 780 nm). For day-night experiments, the LED lamp was set to reproduce the profile of PAR irradiation of a typical summer day in the location of Padova, Italy. Irradiation data were taken from PVGIS Solar Irradiation Data (http://re.jrc.ec.europa.eu/pvgis/), and the month of July was selected as representative of the summer season. Photon flux density (PFD) at the reactor front surface and at the back was measured with a photoradiometer (HD 2101.1 from Delta OHM), which quantifies the PAR. All experiments were carried out in a refrigerated incubator, and the temperature was kept constant at 23 ± 1°C which is suitable for both the species investigated. Excess CO_2 (5% v/v mixed with air, regulated by two flow-meters) was supplied from a sparger placed at the bottom

of the reactor, at a total gas flow-rate of 1 L h^{-1}. CO_2 bubbling also ensured culture mixing, which for *S. obliquus* runs was supplemented by the use of a stirring magnet.

In batch experiments, *N. salina* was inoculated at an initial OD_{750} of 0.45, corresponding to a cell concentration of about 6 x 10^6 cells mL^{-1}, with a total reaction volume of 100 mL. The PBR had an irradiated surface of 125 cm^2 (10x12.5), and a thickness of 0.8 cm. *S. obliquus* was inoculated at initial OD_{750} of 0.5, which corresponds to a cell concentration of about 3 x 10^6 cell mL^{-1}. The reaction volume in this case was equal to 150 mL, in a PBR with equal irradiated surface (125 cm^2) but wider depth (1.2 cm).

In continuous experiments, fresh medium was continuously supplied at constant flow rate Q [mL d^{-1}] from an external sterilized and stirred bottle by means of a peristaltic pump (Sci-Q 400 , Watson Marlow, USA), and the reaction volume was kept constant by an overflow tube through which biomass outlet was withdrawn at the same flow rate. The residence time τ inside the reactor is thus controlled by the peristaltic pump, as it is calculated by:

$$\tau = \frac{V_R}{Q} \qquad \text{(Eq. 3.1)}$$

where V_R is the reaction volume [mL]. Such a system can be reasonably approximated as a Continuous-flow Stirred Tank Reactor (CSTR) (Bertucco et al., 2014). Different light intensities and regimes were used for these experiments. A transient period was observed after changing light conditions, after which a steady state could be reached and maintained for at least 5 days.

3.2.2.1 Spectral-converter

For experiments testing the efficiency of spectral conversion, a commercial product by PhotoFuel SAS (Paris, France) was used. The front PC plate was substituted with a red fluorescent polymethylmethacrylate (PMMA) plate modified with specially designed masterbatches and additives. The red spectral-converter was characterized in terms of absorption and emission spectra, using spectrophotometric and fluorimetric techniques (Cary Eclipse Varian spectrometer fluorometer).

3.2.2.2 PV-PBRs

Silicon PV-PBRs were realized applying flexible solar cells produced by PowerFilm onto the transparent PC front surface, with a measured PV photoconversion efficiency of about 5%; the PV panel (34 x 125 mm) was placed in the middle of the irradiated surface, so that through agitation algal cells moved continuously from illuminated to dark zones inside the reactor volume. The area covered by PV was equal to 1/3 of the total surface. In continuous experiments the surface exposed to light was equal to 222 cm^2 (12 x 18.5 cm), and the reaction volume was 320 mL in the case of *N. salina*, and 400 mL for *S. obliquus*. One third of the irradiated PV-PBR surface was covered with flexible solar cells (3.7 x 18.5 cm), as shown in Figure 3.1A

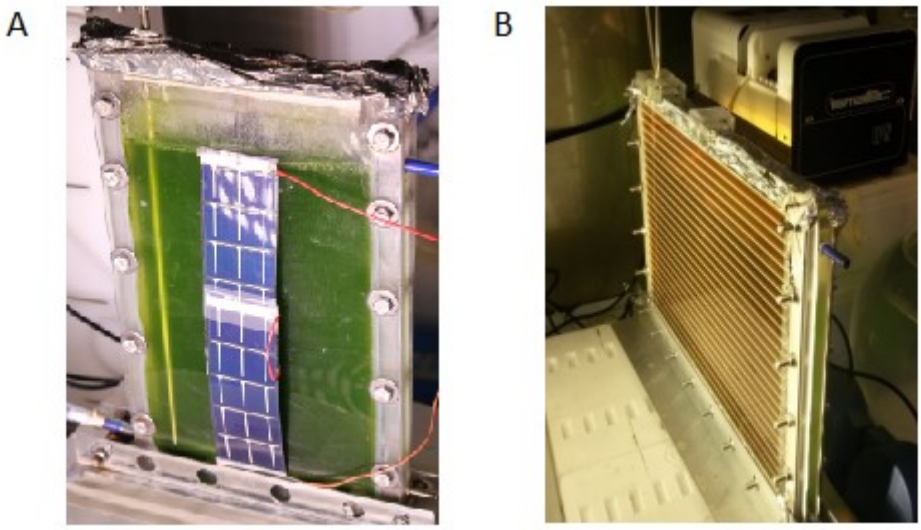

Figure 3.1 *PV-PBRs flat-plate reactors, with standard silicon PV cells (A) and with "orange" DSC (B)*

The other type of PV module tested is a dye sensitized cell (DSC) prototype made by Dyepower. This device is developed on A4-like (20x30) cm^2 conductive glass substrates (7 Ω/sq, 2.2 mm thick, fluorinated tin oxide (FTO) thin conductive oxide (TCO)). The module was composed by 24 cells connected in series with the Z-type connection (Giordano et al., 2013). Each cell was (0.55x29) cm^2 (width x length) and the interdistance among adjacent cells was 2.7 mm. The active area was realized by screen-printing a TiO_2 past, thus obtaining a 3

μm thick transparent titania layer. It was then sensitized with an "orange"-dye. Among several dyes and titania thickness available, those used were chosen in order to assure both good PV performances and high transparency in the wavelength range useful for the PBR. Counter-electrode was obtained by screen-printing a platinum catalysts. As electrolyte, a high stable formulation directly developed in Dyepower was used. The obtained device had different luminous transmittance (Tagliaferro et al., 2013) in the active and non-active regions (Figure 3.2). The equivalent human eye transparencies perceived were 36% and 69%, respectively. Since the active area occupies a 64% ratio of the total area, the total luminous transmittance was about 48%.

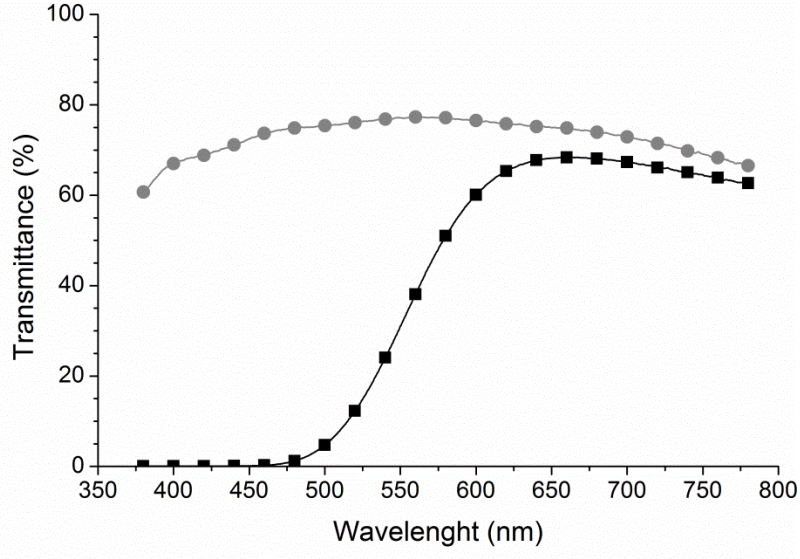

Figure 3.2 *Transmittance profiles of Dyepower DSC module, both of the active area with "orange"-dye (black, squares) and non-active area (grey, circles), performed via a spectrophotometer (Shimadzu UV-2700) in combination with a large sample compartment (Shimadzu MPC-2600)*

In this case, the photobioreactor depth was equal to 1.2 cm, and the irradiated surface measures 30 cm (length) and 19.5 cm (height), for a total culture volume of 700 mL, to match the dimension of the photovoltaic device. The semi-transparent photovoltaic module described was applied directly on the front PC surface of the PBR, covering it entirely (Figure 3.1B).

3.2.3. Analytical procedures

Algal growth in both batch and continuous experiments was monitored daily by measuring the optical density (OD) at 750 nm with a UV-visible UV 500 double beam spectrophotometer (from Spectronic Unicam, UK), correlated to cell concentration, measured with a Bürker Counting Chamber (HBG, Germany). Specific growth rates in batch experiments were calculated as the slope of the linear regression interpolating the logarithms of cell concentration during the exponential phase (tipically 5 or 6 days), taken as the average of two or three independent experiments. At the end of the growth curves, the final biomass concentration was measured as a dry weight (DW), in terms of g L^{-1}. DW was measured gravimetrically by filtering 5 mL of culture with 0.22 μm cellulose acetate filters, which are then dried for 2 h at 90°C in a laboratory oven. In the case of *N. salina*, the 5 mL sample was diluted 1:5 prior to filtration to dissolve salts, and a 0.45 μm filter was used. In continuous experiments biomass concentration in terms of DW was measured daily, and then averaged on 5 to 10 steady state experimental points. Productivity was then calculated from DW measurements, according to:

$$P_x = \frac{DW}{\tau} \qquad \text{(Eq.3.2)}$$

and also averaged on the corresponding number of steady-state experimental points.

Pigment content was determined during the exponential phase of batch experiments and at steady state in continuous ones for both species, following two different procedures. For *N. salina*, Chl-A and total Carotenoids (Car) were extracted from centrifuged cells with 100% N-N'-dimethylformamide, and stored for at least 48 hours in dark conditions at 4°C. In the case of *S. obliquus*, Chl A, Chl B and Car were extracted from 10 x 10^6 centrifuged cells with DMSO, after grinding with quartz powder and incubating at 65°C for 15 min (Gris et al., 2013). Pigment concentration was then evaluated spectrophotometrically by absorbance in the 350-750 nm range, using specific extinction coefficients (Wellburn, 1994).

The efficiency of Photosystems II, expressed as *Fv/Fm* parameter, was measured *in vivo* for batch experiments of *N. salina* at the same day of pigment analysis, using a Dual PAM 100 from WALZ, after 20 min of sample acclimation in dark conditions (Demmig-Adams et al., 1996).

3.2.4. Photoconversion efficiency evaluation

The photoconversion efficiency represents the fraction of light energy impinging the PBR surface that is converted into other energy outputs. When the PV modules are not applied on the front surface (transparent PBR, used as control), it corresponds to the photosynthetic efficiency (i.e. the percentage of radiant energy converted into energy-rich biomass through photosynthesis), and is calculated as:

$$\eta_{PAR} = \frac{DW \cdot Q \cdot LHV}{PFD_{in} \cdot E_p \cdot A_{PBR}} \quad \text{(Eq. 3.3)}$$

$$\eta_{TOT} = 0.476 \cdot \eta_{PAR} \quad \text{(Eq. 3.4)}$$

where LHV is the lower heating value of the dried biomass (assumed equal to 22 MJ kg^{-1}) (Sforza et al., 2015), PFD_{in} the PAR photon flux density hitting the reactor surface (μmol m^{-2} s^{-1}), E_p the energy of photons (J μmol^{-1}), and A_{PBR} is the irradiated surface of the photobioreactor (m^2). η_{PAR} and η_{TOT} represent the energy conversion efficiency referred to the PAR spectrum and to the AM1.5 global reference irradiance spectrum (defined in the *IEC 60904-3* international standard (*IEC 60904-3 (Ed. 2), Photovoltaic devices - Part 3: Measurement principles for terrestrial photovoltaic (PV) solar devices with reference spectral irradiance data.*, 2008)), respectively.

For PV-PBRs the total energy conversion is the sum of the contributions due both to biomass production and the electricity produced by the PV panel:

$$\eta_{PV-PBR} = \frac{(DW \cdot Q \cdot LHV) + (\varepsilon_{PV} \cdot I_{in} \cdot A_{PV})}{I_{in} \cdot A_{PBR}} \quad \text{(Eq. 3.5)}$$

where ε_{PV} and A_{PV} are respectively the efficiency and the surface of the PV panel, and I_{in} is the total irradiation hitting the photobioreactor [kW m^{-2}]. For silicon solar cells a base case was calculated by applying the experimental PV efficiency (5%). In the discussion, an efficiency ranging from 5% to 20% of the total spectrum was considered. The efficiency of the "orange"-dye solar module under different light intensities was measured by the outdoor facility of Dyepower installed in Fonte Nuova (Rome), Italy. The measurement system was composed by a pyranometer (Kipp & Zonen) and a source-meter with a variable load (Keithley) controlled

by a LabView ad-hoc software. Indoor measurements were also performed before and after the main experiments in order to evaluate the degradation of the DSC module. The indoor system was composed by a sun simulator (Solaronix Solixon A70, ABB class) calibrated, using a certified reference solar cell (LOT-QuantumDesign LS0041), at AM1.5G, 1000 W/m^2 and a source-meter (Keithley) controlled by a LabView ad-hoc software.

3.3. Results and discussion

3.3.1. Cultivation of *N. salina* in PBR with a spectral-converter filter

N. salina was cultivated in a batch flat-panel photobioreactor at two different constant light intensities (65 and 150 μmol m^{-2} s^{-1}), in order to test the effect of using a spectral-converter filter on the specific growth rate under limiting irradiances.

The absorption spectrum (400-600 nm) of the spectral-converter filter employed is reported in Figure 3.3: three peaks in the yellow and green range, respectively at 447, 537 and 579 nm were found.

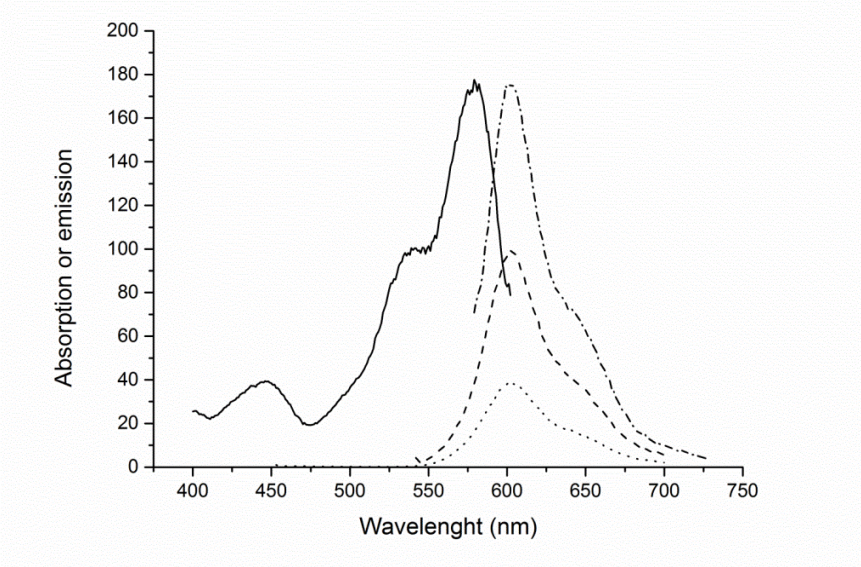

Figure 3.3 *Absorption (solid) and emission spectra of the spectral-converter at different excitation wavelengths: 447nm (dot), 537 nm (dash) and 579 nm (dash-dot)*

The material was therefore excited at each of these three wavelengths, and all the emission spectra obtained show a peak around 600 nm. The spectral-converter filter thus absorbs the

green and yellow wavelengths, and shifts the radiation towards the red range, potentially enhancing the total amount of photons that can be utilized by microalgae for photosynthesis. Moreover, the intensity of each emission peak corresponds to that of the respective wavelength absorption, suggesting a good efficiency of energy shifting.

As mentioned in §3.1, one of the main reasons for a low value of photoconversion efficiency is the limited wavelength absorption by microalgae. As proposed by Mohsenpour and Willoughby (Mohsenpour and Willoughby, 2013) the exploitation of spectral converter can have positive effects under sub-optimal sunlight exposure avoiding the utilization of artificial lights. In this chapter a similar strategy was applied to improve the growth performances of *N. salina* species, which is interesting due to the high lipid content (Rodolfi et al., 2009; Sforza et al., 2012b), but showed a lower photosynthetic efficiency with respect to green algae. Thus, the possibility to increase the light available for photosynthesis by shifting the green portion of the spectrum to the red range was tested. Results of batch experiments at 65 and 150 µmol m^{-2} s^{-1} in a control PBR (walls in PC) and in a PBR with the spectral converter are reported in Figure 3.4: unfortunately, despite the high shifting performances of the material used, no significant difference in growth rate between the control system and the PBR covered with the red spectral-converter was observed (data reported in Table 3.1), even though a slight improvement in final cell concentration was reached.

Table 3.1 *Specific growth rates of N. salina under normal and red-shifted radiation at 150 and 65 µmol m^{-2} s^{-1}*

Light intensity (µmol m^{-2} s^{-1})	**Control PBR (d^{-1})**	**PBR with spectral converter (d^{-1})**
150	0.521± 0.0288	0.510 ± 0.0108
65	0.461 ± 0.0394	0.458 ± 0.0317

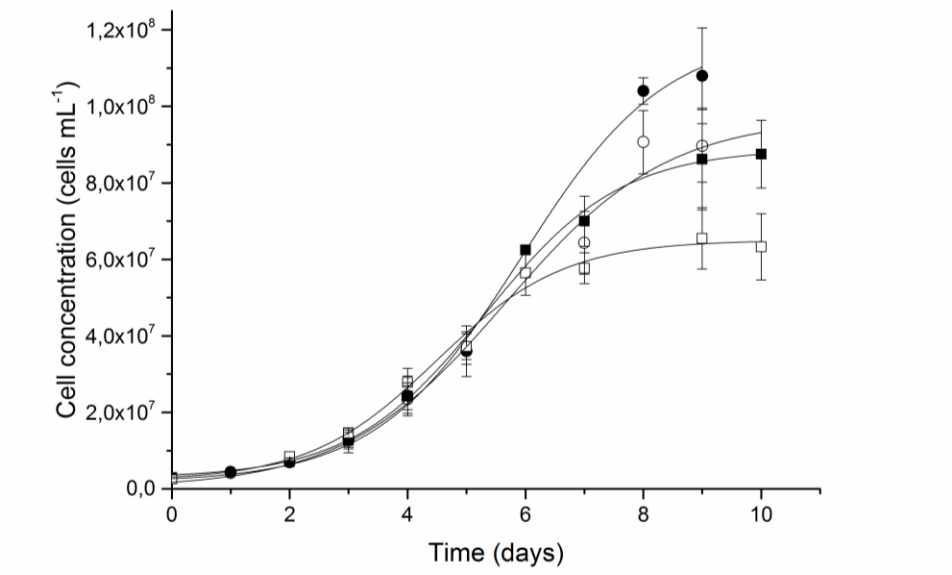

Figure 3.4 *Growth curves of N. salina under normal (open) and red-shifted (filled) radiation, at 150 (squares) and 65 (circles) µmol m^{-2} s^{-1}. Solid lines are eye guides only*

However, this improvement is not statistically significant, suggesting that the use of a front spectral converter does not impact the microalgal growth. On the other hand, as suggested by Wondraczek et al. (Wondraczek et al., 2013), the use of a back spectral converter can improve the algal growth performances, but this configuration may result in more technical issues, such as fouling problems, which should be accounted for in the design of large scale reactor. In addition, when applying spectral converters to the front surface, if no positive effects can be detected for a low cell concentration system (the initial concentration of biomass in the reactor was lower than OD=0.5) this strategy is probably not applicable in reactors with higher cell concentrations, as it is supposed to work in outdoor conditions. In summary, using spectral converters under real irradiances is not a viable strategy, by considering that, for most of the day, the energy impinging the PBR is over the saturation point.

3.3.2. Cultivation of *N. salina* and *S. obliquus* in a Silicon PV-PBR

3.3.2.1 *Nannochloropsis salina*

Batch experiments were carried out with *N. salina* in flat-panel PBRs, with the aim to determine the effect of covering 30% of the irradiated surface with a silicon photovoltaic (PV) panel on cell growth, pigment content and photosynthetic yield. The experiments were

conducted under different values of constant light intensities, ranging from low to high irradiance values (respectively 75, 150, 350 and 750 μmol m^{-2} s^{-1}).

Figure 3.5 shows the specific growth rate values obtained under different light intensities.

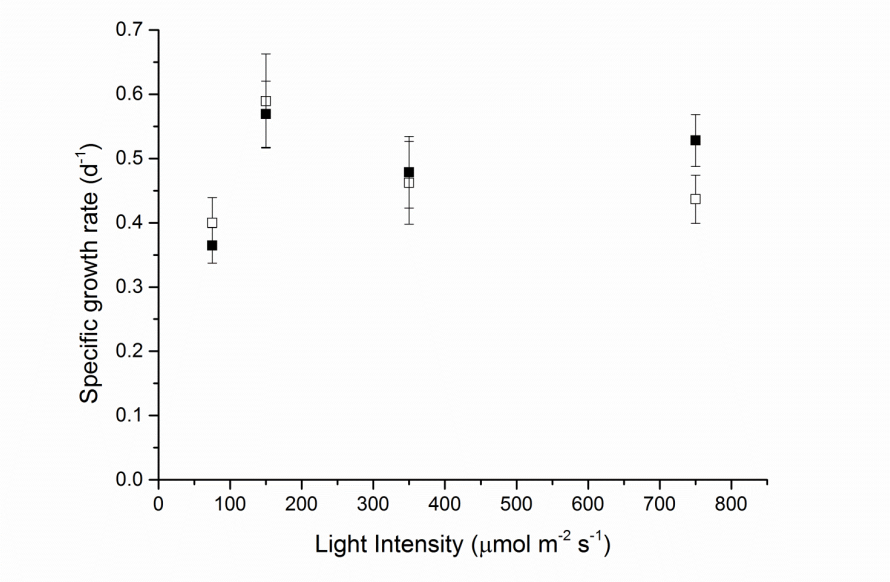

Figure 3.5 *Specific growth rate under different light intensities for N. salina for the control system (open squares) and the PV-PBR (filled squares)*

Consistently with what reported by Sforza et al (Sforza et al., 2012b), the growth rate of the control was maximum at a light intensity of 150 μmol m^{-2} s^{-1}, above which photosaturation and photoinhibition phenomena led to a decreased growth. By comparing the data obtained in the control PBR with those in the PV-PBR, it was observed that at low light intensities the growth rate is not significantly affected by the presence of the PV panel. On the other hand, for high irradiances the growth rate of the partially covered system appeared to be higher compared to that of the control system. This may suggest that when part of the PBR exposed surface is shaded, the alternation of the light intensity has a beneficial effect in reducing the photosaturation and photoinhibition phenomena that take place when algae are exposed to high irradiances.

To understand the physiological effect of a partially covered PBR on microalgae cultivation, the *Fv/Fm* parameter was also monitored at each light condition during the exponential phase, as it is an indicator of the maximum quantum efficiency of PSII. This parameter is useful to detect photoinhibition due to excess irradiances (Maxwell and Johnson, 2000), and is a

meaningful marker of photodamage in the case of *N. salina* (Sforza et al., 2012b). In fact, *Fv/Fm* was found to decrease with the increase of light intensity, as reported in Figure 3.6. However *Fv/Fm* values resulted to be slightly higher for PV-PBRs at each light condition investigated, suggesting a higher efficiency of photosystems. This was further confirmed by a pigment content increase, ranging from 5% to 23% with respect to the control.

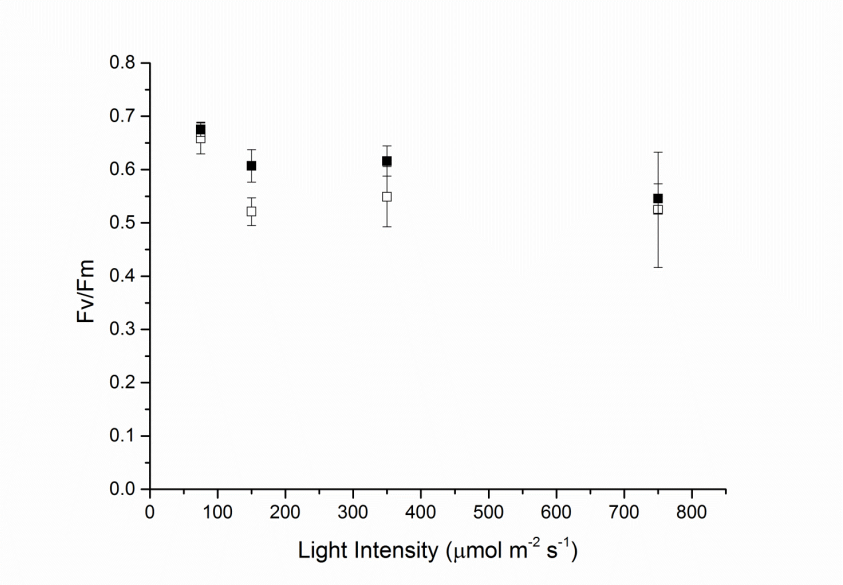

Figure 3.6 *Fv/Fm parameter under different light intensities for N. salina for the control system (open squares) and the PV-PBR (filled squares)*

N. salina was subsequently cultivated in a continuous flat-panel PBR, in order to verify the effect of a PV panel that covers 30% of the irradiated surface on both outlet biomass concentration and overall photoconversion efficiency. In Table 3.2 the average steady state outlet biomass concentration for PV-PBR and control are reported, corresponding to a residence time of 1.69 d and a constant light intensity of 150 μmol m^{-2} s^{-1}. Biomass concentration resulted to be slightly lower in the PV-PBR (0.91 g L^{-1} average compared to 1.03 g L^{-1} obtained with the control system), but this reduction is not statistically significant. Thus, covering 1/3 of the irradiated surface showed a loss of biomass production of only 11.6%.

Table 3.2 *Cells and biomass concentration, biomass productivity and photoconversion efficiency of N. salina continuous cultivation in control PBR and PV-PBR, under 150 µmol m^{-2} s^{-1} and 1.69 d of residence time. The photoconversion efficiency in the case of PV-PBR is calculated by accounting the electrical energy produced by the photovoltaic panel with a 5% of photoconversion efficiency.*

	Light Intensity (µmol m^{-2} s^{-1})	**Biomass concentration (g L^{-1})**	**Cell concentration (10^6 cells mL^{-1})**	**Biomass productivity (g L^{-1} d^{-1})**	**Photosynthetic efficiency %**
Control PBR	150	1.03	60.32±2.20	0.61±0.06	2.62
PV-PBR	150	0.91	52.06±4.51	0.54±0.05	3.98

When considering the overall energy conversion efficiency, on the other hand, the presence of a PV panel on the reactor surface has a larger impact. The photosynthetic efficiency of *N. salina* was equal to 2.62% of the total spectrum in the control PBR, while in the PV-PBR this value increased up to 3.98% of photoconversion. Nonetheless, the values reported are still far from the theoretical maximum value of 12%, despite the low light intensity applied to the reactor. In addition, *N. salina* was found strongly inhibited under higher irradiances and, in the continuous reactor, a steady state was not achieved for irradiances over 150 µmol m^{-2} s^{-1}, due to the strong photodamage, in both control- and PV-PBR.

3.3.2.2 *Scenedesmus obliquus*

Batch experiments were also conducted with *S. obliquus* at various light intensities (50, 150, 350 and 1000 µmol m^{-2} s^{-1}), and the specific growth rate was measured for both PV-PBR and control reactor.

Results confirm those obtained with *N. salina*, showing no substantial difference in growth rate at low light intensities, but a significant improvement at high irradiances in the case of PV-PBR (Figure 3.7). Under 1000 µmol m^{-2} s^{-1} the specific growth rate of *S. obliquus* resulted to be 0.624 ± 0.024 d^{-1}, compared to 0.417 ± 0.041 d^{-1} measured for the control, consolidating the assumption that photoinhibition can be reduced when the irradiated surface is partially covered. The effect of partial covering resulted in a lower pigment content of microalgae, while the *Fv/Fm* was not measured in this case, because no variation of the parameter can be detected for this species as a function of light intensity, as also reported in Gris et al. (Gris et al., 2013).

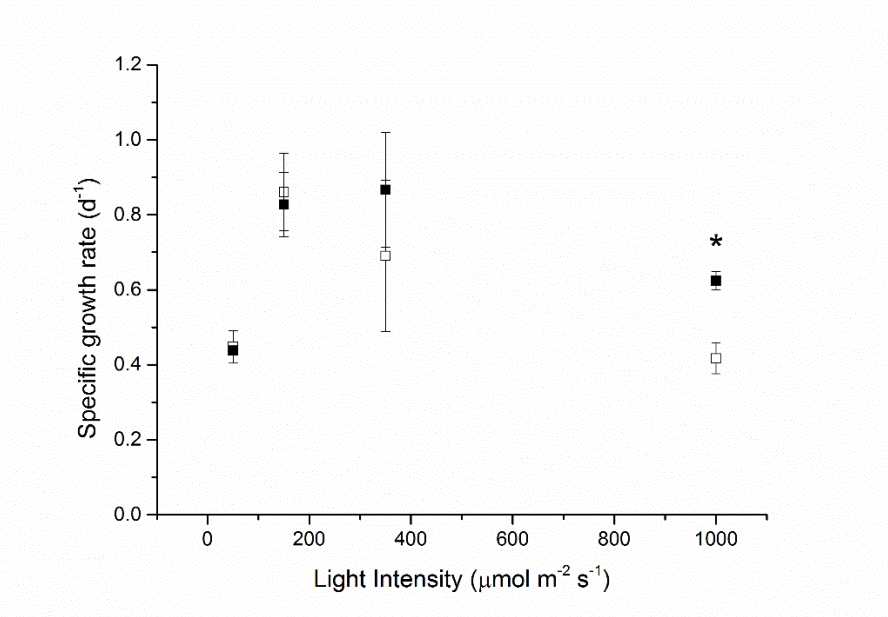

Figure 3.7 *Specific growth rate at different light intensities for S. obliquus for the control system (open squares) and the PV-PBR (filled squares). Statistically significant results are marked with an asterisk*

Continuous experiments with *S. obliquus* were carried out at different constant light intensities (150, 350 and 1000 μmol m^{-2} s^{-1}) with a residence time of the culture inside the reactor equal to 0.9 d. In addition, a simulated day-night irradiation, corresponding to a typical day of summer at middle latitude, was applied, in order to test the effect of the PV-PBR on real irradiation condition, when light intensity is variable along the day, and ranges from limiting to saturating values, as shown in Figure 3.8 (the 24 h integral value is 610 μmol m^{-2} s^{-1}). For this experiment, a residence time of 1.48 days was applied, in order to avoid the washout of the reactor that may occur due to the presence of the night period, without losing too much productivity as it occurs when increasing the residence time (Sforza et al., 2014c). For all continuous experiments P and N consumption were monitored, in order to verify the condition of non-limiting nutrient supply.

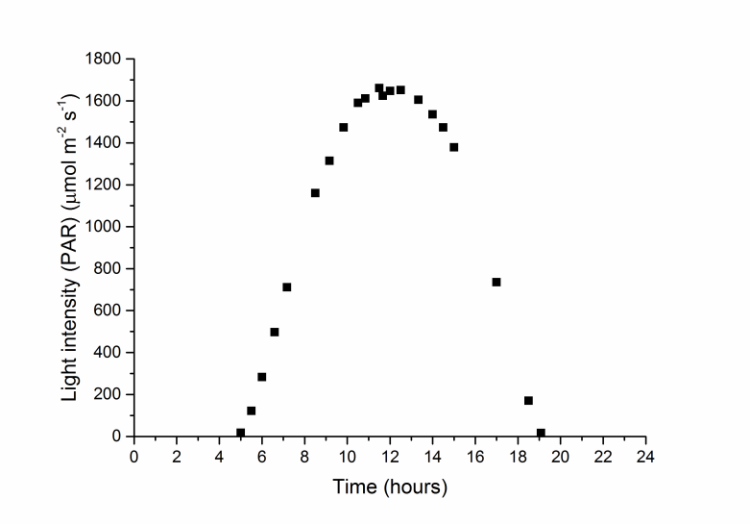

Figure 3.8 *Irradiation profile of the day-night experiments. Dots represent measurements of light intensity at the front surface of the PBR at different times of the day*

The average outlet biomass concentration obtained in PV-PBR and control at the different conditions are summarized in Figure 3.9.

At low light intensities the presence of the PV panel causes a small loss in biomass concentration: at 150 µmol m^{-2} s^{-1} the steady state concentration obtained with the PV-PBR is 14% lower than that of the corresponding control system. In fact, in the former configuration algae cells receive less light at an irradiance that is not inhibiting yet, resulting in a negative effect. Nonetheless, this concentration loss is not high when considering that the presence of the PV panel causes a 30% reduction of the irradiated surface. When the irradiance value increases, the reduction in outlet biomass concentration of the PV-PBR is less evident: at 350 µmol m^{-2} s^{-1} the concentration is reduced by 11% with respect to the control. More interestingly, at 1000 µmol m^{-2} s^{-1} and summer condition, no significant difference between the control system and the PV-PBR is reported. These results confirm those obtained with the previous batch experiments, giving credit to the assumption that covering a portion of the PBR surface, despite causing a small concentration loss at low intensities, leads to positive effects in terms of photodamage protection at the high intensities, which is promising in view of outdoor cultivation systems.

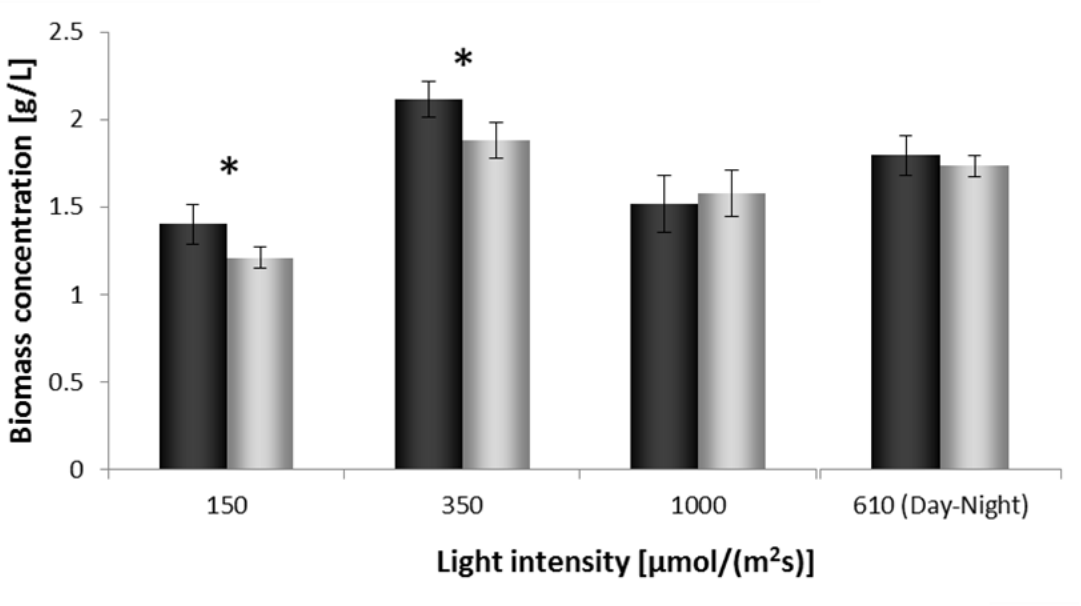

Figure 3.9 *Steady state outlet biomass concentrations of S. obliquus under different irradiation regimes with PV-PBR (grey) and traditional PBR (dark). Statistically significant results are marked with an asterisk*

When considering the energy conversion efficiency, the presence of a PV panel on the reactor surface has a great impact. Table 3.3 reports, for each experimental condition analyzed, the biomass productivity values and the percentage of hitting light that is converted into either biomass or electricity by the system in terms of total radiation (i.e. full spectrum), together with the thermodynamic theoretical limit for photosynthesis, which is equal to 11%.

As already well acknowledged, the photosynthetic efficiency decreases dramatically when light intensity increases, because the photosynthetic apparatus is not able to process the high amount of photons received, which leads to photosystems damage and energy dissipation (Carvalho et al., 2011; Muller et al., 2001).

Photosynthetic efficiency values measured for *S. obliquus* (Table 3.3) are consistent with those found by Sforza et al. (Sforza et al., 2014c). They result to be close to the theoretical limit (9.17% of total radiation) at 150 µmol m^{-2} s^{-1}, decreasing to 5.96% and 1.49% at 350 and 1000 µmol m^{-2} s^{-1} respectively, with a value of 1.8% under simulated day-night irradiation (summer).

Table 3.3 *Cells and biomass concentration, biomass productivity and photoconversion efficiency (PE) of S. obliquus continuous cultivation in control PBR and PV-PBR, under different light intensities and regimes and residence times. The PE in the case of PV-PBR is calculated by accounting the electrical energy produced by the photovoltaic panel with a 5% of photoconversion efficiency*

	Light Intensity (µmol m^{-2} s^{-1})	Residence time (d)	Biomass concentration (g L^{-1})	Cell concentration (10^6 cells mL^{-1})	Biomass productivity (g L^{-1} d^{-1})	PE %
Control PBR	150	0.9	1.41±0.11	65.94±7.40	1.55±0.12	9.36
PV-PBR	150	0.9	1.21±0.06	73.38±7.96	1.34±0.06	9.59
Control PBR	350	0.9	2.12±0.11	103.54±11.88	2.35±0.11	5.99
PV-PBR	350	0.9	1.88±0.10	104.73±5.27	2.08±0.11	6.94
Control PBR	1000	0.9	1.52±0.16	53.44±7.39	1.68±0.17	1.63
PV-PBR	1000	0.9	1.58±0.13	52.80±12.56	1.75±0.14	3.22
Control PBR	610 (summer)	1.48	1.78±0.06	80.17±6.81	1.20±0.04	1.81
PV-PBR	610 (summer)	1.48	1.73±0.07	74.22±4.62	1.16±0.05	3.35

3.3.2.3 Discussion

In this paragraph, the productivity of cultivation of two algal species, which are commonly recognized as interesting for biomass and biofuel production, is evaluated, by proposing a possible integrated PV-PBR to improve the overall conversion efficiency. The relationship between light and the growth rate and productivity of microalgal cultures is complex and can vary depending on the species: the response of each species and strains to the light spectrum varies with their genetic characteristics and adaptation to growth conditions (Gutierrez-Wing et al., 2012). This is particularly true for the two species used in this chapter: even though the maximum growth rate was found at 150 µmol of photons m^{-2} s^{-1}, the growth performances, in the reactor design proposed, were remarkably different for the two species. While *S. obliquus* showed a very high PE in continuous reactor (Table 3.3), the light conversion efficiency of *N. salina* was quite low (§3.3.2.1), according to previous observations (Sforza et al., 2014a).
As mentioned in §3.1, one of the major problems affecting the photosynthetic efficiency in real outdoor PBRs are the photoinhibition and saturation phenomena: even in winter, at middle

latitudes, the maximum intensity can reach 600-700 μmol m^{-2} s^{-1} at noon (data from PVGIS). In the current literature, photoinhibition can be controlled by reducing the total irradiance input, increasing the cycling of the organisms between the light and dark zones of the culture either by mixing or the use of intermittent light pulses reduction of the light source power (Gutierrez-Wing et al., 2012). However, in an outdoor system, the mixing-induced method is difficult to be achieved and precisely controlled because microalgae movement caused by the turbulent fluctuation is random. Moreover, energy consumption is much higher due to the energy required for the additional mixing (Liao et al., 2014). Accordingly, Liao et al (Liao et al., 2014), proposed a novel PBR with a slattered covered area, where the flowing biomass resulted exposed to high frequency light-dark cycles. In this system, operated in batch, they found an increased growth. On the other hand, in a batch system, it is difficult to calculate the biomass productivity and the photoconversion efficiency, because the light changes also along with the time, due to the increasing cell concentration. In addition, in a batch system, the microalgal culture is evolving during time, by adapting to the experimental condition. On the opposite, in a continuous reactor, the adaptation of microalgal biomass occurs during the transient period, and the steady state concentration relies to a stable, well adapted culture.

Here the possibility of using a partial covered PBR to restrain photosaturation and inhibition was tested, for both the species considered. After a first verification of the efficiency of the system in batch experiments, the reactor was operated continuously to quantitatively measure the PE. In batch, for both species, an increased growth was observed under high irradiances when the reactor is partially covered. The positive effect was remarkably higher in the case of *S. obliquus* (growth rate increase of 49% under 1000 μmol m^{-2} s^{-1}). On the opposite, the growth of *N. salina* was found generally strongly affected by high light exposition and the differences between the covered reactor and the control were less pronounced, suggesting that such a covering is not sufficient to guarantee a suitable photoprotection for this species. This assumption was confirmed in continuous experiments: in the case of *N. salina*, the high light drastically causes photoinhibition phenomena so that, under irradiation higher than 150 μmol m^{-2} s^{-1}, no steady state was achieved, even in the case of partially covered PBR. In addition, the photoconversion efficiency is very low even under optimal light condition (150 μmol m^{-2} s^{-1}) with a PE of about 2.6%, which is not substantially increased by the presence of the covering surface.

The PE of continuously cultured *S. obliquus* is, on the other hand, quite high, close to the maximum theoretical value under optimal irradiance, decreasing with the intensity under photoinhibiting irradiances (Figure 3.7). This species showed a higher flexibility to light variation, by well adapting to saturating light in continuous reactor. Interestingly, the presence of the cover under high irradiances resulted in a comparable biomass productivity, slightly higher in the case of 1000 μmol m^{-2} s^{-1} (Figure 3.9). The result is remarkable in particular by considering that a third of the reactor surface is covered, with a loss of biomass no more than 14% with respect to the control. This could likely be attributed to light scattering inside the culture, so that some light is still provided to the zones of the reactor not directly illuminated, but neighboring those who are. The positive effect of the covering was enhanced in the case of batch experiments, and this can be explained by the low cell concentration of such a system, resulting in a higher light supply rate per cell, and consequently in an increased photodamage effect, which is attenuated in the case of PV-PBR.

Of course, by assuming that the effect of photoprotection is due to the presence of a sort of dark-light cycle of cells moving in the different zones of the reactor, with a proper design of the covering, an increased biomass productivity may be achieved, as suggested by Liao et al. (Liao et al., 2014), who modified the frequency of darker zones to set a suitable light-dark cycle frequency.

On the other hand, the main objective addressed in this paragraph is to propose an integrated PV-PBR system, with the aim to not only avoid photosaturation and inhibition phenomena, by partially covering the PBR, but also, by applying silicon PV panels to the covered surface of the PBR, to better exploiting the light energy impinging the system. The Si PV technology is quite well established, and the current research is aimed at improving the efficiency up to 40% of the solar energy (Blankenship et al., 2011). The actual efficiency is about 18%, which is however remarkably high. As reviewed by Blankenship et al. (Blankenship et al., 2011), even if the efficiency of the PV is much higher than PE (real data in outdoor PBR about 3-6%), photosynthesis is unique in its capacity to produce a diverse array of complex organic compounds, because PV devices are not able to deliver selective carbon fixation photochemistry and do not produce an energy source that can be efficiently stored. The integration of a photosynthetic and photovoltaic technology can potentially increase the overall efficiency of solar energy conversion, and provide a range of energy sources that can be

addressed to different fields of application. This is also in agreement with the common opinion that no one renewable approach is capable of solving our energy needs for the future and that a mix of sustainable technologies will be required (Blankenship et al., 2011).

As reported in this paragraph, such PV-PBRs, despite having a lower biomass production at low light intensities, are able to convert part of the photons reaching the PV panel into electricity. Figure 3.10 displays the overall photoconversion of PV-PBR systems (calculated using Eq. 3.5) considering three different values of PV efficiency: 5% and 20% were taken as lower and upper bounds, together with a standard silicon PV efficiency of 12%. The maximum theoretical limit for photosynthesis is also reported.

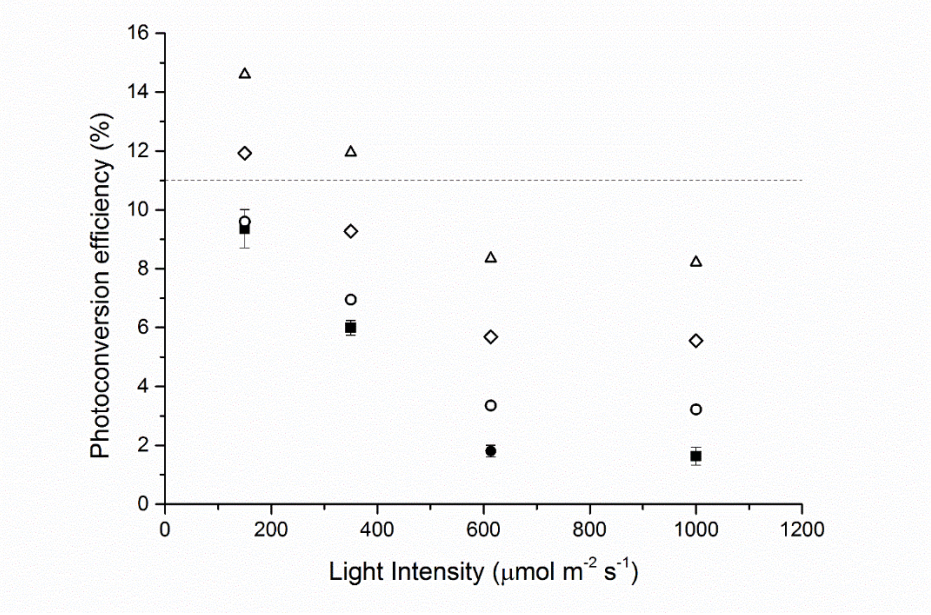

Figure 3.10 *Photoconversion efficiency at different light intensities for S. obliquus cultures with traditional PBR (filled squares) and PV-PBR (open): circles correspond to a PV with 5% efficiency, rhombus to 12%, and triangles to 20%. The dashed line is the theoretical maximum value of photosynthesis. The experimental value at 610 μmol m^{-2} s^{-1} refers to the summer day-night condition (closed circle), as an integrated irradiance value on 24 h basis*

It shows that, considering photovoltaic panel efficiencies in the range investigated, the overall energy conversion of the system can be substantially increased. In particular, in the case of a standard PV efficiency of 12%, the overall conversion is 27%, 54%, 240% and 215% greater for the PV-PBR with respect to the control system at 150, 350 and 1000 μmol m^{-2} s^{-1} and

summer conditions, respectively. As the electricity produced by the PV panel is proportional to the light energy received, the most relevant improvements are reported at the high intensities. Considering a PV efficiency of 20%, the overall photoconversion at 1000 μmol m^{-2} s^{-1} and at average summer irradiation is comparable to that of a traditional PBR operated at 150 μmol m^{-2} s^{-1}. Most importantly, the results obtained show that integrating microalgae cultivation in photobioreactors with photovoltaic allows to reach overall energy conversion values that exceed the theoretical maximum set by photosynthesis alone, overcoming the limit that is otherwise intrinsically connected with microalgae cultivation. In addition, the overall conversion could be further improved, considering advantages in silicon photovoltaic technology, which is constantly improving the efficiency of the light conversion.

3.3.3. Cultivation of *S. obliquus* in a DSC PV-PBR

The second type of PV technology tested in this chapter is the "orange"-dye sensitized cell device described in §3.2.2.2. Continuous cultivation experiments were carried out with *S. obliquus* under different values of constant incident light intensities, ranging from medium-low to high values (220, 615 and 950 μmol m^{-2} s^{-1} respectively), at a residence time τ = 1.6 d, for both transparent PBR (as a control) and DSC-integrated reactor. In addition, a simulated day-night irradiation profile reproducing a typical summer day (July) in Padova, Italy, was applied in order to verify the performances of the system under realistic illumination conditions, with light intensities ranging from limiting to saturating/inhibiting values, alternated with long dark periods. In this case, the average incident light intensity in this case was equal to 564 μmol m^{-2} s^{-1}, with a peak value of 1500 μmol m^{-2} s^{-1}. The complete irradiation profile used is shown in Figure 3.11.

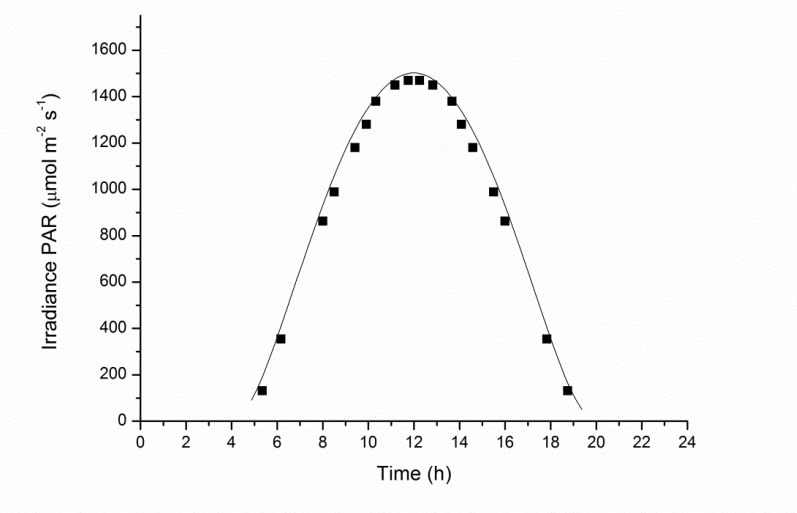

Figure 3.11 *Light profile (PAR) for a typical summer day in Padova, Italy. Solid line represents data from PVGIS, while dots indicate experimental measurements*

3.3.3.1 Biomass productivity

The biomass productivity, (calculated according to Eq. 3.2) obtained at the different experimental conditions for both the control and integrated DSC-PBR is represented in Figure 3.12. Note that, since the residence time was the same in all conditions, productivity and biomass concentration (DW, g L^{-1}) have the same trend.

The presence of the semi-transparent solar cell on the PBR surface has a strong influence on biomass productivity. In fact, it absorbs part of the incident radiation which is converted to electricity. In particular, about 45% of the incident PAR radiation was measured to be absorbed by the photovoltaic module in all conditions, while the remaining 55% is transmitted to the algal culture, with the spectral distribution reported in Figure 3.2. When the incident light intensity is low (220 μmol m^{-2} s^{-1}), this leads to a significant decrease in the biomass concentration, and the productivity drops accordingly, from 1.63 ± 0.06 g L^{-1} d^{-1} to 0.89 ± 0.04 g L^{-1} d^{-1}. Interestingly, the productivity reduction caused by the presence of the photovoltaic device is equal to 45% with respect to the control, which corresponds exactly to the percentage of photon flux absorbed by the solar cell. This suggests that an irradiance of 220 μmol m^{-2} s^{-1} is still below the saturation value for the species considered, according to what discussed in Chapter 2, where it was shown that under 250 μmol m^{-2} s^{-1} the light provided is still limiting

for *Scenedesmus* growth. Therefore, a reduction of the light transmitted to the culture in the presence of the PV module resulted in a corresponding reduction of biomass productivity. Increasing the light intensity to a value of 615 µmol m^{-2} s^{-1} allowed obtaining higher biomass concentration and productivity as a consequence of an increased energy input, reaching, in the control PBR, a value of 4.37 ± 0.22 g L^{-1} of dry weight. This trend was also found in other similar works cultivating *S. obliquus* in continuous flat-panel PBRs (Sforza et al., 2015, 2014c). Under these light conditions, the semi-transparent solar module still caused a productivity decrease, but the difference with respect to control PBR was only 15% (from 2.74 ± 0.14 to 2.32 ± 0.10 g L^{-1} d^{-1}). This can be explained considering that under these illumination intensities light becomes saturating. Hence, even if in the control the algal culture receives 45% more photons than in the DSC-integrated system, the benefit in biomass production is less marked.

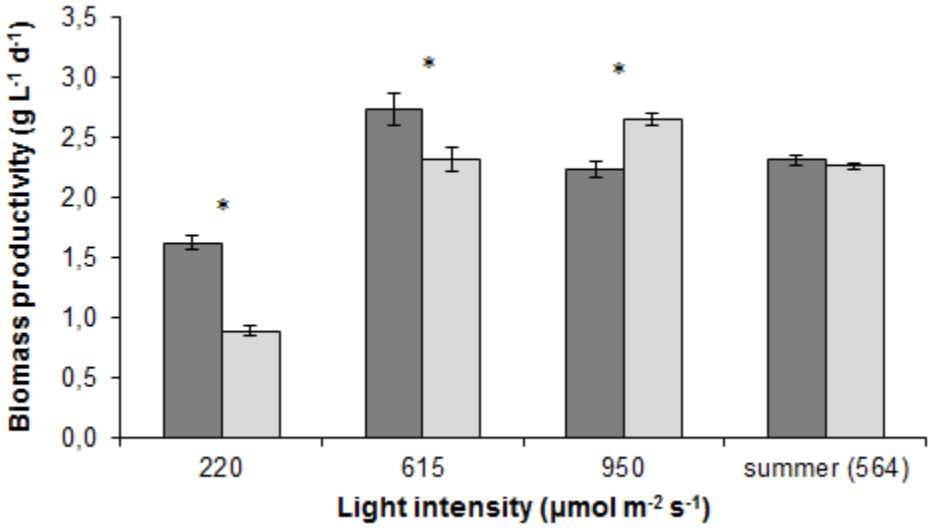

Figure 3.12 *Biomass productivity under different light intensities and regime for control PBR (dark grey) and DSC-PBR (light grey). Statistically different results are marked with an asterisk*

On the other hand, in the case of control PBR, a further irradiance increase up to 950 µmol m^{-2} s^{-1} led to a substantial productivity decrease with respect to the same system under previous light conditions. It means that under such high irradiance values photoinhibition takes place, causing damage in the photosystems, which results in reduced algal growth and production. In

this case, the presence of the semi-transparent photovoltaic module on the PBR surface was found to have a significantly beneficial effect in terms of biomass productivity, which increased from 2.23 ± 0.07 g L^{-1} d^{-1} to 2.66 ± 0.04 g L^{-1} d^{-1} (about 20% higher). In fact, the actual photon flux transmitted to the microalgal culture is decreased to a value of 505 µmol m^{-2} s^{-1}, at which photosaturation and especially photoinhibition phenomena are much reduced. In summary, when light is limiting, the presence of the PV cell reduces the microalgal productivity but, under photoinhibiting condition, covering the PBR by PV results in and enhanced biomass concentration.

Given the interesting results obtained under constant light intensity, *S. obliquus* was cultivated under the day-night irradiation profile shown in Figure 3.11, where PBR is exposed to variable light intensities, ranging from limiting to saturating photon flux densities. In this case the productivity resulted to be the same both for control and DSC-integrated photobioreactor. These results suggest that, even though the peak of light irradiation (midday) is far beyond the saturation point of the photosynthesis, the alternated light-dark cycle with sinusoidal trend leads to a complex acclimation response. In particular, the presence of long dark periods are likely to induce a preponderant respiration metabolism at night. Consequently, even though a steady-state productivity is reached, the light intensity received by the cells continuously changes in a cyclical way, leading to a cyclic steady state (Bertucco et al., 2014). In these conditions, algae are exposed to changing irradiances and the negative and positive effect of the semi-transparent device can be supposed to compensate, so that no difference can be noticed in overall biomass production when the PV is applied. In this regard, Cannavale et al. (2015), recently proposed a perovskite-based photovoltachromic device with self-adaptive transparency, able to undergo a chromic transition from neutral-color semi-transparent to dark blue-tinted when irradiated with solar light, without any additional external bias. This would be most desired, as the shading effect could be tuned to very low under limiting irradiances, and maximal at high irradiances, protecting cells from photodamage and potentially keeping the culture in almost stationary light regime. Anyway, the result obtained is promising, showing that a DSC-integrated PBR has the potential not to decrease biomass productivity, even if the irradiation surface is covered, but at the same time the overall photoconversion efficiency is enhanced, by exploiting the light to produce electricity, thus improving the land use.

3.3.3.2 Pigments content and light spectrum utilization

The results obtained in terms of biomass concentration and productivity under different values of constant incident light intensities are certainly of interest also as they allow to understand more deeply the effect of photon flux spectrum on microalgal growth. Photosynthetic pigments (i.e. chlorophylls) absorb mainly in the blue and red ranges of the PAR. The semi-transparent DSC module, as previously shown, absorbs the blue wavelengths, and the red range is transmitted to the culture. To better understand a possible effect of the spectrum change on algal cells, total chlorophyll content (Chl *a* and Chl *b*) was measured in all light conditions. The results obtained are shown in Figure 3.13. When chlorophyll content is plotted against incident light intensity (i.e. the photon flux hitting the front surface of the PBR, equal in the two configurations), in the DSC-integrated PBR it results to be higher than in the control (Figure 3.13A), as a consequence of the reduced light intensity. As also reported by Gris et al. (Gris et al., 2013), *S. obliquus*, like other photosynthetic organisms, shows an acclimation response by decreasing the chlorophyll content under higher light intensities to reduce light-harvesting ability. However, it is more interesting considering the trend of total chlorophyll content as a function of the transmitted light intensity, i.e. the photon flux actually received by the algal culture.

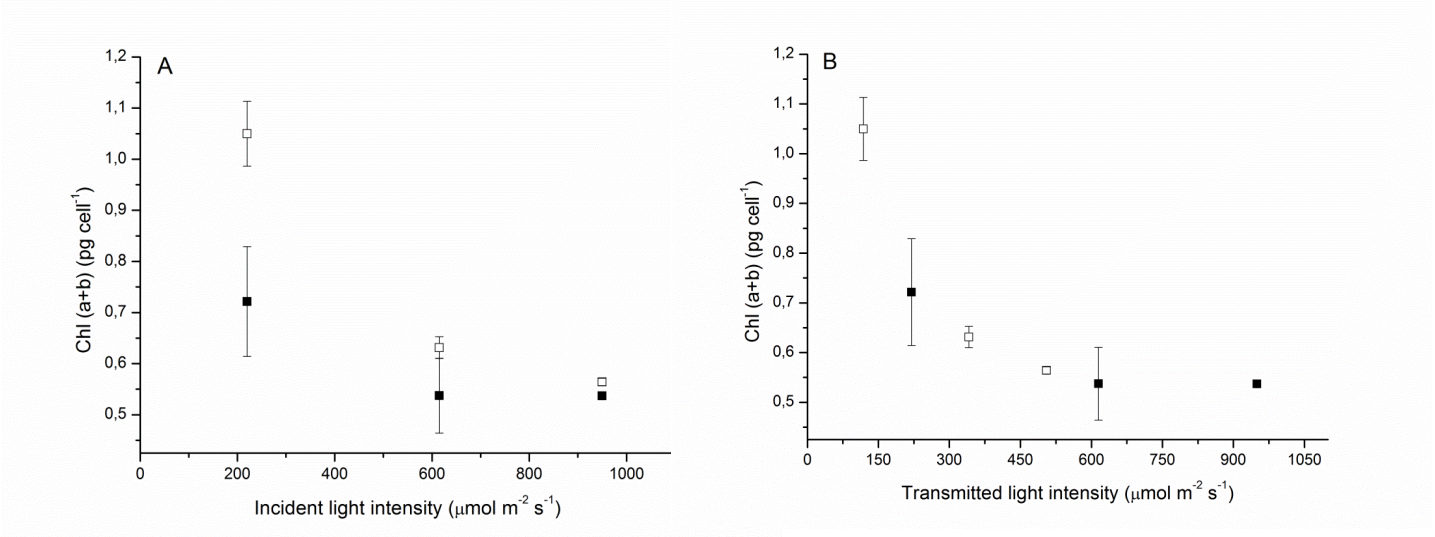

Figure 3.13 *Chlorophyll content per cell as a function of incident (A) and transmitted (B) light intensity, for control PBR (full dots) and DSC-integrated PBR (empty dots)*

In this case, even though the wavelengths of the photons received are different, the chlorophyll content per cell appears to follow an aligned trend (Figure 3.13B), suggesting that in the specific case algal cells are influenced, more than by the quality of the spectrum, by the global intensity of the photon flux received.

As a matter of fact, photosynthesis uses different radiant energy wavelengths with different efficiencies and, even if the energy of a blue photon is about 75% higher than that of a red photon, the higher excited chlorophyll states undergo very rapid relaxation, so that photochemistry is driven to the reaction center with the energy of a red photon (700 nm), regardless the wavelength originally absorbed (X.-G. Zhu et al., 2008). The additional energy contained in blue photons is therefore lost. For this reason, the "orange"-dye sensitized solar cell used in this study appears to be suitable for the purpose of the work, as it reduces the global photon flux hitting the algal culture (thus limiting photosaturation and inhibition phenomena), and allows to exploit the higher energy PAR photons (blue) to produce electricity, while transmitting the portion of spectrum that algae use with higher efficiency. Based on these considerations, as long as photons in the ranges absorbed by photosynthetic pigments are provided, the parameter of influence is represented by the global photon flux intensity transmitted to the microalgae. It is therefore interesting to evaluate the trend of productivity as a function of the transmitted light intensity (Figure 3.14).

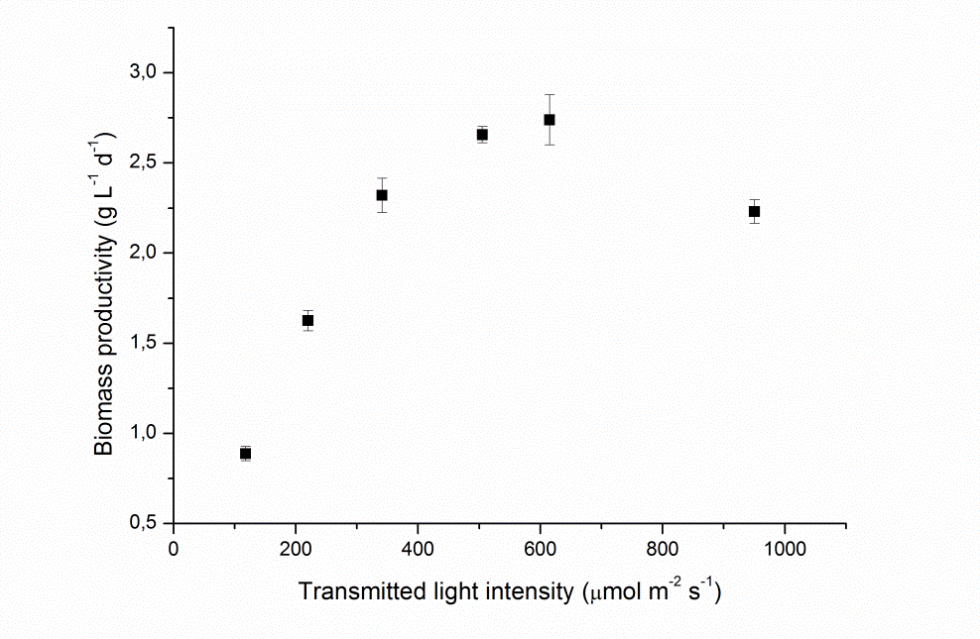

Figure 3.14 *Biomass productivity as a function of transmitted light intensity*

Similarly to the chlorophyll content considered previously, also in this case the trend of biomass production is aligned despite the difference in light spectrum received between control and DSC PV-PBR. The graph obtained allows to draw some remarks on light saturation and inhibition for the species considered: it appears that saturation occurs above irradiance values greater of about 500 μmol m^{-2} s^{-1} while, as previously mentioned, a light intensity of 950 μmol m^{-2} s^{-1} a clear inhibition is evidenced. Interestingly, photosaturation and photoinhibition appear to occur at quite higher irradiance values compared to those usually reported in the literature (half-saturation constants range between 100-150 μmol m^{-2} s^{-1}) (Munoz-Tamayo et al., 2013; Takache et al., 2012). This could be explained considering that these values are often determined from batch experiments, in which algal cells do not have the time to fully adapt to high light conditions. On the other hand, in a continuous culture, after a transient period that allows cells to adapt to the new conditions, a steady-state is reached in which microalgae are fully acclimated.

A reduction of pigment content was observed in the case of summer irradiation (corresponding to 0.32 ± 0.02 for the control and 0.41 ± 0.02 in the case of PV-PBR), which is a typical response to a sinusoidal irradiation (Sforza et al., 2014c). However, in the presence of PV, the pigment content is higher than the control, suggesting that, also in this case, a photoprotective effect is carried out by the PV device.

3.3.3.3 Energy conversion efficiency

In order to evaluate the energy and light utilization efficiency of the system, the performances of the DSC module were measured at the different light irradiances investigated (referred to the global solar spectrum), and the overall photoconversion calculated accordingly by Eqs 3.3-3.5.

The efficiency of such PV devices can be expressed in terms of active area (in this case equal to 381 cm^2), or in terms of aperture area (in this case 564 cm^2), which takes into account the surface of the module including the non-active portions among the cells (occupied by seal and interconnections) (Green et al., 2012). The latter one was used in the calculations, but the first parameter is also interesting, as the ratio between active/non active areas might be improved in the future technological developments.

At the end of the main experiments, the efficiency of the DSC module in indoor condition (1000 W/m^2, AM1.5G, ~40 °C, similar to standard test condition (STC) except for the temperature) was equal to 2.21% in terms of aperture area (3.21% in terms of active area). In the same conditions, before the main experiments were carried out (about one year earlier), the device had efficiencies equal to 2.23% and 3.30% respectively, thus demonstrating a longer stability of the DSC module used. However, the efficiency of the DSC module depends on light intensity. For this reason, its value was measured at different outdoor irradiances. For the summer conditions, the efficiency at minimum (131 μmol m^{-2} s^{-1}), maximum (1500 μmol m^{-2} s^{-1}) and three intermediate irradiance values were considered, together with the average one (564 μmol m^{-2} s^{-1}). As it can be seen in Figure 3.15, the PV efficiency decreases when the light intensity increases. Under low light intensities its value reaches about 4% of energy conversion, while it drops to values between 2-3% at higher irradiances. Figure 3.16 represents the overall photoconversion efficiency of control and DSC-integrated PBRs, respectively, under the different light conditions. It can be seen that light energy conversion is always higher when the photobioreactor is integrated with the semi-transparent DSC module under all the conditions investigated.

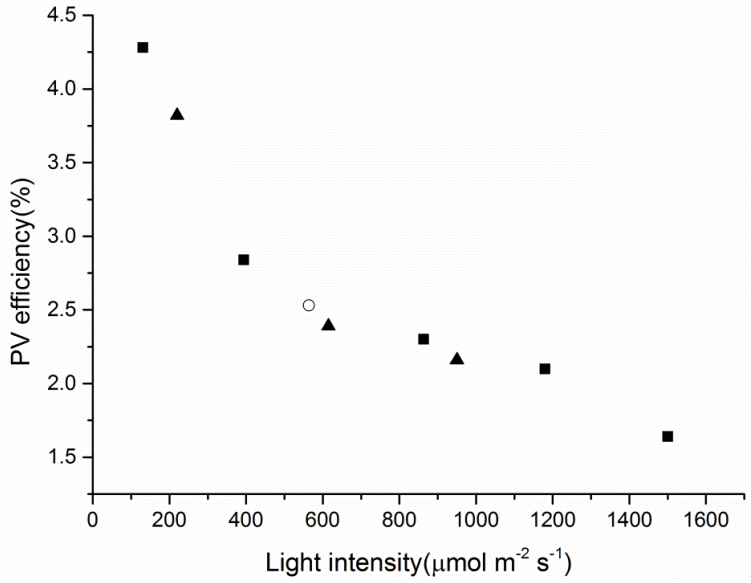

Figure 3.15 *Efficiency values, in terms of aperture area, of the DSC module under different light intensities (outdoor measurements): summer regime (squares), averaged summer (circle), continuous light (triangles)*

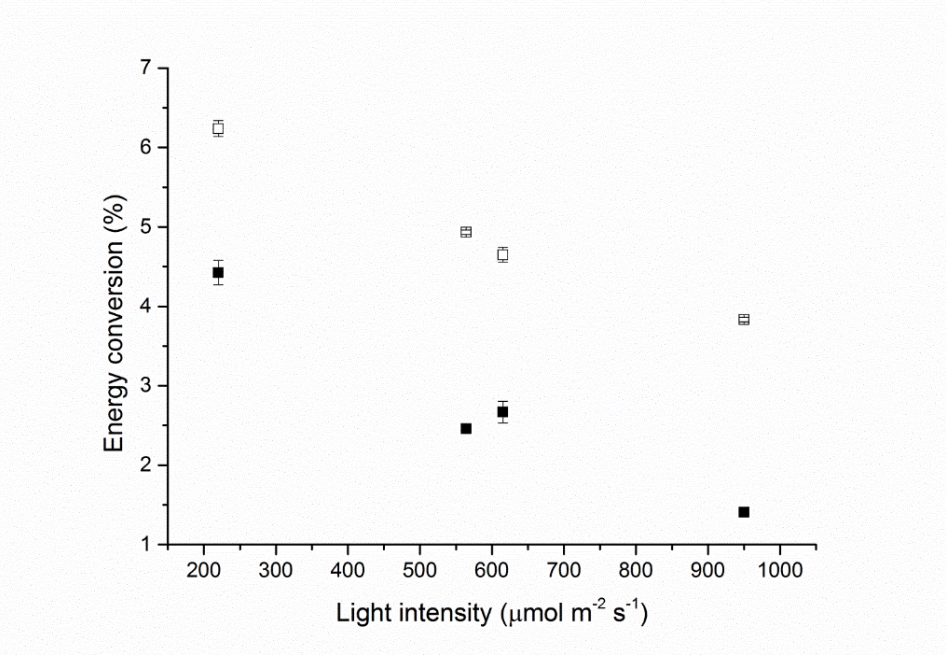

Figure 3.16 *Overall photoconversion efficiency under different light intensities for control PBR (filled squares) and DSC-PBR (open squares)*

In particular, the energy output was found to be 41%, 74%, 172% and 100% higher compared to the transparent PBR for the three constant light intensities and for the summer irradiation condition respectively. All the results are summarized in Table 3.4.

Table 3.4 *Summary of energy conversion efficiency*

Light (μmol m^{-2} s^{-1})	**DW (g L^{-1})**	**$E_{out,bio}$ (kJ d^{-1})**	**ε_{PV} (%)**	**$E_{out,PV}$ (kJ d^{-1})**	**η_{TOT} (%)**
220 (Control)	2.59 ± 0.09	25.03 ± 0.87	-	-	4.43 ± 0.15
220 (PV)	1.42 ± 0.06	13.68 ± 0.57	3.8	21.61	6.24 ± 0.10
615 (Control)	4.37 ± 0.22	42.19 ± 2.13	-	-	2.67 ± 0.14
615 (PV)	3.7 ± 0.15	35.74 ± 1.47	2.4	37.79	4.65 ± 0.09
950 (Control)	3.56 ± 0.10	34.36 ± 1.01	-	-	1.41 ± 0.04
950 (PV)	4.24 ± 0.07	40.92 ± 0.69	2.2	52.76	3.84 ± 0.03
Summer (Control)	3.69 ± 0.07	35.64 ± 0.72	-	-	2.46 ± 0.05
Summer (PV)	3.61± 0.04	34.83 ± 0.40	2.5	36.69	4.93 ± 0.03

The results obtained highlight the promising potential of combining microalgae production with this novel photovoltaic technology. The integration of different renewable energy sources is highly encouraged by the fact that single approaches would not be able to solve the energy demands for the future, and a combination of more sustainable technologies should be adopted (Blankenship et al., 2011). In this case, even though under limiting light intensities the biomass productivity was reduced, the overall light utilization was found to be greatly improved in all the conditions investigated. Moreover, under day-night outdoor irradiation, the energy conversion efficiency was doubled, while the microalgal productivity was not affected.

Despite the efficiency of dye-sensitized solar cells is still quite low compared to the well-developed silicon photovoltaic, its semi-transparency allows the entire PBR irradiated surface to be uniformly covered by PV, while in this case only a certain portion can be utilized for electricity production. Moreover, being this a novel technology, there are still wide prospects for further efficiency improvements, and different combinations of titania thickness, dyes and module layouts should be compared in addition to a PBR system.

3.4. Final remarks

In this chapter two strategies to improve the energy conversion in photobioreactors were considered: according to the first one, a commercially available spectral converter was applied to the surface of a flat panel reactor increasing the portion of spectrum available for photosynthesis. Even though the filter used is able to efficiently absorb the green wavelengths and shifts this radiation to the red range, no significant effect was observed on algal growth, even under low irradiances.

On the other hand, integrating microalgae photobioreactor (PBR) with different photovoltaic (PV) devices, remarkably increased the overall photoconversion efficiency of the system, by producing directly available electrical energy together with microalgal biomass. Moreover, under higher irradiances, the presence of the PV module (a partial cover of the reactor surface in the case of Si PV-PBR and a partial light absorption with the DSC-PBR) resulted in reduced photosaturation and photoihibition phenomena. Most importantly, under certain conditions, integrating microalgae cultivation in photobioreactors with photovoltaic allows to reach

overall energy conversion values that exceed the theoretical maximum set by photosynthesis itself.

Overall, the results discussed in this chapter show that the configuration proposed, combining biomass production with photovoltaic technology, could be a valid way to improve light energy utilization and efficiency in microalgal production.

Chapter 4

Energy and economic analysis of microalgae cultivation in Algreenhouse (a photovoltaic-assisted greenhouse)

Microalgae are photosynthetic organisms able to convert sunlight energy into chemical energy stored as biomass. However, in industrial scale applications, their photosynthetic efficiency is quite low so that high surface area is required for massive production, resulting in unacceptable production costs. In this chapter, a possible optimization of land use for microalgae cultivation is proposed, by combining biomass and electricity production with photovoltaics. To this purpose, microalgal cultivation in a continuously operated open pond placed inside a greenhouse is considered, at two different Italian latitudes, as a case study. The greenhouse roof area is partially covered with commercial photovoltaic modules, having the double purpose of shading the pond to limit photoinhibition, and of better exploiting incoming photons to produce electricity. The solar radiation profile at ground level and the average temperature inside the greenhouse are simulated for different seasons, and the corresponding microalgal productivities are calculated based on a validated growth model. The performances of the photovoltaic-greenhouse system are compared, from the energy efficiency point of view, to those of an identical system without PV modules. Moreover, an economic analysis is carried out to assess the profitability of such a cultivation system with respect to an area of 1 hectare.

[0]Part of this chapter has been submitted to Energy

4.1. Introduction

Microalgae cultivation has received a growing interest in the latest years, thanks to the ability of these photosynthetic microorganisms to convert sunlight energy into biomass with high heating value, rich in lipids and valuable compounds that can be destined to a wide variety of uses, spanning from biofuels production to cosmetic and nutraceutical applications (Milledge, 2010; Zhu, 2015). It is well known that microalgal biomass offers higher growth rate and solar energy conversion efficiency compared to terrestrial plants. However, the photoconversion efficiency can never exceed the thermodynamic limit set by photosynthesis, which is estimated to be about 11-12% for sunlight energy (Blankenship et al., 2011). In addition, this limit is far from being reached in large scale system applications, so that actual values show that only between 2-4% of the total light received can be converted into biomass by photosynthesis (Chisti, 2013). This is due to various phenomena, among which photosaturation and photoinhibition under high light intensities play a major role. In fact, when exposed to strong irradiations, like those occurring even in a typical winter day at mid-latitudes, photosystems are not able to process the entire flow of photons received, and get saturated or damaged, while excess light is dissipated as heat or chlorophyll fluorescence, leading to substantial energy and productivity losses. On the other hand, photovoltaic (PV) panel technology available in the market is currently able to convert light energy into electricity with yields above 20% (Blankenship et al., 2011; Green et al., 2015).

In Chapter 3, an integrated photovoltaic-photobioreactor was tested with the aim of improving the photoconversion efficiency of a light capturing system, and showed that covering 30% of the irradiated surface with standard PV panels did not result in a significant microalgae productivity reduction. In particular, at high irradiations, photosaturation and photoinhibition were attenuated by the presence of a dark zone in the culture volume, and the overall photoconversion efficiency was greatly increased, thanks to the photons that are converted into electricity. In the same chapter, a similar concept has been applied by using a dye-sensitized PV module directly placed on the photobioreactor, confirming that microalgal productivity is not substantially decreased by the shading effect due to the PV panels except for low irradiations, when the light is limiting itself. From the industrial point of view, this concept could be profitably applied by placing the microalgal cultivation system inside a greenhouse,

whose roof is partially covered by silicon photovoltaic panels. An integration of PV and PBR technologies has been recently proposed by several authors, and the effect of PV on microalgal cultivation is under strong investigation (Bernard et al., 2015; Detweiler et al., 2015; Parlevliet and Moheimani, 2014).

Photovoltaic greenhouses have indeed been widely studied and applied at least in southern Europe, especially Spain, France and Italy, in the agronomic field (Cossu et al., 2014). The possibility of exploiting the abundance of solar energy for producing, in addition to biomass, electricity that could be locally used to meet the power demand of the facility, or injected into the grid, makes it an interesting and attractive solution. Nonetheless, many works related to agricultural applications of photovoltaic greenhouses report negative results, as the partial shading of the cultivation surface causes either a reduction in productivity, or a negative effect on fruit size, hardness and color, depending on type of crop (Cossu et al., 2014; Marrou et al., 2013; Yano et al., 2010). With respect to this, microalgae cultivation luckily differs from that of terrestrial crops as, in the simplest cultivation system, the liquid culture suspension flows along a raceway pond, and algal cells move alternatively and continuously from irradiated to shaded zones. This fast alternation between high and low light intensity exposures could be beneficial in reducing phosaturation and photoinhibition effects. Cultivation of microalgae inside greenhouses, in addition, can help reducing external contaminations and protecting the system from climatic factors such as wind and rain. On the other hand, integrating a greenhouse with high efficiency PV module could render the whole process self-sufficient with respect to energy duties and maybe also economically attractive.

The objective of this chapter is to assess the profitability of microalgal cultivation in photovoltaic greenhouses both energetically and economically, and to compare its performances with those of an identical system without PV panels on the roof. Extensive process simulation is carried out based on literature models with parameters values derived from previous experimental work when needed, as described in Chapter 2. A standard-type Cost Benefit Analysis (CBA) is then performed with reference to a microalgal greenhouse (Algreenhouse) of 1 hectare extension. Two different Italian locations (Venice, in the North, and Palermo, Sicily, in the South) were considered as examples of the analysis, in order to take into account the effects of local irradiance and temperature on the performances, with the aim

of evaluating the feasibility of the proposed system and highlighting its main advantages and disadvantages in a real environment.

4.2. Methods

4.2.1. Greenhouse and cultivation system configuration

In this chapter, a commercially available greenhouse covering an area of 10,835 m^2, made of 29 pitched-roof spans (71 m long and 5.26 m wide each, east-west oriented) was considered, giving an overall width equal to 152.6 m. The gutter height is 2 m, and the roof slope is 35° with respect to the ground, while the total height is equal to 3.84 m. The south-oriented roof of each span is covered on the upper half only by 68 silicon PV modules (E19-320 by SunPower, 1.6 m x 1.046 m), with an average electricity conversion efficiency of 19.8%. The characteristics of one span are shown in Figure 4.1, while the specifications of the PV modules considered are summarized in Table 4.1.

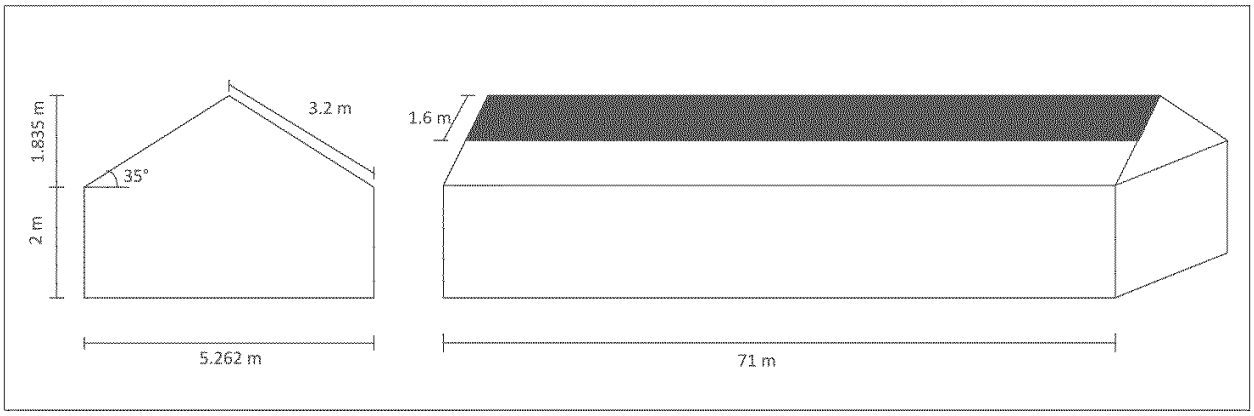

Figure 4.1 *Dimension characteristics of one span of the greenhouse*

The microalgal cultivation system placed inside the greenhouse covers an overall area of 1 ha, and is divided into 6 equal raceway-pond modules of 50 x 33.3 m, in order to ensure a safer operation and to limit production losses in case of malfunctioning conditions. Each raceway module is 10 cm deep, and is designed as an open pond circuit made of 10 channels of 3.33 m width. The system is operated in continuous mode, meaning that nutrients are continuously fed at the inlet, and biomass is continuously harvested from the outlet. Partial recirculation of the

outlet stream is necessary in order to avoid complete wash-out of biomass from the system and to prevent microalgae from settling by enhancing the convective velocity through the pond.

Table 4.1. *Technical specifications of the PV module*

PV module	
Name	E19-320
Type	Mono-crystalline silicon
Dimensions	1559 x 1046 x 46 mm
Efficiency	19.8%
Weight	18.6 kg
Electrical data	
Nominal power	320 Wp
Nominal power voltage	54.7 V
Nominal power current	5.86 A
Open circuit voltage	64.8 V
Short circuit current	6.24 A

The residence time of the microalgal culture inside the reactor, is defined as:

$$\tau = \frac{V_R}{Q} \qquad \text{(Eq. 4.1)}$$

where V_R is the reactor volume and Q the inlet/external volumetric flow-rate. The value of τ is adjusted to the different irradiation conditions along the year.

The algal species to which all simulations are referred is *Scenedesmus obliquus*, because it yields high productivity and photosynthetic efficiency compared to other species, and can be interesting from the industrial point of view (Sforza et al., 2014c; Tang et al., 2011). However, this approach can be easily extended to many other species as well.

4.2.2. Irradiance and temperature simulations

The light radiation distribution at ground level inside the greenhouse was simulated using the software DIALux 4.12 (from DIAL GmbH). Four days were chosen as representative for the various seasons, respectively January 15th for winter, April 15th for spring, July 15th for summer, and October 15th for autumn. Clear sky was assumed in all the simulations. Venice

was chosen as the location representative for Northern Italy, while Palermo for the South. With such specifications, the software retrieves sunlight irradiation data from its data bank.

Regarding optical properties, it was assumed that photovoltaic panels are completely opaque to solar radiations, while a transmissivity value of 90% was used for the greenhouse. This value was then reduced by considering a pollution factor of 0.9 (for low-density rural environments) and a factor of 0.95 that takes into account the reduction due to the greenhouse structure. Radiation distribution simulations were performed by means of DIALux at different hours during the day considered both for the greenhouse covered with PV panels and for the one without them. In order to reduce the calculation time required by the simulations, only 1/3 of the entire greenhouse surface was considered (10 spans instead of 29), assuming that the units are repeatable.

Assuming to operate without a temperature regulation system in the pond, the air temperature both outside and inside the greenhouse was evaluated using CASAnova software (rel. 3.3- Universitat Siegen, Fachgebeit Bauphysik & Solarenergie). Typical values of transmittance and transmissivity for greenhouses have been taken, i.e. 3.5 W m^{-2} K^{-1}.

In addition, the greenhouse was assumed to be closed in winter (0.6 volume make up per hour, due to imperfect seal of the walls) and partially open in summer (4 volume make up per hour) to prevent temperature from getting too high in the hot season.

Considering the long residence time and the small hydraulic hold-up in the PBR, the water temperature was reasonably set equal to the air temperature inside the greenhouse at each time of the year.

4.2.3. Productivity simulations and energy balances

In order to evaluate the biomass productivity along the year in each of the conditions considered, the model of Pruvost et al. (2011) (Pruvost et al., 2011b) for eukaryotic microalgae in a rectangular cultivation system was used, as previously detailed in Chapter 2.

Assuming a perfectly mixed continuous reactor, the material balance referred to the dry biomass is therefore expressed by:

$$\frac{dc_x}{dt} = r_x - \frac{c_x}{\tau} \qquad \text{(Eq. 4.2)}$$

where c_x and r_x represent the biomass concentration in the reactor (g L^{-1}) and its growth rate (g L^{-1} d^{-1}).

Since in such a geometry the light intensity can be assumed to vary only along the reactor depth (z), the local growth rate is expressed as follows:

$$r_x(z) = (\rho_m \frac{K}{K + I(z)} \Phi I(z) E_a c_x - \mu_e) \cdot \Phi_T \quad \text{(Eq. 4.3)}$$

where ρ_m is the maximum energetic yield for photon conversion, K the half saturation constant for photosynthesis, Φ the mass quantum yield for the Z-scheme of photosynthesis, E_a the light absorption mass coefficient, and μ_e the maintenance coefficient.

The net average biomass growth rate is then obtained integrating the local growth rate along the reactor depth H:

$$r_x = \frac{1}{H} \int_0^H r_x(z) dz \quad \text{(Eq. 4.4)}$$

The factor Φ_T in Eq. 4.3 was added to account for the effect of temperature on microalgal growth. It is evaluated according to the model proposed by Bernard and Remond (2012) (Bernard and Rémond, 2012), which considers three temperatures: T_{min} and T_{max} (i.e., the values below and above which microalgal growth is equal to 0), and T_{opt} (i.e., the temperature at which the growth rate is maximal). The values of parameters used in simulation of *S. obliquus* growth were the same described in Chapter 2, while temperature parameters were retrieved from Xi et al. (2010). All of them are summarized in Table 4.2. The daily irradiation profile as obtained from DIALux simulations was applied, considering the average irradiance profile at ground level inside the greenhouse, and an angle of incidence on the culture of 0°. In fact, within the greenhouse it was assumed that sunlight energy is mainly in the form of diffuse radiation.

Finally, the average biomass productivity per unit volume was evaluated taking the average of the cyclical steady-state biomass concentration value achieved, according to:

$$\overline{P_{x,v}} = \frac{\overline{c_x}}{\tau} \quad \text{(Eq. 4.5)}$$

where $\overline{c_x}$ is the integral mean of the reactor outlet concentration over time.

On the other hand, the average productivity per unit area can be calculated by:

$$\overline{P_{x,A}} = H\overline{P_{x,v}} \qquad \text{(Eq. 4.6)}$$

Eventually, the photosynthetic efficiency η referred to total radiation was evaluated by:

$$\eta = \frac{H \cdot LHV \cdot \overline{P_{x,v}}}{PFD_{abs} \cdot E_p} \qquad \text{(Eq. 4.7)}$$

where *LHV* is the lower heating energy value (assumed equal to 22 kJ g^{-1} for *S. obliquus* (Gons and Mur, 1980)), PFD_{abs} the photon flux density absorbed by the culture (μmol m^{-2} s^{-1}), assumed equal to the average (i.e. integral mean) intensity within the greenhouse, and *Ep* is the energy of the photon (0.223 J μmol^{-1}).

Table 4.2 *Parameters used in the simulations for the North (a) and South (b)*

a)

Case	Season	K (μmol m^{-2} s^{-1})	ρ_m (-)	Φ (kg μmol^{-1})	E_a (m^2 kg^{-1})	μ_e (d^{-1})
with PV	**Spring**	325	0.8	$2.84 \cdot 10^{-9}$	182	0.231
	Summer				172	0.292
	Fall				204	0.151
	Winter				230	0.108
without PV	**Spring**	325	0.8	$2.84 \cdot 10^{-9}$	169	0.314
	Summer				162	0.383
	Fall				188	0.201
	Winter				212	0.133

b)

Case	Season	K (μmol m^{-2} s^{-1})	ρ_m (-)	Φ (kg μmol^{-1})	E_a (m^2 kg^{-1})	μ_e (d^{-1})
with PV	**Spring**	325	0.8	$2.84 \cdot 10^{-9}$	171	0.302
	Summer				178	0.252
	Fall				195	0.175
	Winter				215	0.129
without PV	**Spring**	325	0.8	$2.84 \cdot 10^{-9}$	161	0.390
	Summer				167	0.334
	Fall				180	0.238
	Winter				197	0.168

The product $LHV \cdot \overline{P_{x,v}}$ expresses the energy per unit time in the biomass. Note that the plant operation simulation was stopped when the temperature and/or the sunlight energy were too low to sustain growth. For the calculation of the energy efficiency of the PV-PBR system, also the power produced by PV panels in excess was considered to supply the process electricity duty. This can be done in two ways, by simply adding it to the biomass energy or, more correctly, by doing this after upgrading the electrical energy by a factor of 2.18, which takes into account the average conversion efficiency of heat into electricity (average value for Italian electricity production ("Circ.18-12-2014, law 09-01-1991 n10, Ministero dello Sviluppo Economico, Italy," 2014)). Energy duties of the entire process were estimated by applying mass and energy conservation balances to all the process units, according to the simplified block flow diagram depicted in Figure 4.2. PV modules have been added so that PV electricity production is fully supporting the energy requirements of all the pieces of equipment in the plant (CO_2 and nutrients feed systems, recirculation of the suspension within the reactor, thickening, centrifugation. Drying was instead achieved by heating).

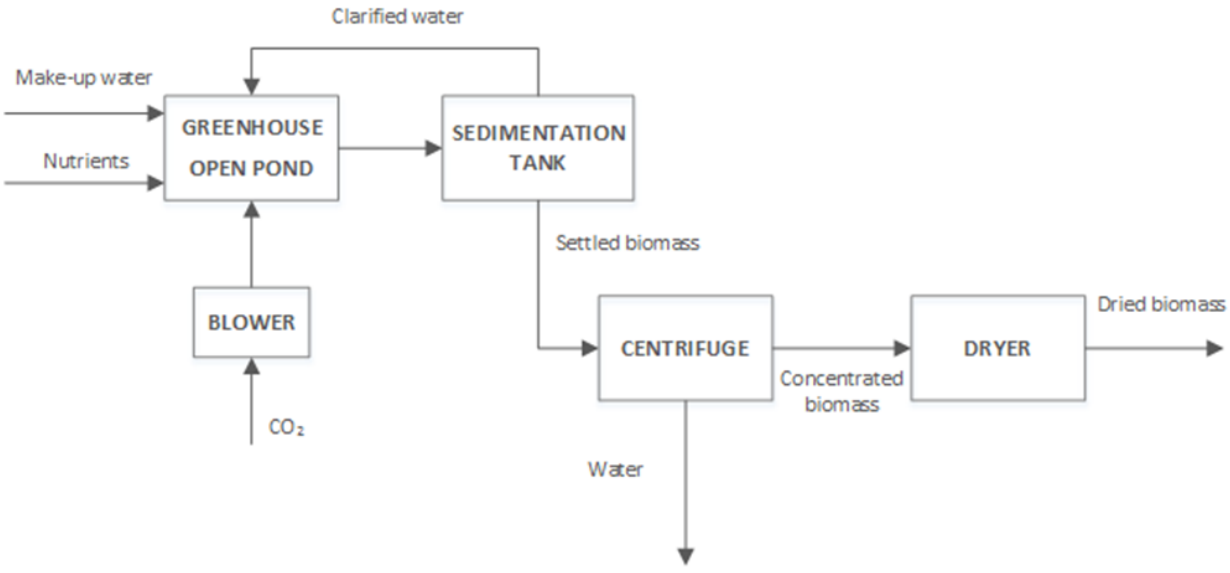

Figure 4.2. *Block Flow Diagram of the process considered*

4.2.4. Economical evaluation of the process

As for energy, also units other than the photobioreactor have to be taken into account to evaluate the production costs of microalgae in the greenhouse. The analysis was referred to the process depicted in Figure 4.2, according to which dried microalgal biomass is the product, while carbon is supplied as a CO_2-enriched gaseous stream freely available from flue gases, and other nutrients are bought from the market. Alternately, the cost of nutrient supply could be minimized by exploiting wastewater sources to this scope, but this possibility was not investigated in thid Chapter (Sforza et al., 2014b).

The procedure applied is according to the paper by Ramos Tercero et al. (2014), which is based on a cost benefit analysis (CBA) approach proposed by Douglas (1988). In order to develop this analysis, both IC (installation costs) and OC (operation costs) related to all equipment and utilities of the process under study were evaluated. For the calculation of annual operating costs, a stream factor of 0.93 was considered and, in order to identify and compare the IC and OC which are more relevant for the process, the ICs were annualized using the Capital Charge Factor (CCF) of 1/3 $year^{-1}$ (Douglas, 1988).

For the process profitability analysis the Total Capital Investment (TCI) and the Total Product Cost (TPC) were estimated, with a level of accuracy between +30% and -20%. The calculation of the economic profitability is based on the cash flow profiles according to three indexes: the discounted payback time, the NPV (Net Present Value) and the IRR (Internal Rate of Return).

$FCI = TCI/1.30$ TCI is derived from the value of total IC, while FCI (Fixed Capital Invested) is based on TCI according to:

$$TCI = 2.36(IC) \quad \text{(Eq. 4.8)}$$

$$FCI = TCI/1.30 \quad \text{(Eq. 4.9)}$$

By taking out the land cost from FCI, the parameter needed for cash flow calculation (i.e. FCI_L) can be evaluated. An average land cost of \$7,500/ha was assumed ("http://www.agenziaentrate.gov.it/," n.d.).

The estimate of the TPC_{wd} (Total Product Cost excluding depreciation) is given by (Douglas, 1988):

$$TCP_{wd} = (1.03 \cdot OC) + (0.18 \cdot IC) + (1 \cdot 10^5 \cdot No.workers) + (0.025 \cdot Revenues) \quad \text{(Eq. 4.10)}$$

Note that Eqs. 4.8 to 4.10 have been proposed to perform CBA of chemical/biochemical processes (Douglas, 1988). Therefore, these equations have been applied to all units and pieces of equipment of our process, excluding IC of PV modules (including maintenance), which were directly accounted for in the cash flow analysis, according to actual market price due to the large availability of table of investment cost for this kind of plants.

A number of workers equal to 5 was assumed, and the revenues were calculated taking into account both the biomass and the electrical energy produced. The annual revenues from sales depend on the unit selling price of electricity, which was set equal to 0.16 €/kWh (average cost of kWh for the Italian energy market) and of the microalgae, whose value was determined iteratively by the cash-flow analysis in order to reach the breakeven point in ten years (Internal Rate of Return = 0%), according to the following hypothesis:

- useful life of the plant is 10 years, the first 2 of which are used for its construction;
- land is purchased at the end of year 0;
- 60% of FCI_L (FCI excluding the land cost) is invested in the first year, the remaining 40 % in year 2;
- at the end of year 2, the WC (Working Capital) and StC (Start-up Costs) are invested, to start the operations of the plant. WC is assumed as 15% of TCI, and StC as 10% of FCI (Douglas, 1988);
- an income tax rate of 45%, is taken based on Italian situation (Istituto nazionale di Statistica, 2013);
- depreciation in the first 7 years of life is evaluated by DDB (Double Declining Balance);
- salvage value of the plant is 10% of FCI_L (Douglas, 1988);
- the discounted cash flows are calculated taking the year of plant construction as "year zero".

4.3. Results and discussion

4.3.1. Irradiances inside the greenhouse with and without PV

First of all the irradiances inside the greenhouse were simulated for the different months of the year by means of DIAlux, both with the roof of the greenhouse partially covered by PV modules, and without them (i.e. with a fully transparent greenhouse). This was done at various times of the day, for the two geographical positions considered (Northern and Southern Italy, respectively).

When PV modules are installed, at the raceway pond level the sunlight intensity profiles lead to alternately shaded and illuminated areas, as shown in Figure 4.3. Here, two examples are reported at noon time: a Summer day (Figure 4.3A) and a Winter day (Figure 4.3B). Clearly, due to the sun inclination, the shaded area is much larger in winter than in summer, and this is true all along the day.

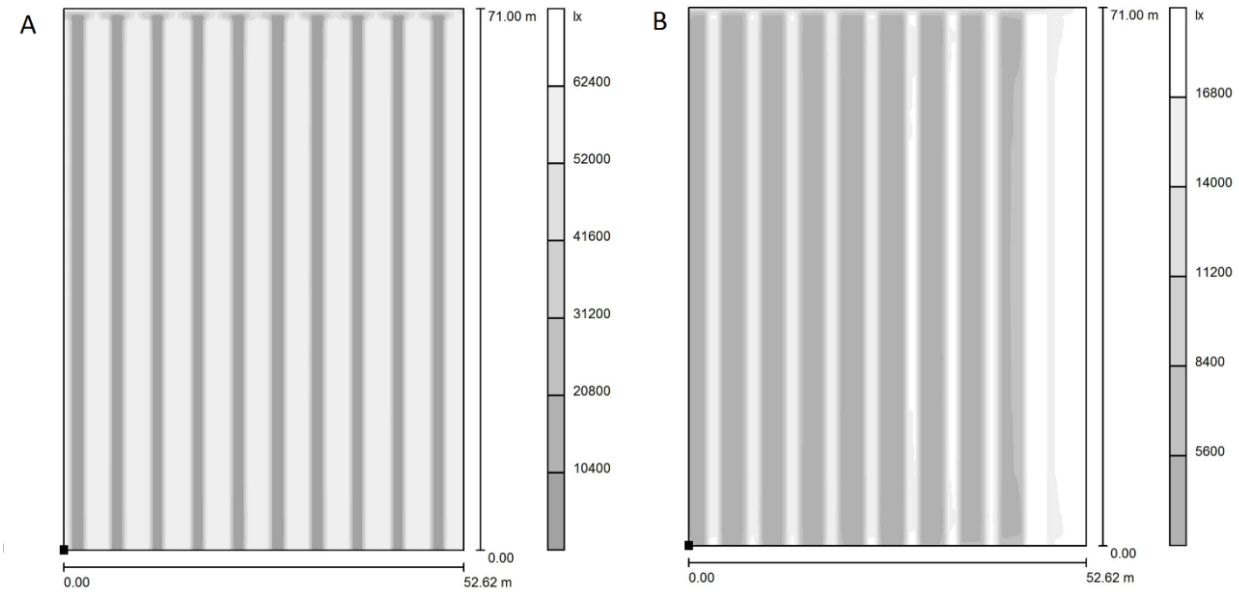

Figure 4.3. *Irradiation and shading pattern inside the greenhouse at ground level at noon in Summer (A) and in Winter (B) for the Southern location*

The values of sunlight radiation intensity as a function of the time of the day are reported in Figure 4.4, again with respect to the Southern location, in both the shaded and the illuminated position. In Figure 4.4 only the maximum (for illuminated), minimum (for shaded) and surface

averaged irradiance are plotted, but all the punctual radiation values along the surface are available. In the same plots, also the light impinging the greenhouse roof (from PVGIS data) is displayed, for the four seasons.

It can be concluded that in all the seasons and apart of the effect of the PV modules, a reduction of light available for microalgal growth is caused by the greenhouse itself, due to the absorption/reflection of its walls. Of course, the light reduction effect is stronger in the winter season when the PV panels are present, as because of the sun inclination the shaded bands at the ground level are larger (i.e., the surface-averaged irradiance is lower).

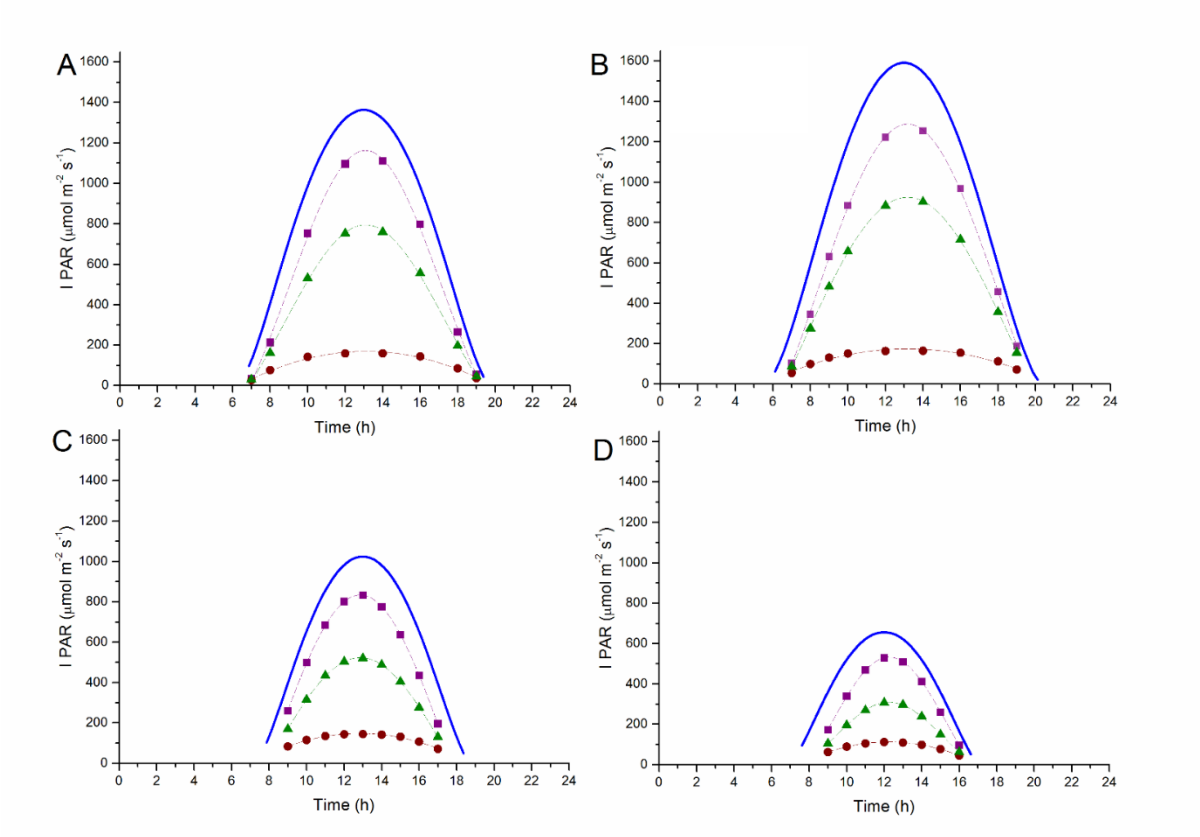

Figure 4.4. *Sunlight intensity both outside (continuous blue line) and inside the greenhouse for spring (A), summer (B), fall (C) and winter (D) of Southern location. Purple quares indicate the irradiated zone of the greenhouse, red circles the dark one and green triangle the surface-averaged data of irradiation.*

4.3.2. Temperature inside the greenhouse with and without PV

By means of the simulator CASANOVA the temperatures, both inside (room) and outside (outdoor) the greenhouse were simulated. An example is shown in Figure 4.5 for the Southern position in the spring season.

To summarize these results the average intensity and temperature within the greenhouse for each season are reported in Table 4.3, both with (A) and without (B) PV cells.

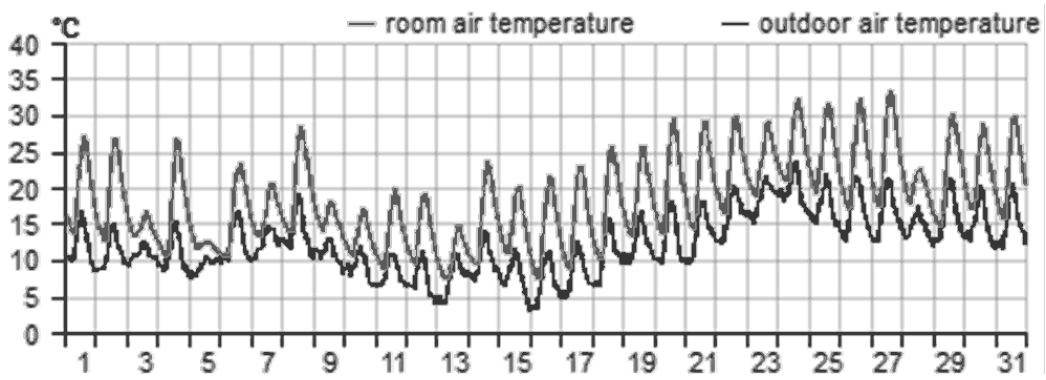

Figure 4.5 *Monthly temperatures outside (black) and inside (gray) the greenhouse for the Southern location in the spring season*

4.3.3. Productivity

Table 4.3 summarizes also the residence times used in the open pond simulations and the corresponding average microalgae concentrations calculated in the reactor by considering the daily irradiation profile inside the greenhouse (third and fourth columns). Accordingly, the volumetric and areal biomass productivities were also evaluated (fifth and sixth columns of Table 4.3). Eventually, values of photosynthetic efficiency referred to both the intensity inside the greenhouse (i.e., that available to the algal culture) and the incident sunlight (i.e. the light impinging the greenhouse) are reported in the last two columns of Table 4.3. It should be noticed that the values of photosynthetic efficiencies obtained are realistic, and correspond to the range of data obtained in actual pilot scale systems (Chisti, 2013).

Table 4.3. *Irradiances, averaged temperatures and seasonal productivities at North (a) and South (b)*

a)

Case	Season	I_avg (µmol m^{-2} s^{-1})	T [°C]	τ_{min} (d)	c_x (g L^{-1})	$P_{x,v}$ (g L^{-1} d^{-1})	$P_{x,A}$ (g m^{-2} d^{-1})	η_{in} (%)	η_{out} (%)
with PV	Spring	215	17	1.83	0.205	0.112	11.18	2.55	1.39
	Summer	302	24.9	1.13	0.270	0.239	23.90	3.88	2.98
	Fall	101	11	4.53	0.132	0.029	2.91	1.41	0.36
	Winter	40	6.2	19.3	0.000	0.000	0.00	0.00	0.00
without PV	Spring	334	19	1.81	0.246	0.136	13.58	2.00	1.69
	Summer	432	26.9	1.17	0.318	0.272	27.20	3.09	3.39
	Fall	172	13	3.61	0.143	0.039	3.95	1.13	0.49
	Winter	75	8.2	12.14	0.000	0.000	0.00	0.00	0.00

b)

Case	Season	I_avg (µmol m^{-2} s^{-1})	T (°C)	τ_{min} (d)	c_x (g L^{-1})	$P_{x,v}$ (g L^{-1} d^{-1})	$P_{x,A}$ (g m^{-2} d^{-1})	η (%)	η_{out} (%)
with PV	Spring	245	23.7	1.18	0.147	0.124	12.45	2.49	2.59
	Summer	317	27.5	1.13	0.268	0.237	23.73	3.67	1.36
	Fall	135	24.0	1.36	0.174	0.128	12.77	4.65	1.39
	Winter	69	18.4	2.70	0.134	0.050	4.98	3.54	0.54
without PV	Spring	363	25.7	1.13	0.178	0.158	15.78	2.13	2.50
	Summer	442	29.5	1.37	0.313	0.229	22.87	2.54	1.72
	Fall	225	26.0	1.13	0.118	0.105	10.47	2.28	1.14
	Winter	125	20.4	1.67	0.162	0.097	9.69	3.80	1.06

These results clearly show that the production of microalgal biomass is only slightly reduced by the presence of PV modules in the northern location, due to the shading effect. Accordingly, the photosynthetic efficiency, which spans between 2% and 5%, is increased. As about the southern location, where the irradiance is higher and photoinhibition is likely to occur, the beneficial effect of covering the greenhouse also lead to an increased areal productivity, for summer and fall. This is in agreement with experimental evidences, for instance the data reported in Chapter 3. In Table 4.3, it can also be seen that, for the Northern location, zero production was obtained when simulating the Winter season, where calculations show that the sunlight energy available and especially the water temperature are insufficient to sustain microalgal growth with acceptable residence times (i.e. less than 10 d). It means that plant operation has to be stopped in December, January and February at the Northern position.

4.3.4. Energy balance and yield

The energy powers available from PV modules and those required to run the plant equipment are summarized in Tables 4.4A and 4.4B for the Northern and Southern positions, respectively. It is seen that, in all the seasons, the power supplied by PV is largely sufficient to sustain the plant operation energy duties for both of these geographical locations.

Table 4.4 *PV power and energy consumed for operation reported as MWh per season in the case of Northern (a) and Southern (b) location*

a)

Case	Season	PV power	Centrifuge	Dryer	Blower CO2	Mixing
with PV	**Spring**	199.9	6.14	31.58	5.15	2.66
	Summer	246.5	9.95	67.51	11.02	2.66
	Fall	141.4	2.48	8.21	1.34	2.66
	Winter	95.4	0.00	0.00	0.00	0.00
without PV	**Spring**	0.00	6.21	38.36	6.26	2.66
	Summer	0.00	9.61	76.82	12.54	2.66
	Fall	0.00	3.11	11.15	1.82	2.66
	Winter	0.00	0.00	0.00	0.00	0.00

b)

Case	Season	PV power	Centrifuge	Dryer	Blower CO2	Mixing
with PV	**Spring**	257.3	9.52	35.16	11.48	2.66
	Summer	267.5	9.95	67.01	21.87	2.66
	Fall	211.9	8.26	36.07	11.78	2.66
	Winter	146.5	4.16	13.99	4.57	2.66
without PV	**Spring**	0.00	9.95	44.57	14.55	2.66
	Summer	0.00	8.20	64.59	21.08	2.66
	Fall	0.00	9.95	29.57	9.65	2.66
	Winter	0.00	6.73	27.38	8.94	2.66

By comparing the energy stored as biomass and that from PV panels it can be concluded that the case with PV modules on the greenhouse roof is highly advantageous. In fact, the ratio between electrical energy and biochemical energy produced ranges from about 2.15 (North) to 2.55 (South) (Figure 4.6A).

This is even more evident when accounting for the higher quality of the electricity with respect to heat: PV modules are able to catch about 5.38-6.36 times more than microalgae of the available sunlight energy (Figure 4.6B), increasing the overall exploitation of sunlight in the given area.

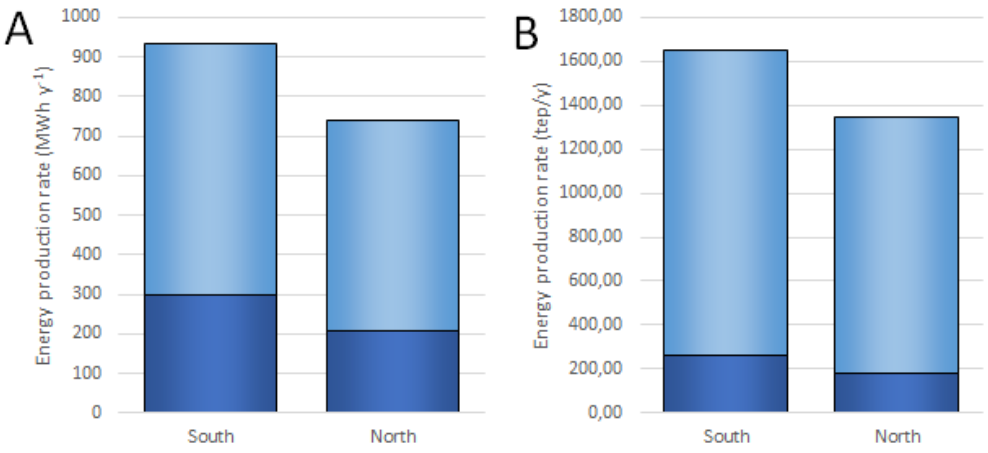

Figure 4.6 *Energy produced by biomass (dark) and PV (gray) for southern and northern locations. In 4.6A the energy produced is directly compared, by applying the LHV value for biomass. In 4.6B a comparison based on Tonns of Oil Equivalent (tep) was made.*

4.3.5. Economic analysis

A first important result from CBA relates to the share of IC and OC within the total production costs of the dried microalgal biomass. This is displayed in figures 4.7A and B, with PV modules and without them, respectively, for the Southern location on an annual basis (similar results were obtained for the Northern one).

Clearly, the PV modules costs are most relevant, accounting for about 50% of the total value and increasing it by 90% with respect to the greenhouse without PV. Second in the list is the greenhouse capital cost.

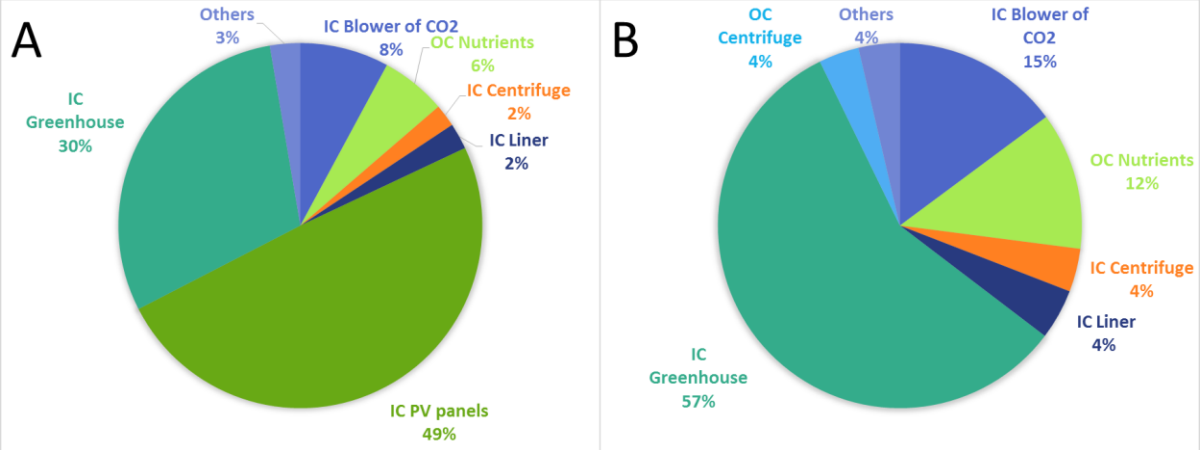

Figure 4.7 *Annualized IC e OC for Southern location with PV (A) and without PV (B)*

All other items are less important with PV, summing up to almost 20% of the total, and raise to about 40% when PV is not present.

A second key point is the return of the investment in the different cases considered. Table 4.5 reports the break-even market price of dry biomass to ensure saving the capital invested within a 10-year perspective. These values span from 13.8 \$ kg^{-1} (with PV, South) to 23 \$ kg^{-1} (without PV, North) and are very well positioned with respect to the market price of biomass of other species like *Chlorella* or *Spirulina* (Doucha and Livansky, 2014; "www.fao.org/3/a-az386e.pdf," n.d.).

Table 4.5 *Market price of microalgal biomass (\$ kg^{-1}) needed to ensure saving the capital invested within a 10-year perspective*

	North		South	
	with PV	**no PV**	**with PV**	**no PV**
\$ kg^{-1}	22.3	23	13.8	16.4

In Figure 4.8, the cumulated cash-flow profile is represented for the Southern location. Even though the energy produced by the PV modules is much higher than that accumulated as biomass (§4.3.4), the revenues from biomass sale are far more relevant than those obtained from the sale of electrical energy, due also to the fixed value of the market price of electricity. However, the PV plant itself has a quite fast return of investment (about 6.7 years for the North and 5.7 for South), thus increasing the inlet cash-flow with respect to the case without PV.

In summary, this analysis shows that integrating microalgae production with PV results to be always beneficial, as its break-even point value is lowered by about 16% at the Southern location, and about 3% at the Northern one.

This is a general result, but both the biomass and electricity production, and the corresponding economic advantage that can be achieved, depend on the assumptions done, especially on the fraction of greenhouse surface covered by PV modules. As the energy duty of the whole microalgae cultivation process is by far less than the electricity produced with 50% of coverage, the latter could be reduced, especially in locations with less radiation, resulting in larger biomass throughput. However, optimizing the PV roof coverage is outside the scope of this chapter. It also needs to be pointed out that technological advancement is likely to reduce installation costs of Algreenhouse within a shorter time, thus making the perspective of its application more and more attractive in the years to come.

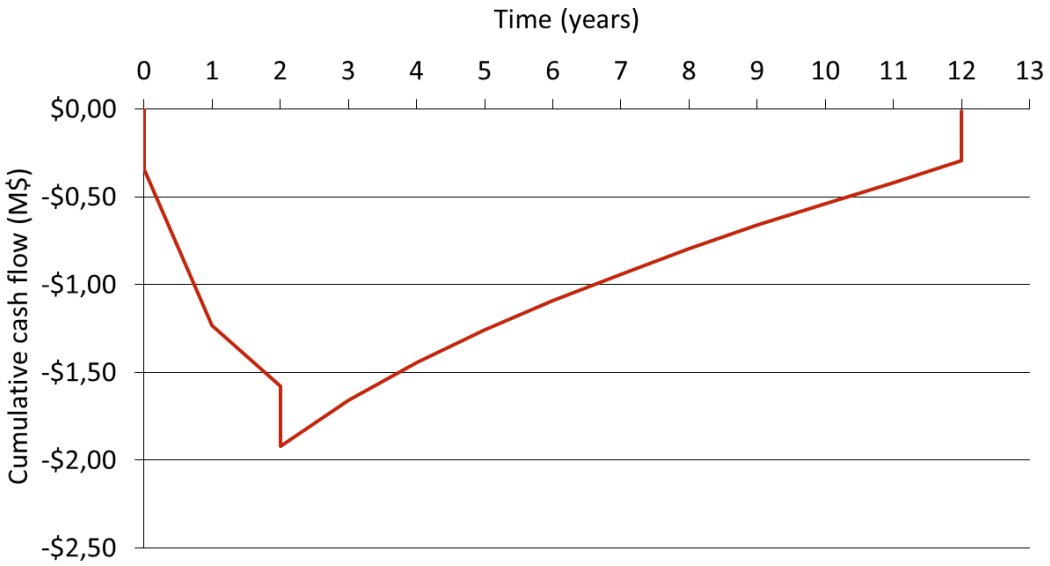

Figure 4.8 *Cash flow of plant with PV in the case of Southern location*

4.4. Final remarks

In this Chapter a microalgae open-pond cultivation system placed inside a greenhouse partially covered by PV modules (Algreenhouse) was addressed.

Two different Italian latitudes and the corresponding irradiations and temperatures were considered to calculate the biomass and electricity productions, the process energy efficiency and a cost benefit analysis of the plant. The open-pond performances of a number of configurations were simulated taking into account light attenuation, temperature and biomass growth according to validated models.
The presence of commercial photovoltaic modules showed to be beneficial with respect to biomass productivity under high irradiation, due to the shading effect which decreases photoinhibition phenomena, but lead to a decreased production, especially in the winter season, when light is limiting. It was found that the presence of PV modules strongly increases the overall sunlight conversion efficiency, and the electricity produced by PV can be exploited to energetically self-sustain the process.

From the economic standpoint, in spite of the large increase of capital cost due to PV modules, the return of investment of the PV installation is fast. Thus, the cash flow of the entire process is improved, and the break-even market price of the biomass produced is lower when using the Algreenhouse system, for both the locations considered. Although these calculations were performed for a fixed value of the percent of greenhouse roof covered by PV modules, this variable can be optimized in view of a specific goal.
In summary, the results presented show that, in spite of the higher investment required when coupling photovoltaics with raceway ponds in a greenhouse, the economicity of the process to produce microalgal biomass is substantially improved compared to the case of a transparent greenhouse. Therefore, the Algreenhouse system proposed could become an attractive technology for large-scale production of microalgal biomass.

Chapter 5

Cultivation of *Scenedesmus obliquus* and *Nannochloropsis gaditana* in the liquid hydrolysate obtained from flash hydrolysis of the same microalgae

The production of biofuels from microalgae is associated with high demands of nutrients (nitrogen and phosphorus) required for growth. Recycling nutrients from the residual biomass is essential to obtain a sustainable production. In this chapter, the aqueous phases obtained from flash hydrolysis of the freshwater alga *Scenedesmus sp.* and of the marine species *Nannochloropsis gaditana* were used as cultivation medium for a microalga of the same genus respectively, to assess the feasibility of this technique for nutrient recycling purposes. Batch and continuous cultivations were carried out, to determine growth performances in this substrate compared to standard media, and verify if a stable biomass production could be obtained. In continuous experiments, the effect of hydrolysate inlet concentration and of residence time were assessed to optimize nutrient supply in relation to productivity. The results obtained show that *Scenedesmus obliquus* was able to grow efficiently in the hydrolysate, exploiting the organic nitrogen and carbon available in the medium, as well as all the micronutrients. Experiments with *N. gaditana* instead show that this species was also able to grow in this medium, but the release of inorganic ammonium from amino-acids and peptides is necessary. However, phosphorus resulted to be readily available. In summary, the results contained in this chapter show that nutrient recycling is feasible by treating biomass with flash hydrolysis, even though the growth performances are related to the species considered.

[0]Part of this chapter was published in Bioresource Technology (Barbera E., Sforza E., Kumar S., Morosinotto T., Bertucco A., 2016. 207:59-66) and in AIChE Journal (Teymouri A., Kumar S., Barbera E., Sforza E., Bertucco A., Morosinotto T., 2016. *In Press*)

5.1. Introduction

Microalgae have been widely recognized as a very promising feedstock for biofuels and bio-products, aiming at replacing traditional fossil fuels and reducing greenhouse gas emissions, especially for the transportation sector. The numerous advantages that these microorganisms offer compared to terrestrial plants are very well established, such as the possibility of cultivation on non-arable land, the ability of capturing CO_2 from flue-gases, together with higher growth rates, productivities and photosynthetic efficiencies (Mata et al., 2010; Quinn and Davis, 2015; Ullah et al., 2015). Nonetheless, several issues have still to be addressed and solved in order for microalgae-based biofuels production to be sustainable (Chisti, 2013).

Clearly, in order to achieve significant displacement of petroleum-based fuels, very large volumes of microalgal biomass need to be produced. This is associated with the necessity of consistent amounts of nutrients that are required for growth, mainly nitrogen (N) and phosphorus (P). Even though at the beginning nutrients were often neglected when evaluating costs estimates, they are emerging as one of the highest operational costs (Pate et al., 2011). In addition to economic implications, extensive nutrients requirements raise also environmental and sustainability issues. In fact, based on a typical microalgae elemental composition, it can be estimated that, assuming 100% nutrient uptake, roughly 88 kg of N and 12 kg of P are required for producing 1 ton of algal biomass. Pate et al. (Pate et al., 2011) reported that, considering a target biofuels production of 10 billion gallons per year and a biomass oil content of 20%, the nitrogen and phosphorus required for algae cultivation would account for 107% and 51% of overall US consumption, respectively. Moreover, it has to be considered that N and P fertilizers are currently derived from mineral or fossil resources, whose availability is therefore limited. This is particularly critical for phosphorus, since the natural reserves of phosphate rocks are finite, and expected to be depleted in the future (Gifford et al., 2015; Markou et al., 2014; Pate et al., 2011; Ward et al., 2014). Nitrogen is on the contrary more abundant, but its production requires energy intensive processes (Haber-Bosh) (Peccia et al., 2013). Based on these considerations, it is clear that the only way to obtain an economically and environmentally sustainable microalgal biofuels production is to recycle the nutrients, the majority of which is not included in the lipid fraction destined to biofuels, and remains in the residuals. This possibility is clearly highly connected with the method employed for biomass

treatment after harvesting. In this regard, different alternatives have been recently proposed (Rösch et al., 2012; Zhang et al., 2014), from anaerobic digestion after lipid extraction (Bruno Sialve et al., 2009; Ward et al., 2014), to hydrothermal treatments (Biller et al., 2012; Garcia Alba et al., 2013; Heilmann et al., 2011; Levine et al., 2013; López Barreiro et al., 2013). Among hydrothermal processes, flash hydrolysis (FH) has been proven to be an interesting and environmentally friendly strategy to extract energy dense molecules from biomass: it consists in processing the algae slurry, harvested from the cultivation system, in a continuous-flow reactor under subcritical water conditions (200°C – 300°C) and few seconds of residence time (6s – 10s) (Garcia-Moscoso et al., 2015, 2013). This treatment allows obtaining two phases. The main product of the process is a low-N, high-C solid, that retains the lipid fraction, and is therefore an intermediate for biofuels production (Garcia-Moscoso et al., 2015, 2013). Lipids in this biofuels intermediate are more concentrated and easily extractable compared to the original biomass. The second phase is a liquid hydrolysate that contains the hydrolyzed proteins in the form solubilized peptides and amino acids (up to 66% of the initial N content), as well as other inorganic elements (e.g. P, S, K, Na, and Ca), that can be recycled to sustain a new cycle of algal growth. Compared to conventional hydrothermal liquefaction (HTL), which is characterized by longer residence times (generally from few minutes to 1 h), flash hydrolysis offers several advantages. Firstly, lipids are retained and preserved in the solid fraction, while the former produces an organic liquid phase (biocrude), which has to be separated and refined prior to use as fuel for transportation. Also, the amount of phenolic compounds produced, which are known to have inhibitory effects on algae growth when the liquid phase is recycled, is reported to be much lower in the hydrolysate obtained from FH compared to the aqueous phase from HTL (Garcia-Moscoso et al., 2015).

This work aims at assessing the feasibility of using residuals from flash hydrolysis for nutrient recycling to improve the sustainability of biofuels production. For this purpose, two different microalgae species, the freshwater *Scenedesmus obliquus* and the marine *Nannochloropsis gaditana* were cultivated in the liquid hydrolysates obtained from flash hydrolysis of algae biomass belonging to the same genus, respectively. Firstly, batch experiments were carried out under different experimental conditions to compare the growth potential in this substrate with a synthetic cultivation medium where all the nutrients are supplied as soluble inorganic salts. However, despite batch studies are fundamental to determine growth parameters, continuous

cultivation is preferable when considering large-scale industrial plants, as it allows reaching steady-state, stable and continuous biomass production (Sforza et al., 2014a). For this reason, *S. obliquus* was also cultivated in a continuous laboratory-scale photobioreactor (PBR) fed with the hydrolysate, to assess the performances achievable in terms of biomass productivity and efficiency. Specific attention was given to nutrients consumptions and corresponding content in the biomass produced, in order to minimize the amount supplied to the culture while at the same time maintaining an acceptable productivity. Finally, the effect of the residence time of the culture inside the PBR on productivity and on nutrients content was taken into consideration.

5.2. Materials and methods

5.2.1. Algae strains and culture media

Scenedesmus obliquus 276.7 (obtained from SAG-Goettingen, Germany) was maintained in sterile BG11 medium, with 1.5 g L^{-1} $NaNO_3$ (247 mg L^{-1} N) and 30.5 mg L^{-1} K_2HPO_4 (5.4 mg L^{-1} P), buffered with 10 mM HEPES pH 8. For all control experiments, BG11 was modified so that N was supplied as NH_4Cl (keeping an equivalent concentration of 247 mg L^{-1} N). In continuous experiments, BG11 was further modified in order to guarantee non-limiting nutrient concentrations: 494 mg L^{-1} of N (NH_4Cl) and 89 mg L^{-1} of P (K_2HPO_4) (Sforza et al., 2014c).

Nannochloropsis gaditana (strain 849/5, obtained from CCAP) was maintained in sterile f/2 medium, with 33 g L^{-1} sea salts (Sigma -Aldrich), having a concentration of 1.5 g L^{-1} $NaNO_3$ (247 mg L^{-1} N) and 5 mg L^{-1} of $NaH_2PO_4 \cdot H_2O$ (1.12 mg L^{-1} of P), buffered with 40 mM TRIS HCl pH 8. The same medium was used for all control experiments.

The characteristics of the hydrolysate are slightly different for *S. obliquus* and *N. gaditana* respectively. They were obtained from FH of *Scenedesmus* sp. (Garcia-Moscoso et al., 2013) and *Nannochloropsis gaditana* at 280°C and 9 s of residence time. Both were stored, at 4°C, as a freeze-dried powder with the composition summarized in Table 5.1. Nitrogen was available in the medium mainly as soluble peptides and amino acids, with a small fraction (about 30% of the total N for *Scenedesmus* and 10% for *Nannochloropsis*) present as ammonia.

For all batch experiments, an appropriate amount of freeze-dried powder was re-dissolved in distilled water in order to match the same total N concentration of BG11 and f/2 used as a controls (247 mg L^{-1}).

Table 5.1 *Composition of the hydrolysate freeze-dried powder for the two microalgal species*

Element	*Scenedesmus* sp. wt%	*N. gaditana* wt%
C	46.5	35.8
H	7.3	5.8
N	9.6	8.0
P	1.37	1.3
S	2.87	1.0
Ca	0.41	1.6
K	1.65	4.5
Mg	0.06	0.3
Cl	0.07	15.8
Na	-	1.1

This corresponds to a P concentration of 35 mg L^{-1} and 40 mg L^{-1} for the two species respectively (mainly present as phosphate, PO_4-P). For experiments with *N. gaditana* in addition, 33 g L^{-1} of sea salts were added to the medium. In continuous experiments with *S. obliquus*, the hydrolysate concentration was varied as described in §5.3.3. No sterilization was carried out on the hydrolysate prior to inoculation.

5.2.2. Experimental set-up

Experiments were conducted in both batch and continuous mode. The temperature was kept constant at 23 ± 1 °C for all the experiments, in a refrigerated incubator. Artificial white light was provided by a LED Lamp (Photon System Instruments, SN-SL 3500-22), and the photon flux density (PFD) provided to the culture was measured with a photoradiometer (HD 2101.1 from Delta OHM), which quantifies the PAR (Photosynthetically Active Radiation, 400-700 nm). Except when explicitly specified, CO_2-enriched air (5% v/v, regulated by two flowmeters) was supplied to the cultures, at total flow-rate of 1 L h^{-1}.

Batch experiments were carried out in Drechsel bottles with 5 cm diameter, at a light intensity of 120 µmol m^{-2} s^{-1} and 150 µmol m^{-2} s^{-1} for *S. obliquus* and *N. gaditana* respectively. Each batch experiment started with an initial microalgae inoculation of OD_{750} = 0.5 in the case of *S. obliquus* and OD_{750} = 0.45 for *N. gaditana*, which correspond to a cell concentration of about $5 \cdot 10^6$ cells mL^{-1}. The culture volume was 100 mL. All experiments were carried out at least in duplicates.

Continuous experiments were performed in a thin vertical flat-plate polycarbonate (PC) PBR with 100 cm^2 irradiated surface and 1.3 cm depth, to maximize light utilization (Sforza et al., 2014a), at a continuous constant light intensity of 150 µmol m^{-2} s^{-1}. CO_2-air mixture was sparged from the bottom of the reactor, ensuring culture mixing, which was also aided by a stirring magnet. Fresh medium was continuously supplied by means of a peristaltic pump (Sci-Q 400, Watson Marlow, USA) that allows to regulate the inlet flow-rate. The reaction volume was kept constant by an overflow tube, through which biomass was withdrawn at the same flow-rate. A scheme of the continuous experiments set-up is shown in Figure 5.1.

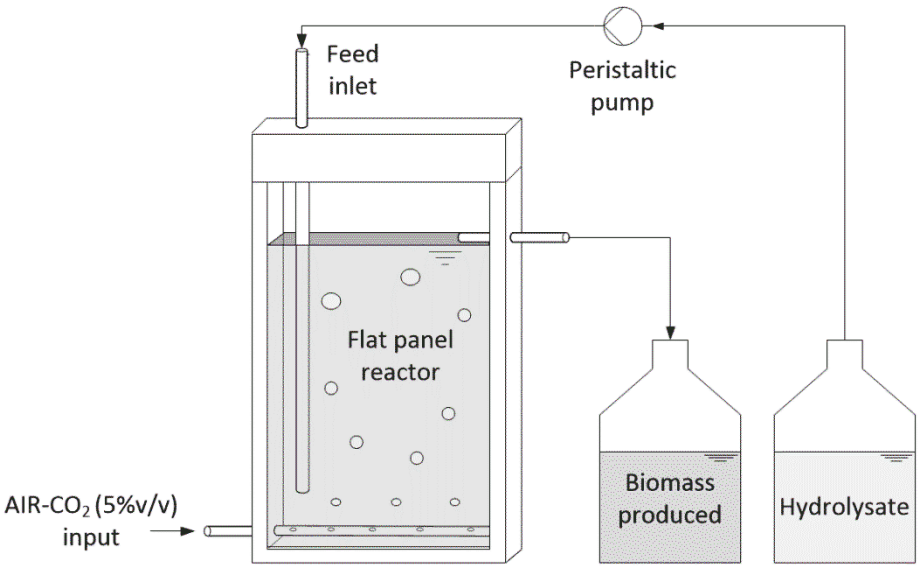

Figure 5.1 *Scheme of the flat-panel photobioreactor used in continuous experiments*

The residence time of the culture inside the PBR is regulated by the pump, and calculated according to:

$$\tau = \frac{V_R}{Q} \quad \text{(Eq. 5.1)}$$

where V_R is the reactor volume (130 mL) and Q the volumetric flow-rate. After a transient, observed when changing experimental conditions, the biomass concentration was found stable, and a steady state was achieved. As the PBR described can be approximated to a CSTR (Bertucco et al., 2014), steady state productivity P_x was then calculated by:

$$P_x = \frac{c_x}{\tau} \quad \text{(Eq.5.2)}$$

c_x being the average outlet biomass concentration, of at least 4 experimental measures in different days at steady state. The photosynthetic efficiency (PE), referred to the irradiated PAR, is evaluated as:

$$\eta_{PAR}\% = \frac{c_x \cdot Q \cdot LHV}{PFD_{in} \cdot E_p \cdot A_{PBR}} \cdot 100 \quad \text{(Eq. 5.3)}$$

where LHV is the lower heating value of the biomass (22 MJ kg^{-1} (Sforza et al., 2014c)), PFD_{in} the radiation hitting the PBR front surface (μmol m^{-2} s^{-1}), E_p the energy of photons (kJ μmol^{-1}), and A_{PBR} the irradiated surface of the flat-panel reactor.

5.2.3. Analytical procedures

Algal growth was monitored daily in both batch and continuous experiments, by measuring the optical density (OD) at 750 nm with a UV-visible UV 500 double beam spectrophotometer (from Spectronic Unicam, UK). In addition, cell concentration was measured using a Bürker Counting Chamber (HBG, Germany). Specific growth rate of batch experiments were obtained by linear regression of the logarithm of multiple experimental points of the exponential phase of growth, taken as the average of two independent biological replicates. At the end of the batch growth curves, and daily in continuous experiments, biomass concentration was measured as dry weight (DW, g L^{-1}). DW was measured gravimetrically by filtering 5 mL of culture sample with 0.22 μm cellulose acetate filters, which are then dried for 4 h at 90°C in a laboratory oven. In the case of *N. gaditana*, the sample was previously 1:5 in order to dissolve salts, and 0.45 μm filters were used. In the case of growth experiments using the hydrolyzate,

the DW of the medium itself was previously measured and subtracted from that of the total sample. N, P and Chemical Oxygen Demand (COD) concentrations were measured spectrophotometrically, using standard test kits, at initial and final points for batch experiments, and in the inlet and outlet streams, for at least three days of steady state, in continuous experiments. A sample of culture was filtered (0.22 μm) to measure only the dissolved nutrients. Total nitrogen (TN) was measured using HYDROCECK MONOTEST (provided by Reasol®), based on oxidation of all nitrogen compounds to nitrates. By reaction with 2,6-dimethylphenol a dying molecule is then produced and detected at 340 nm using Spectronic Unicam UV-500 UV-visible spectrometer. Ammonium (NH_4-N) was measured with HYDROCHECK SPECTRATEST (Reasol®), by reaction with Nessler reagent in alkaline conditions, and subsequent absorbance measurement at 445 nm. Phosphorus (PO_4-P) is measured by the absorbance (at 705 nm) of a dying complex between ortophosphate ions and molybdenum under reducing environment. Finally, COD was measured by an analytical kit provided by Sigma-Aldrich, USA (AQUANAL®) and is based on oxidation of organic compounds by potassium dichromate in sulfuric acid solution.

5.3. Results and discussion

5.3.1. Batch experiments with *Scenedesmus obliquus*

Batch experiments were conducted in Drechsel bottles using the hydrolysate obtained from flash hydrolysis as culture medium, in order to test the microalgal ability to grow in this substrate, and assess the feasibility of using this technique for nutrient recycling. The growth of *Scenedesmus obliquus* was measured, both in the hydrolysate and in BG11, in different experimental conditions, namely under both a continuous and alternated light (12 h of constant light followed by 12 h of dark) of 120 μmol m^{-2} s^{-1}, and with or without bubbling of air enriched with CO_2 (5% v/v), respectively. The growth curves obtained in each condition are reported in Figure 5.2, and the corresponding specific growth rates (d^{-1}) summarized in Table 5.2.

Table 5.2 *Specific growth rate of Scenedesmus obliquus in the hydrolysate and in BG11 (control), under different experimental conditions. Statistically different results are marked with the same letter.*

Specific growth rate k (d^{-1})	Hydrolysate	BG11 (control)
Continuous light, CO_2 (5% v/v)	1.05 ± 0.141^a	0.566 ± 0.031^a
Alternated light, CO_2 (5% v/v)	0.347 ± 0.004	0.358 ± 0.030
Continuous light, no CO_2	0.343 ± 0.030^b	0.096 ± 0.025^b
Alternated light, no CO_2	0.223 ± 0.061^c	0.100 ± 0.020^c

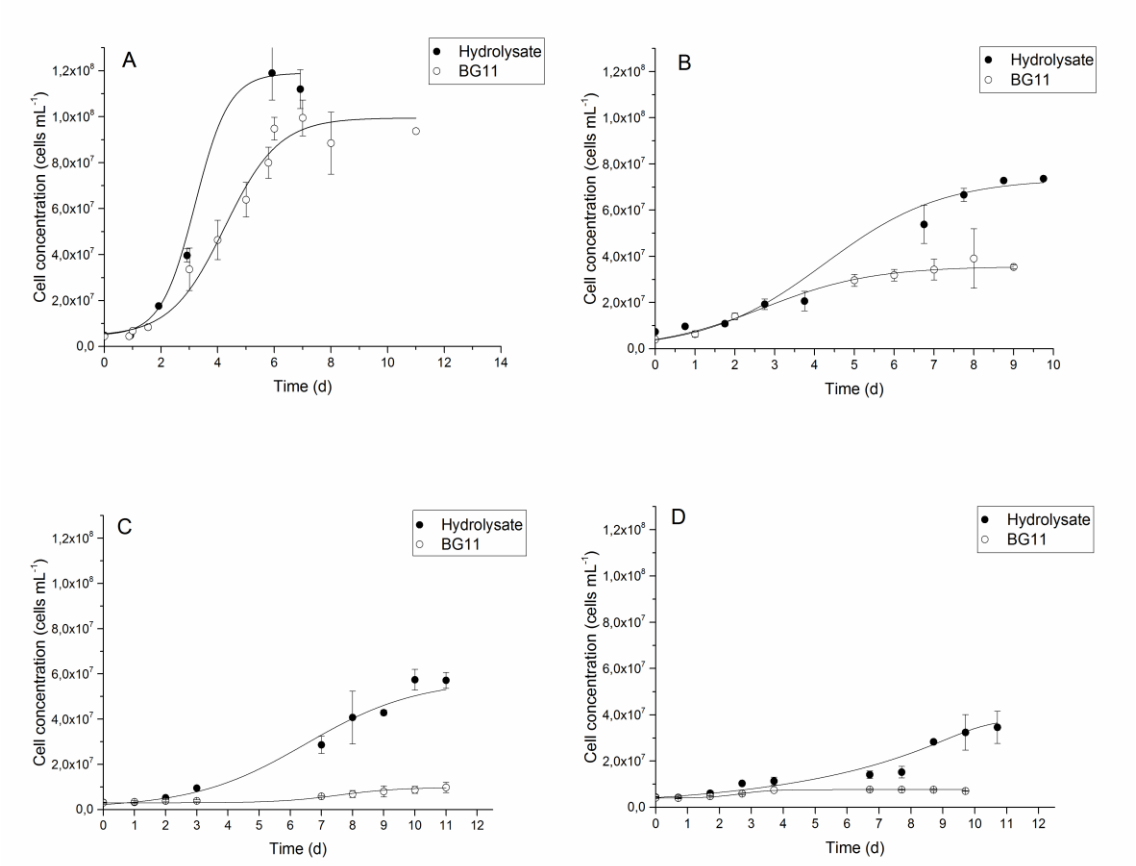

Figure 5.2 *Growth of Scenedesmus obliquus in hydrolysate (full circles), and BG11 (open circles), under different conditions: continuous light and CO_2 bubbling (A), alternated light and CO_2 bubbling (B), continuous light and no CO_2 bubbling (C), alternated light and no CO_2 bubbling (D)*

Under continuous light and bubbling of CO_2 (5% v/v) *S. obliquus* was able to grow efficiently in the hydrolysate, and the specific growth rate resulted to be almost twice the one obtained in the control grown in BG11. Nutrients consumption analyses show that this species was able to uptake the organic nitrogen, available in the medium mainly in the form of amino acids and soluble peptides. In fact, even though roughly 30% of the nitrogen in the hydrolysate is present as ammonium, the consumption of this inorganic form represents only a small fraction of the total nitrogen consumption (Figure 5.3A). This is consistent with results reported in the literature showing the capability of certain microalgal species to utilize simple organic forms (such as urea but also some amino acids) as nitrogen sources, both in autotrophic and heterotrophic cultivation mode (Markou et al., 2014). In particular, Gu et al.(Gu et al., 2015) also found that *Scenedesmus acutus* was able to assimilate nitrogen contained in amino acids, yeast extracts and proteinaceous algal residuals. Phosphorus consumption was also measured, verifying that its concentration was not limiting (Figure 5.3B). Besides N and P, the hydrolysate provided also all the other micronutrients required for growth, as proven by the high growth rate obtained. The high growth rate also confirms that the concentration of toxic molecules in the medium is low, as reported by Garcia Moscoso et al. (Garcia-Moscoso et al., 2015). In addition to nutrients, a COD consumption of 19 to 60% with respect to the initial concentration was also observed (Figure 5.3C).

The possibility of growing microalgae mixotrophically is very interesting, as the possible exploitation of organic carbon may sustain growth when light is not available (i.e. during night). Thus, some experiments were carried out by exposing the culture to day/night cycles. When the light was provided alternating 12 h of illumination with 12 h of dark, in the presence of CO_2 bubbling, the measured growth rate was lower, both in the hydrolysate and in the control, as a consequence of the reduced light energy input. Comparing the two different cultivation media, they both showed the same growth kinetic k (Table 5.2), but the final biomass concentration reached in the hydrolysate was significantly higher. In addition, COD consumption was increased (from 19 up to 44%) compared to the case of constant illumination, suggesting that in the dark algal cells consume more organic carbon to compensate the lack of light energy.

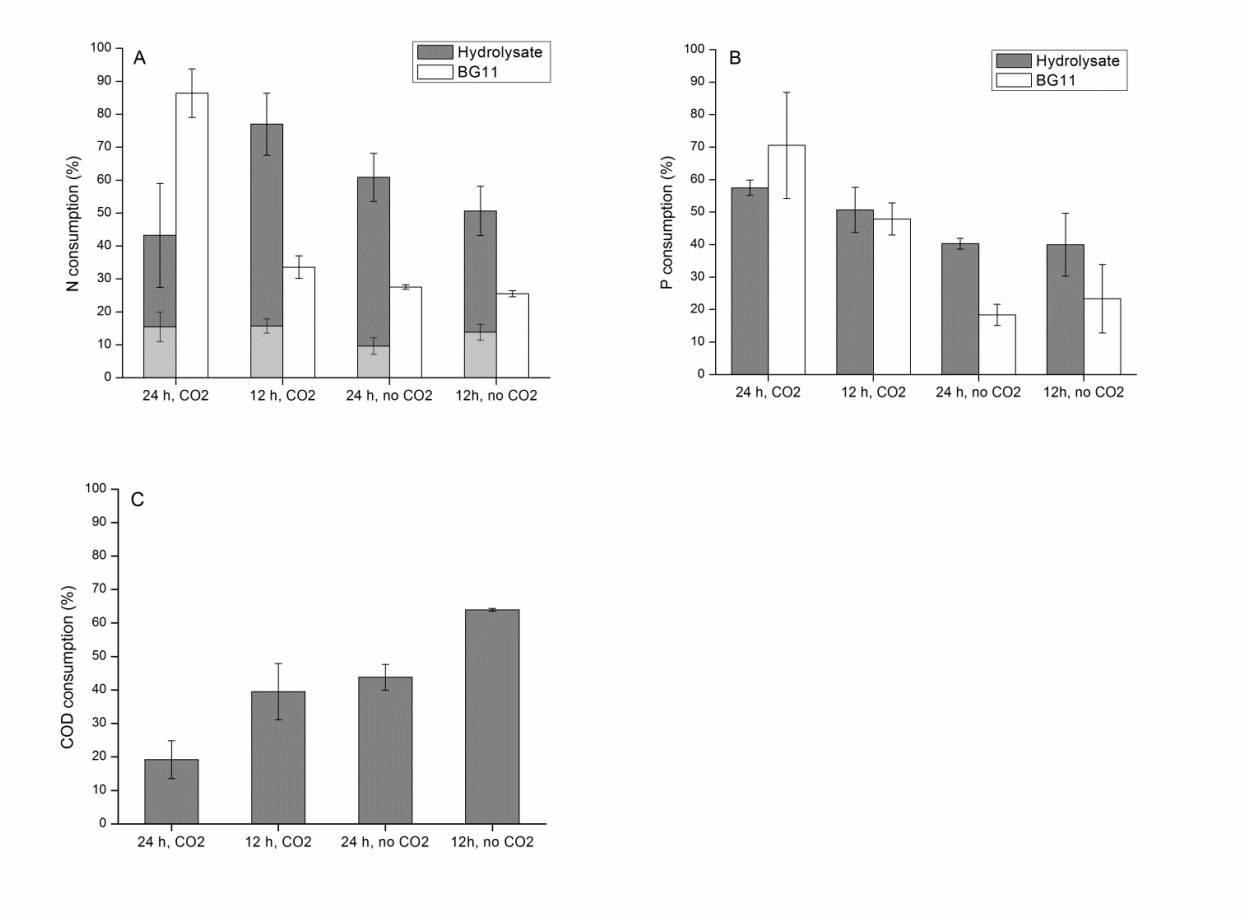

Figure 3 *Nitrogen (A), phosphorus (B) and COD (C) consumption of the hydrolysate cultures (grey) and BG11 controls (white) in different experimental conditions. 24 h stays for continuous light, while 12 h indicates alternated light. In Figure 3A light grey bars indicate the fraction of ammonium consumed with respect to the total initial concentration*

In a previous work, Sforza et al. (2012a) verified that CO_2 inhibits mixotrophy in the cultivation of *Chlorella protothecoides* and *Nannochloropsis salina*, likely because of an inhibition on respiration, and therefore experiments were also carried out without supplying the CO_2-enriched air mixture. When no additional CO_2 was provided to the cultivation system, *S. obliquus* growth in the hydrolysate was much higher than in the control, both in the case of continuous illumination and day/night cycles. The reduced growth in the control is easily explainable by a strong limitation in carbon availability, since the low CO_2 content in atmospheric air is well known to limit productivity. In the hydrolysate, on the contrary, this limitation is less significant because algal cells were able to exploit the organic carbon

available in the medium for their growth, reaching, in the case of continuous illumination, satisfactory cell concentrations and specific growth rates. An alternated illumination resulted again in a reduced growth (except in the control, where carbon instead of light was the limiting factor), but in an increased COD consumption (64% instead of 44% measured for continuous light), strongly supporting the hypothesis that *Scenedesmus* cells can consume organic carbon present in the hydrolysate as an energy source, especially during the dark periods.

The results obtained show that *Scenedesmus obliquus* grows very well in the hydrolysate obtained from flash hydrolysis of the same genus, without the need of sterilization, and growth kinetics and biomass productivities are even better than in the control medium in the various experimental conditions investigated. This may be due to its capability of exploiting the available organic carbon (and nitrogen) and growing mixotrophically. Although these were not specifically monitored, the high growth measured also allows concluding that the hydrolysate contained all micronutrients (e.g. K, Ca, Fe, and Mg) required for the algal growth. When exposed to long dark periods, the increased consumption of COD suggests that organic molecules are used by the cells to get the energy for their growth. However, the great decrease in the specific growth rate obtained in these light conditions (both with and without CO_2 bubbling), compared to the case of continuous illumination, indicates that photosynthesis provides additional advantages and that mixotrophy is preferred over heterotrophy. Finally, *S. obliquus* was seen to be able to use the sole organic carbon available in the recycled medium as a source for growth when no inorganic forms were provided. Nonetheless, the inorganic CO_2 is a highly preferred carbon source, as clearly shown by the much higher growth rates obtained with 5% v/v air-CO_2 bubbling (both under continuous and alternated illumination), and by the lower COD consumption measured when inorganic carbon was also present in the medium. This result is also consistent with what reported by Sforza et al. (Sforza et al., 2012a), who found that an excess CO_2 supply had an inhibitory effect on the organic substrate consumption in mixotrophic growth. The conditions of CO_2 supply appear to be the most favorable also in terms of nutrients consumption, which, from the recycling point of view, should be as high as possible. In fact, when the inorganic carbon is available, roughly 80% of nitrogen and 55% of phosphorus are consumed (Fig. 5.3A and B). When instead this inorganic source is absent, both N and P consumption values drop, resulting in a less efficient exploitation of the nutrients recycled by flash hydrolysis.

5.3.2. Batch experiments with *Nannochloropsis gaditana*

In order to ascertain the capability of a different microalgal species of exploiting the nutrients recycled through FH for growth, *N. gaditana* was cultivated in the corresponding hydrolysate. Results are shown in Figure 5.4. It can be seen that *N. gaditana* was able to grow in the hydrolysate, reaching a final cell concentration of about 40×10^6 cells mL^{-1}. In this case however, the growth rate appeared to be lower compared to that obtained in sterile f/2 medium, used as control, showing in addition an initial lag-phase, which indicates cells adaptation to the new cultivation conditions. In particular, the growth rate resulted to be equal to 0.46 d^{-1} in f/2, and 0.29 d^{-1} in the hydrolysate. Nonetheless, the final biomass concentration measured as dry weight resulted to be similar in the two cases (0.97 ± 0.21 g L^{-1} and 0.93 ± 0.18 g L^{-1} for control and hydrolysate cultures respectively).

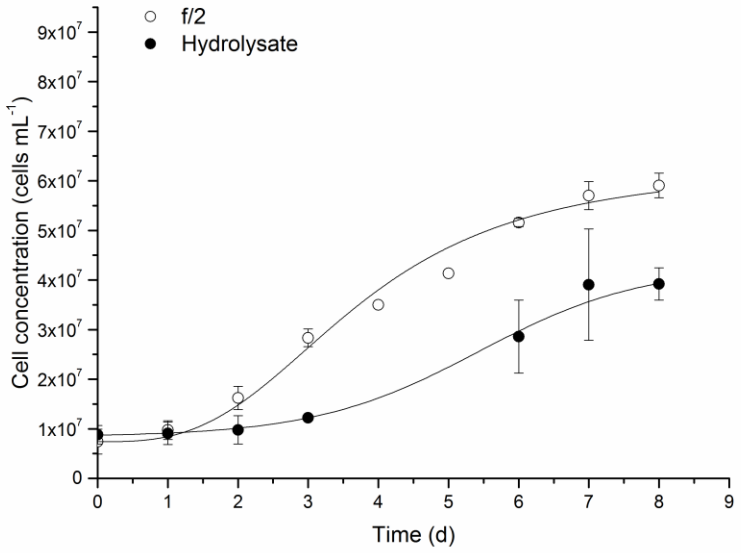

Figure 5.4 *Growth curve of Nannochloropsis gaditana in f/2 (open circles) and in the hydrolysate (full circles)*

In order to determine the bio-availability of the nutrients contained in the hydrolysate, initial and final concentrations were measured. As previously reported, nitrogen is mainly present in the hydrolysate in the form of soluble peptides and amino acids, while only about 10% is available as ammonium (NH_4-N). In the previous paragraph, it was shown that *Scenedesmus*

sp. was able to uptake the organic nitrogen forms contained in the medium and use that for growth. However, the capability of up-taking simple organic nitrogen is species-dependent, and has therefore to be assessed for the species considered (Markou et al., 2014). As reported in Figure 5.5, about 20% of the initial nitrogen (measured as TN) contained in the hydrolysate was consumed by the culture. On the other side, COD measurements show that no consumption of organic carbon is verified (Table 5.3), suggesting that *N. gaditana* did not in fact consume the organic nitrogen available in the medium. This result is consistent with what was reported in the work of López Barreiro *et al.* (López Barreiro et al., 2015) in which no significant organic carbon consumption is measured for *N. gaditana* grown in the aqueous phase obtained from HTL. This is consistent with the limited ability of this species to use organic carbon in mixotrophic conditions (Sforza et al., 2012a).

Interestingly, as also shown in Table 5.3, the concentration of NH_4-N, initially very low, was found to be much higher at the end of the growth curve. This seems to suggest that ammonium was slowly released in the medium, and that the slower growth rate obtained in the hydrolysate compared to that in f/2 could be due to an initially limiting inorganic nitrogen concentration. The slow release of ammonium in the medium is therefore necessary in order to allow algal growth, since this microalga is not able to use organic nitrogen molecules.

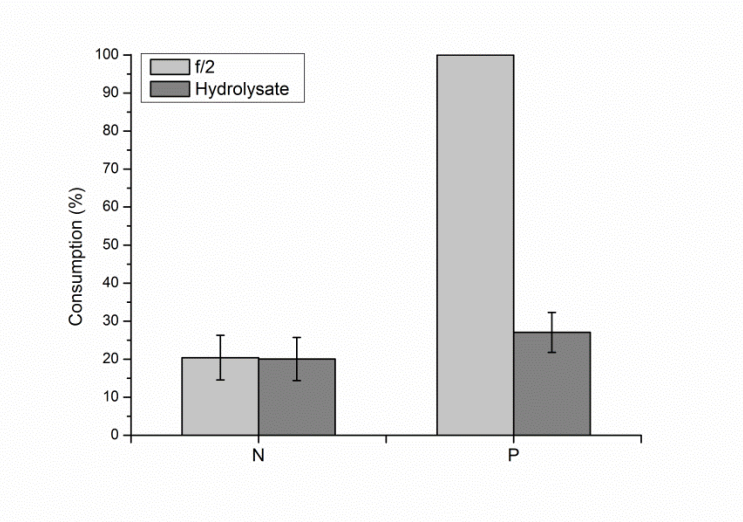

Figure 5.5 *Nitrogen and phosphorus consumption in f/2 (light grey) and hydrolyzate (dark grey)*

Table 5.3 *Initial and final nutrients concentrations in f/2 and hydrolyzate cultures*

	Nutrient	Initial concentration	Final concentration
f/2	N (NO_3-N)	249.07 ± 14.07	198.20 ± 2.56
	P (PO_4-P)	0.68 ± 0.25	0
Hydrolyzate	N (TN)	203.71 ± 11.23	162.88 ± 1.60
	N (NH_4-N)	18.16 ± 0.17	102.13 ± 1.03
	P (PO_4-P)	22.77 ± 1.05	16.60 ± 0.49
	COD	840.19 ± 158.37	1040.58 ± 80.58

Phosphorus, on the other hand, was mainly available in the hydrolysate in the form of orthophosphates, and could be efficiently assimilated by microalgal cells. While the P in f/2 was entirely consumed, being it the limiting nutrient under these experimental conditions, only 27% of that present, in significantly higher concentration, in the hydrolysate was uptaken by the culture (Figure 5.5), likely due to the limiting nitrogen bio-available in this case.

Overall, the liquid hydrolysate obtained from FH of *Nannochloropsis gaditana* was proved to be able to sustain growth of a microalga of the same genus, even without the addition of other macro and micro-nutrients, highlighting the good potential of this technique for direct nutrient recycling. However, the species considered was found to have a low capability of assimilating the organic nitrogen forms present in the medium, requiring first inorganic ammonium to be released, which leads to slower growth rates. Nonetheless, the partial addition of other inorganic nitrogen forms (e.g., nitrates) can help to improve the growth during the first days of cultivation. At the same time, the hydrolysate could be used as the sole source of phosphorus, providing therefore a quantitative recycle of this strategic resource.

5.3.3. Continuous experiments with *Scenedesmus obliquus*

Once verified that the hydrolysate is able to sustain an efficient microalgal growth and provides itself all the nutrients and micronutrients required, continuous experiments were carried out with *S. obliquus* to assess if a stable microalgal production could be obtained in this medium, and subsequently optimize the nutrients supply (i.e., the hydrolysate feed concentration).

5.3.3.1 Effect of inlet concentration

S. obliquus was cultivated in a flat-panel PBR, under bubbling of CO_2-enriched air (5% v/v), at a residence time $\tau = 4$ d, and under continuous light intensity of 150 μmol m^{-2} s^{-1}. Since the objective is that of optimizing nutrients consumption, an optimal light intensity for the growth of *S. obliquus* in flat-panel PBRs was chosen (Gris et al., 2013). Since the uptake of nutrients in case of day-night irradiation is quite complex (Sforza et al., 2014c), a continuous illumination regime was chosen to focus on a single variable. The various feed concentrations used, always in non-sterile conditions, are summarized in Table 5.4.

Firstly, the system was fed with BG11 modified, as explained in §5.2.1, with large excess of both N and P in order to assure non-limiting concentrations (Sforza et al., 2014c), and the steady-state biomass concentration, productivity and nutrients consumption were measured in these conditions as a control.

Table 5.4 *Nutrients inlet concentrations of the different experimental conditions, and corresponding N/P ratio*

Concentration (mg L^{-1})	**N**	**P**	**N/P**
Control (BG11)	494	89	5.55
Hydrolysate 1	350	68	5.15
Hydrolysate 2	350	50	7
Hydrolysate 3	300	43	7
Hydrolysate 4	250	36	7

The biomass concentration resulted to be 3.08 ± 0.141 g L^{-1} (Figure 5.6A) and the corresponding productivity 0.77 ± 0.035 g L^{-1} d^{-1}. N and P difference between inlet and outlet concentration was 320 mg L^{-1} and 62 mg L^{-1} respectively. Considering these values as a reference, the feed was substituted with the hydrolysate properly diluted, in order to obtain a concentration of 350 mg L^{-1} of nitrogen. The phosphorus concentration was adjusted in order to maintain the same conditions of the control. Given the composition of the hydrolysate (§5.2.1), the dilution made to obtain 350 mg L^{-1} of N corresponds to 50 mg L^{-1} of P, therefore the remaining 18 mg L^{-1} were added as K_2HPO_4, thus reaching a final concentration of 68 mg L^{-1} of elemental phosphorus. In these conditions, the biomass concentration obtained with the

hydrolysate was equivalent to the control: 3.11 ± 0.155 g L^{-1} of DW, corresponding to a productivity of 0.78 ± 0.089 g L^{-1} d^{-1}.

Interestingly, nutrients (total N and P) were not entirely consumed, but instead their consumption percentage with respect to the inlet concentration was more or less the same for all dilutions tested (Figure 5.6B) and significant concentrations were measured in the outlet stream.

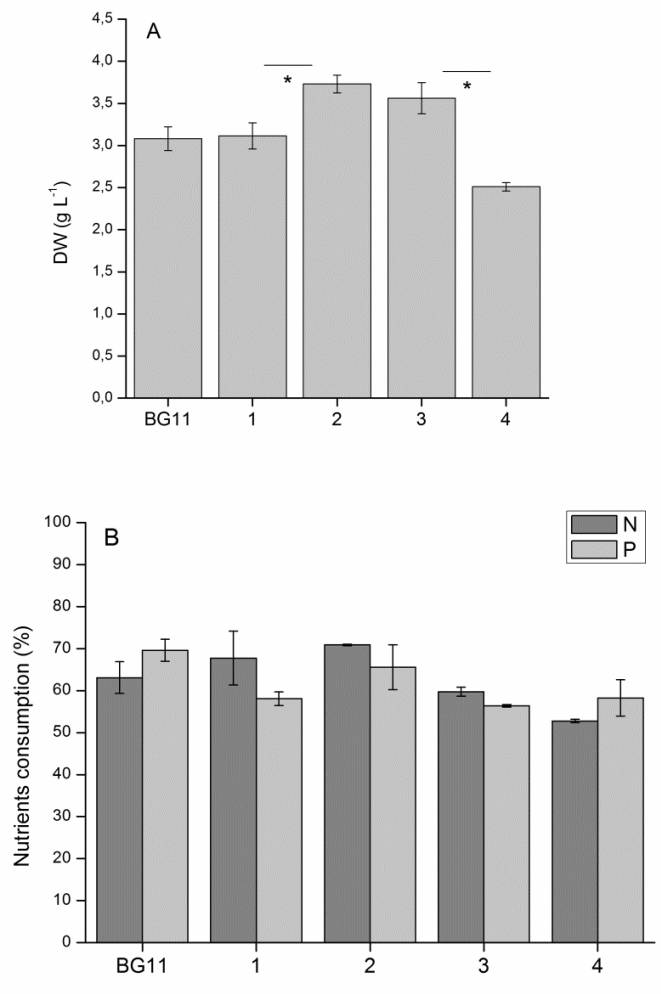

Figure 5.6 *Biomass concentration (A) and nutrients consumption (B) at steady state for the different feed conditions. Dashed asterisks indicate statistically significant differences between two consecutive steady-states*

Even in this case, a consumption of COD was observed (around 66% of the initial value), confirming mixotrophic growth also in continuous cultivation conditions.

In view of an efficient nutrient recycling, it is important to exploit the nutrients present in the medium as much as possible. Consequently, given the presence of non-consumed nutrients in the outlet stream, the inlet feed concentration was modified, keeping the same hydrolysate concentration, but without further addition of phosphate. This reduction of phosphate concentration, and the consequent increase of the N/P ratio in the feed, resulted in a significant increase in biomass concentration, up to 3.73 ± 0.105 g L^{-1}. The productivity increased, accordingly, to a value of 0.932 ± 0.026 g L^{-1} d^{-1}.

The reason of such an increment in the biomass production could be explained considering a possibly slowed growth due to high phosphorus concentration, related also to the phenomenon of luxury up-take. Different authors have reported that some microalgae, and in particular *Scenedesmus* sp., have the ability to over-uptake phosphorus when the N/P ratio in the growth medium differs from the normal elementary composition of the cells (Xin et al., 2010), and to accumulate it in the form of polyphosphate to be used as an internal source in case of starvation periods (Powell et al., 2009). Polyphosphates metabolism is quite complex (John and Flynn, 2000), however it is known that the growth rate tends to decrease with the progressive saturation of internal P pools (Valiela, 1995). Considering the nutrients content in the biomass (i.e. the uptake normalized on the dry weight), shown in Table 5.5 and calculated as:

$$Y_{i/x}\% = \frac{c_{i,in} - c_{i,out}}{DW} \cdot 100 \qquad \text{(Eq. 5.4)}$$

where *i* stays for a specific nutrient, and *in* and *out* indicate the inlet and outlet concentrations respectively, it can be seen that both in the control and in the first hydrolysate condition the percentage of P is higher than the typical content, which ranges between 0.3-1% by dry weight, suggesting there is indeed a luxury uptake. In both cases, in fact, the N/P ratio of the feed was lower than the typical microalgal elementary composition (N/P 7.2:1 by weight) (Redfield, 1934), as reported in Table 5.4. When the phosphorus concentration was reduced, also $Y_{P/X}$ decreased to a value of 0.77 %.

Table 5.5 *N and P content in biomass produced for the different feed concentrations tested*

	$Y_{N/X}$ %	$Y_{P/X}$ %	$Y_{N/X}$ / $Y_{P/X}$
Control (BG11)	11.01± 0.66	2.14 ± 0.08	5.16 ± 0.36
Hydrolysate 1	6.96 ± 0.66	1.36 ± 0.03	5.12 ± 0.51
Hydrolysate 2	6.09 ± 0.02	0.77 ± 0.07	7.84 ± 0.64
Hydrolysate 3	4.92 ± 0.09	0.632 ± 0.03	7.78 ± 0.39
Hydrolysate 4	4.84 ± 0.04	0.67 ± 0.05	7.18 ± 0.53

Despite the increase in productivity, both N and P were still present in the outlet stream. Thus, the hydrolysate was diluted to a level corresponding to 300 mg L^{-1} of N and 43 mg L^{-1} of P. Note that the N/P ratio is now fixed by the hydrolysate composition (7:1). In this case, the biomass production was comparable to the previous conditions (Figure 5.6A). A further feed concentration reduction (250 mg L^{-1} of N and 36 mg L^{-1} of P) resulted instead in a severe decrease in biomass concentration and productivity, to 2.51 ± 0.05 g L^{-1} and 0.628 ± 0.012 g L^{-1} d^{-1} respectively, meaning that in these conditions nutrients become limiting for growth. It has to be noted that even in this case N and P were not entirely consumed (Figure 5.6B). This might suggest that the actual limitation could be due not to nitrogen or phosphorous but to other micronutrients that became too diluted. Hence, the optimum hydrolysate concentration to obtain the maximum productivity (0.932 ± 0.026 g L^{-1} d^{-1}) with minimum nutrient supply was identified as 300 mg L^{-1} of N and 43 mg L^{-1} of P. The corresponding photosynthetic efficiency PE resulted to be 9.14 ± 0.26 % of the irradiated PAR.

Concerning the nutrients consumptions, it is worth noticing that N and P are never entirely consumed. Instead, the consumption percentage of both nutrients appears quite unvaried for all the conditions investigated and ranges between 60% and 70% of inlet concentration, regardless the hydrolysate feed concentration, while the absolute values (ΔN and ΔP) decrease with decreasing inlet concentration. This is also reflected in the fact that the nutrient contents in the biomass are seen to decrease together with the feed concentration, meaning that microalgal cells use smaller amounts per gram of biomass produced. However, the N and P content in the biomass is also influenced by the N/P ratio of the feed: in fact, as reported in Table 5.4 and 5.5 the ratio between $Y_{N/X}$ and $Y_{P/X}$ matches the inlet N/P ratio, as was also reported by Xin et al. (Xin et al., 2010) for batch cultivation of *Scenedesmus* sp.

Therefore, it is essential to minimize the nutrients supply to avoid luxury-uptake phenomena that, from the recycling point of view, represent a waste. In addition, also the N/P ratio of the feed plays a major role, both in relation to luxury-uptake and actual biomass productivity. The hydrolysate considered in this chapter, having a N/P ratio of 7:1, which is very close to the Redfield value (Redfield, 1934), proved to be a good substrate for continuous cultivation of *Scenedesmus obliquus*, allowing satisfactory productivities once the inlet concentration is optimized.

5.3.3.2 Effect of residence time

In addition to the inlet concentration of the hydrolysate (i.e. of nutrients), another operating parameter that is known to strongly influence the nutrients content in the biomass in a continuous reactor is the residence time (Sforza et al., 2014c). For this reason, two other values of τ were investigated, respectively 2.5 d and 1.5 d, keeping the inlet hydrolysate concentration fixed at 250 mg L^{-1} of N and 36 mg L^{-1} of P, with the aim of seeing if better consumptions could be achieved. The biomass concentration decreased with the residence time τ (Figure 5.7A), while the productivity showed an increasing trend, up to a maximum (Figure 5.7B), in agreement with what is already published in the literature (Takache et al., 2010). However, the difference in productivity between a residence time of 2.5 d and 1.5 d is not statistically significant and the optimum residence time is likely to be between these values.

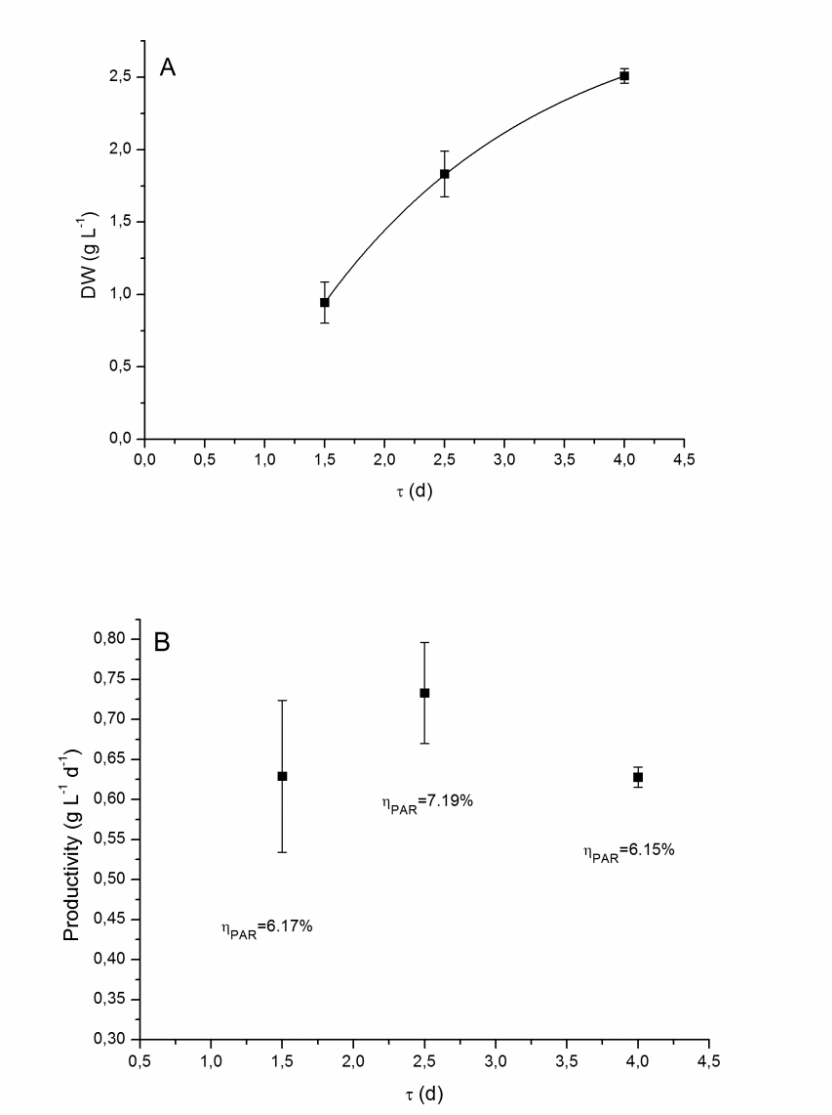

Figure 5.7 *Biomass concentration (A) and productivity (B) as a function of the residence time. In Figure 5.7B also the photosynthetic efficiency values are reported*

When considering the consumption percentage of nitrogen and phosphorus, it appears not to change significantly with the residence time. On the other hand, the nutrients content in the biomass is significantly affected by this operating parameter for both N and P, and in particular the value increases when the residence time is lower (Figure 5.8). Thus, while the biomass concentration decreases with τ, the amount of nutrients consumed per gram of biomass produced is higher. This behavior was also found by Sforza et al., (Sforza et al., 2014c), and

explained considering that at lower residence times the respiration rate and maintenance requirements of microalgal cells were found to increase.

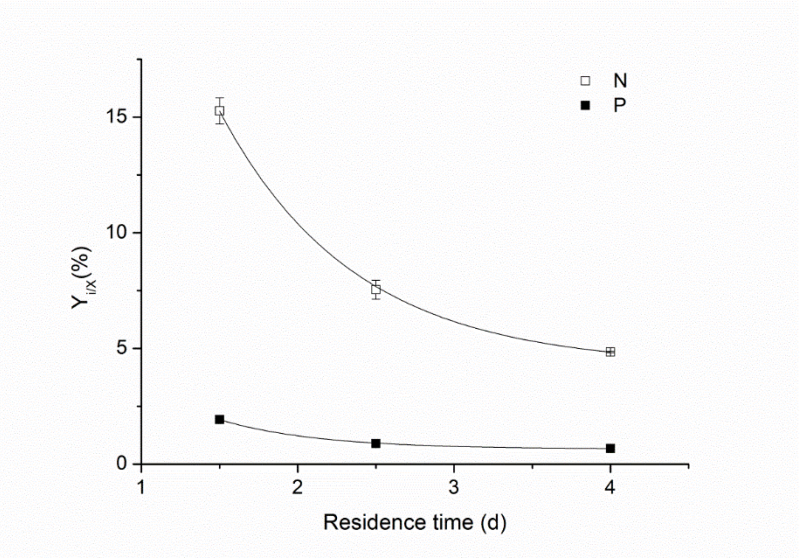

Figure 5.8 *Nitrogen (white) and phosphorus (black) content in the biomass produced as a function of residence time*

However, since the global nutrients consumption remains quite unvaried, even though it never reaches 100%, it is clear that the photobioreactor should be operated at the value of residence time that guarantees the maximum productivity in the specific experimental conditions.

5.4. Final remarks

In this chapter the growth of *Scenedesmus obliquus* and of *Nannochloropsis* in the liquid hydrolysate obtained from flash hydrolysis of the same microalgal genus is evaluated, in order to assess the feasibility of using this technique for nutrient recovery and recycling, and to reduce the N and P inputs to the process.

Batch experiments showed that the hydrolysate without prior sterilization was able to efficiently sustain microalgal growth and provide all the necessary macro and micronutrients. In particular, the *S. obliquus* was able to assimilate nitrogen, even if available in the medium mainly in the organic form of soluble peptides and amino acids. It also was able to exploit organic carbon for supporting growth, reaching generally higher growth rates compared to

cultivation in standard medium. *N. gaditana* was also able to grow in this medium, even though in this case the release of inorganic ammonium from amino-acids and peptides is necessary, as this species was found not to consume the organic carbon and nitrogen. Nonetheless, phosphorus resulted to be readily available in the hydrolysate and could be exploited.
In continuous cultivation of *S. obliquus*, stable and satisfactory productivities and efficiencies were obtained using the hydrolysate, in all experimental conditions. A particular attention was dedicated to nutrients consumptions, with the aim of optimizing their utilization in a recovery and recycling perspective. The results showed that the inlet concentration needs to be optimized in order to avoid luxury up-take phenomena, which represent a waste of nutrients and do not provide any advantage in growth. In addition, the N/P ratio in the feed was found to have a relevant influence on the culture, and the hydrolysate composition, having a ratio of 7:1, results to be a suitable substrate from this point of view without any further modification. The residence time was found to affect the nutrient content in the biomass, while the global consumptions did not vary significantly. However, this operating parameter has a strong influence on the biomass productivity, therefore the photobioreactor should be operated in order to guarantee the maximum performances in these terms.

Overall, the results obtained show that FH could be a very promising and viable process to recycle the nutrients necessary for algal growth, hence reducing the amount of fertilizers required and improving the performances of biofuels production from microalgae.

Chapter 6

Recycling minerals in microalgae cultivation through hydrothermal mineralization

The high demand of nutrients represents one of the major limitations to a sustainable large-scale production of microalgae-derived biofuels. This is particularly critical for phosphorus, whose natural reserves will soon be depleted. This chapter aims at testing the possibility of recycling phosphorus from the microalgal biomass in the form of stable fertilizers suitable for transportation and storage purposes, obtained through rapid subcritical water extraction (flash hydrolysis, FH) followed by precipitation. Through this process, also called hydrothermal mineralization, two main minerals can be precipitated depending on the operating conditions, namely magnesium ammonium phosphate (MAP, also known as struvite) and hydroxyapatite (HAP). To this goal, growth experiments were carried out with the microalga *Scenedesmus* sp., in both batch and continuous lab-scale photobioreactors, using first pure MAP and HAP, and subsequently the actual precipitates recovered from FH of the same microalga to replace traditional phosphate fertilizers in the cultivation medium. Results show that the growth rate and productivity obtained when using the recycled minerals as phosphorus source equal those achieved in the standard medium, suggesting that the proposed process could be a viable way to increase the sustainability of microalgal production at large-scale.

[0]Part of this chapter was published in ACS Sustainable Chemistry & Engineering (Barbera E., Teymouri A., Stuart B., Bertucco A., Kumar S., 2017. 5:929-935)

6.1. Introduction

Microalgae are currently the subject of many research efforts due to their promising potential as feedstock for the production of renewable fuels. It is worldwide acknowledged that fossil fuels, which currently represent the major source for the global energy production and consumption, will be unsustainable to meet the increasing demand in the medium to long term (Chisti, 2013; Ribeiro et al., 2015). These photosynthetic microorganisms are being widely investigated especially as a source of transportation fuels, due to the several advantages they offer compared to other types of crops, among which their high growth rate per unit area, and the fact that they do not require arable land, hence they do not compete with food production (Han et al., 2015; Quinn and Davis, 2015; Ribeiro et al., 2015).

However, the large amount of nutrients required for microalgal cultivation at a scale able to significantly displacing petroleum-based fuels has recently raised a lot of concern in terms of sustainability and economic perspectives. Pate et al. (Pate et al., 2011) estimated that, assuming 100% nutrients uptake efficiency, 88 kg of nitrogen and 12 kg of phosphorus would be required to produce 1 ton of algal biomass, while in the work of Canter et al. (Canter et al., 2015) 50-60 kg of N and 0.9-19 kg of P_2O_5 are reported for *Chlorella* and *Nannochloropsis* species, respectively. The major concerns are related particularly to phosphorus, which is an irreplaceable and already strained nutrient derived from non-renewable phosphate rocks through direct mining (Canter et al., 2015; Gifford et al., 2015; Markou et al., 2014; Pate et al., 2011). At present, it is estimated that global phosphate reserves will be depleted in 50-100 years, with an expected peak production around the year 2030 (Cordell et al., 2009). Modern agriculture is in fact highly dependent on this resource in order to produce fertilizers, required to meet the increasing demand of food crops production.

In this context, it appears clear that cultivation of microalgae on a large scale would affect the phosphate market, potentially raising fertilizers prices. Canter et al. (Canter et al., 2015) estimated that the production of 19 billion liters per year of algal oil-based fuels (which represents about 23% of the target of the 2007 U.S. Energy Independence and Security Act (U.S. Congress, 2007)) would consume roughly 15-23% of the P_2O_5 currently used in the U.S. and, more in general, 32-49% of the current world P_2O_5 fertilizers surplus. If the production

were doubled, there would not be enough fertilizers to meet the demand for microalgal production.

The only possibility to develop an economically and environmentally sustainable production of microalgae-derived biofuels is to recover the phosphorus (which is not desired in the fuel products) from the biomass, and recycle it for further algal growth, reducing the input of fresh fertilizers required. To this purpose, several process alternatives have been developed in the latest years, among which hydrothermal liquefaction (HTL) has received a wide interest (Biller et al., 2012; Garcia Alba et al., 2013; López Barreiro et al., 2015). In the area of hydrothermal treatments Flash Hydrolysis (FH), a type of rapid-HTL characterized by very short residence times (few seconds) under subcritical water conditions (200-300°C), has been shown to be a viable and environmentally benign process that allows to extract nutrients from the algal biomass into the aqueous phase (hydrolysate), while preserving the lipids in an energy-rich solid intermediate for subsequent biofuels production (Garcia-Moscoso et al., 2015, 2013). About 80% of the phosphorus and 60% of the nitrogen contained in the initial biomass can be extracted in the hydrolysate. The former is mainly directly available as orthophosphates, while N is mostly present in the form of soluble peptides and amino acids derived from hydrolyzed proteins, with a small percentage (about 10%) of ammonium.

In the previous chapter, it was shown that such hydrolysate could be successfully used for direct nutrient recycling, both in batch and continuous cultivation processes, and with different microalgal species. However, direct recycling may not always be the best option in large-scale operation, considering that such a medium could not be stored for long periods due to its organic carbon content and related instability. As an alternative option, nutrients could be precipitated from the hydrolysate and recovered as minerals, which would be suitable for long-term storage and transportation purposes. This FH-precipitation process, also called hydrothermal mineralization (HTM), allows to obtain two main minerals, depending on the operating conditions: under high temperature and pressure (i.e., right after FH), phosphate can precipitate as hydroxyapatite (HAP, $Ca_{10}(PO_4)_6(OH)_2$), while at atmospheric conditions N and P can be recovered in the form of magnesium ammonium phosphate or MAP ($MgNH_4PO_4 \cdot 6H_2O$, also known as struvite).

A few authors have recently shown that MAP, which is a major precipitate in wastewater streams having high concentration of PO_4^{3-} and NH_4^+, could represent a good alternative source

of phosphorus, and partially of nitrogen, for microalgae cultivation (Davis et al., 2015; Moed et al., 2015), while no works are reported on the possibility of using HAP.

In this chapter, the possibility of precipitating the phosphate and ammonium contained in the hydrolysate obtained from FH of *Scenedesmus* sp. as struvite or hydroxyapatite powder, and recycling it for further growth of the same microalga, is investigated. To this aim, preliminary batch cultivation experiments were carried out with pure MAP and HAP respectively, in order to compare the algal growth performances with those obtained in a standard synthetic medium (BG11). Possible slow-release effects of these minerals were also taken into consideration by monitoring phosphate dissolution in BG11 without algae inoculation. Subsequently, the real precipitates obtained from the hydrolysate were used for both batch and continuous cultivation experiments, in order to close the loop and determine the potential of the proposed process to recycle phosphorus, in the prospect of the development of a more sustainable large-scale algae production.

6.2. Materials and methods

6.2.1. Algae strain and culture media

Scenedesmus sp. was obtained from Carolina Biological (NC, USA), and maintained in AM-14 medium (Talbot et al., 2016), under continuous aeration. Control experiments were performed in BG11 medium, buffered at pH 7.15 with 10 mM HEPES, having a concentration of 5.4 mg L^{-1} of P (as K_2HPO_4) and 43.2 mg L^{-1} of N (as $NaNO_3$), in order to have a mass ratio N:P equal to 8 (17:1 by mole), close to the Redfield number (Redfield, 1934). For the continuous experiment, BG11 was further modified to guarantee non-limiting nutrients concentrations, with 494 mg L^{-1} of N ($NaNO_3$) and 61.75 mg L^{-1} of P (K_2HPO_4), and a double concentration of all the other micronutrients.

For the preliminary experiments, pure MAP (from Alfa Aesar, MA, USA) and HAP (from Sigma-Aldrich) were dissolved in BG11 to replace 100% of the P. In the former case, increasing concentrations were used in order to obtain different N replacement. Excess nitrogen needed to meet the control BG11 concentration was supplied as $NaNO_3$.

Batch and continuous experiments using the real precipitates obtained from the hydrolysate (section 2.2) were carried out dissolving the powder in BG11 in order to replace 100% of the

P with respect to the corresponding control (5.4 mg L^{-1} and 61.75 mg L^{-1} respectively). Even in this case, the amount of nitrogen necessary to reach the same final concentration of the BG11 control was added as $NaNO_3$. No sterilization was carried out on the culture media prior to inoculation.

6.2.2. MAP precipitation

Magnesium ammonium phosphate was precipitated from the liquid hydrolyzate obtained from FH of *Scenedesmus* sp. at 280 ºC and 9 s of residence time (Garcia-Moscoso et al., 2013). The precipitation was carried out in a 1 L Erlenmeyer flask at room temperature (20 ˚C) with a mixing rate of 350 rpm using a magnetic stirrer and Fisher Scientific Isotemp hot plate, while pH was continuously monitored and set at a value of 9 (by addition of NaOH 1 N) as the optimum condition for struvite precipitation (Doyle and Parsons, 2002). $MgCl_2$ was added as the magnesium source (Marti et al., 2010; Rahman et al., 2014) using a Mg:P molar ratio of 2:1. Pure struvite was also used as a seed in order to promote crystallization (Kim et al., 2007). After 1 h of reaction, the hydrolyzate containing the precipitates was vacuum filtered using Whatman 47mm glass microfiber filters and the separated solids were oven dried at 65 ˚C for 24 h. A yield of phosphate and ammonium removal from the hydrolyzate of about 66 wt% and 30 wt% were obtained, respectively. The optimization of the FH-precipitation process and phosphate recovery lies outside the scope of the present work and will be discussed elsewhere. The MAP powder obtained was characterized by means of XRD (MiniFlex II X-Ray Difractometer, Rigaku Corporation, Japan), in the range from 10 to 60 degrees ($2\theta/\theta$) at 30 kV and 15 mA, and also in terms of Elemental Analysis (Thermo Finnigan Flash EA 1112 Automatic Elemental Analyzer, Thermo Fisher Scientific, Waltham, MA), in order to quantify the carbon carry-over from the hydrolyzate.

6.2.3. Experimental set-up

Cultivation experiments were conducted in both batch and continuous mode, in glass bottles having 8.5 cm diameter. Atmospheric air was continuously supplied by means of an air stone placed inside the bottles, which also ensured complete mixing of the algal culture. Light was provided at a continuous and constant light intensity of about 150 μmol m^{-2} s^{-1} (measured with

a digital light meter) using fluorescent lamps (SUN-904302 Fluorescent 157 Grow Light Fixture; full spectrum 6500K) placed on the two opposite sides of the bottles. The culture temperature was measured daily and was equal to 25 ± 2 ºC for batch experiments and 28 ± 1 ºC for continuous ones.

Batch experiments were inoculated at an initial microalgae cell concentration of $3 \cdot 10^5$ cells mL^{-1}, with a culture volume of 400 mL, and were carried out in duplicate.

The volume of the continuous culture experiment was equal to 650 mL. Fresh medium was continuously supplied, and biomass was continuously removed from the reactor by means of a peristaltic pump (MasterFlex® L/S™ 7519-06) at the same flow-rate Q (mL d^{-1}). The residence time of the culture inside the reactor is calculated according to:

$$\tau = \frac{V_R}{Q} \qquad \text{(Eq. 6.1)}$$

where V_R is the culture volume, and it was set equal to 2.94 d.

After an initial transient period observed when changing the experimental conditions, the continuous system reached steady-state, and a constant biomass concentration was obtained. The steady-state biomass productivity was hence calculated as:

$$P_x = \frac{c_x}{\tau} \qquad \text{(Eq. 6.2)}$$

c_x being the average biomass concentration (g L^{-1}) of at least 4 experimental points measured at different days of steady-state.

6.2.4. Analytical procedures

Algal growth was monitored daily in both batch and continuous experiments by measuring the cell concentration (cells mL^{-1}) with a Neubauer improved hemocytometer. Specific growth rates (d^{-1}) in batch experiments were then calculated from the linear regression of the logarithm of cell concentrations during the exponential phase, taken as the average of two independent biological replicates.

In continuous experiments, biomass concentration was measured daily as TSS (g L^{-1}) by filtering 5 mL of culture sample with previously dried filters (Whatman 192 934-AH glass fiber discs; 1.4 micron pore size; 47 mm). The filters were then dried in the oven at 60 ºC for

24 h. To account for possible undissolved particles, in the experiment using MAP as a phosphate source the TSS of the medium was also measured and subtracted from that of the algal culture.

Nutrients were measured every 2 days in batch cultures, and at the inlet and outlet for at least three days of steady state in the continuous experiments. Nutrients concentrations were measured by Ion Chromatography (Dionex ICS-5000, using an AS23 IonPac™ column for nitrate and phosphate, and CS16 IonPac™ column for ammonium).

6.3. Results and discussion

6.3.1. Batch experiments with pure MAP and HAP

Preliminary batch experiments were carried out using pure struvite and hydroxyapatite, in order to determine if these type of minerals are suitable sources of phosphorus, and partially of nitrogen, for the cultivation of *Scenedesmus* sp. To take into account possible slow-release effects of this mineral, PO_4^{3-} concentration was measured during time in a highly supersaturated solution of MAP and HAP in BG11, respectively. As it can be seen in Figure 6.1A, in the case of MAP a constant concentration of about 98 mg L^{-1} of PO_4-P was reached after less than 2 hours, showing that this nutrient is in fact readily available in the medium from this source for microalgae cells to uptake.

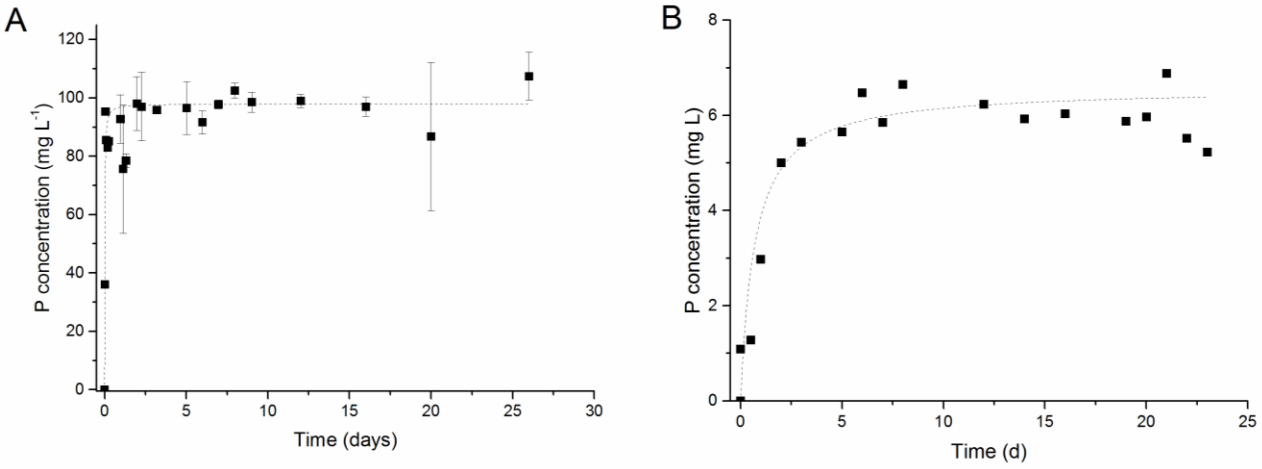

Figure 6.1 *Phosphorus dissolution from MAP (A) and HAP (b) in BG11 medium*

HAP dissolution and solubility resulted instead to be much lower, with a P concentration of about 6 mg L^{-1} reached after 3 days (Figure 6.1B). However this concentration would be enough to match that of BG11 (5.4 mg L^{-1}).

Since the main focus of this chapter is directed towards P as a strategic nutrient, the pure minerals were used to replace 100% of this element in BG11 which, in the case of struvite, corresponds to 5.6% of N as well. As it can be seen from Figure 6.2, the algal growth obtained when 100% of P is provided in the form of struvite matches that of the control, with a specific growth rate equal to 1.094 ± 0.146 d^{-1} compared to 1.096 ± 0.121 d^{-1}. This result confirms the fact that struvite is a good source of phosphate for the growth of *Scenedesmus* sp., and could entirely replace common P fertilizers. On the other hand, when HAP is used to provide phosphate, the growth resulted to be much lower, with an initial specific growth rate of 0.613 ± 0.022 d^{-1}, which stopped at a final cell concentration of about $4 \cdot 10^6$ cells mL^{-1}.

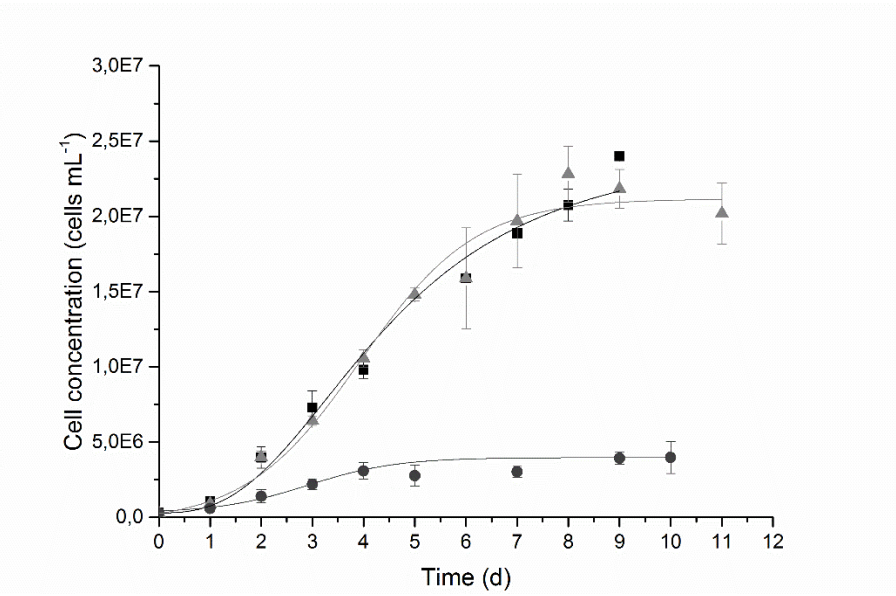

Figure 6.2 *Growth curve of Scenedesmus sp. in control BG11 (black squares), and with 100% P replacement by MAP (grey triangles) and HAP (dark grey circles)*

This can be explained considering that the initial P concentration in the medium resulted to be low (1.19 ± 0.01 mg L^{-1}), in agreement also with results of Figure 6.1B. This suggests that, even though HAP dissolution would finally reach a P concentration sufficient to meet that of BG11, the release of this nutrient appears to be too slow to sustain microalgal growth. In the case of MAP

instead, P resulted to be immediately available for algal cells to uptake, with an initial concentration of 5.76 ± 0.21 mg L^{-1}.

Building on this, MAP concentration was increased to assess whether higher percentages of nitrogen (24% and 50% respectively) could also be replaced, as ammonium, using this source. It has to be noted that, according to the N:P molar ratio of struvite (1:1), increasing the N replacement corresponds to excess phosphorus in the medium. The growth curves obtained are shown in Figure 6.3. Initial nitrogen and phosphorus concentrations for all MAP experiments are summarized in Table 6.1.

Table 6.1 *Initial P and N concentration of batch experiments with pure MAP*

Experiment	PO_4-P (mg L^{-1})	NH_4-N (mg L^{-1})	NO_3-N (mg L^{-1})
Control BG11	5.4	-	43.2
100% P	5.4	2.4	40.8
24% N	22.8	10.3	32.9
50% N	47.8	21.6	21.6

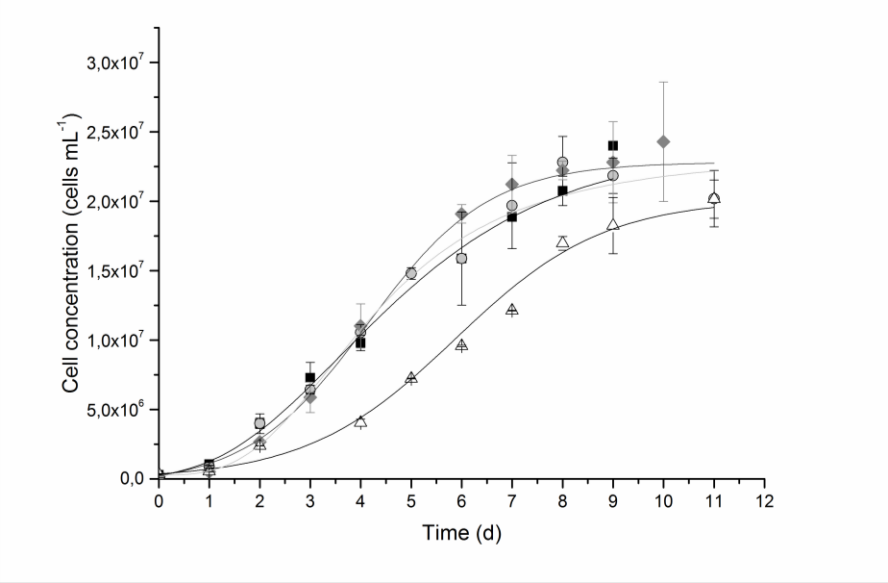

Figure 6.3 *Growth curve of Scenedesmus sp. in control BG11 (black squares), and at different MAP concentrations to replace: 100% P (light grey circles), 24% N (dark grey rhombus) and 50% N (open triangles)*

In both cases, the performances obtained in terms of growth were good, even though at the highest MAP concentration investigated (50% N replacement) the growth rate resulted to be slightly lower (0.652 ± 0.012 d^{-1}). However, the final cell concentration reached is comparable to the previous cases. It has to be considered that in this case the N:P ratio is extremely different from the typical algal composition (about 8:1 by weight), with a P concentration that is even higher than that of N.

As about the nutrients consumption, it is seen that the ammonium supplied as struvite is almost entirely consumed in all the conditions investigated (Figure 6.4A), being moreover the preferred nitrogen form over nitrate, in agreement with what reported in the literature (Markou et al., 2014). These results suggest that increasing the struvite concentration in the medium could potentially help reducing also the amount of fresh nitrogen fertilizers required, providing a readily available source of this important nutrient as well.

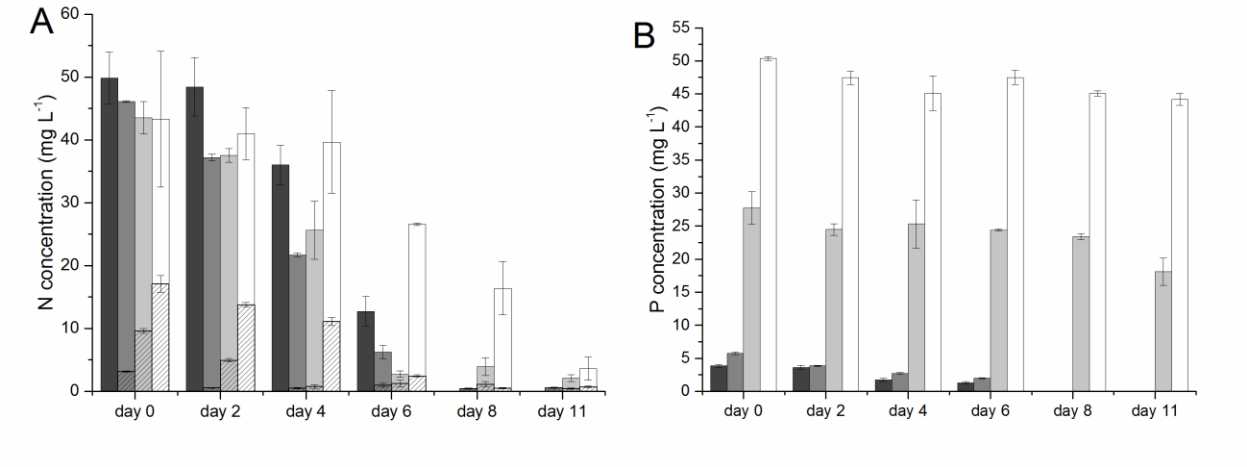

Figure 6.4 *Nitrogen (A) and phosphorus (B) concentration during time for control BG11 (dark grey), and experiments using pure MAP to replace: 100% P (grey), 24% N (light grey) and 50% N (white). In Figure 6.4A, filled columns represent ammonium concentration*

Nonetheless, as previously mentioned, increasing the ammonium concentration by means of struvite necessarily implies a higher phosphorus concentration in the medium, which however did not result in increased growth or productivity. As a matter of fact, in the 24% N replacement the growth rate and final biomass concentration were equal to that of the control, even though a higher consumption of P was measured (9.63 mg L^{-1} compared to roughly 5 mg L^{-1} of control

and 100% P replacement conditions) (Figure 6.4B). This phenomenon is known as luxury uptake (Powell et al., 2009), and should in fact be avoided in mass production of microalgae, as it represents a waste of this valuable nutrient. A further increase in the excess P concentration (50% N replacement), moreover, appears to somehow slightly hinder the growth (which is also reflected in the slower nitrogen consumption seen in Figure 6.4A).

In summary, even though MAP could serve as a good source of both phosphorus and nitrogen for the growth of the microalgal species used, results suggest that it would be better to use this mineral for a full replacement of phosphate in the medium, while supplying external fresh nitrogen to meet a suitable N:P ratio, and maximize the utilization of P as a more sensitive element.

6.3.2. Batch experiments with precipitated MAP

Given the results obtained with the pure minerals, only MAP was precipitated from the liquid hydrolysate to assess phosphorus recycling potential for further microalgal cultivation through HTM. It has to be pointed out that however, HAP could be recovered in any case as a valuable product (through a two-stage precipitation process) and destined to several other applications, especially in the biomedical field (Yang et al., 2014). Hence, growth experiments were performed using the real precipitates recovered from *Scenedesmus* sp. hydrolysate to replace 100% of the phosphorus in BG11 (5.4 mg L^{-1}). XRD analysis revealed that the powder obtained corresponds to the monohydrate form of MAP (also known as dittmarite, $MgNH_4PO_4 \cdot H_2O$), rather than the hexahydrate compound, as shown in Figure 6.5.

The solubility of dittmarite in water is reported to be slightly lower than that of struvite (Bridger et al., 1962), as it first gradually hydrates to the hexahydrate form (Bhuiyan et al., 2008). Elemental analysis of the powder showed the presence of 9.27 ± 0.15 % of carbon, as a carry-over from the carbon-rich hydrolyzate. The presence of carbon as an impurity might in fact have a beneficial effect on the growth, as it is the main element in microalgal biomass (roughly 50% by weight) (Markou et al., 2014). However, the MAP concentration used in this case corresponds to only 2.5 ± 0.04 mg L^{-1} of C, hence its contribution would not be significant.

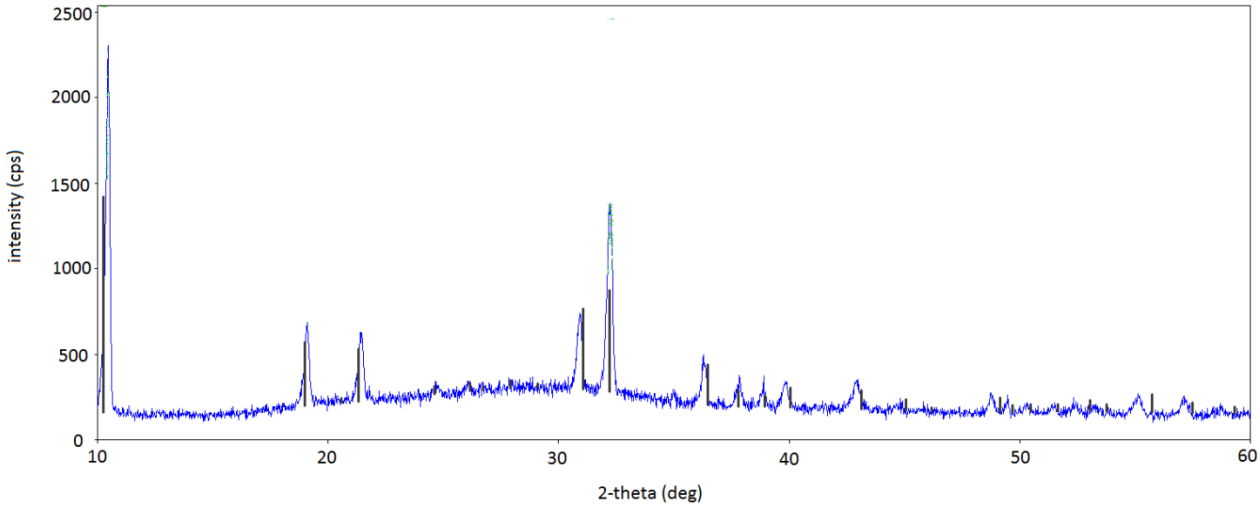

Figure 6.5 *XRD analysis of hydrolysate precipitates (blue line) compared to dittmarite standard (black bars)*

The growth curve obtained in this case is shown in Figure 6.6, together with those of control BG11 and the corresponding 100% P replacement with pure MAP, as a comparison.

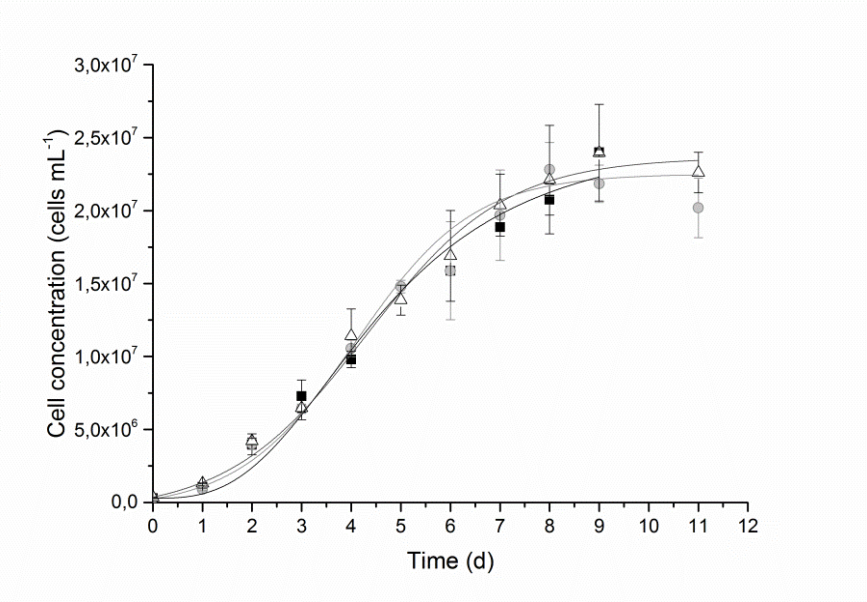

Figure 6.6 *Growth curve of Scenedesmus sp. in control BG11 (black squares) and with 100% P replacement by pure MAP (light grey circles) and precipitated MAP (open triangles)*

As can be seen, the dittmarite precipitated from the hydrolyzate also proved to be very suitable to sustain microalgal growth, with a specific growth rate similar to that obtained with pure MAP (0.98 ± 0.14 d^{-1}). Even in this case, phosphorus was immediately available for the algal

cells to uptake, with a measured initial concentration of 5.215 ± 0.319 mg L^{-1}. Nitrogen consumption also followed the same trend, with the ammonium fraction (2.323 ± 0.004 mg L^{-1}) being utilized first, followed by nitrate.

These results show that MAP minerals could be recovered directly from the microalgal biomass and actually recycled for further algal growth, reducing the requirement of external P and, even if to a smaller extent, of N fertilizers supply, while at the same time ensuring growth performances equal to those obtained with standard media or pure struvite purchased from the market. Besides, even though it is true that recycling the aqueous hydrolyzate directly after flash hydrolysis (without MAP precipitation) would provide a quantitative replacement of both phosphorus and nitrogen in the cultivation system, the latter one is mainly present as simple organic compounds (amino acids and oligopeptides (Garcia-Moscoso et al., 2015, 2013)), while only a small fraction is available as inorganic ammonium. In the previous chapter, it was shown that *Scenedesmus obliquus* was indeed able to exploit the organic nitrogen from the liquid hydrolyzate and could grow efficiently in this substrate without the need of any external macro and micronutrients supply. However, the capability of up-taking these simple organic nitrogen forms is known to be highly dependent on the microalgal species (Markou et al., 2014), and it was also seen that, for example, the marine alga *Nannochloropsis gaditana* could not grow as well in the hydrolyzate as in the control medium, as it needs inorganic ammonium to be released. Through MAP precipitation, a good percentage of the ammonium present in the hydrolyzate after FH could actually be recovered and immobilized together with phosphorus in a stable mineral fertilizer, which is likely to be a suitable nutrient source for different algal species (as proved here for *Scenedesmus* sp., as well as for *Chlorella* (Moed et al., 2015) and *Nannochloropsis* (Davis et al., 2015)). In addition, the clear liquid phase remaining after separation of the solid precipitates, which contains the residual organic fraction of amino acids and soluble oligopeptides, could be used for the production of valuable coproducts, such as arginine and peptides (Garcia-Moscoso et al., 2015), or even polyurethanes (Kumar et al., 2014).

6.3.3. Continuous experiments with precipitated MAP

Even though batch experiments are fundamental in order to assess growth performances and nutrients utilization, especially when using different cultivation media and nutrient sources, from the industrial point of view a continuous operation mode is certainly preferable, as it allows a stable and continuous production of biomass, to be sent to downstream units for conversion to biofuels or other products. For this reason, once verified that *Scenedesmus* sp. grew well in batch conditions using precipitated MAP as a phosphate source, the same powder was used in continuous cultivation to assess if a stable biomass production could also be obtained, and to compare the performances with those achieved in standard BG11. The residence time of the culture inside the reactor was 2.94 d, and nutrients were provided in large excess (§ 6.2.1).

The results obtained in terms of biomass concentration (TSS, g L^{-1}), productivity (g L d^{-1}) and phosphorus utilization are summarized in Table 6.2. As can be seen, the steady-state biomass concentration reached in the photobioreactor (and consequently, as the residence time is constant, also the productivity) resulted to be the same for the control BG11 and 100% P replacement with MAP, confirming that the positive results previously obtained in batch experiments are valid for continuous cultures as well.

Table 6.2 *Summary of results of continuous experiments (τ = 2.94 d)*

Statistically different results are marked with an asterisk

	Biomass concentration TSS (g L^{-1})	**Biomass productivity (g L^{-1} d^{-1})**	**Phosphorus consumption (mg L^{-1})**	**Phosphorus on biomass yield $Y_{P/X}$ (%)**
Control BG11	0.980 ± 0.023	0.333 ± 0.008	11.04 ± 1.126*	1.13 ± 0.134*
MAP	0.965 ± 0.024	0.328 ± 0.008	5.133 ± 0.815*	0.53 ± 0.08*

In this case, however, the inlet phosphorus concentration measured in the MAP medium resulted to be lower than the desired one (48.35 ± 1.28 mg L^{-1} instead of 61.75 mg L^{-1}). This seems to be due to an incomplete dissolution of the dittmarite powder, as suggested by a TSS of the inlet medium of roughly 0.2 g L^{-1} measured daily, rather than to slow-release effects, as

the P concentration in the feed was anyway constant during time. Even though this did not affect the biomass productivity, as the concentration of P was still provided in large excess, it appears to have an effect on the uptake of this nutrient. In particular, the phosphorus on biomass yield (i.e. the consumption normalized on the biomass concentration, which reflects the P content in the biomass), calculated as:

$$Y_{P/X}\% = \frac{c_{p,in} - c_{p,out}}{c_x} \cdot 100 \qquad \text{(Eq. 6.3)}$$

where *in* and *out* indicate the inlet and outlet concentrations respectively, results to be much lower (roughly half) that of the control. This again suggests that in the first case the higher concentration of phosphates available in the medium leads to some luxury uptake phenomena, with an increased P percentage in the biomass without an enhancement of productivity. The lower solubility of MAP allowed instead a more efficient utilization of this nutrient with regard to biomass production, consistently to what reported also in the previous chapter. Clearly, these results depend on the experimental conditions investigated (i.e., residence time, light intensity and regime, CO_2 supply), and the concentration of MAP in the feed could be optimized in order to minimize the phosphorus input required to obtain a certain efficient productivity, i.e. optimizing its utilization. Nonetheless, the results presented here serve as a good proof-of-concept to show that the MAP recovered from the hydrolyzate is an effective source of phosphate for microalgal growth. Even though the maximum P concentration achievable in the medium resulted to be about 48 mg L^{-1} because of solubility limitations of the powder, a stable steady-state biomass production can be achieved under continuous operation with performances comparable to those obtained using standard cultivation media.

6.4. Final remarks

This chapter investigates the possibility of using minerals recovered from flash hydrolysis of microalgae biomass followed by precipitation (i.e., hydrothermal mineralization, HTM) as magnesium ammonium phosphate (MAP) or hydroxyapatite (HAP) for further growth of the same species (*Scenedesmus* sp.), with the aim of recycling phosphorus and increasing the sustainability of algal biofuels production.

Preliminary experiments with pure minerals showed that struvite can be a good source to replace both phosphorus (as PO_4^{3-}) and also up to 50% of nitrogen (as NH_4^+), while microalgal growth was not efficient when using HAP likely, due to lack of P availability (slow-release). The N:P ratio of MAP however, being much lower than that of the typical microalgae elemental composition, suggests that it would be preferable to add fresh nitrogen to compensate the stoichiometric mismatch, to avoid wasting phosphorus as a precious nutrient.

Experiments carried out with the actual precipitates recovered directly from the algal hydrolyzate, which resulted to be monohydrate MAP or dittmarite, proved that recycling these minerals to replace common P fertilizers allows to obtain growth performances comparable to those achieved with standard cultivation media, both in batch and continuous operation.

The process proposed could therefore be a valid and viable way to recover nutrients (especially phosphorus) into stable fertilizers to be later efficiently used for further microalgae production when direct recycling of the liquid hydrolyzate is not possible, allowing a more strategic management of this precious nutrient.

Chapter 7

Anaerobic digestion of lipid-extracted microalgae: enhancing nutrient recovery towards a closed loop recycling

Nutrient recycling is essential to make microalgae cultivation processes sustainable on an industrial scale. To this aim, in this chapter lab-scale anaerobic digestion experiments of *Chlorella vulgaris* biomass after lipid extraction were carried out to evaluate digestion yields, in terms of biogas produced and nutrients recovery. The biological methane potential was evaluated by standard methods. The digestate was centrifuged and the liquid fraction was analysed to measure the concentration of nutrients dissolved. Then, the autotrophic growth rate of the same microalgal species was measured in this liquid, with suitable dilution and nutrient integration when necessary, to assess the possibility of re-cultivating microalgae in a closed loop nutrient recycling process. In the re-growth experiments, the liquid phase from microalgal digestate showed a lack of sulphate and phosphorus. In particular, the low recovery of P was due to the precipitation in the solid phase during digestion. Several techniques were hence tested to enhance phosphorus solubilisation. Eventually, *C. vulgaris* was grown in such treated digestate, obtaining a final biomass production comparable to that of the corresponding control, without the need of external phosphorus supply.

[0]Part of this chapter has been submitted to Biochemical Engineering Journal

7.1. Introduction

The progressive depletion of fossil fuels, together with the increasing world energy demand, has led to the development of several alternative and renewable energy sources. Among these, microalgae have received wide attention as a prospective biomass feedstock for biofuels and bioenergy production, especially related to liquid fuels for transportation, as they are characterized by fast growth rates and high lipid contents compared to other crops (Chisti and Yan, 2011; Mata et al., 2010).

Nonetheless, in order to quantitatively replace fossil fuels with third-generation biofuels derived from microalgal biomass a number of issues have to be properly addressed and solved yet. In terms of both economic and environmental sustainability, the problem of nutrients (particularly N and P) supply required by microalgae to grow is of greater concern, as a simple mass conservation balance suggests that huge amounts of fertilizers would be needed in view of a quantitative replacement of transportation fossil fuels by biofuels. These amounts are in competition with food crops cultivation (in the case of nitrogen) and well beyond the available natural resources (for phosphorus) (Canter et al., 2015). On the other hand, biofuels do not need to be based on components other than mixtures of hydrocarbons, which do not contain either N or P, whereas microalgae, as well as any other biomass, need them to grow and to produce hydrocarbon precursors. Therefore, the only possibility and goal are pursuing maximum nutrient recovery from the spent biomass and subsequently recycle them for further cultivation.

Among the possible techniques available to this aim, anaerobic digestion (AD) appears to be a viable and promising solution, as it allows obtaining a liquid phase in which nutrients are re-mineralized, while at the same time producing biogas as an additional energy output (Gonzalez-Fernandez et al., 2015; B. Sialve et al., 2009; Ward et al., 2014; Xia and Murphy, 2016). The literature is quite rich of papers about AD of different microalgal species, both on whole-cells (Acién Fernández et al., 2012; Prajapati et al., 2014; Ras et al., 2011) and after lipids extraction (Alzate et al., 2014; Bohutskyi et al., 2015; Ehimen et al., 2011), proving that this type of biomass can be a good substrate for biogas production. In addition, the possibility of growing microalgae on the liquid digestate effluent originated from AD of various feedstocks (e.g., cow or swine manure, municipal wastewaters, etc.), rich in nutrients such as

ammonium nitrogen and phosphorus, has also been investigated and proved to be feasible for different algal species (Bjornsson et al., 2013; Cai et al., 2013; Uggetti et al., 2014).
However, the composition of the biomass fed to the anaerobic digester clearly influences the final composition of the digestate. So that, if a given nutrients ratio is required by algae growth, and the same biomass is digested, some unbalanced recovery of nutrients may occur. This fact is likely to affect the suitability of algal digestate as nutrients source. In the perspective of an industrial-scale microalgal process development, a closed-loop should be considered, where the algae-based digestate is recycled to the culture, but the availability of nutrients in the correct ratio must be checked, when the same biomass is used for anaerobic digestion. Prajapati et al. (Prajapati et al., 2014) investigated the possibility of a closed-loop cultivation/AD process using the cyanobacteria *Chroococcus* sp. In their work, the biomass produced after cultivation is sent directly to the anaerobic digester, so that such a process is aimed at the production of biogas as the main and only fuel. When instead the main goal is obtaining algal liquid fuels for transportation, the lipid fraction has to be previously extracted from microalgae, then the residual biomass (which has a somehow different composition) is sent to AD for additional energy production and nutrients recycling.
In this chapter, a lipid-extracted microalgal biomass (*Chlorella* vulgaris) was used for anaerobic digestion, and the liquid digestate was assessed as cultivation medium to re-grow the same species and evaluate the availability of macro and micronutrients, in order to highlight and quantify the need of nutrients make up.

7.2. Materials and methods

7.2.1. Lipid extraction and BMP tests

Pre-dried *Chlorella vulgaris* (provided by NEOALGAE^{TM}) was used for anaerobic digestion experiments. Lipids were extracted using a Soxhlet apparatus and a mixture of ethanol-hexane (2.5:1 volumetric ratio) as extraction solvent. Such a mixture was chosen as, even though chlorinated solvents are more efficient in extracting lipids from the biomass, their residuals cause inhibition of the digestion process (Tercero et al., 2014). Laboratory scale tests were then performed to evaluate the Biochemical Methane Potential (BMP) of the lipid-extracted algal

biomass (LEA). Batch tests were carried out using six 500 mL glass bottles, with a working volume of 250 mL. In addition, two bottles were added containing only inoculum (no algae), as a control. These were subsequently sealed with silicon plugs. Anaerobic sludge collected from an anaerobic digester of sewage sludge from a municipal wastewater treatment plant located in Padova, Italy, was used as inoculum. Microalgal concentration and microalgae/sludge ratio (F/M, i.e. food to microorganism) were 2.76 gVS L^{-1} and 0.5 gVS gVS^{-1} (Tercero et al., 2014), respectively. The bottles were flushed with N_2 gas for 3 minutes to ensure anaerobic conditions and incubated at a temperature of 35 ± 1ºC. Total solids (TS) and volatile solids (VS) of the inoculum and LEA were analysed according to standard methods (APHA, AWWA, W., 1999).

The volume of biogas produced during the anaerobic digestion process was measured by means of the water displacement method. The produced gas composition in terms of CH_4 and CO_2 was analysed using a portable gas analyzer (LFG 20-ADC, Gas Analysis Ltd).

Methane and carbon dioxide volumes produced during the first and second stages of AD were calculated according to Ginkel et al. (Van Ginkel et al., 2005):

$$V_{c,t} = C_{c,t}V_{b,t} + V_H(C_{c,t} - C_{c,t-1}) \quad \text{(Eq. 7.1)}$$

where:

$V_{c,t}$= Volume of CH_4 or CO_2 produced between intervals of t and t-1

$V_{b,t}$= Volume of total biogas produced between intervals of t and t-1

V_H= Volume of headspace of bottles (300 mL)

$C_{c,t}$= Concentrations of intervals CH_4 or CO_2 in headspace in time of t

$C_{c,t-1}$= Concentrations of intervals CH_4 or CO_2 in headspace in time of t-1.

Only the net production of biogas was considered, by subtracting the amount of biogas produced by control experiments (bottles without algal biomass).

At the end of BMP tests, the digestate was collected: part of it was centrifuged and filtered to separate the liquid fraction from the solids, while the remaining was kept for subsequent phosphorus solubilisation treatments. All the products were stored in a refrigerator at -20°C until use.

7.2.2. Algae strain and culture media

Chlorella vulgaris Emerson/3 was used for growth experiments.

The culture was maintained in sterile BG11 medium with 1.5 mg L^{-1} $NaNO_3$ (247 mg L^{-1} N) and 30.5 mg L^{-1} K_2HPO_4 (5.4 mg L^{-1} P), buffered with 10 mM HEPES pH 8, in 250 mL Drechsel bottles, as a pre-inoculum. Since in the anaerobic digestate nitrogen is mainly present as ammonium, for the control experiment BG11 was modified so that this nutrient was supplied as NH_4Cl, keeping an equivalent concentration of 247 mg L^{-1} N. All other nutrients were provided in the same amount and form as standard BG11.

For experiments carried out in the digestate, the medium was diluted with distilled water in order to have the same N concentration of control BG11. When necessary, additional P and S were added as K_2HPO_4 and $MgSO_4 \cdot 7H_2O$ salts, respectively, at the concentration reported in subsequent sections. The pH was measured daily and kept in the range of 7.3-7.7 by addition of NaOH or HCl solutions. No sterilization was carried out on the digestate prior to algae inoculation, to effectively measure the growth capability in conditions similar to industrial ones.

7.2.3. Cultivation set-up and analytical procedures

Growth experiments were performed in Drechsel bottles having 5 cm diameter, with a culture volume of 100 mL. A mixture of CO_2-enriched air (5% v/v, regulated by two flow-meters) was continuously bubbled through the microalgal suspension at approximately 1 L h^{-1} total flow, to ensure non-limiting carbon supply. To avoid sedimentation, the culture was continuously mixed by a stirring magnet, placed at the bottom of the reactor. Light was provided by fluorescent lamps, placed in front of the cultivation bottles. The light intensity used for the experiments was equal to 120 μmol m^{-2} s^{-1} of PAR (Photosynthetically Active Radiation, 400-700 nm), measured with a photoradiometer (Delta OHM HD 2102.1). The cultures were placed in a refrigerated incubator, at a constant temperature of 28 ± 1 °C. Each experiment started with a microalgae inoculation of OD_{750} = 0.2, which corresponds to a cell concentration of about $2 \cdot 10^6$ cells mL^{-1}, and was carried out at least in duplicate.

Microalgal growth in batch cultivation experiments was monitored daily by measuring the optical density at 750 nm (OD_{750}) using a UV-visible double beam spectrophotometer (UV

500, from Spectronic Unicam, UK). Cell concentration was also measured daily using a Bürker Counting Chamber (HBG, Germany). Specific growth rate constants (μ) were then calculated as the slope of the linear regression of the logarithm of cell concentration, during the exponential phase of growth. At the end of each curve, the final biomass concentration C_x was measured as dry weight (g L^{-1}), by filtering 5 mL of culture sample with 0.2 μm pore size pre-dried nitrocellulose filters. The filters were then dried in a laboratory oven at 90°C for 4 h. In the experiments carried out in the digestate, the dry weight of the medium was measured as well and subtracted from that of the biomass.

$N\text{-}NH_4^+$ and $P\text{-}PO_4^{3-}$ in the liquid digestate, and at the initial and final times of batch experiments, were analysed spectrophotometrically using standard test kits. Ammonia nitrogen was measured with HYDROCHECK SPECTRATEST (Reasol®), by colorimetric reaction with Nessler reagent (potassium tetraiodomercurate) in alkaline conditions, and subsequent absorbance measurement at 445 nm. Orthophosphate phosphorus was measured with the molybdate/ascorbic acid method, which involves the formation of a blue dying complex between orthophosphate ions and molybdenum under reducing environment, whose absorbance is then measured at 705 nm. The characterization of micronutrients (trace metals and other elements) in the liquid digestate was performed by professional laboratories (Chelab S.r.l. and Microanalysis Lab of DISC-UniPD).

Student's t tests were applied to ascertain significant differences in specific growth rate and final biomass concentration of growth curves. The level of statistical significance was $p<0.05$.

7.2.4. Phosphorus solubilisation

Four protocols for re-solubilisation of phosphorus from the solid to the liquid phase of digestate were carried out.

In the first case, the phosphorus extraction process was performed by treating the raw digestate (before separating the liquid from the solid phase by centrifugation) with different concentrations of chloridric acid (HCl), to reach different pH values (Mehta and Batstone, 2013). Then, the mixture was left in a magnetically stirred beaker for 15 min at room temperature, and was then centrifuged at 1500 rpm for 3 min to eliminate the solid particulate. The orthophosphate content in this final liquid was determined as reported in §7.2.3.

In the second case, an acidified (pH=2) and centrifuged fraction of digestate was neutralized at different pH (which are more compatible to algal growth range) by adding NaOH, as explained in §7.3.2.1 below. The solid formed due to the neutralization was removed both by sedimentation or centrifugation at 1500 rpm for 3 min.

In the third case, EDTA (ethylendiaminetetraacetic acid) in a range of concentrations between 200 and 3000 mg L^{-1} was added after the acidification treatment, with the aim to sequester metallic ions that would instead precipitate as insoluble phosphates. The mixture was left to react for 15 minutes, then treated with NaOH for neutralization, centrifuged and measured in its phosphate content.

In the fourth case, different concentrations of $NaHCO_3$ (0.05 - 0.5 M) were added to the raw digestate, following the "Olsen method" principles, which is usually applied for phosphorus extraction in soils: bicarbonate ions (HCO_3^-) reduce the availability of metallic ions in solution such as Ca^{2+} and Al^{3+}, thus increasing phosphate solubility (Horta and Torrent, 2007). The mixture was left under stirring for 1.5 h at room temperature. After the treatment with bicarbonate, the mixture was centrifuged at 1500 rpm for 3 min or sedimented, and the phosphates in solution were measured.

7.3.Results and discussion

7.3.1. Anaerobic digestion experiments and BMP evaluation

Anaerobic sludge inoculum and LEA were characterized by their TS and VS contents, and the results are reported in Table 7.1.

Table 7.1 *Total solids (TS) and volatile solids (VS) content in anaerobic sludge and LEA*

Anaerobic sludge		**Lipid-extracted algal biomass**	
gTS L^{-1}	11.3 ± 0.13	**gTS L^{-1}**	2.96 ± 0.1
gVS L^{-1}	5.52 ± 0.04	**gVS L^{-1}**	2.76 ± 0.1
VS/TS (%)	48.6 ± 0.5	**VS/TS (%)**	93 ± 0.1

Cumulative methane production potential for the LEA is shown in Figure 7.1. Lag phase was almost nil, due to the fact that the F/M ratio equal to 0.5 is low enough to enable a fast substrate degradation operated by a high number of bacteria. Moreover, it can be observed that the plateau related to methane production was reached within the first 15 days of anaerobic digestion. This is not the case of the biogas production, which keeps increasing for additional 20 days. Until day 15, biogas contains at least the 50% of CH_4, while its percentage drops to 43% at the end of the experiments. After running the test for 40 days, the cumulative biogas and methane production was 347.3 ± 37.6 and 150.2 ± 14.6 NmL gVS^{-1}, respectively. These values are in agreement with the results reported in previous studies analysing LEA (Rodriguez et al., 2015; Tercero et al., 2014). Clearly, they are lower if compared to the theoretical methane yield, which can be calculated from the elemental composition of the biomass according to the Buswell equation (444.2 NmL gVS^{-1}), due to incomplete degradation by the anaerobic bacteria. In order to enhance the degradation of the algal walls and improve biogas and methane yield, a number of pretreatments could be applied to the extracted biomass prior to the anaerobic digestion process, but such an aspect was outside the scope of the work.

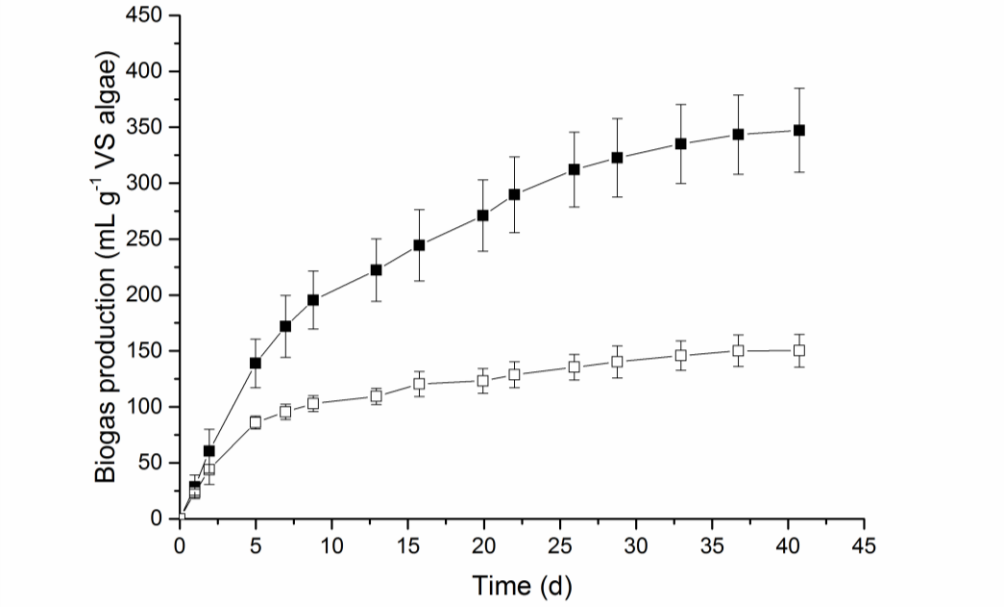

Figure 7.1 *Cumulative biogas (black squares) and biomethane (open squares) production potential of lipid-extracted C. vulgaris*

The effluent from anaerobic digestion was centrifuged and filtered in order to separate the solid fraction from the liquid one, to be recovered as a nutrient source in culture media. Nutrients

content of liquid digestate was first analysed and the composition is reported in Table 7.2. Here it can be seen that ammonium and almost all micronutrients are present in the diluted liquid digestate with a higher concentration with respect to standard BG11, while P and S are almost absent. The absence of S is due to the digestion process that produces H_2S, which is lost in gaseous phase (Möller and Müller, 2012). In particular, N-NH_4 concentration in the digestate resulted to be 524 mg L^{-1}.

Table 7.2 *Composition of liquid digestate (before and after dilution) and of BG11*

Element (mg L^{-1})	Liquid digestate	Liquid diluted digestate	BG11
N-NH_4^+	524	247	247
P- PO_4^{3-}	0.88	0.41	5.4
S	0	0	9.8
Ca	177	83.4	9.8
Co	<1	<1	0.012
Fe	6.1	2.9	1.279
Mg	51	24	7.398
Mn	<2.5	<2.5	0.503
Mo	<1	<1	$1.7 \cdot 10^{-4}$
K	83	39.1	13.7
Cu	<1	<1	0.020
Zn	<1	<1	0.051

7.3.2. Growth in liquid digestate

The liquid fraction of the anaerobic digestate was used to assess the microalgal growth capabilities on this substrate. The light absorbance of the diluted medium (OD_{750}) was equal to 0.06, i.e. it allows high light penetration for photosynthetic growth. The growth curves in the digestate were compared to a control curve in standard growth media (BG11, modified as described in §7.2.2). The specific growth rate of the control was 2.040 ± 0.087 d^{-1} and the final biomass concentration was equal to 2.147 ± 0.070 g L^{-1}. Absolute and relative nutrient consumptions and yields are summarized in Table 7.3: all the phosphorus present in the medium was consumed, suggesting a limiting role in growth.

To perform growth experiments in digestate, with the composition reported in Table 7.2, a dilution was made so to obtain the same N concentration of the control (247 mg L^{-1} N as in BG11).

Table 7.3 *Specific growth rate, final biomass concentration, nutrient consumptions (absolute and relative) in digestate with different levels of nutrient addition. Statistically significant results of growth rate and final biomass concentration with respect to the control are marked with an asterisk.*

Medium	Control	Liquid diluted digestate	Liquid diluted digestate +P	Liquid diluted digestate +P +S
μ (d^{-1})	2.04 ± 0.09	1.03 ± 0.02*	1.98 ± 0.07*	2.07 ± 0.02
C_x (g L^{-1})	2.15 ± 0.07	0.09 ± 0.01*	0.88 ± 0.28*	1.99 ± 0.16
ΔN (mg L^{-1})	126.1 ± 29.1	6.07 ± 2.43	46.89 ± 13.76	105.73 ± 4.45
ΔP (mg L^{-1})	4.95 ± 0.04	0.18 ± 0.04	2.62 ± 0.30	3.90 ± 0.18
Y_N%	57%	3%	22%	49%
Y_P%	100%	28%	43%	88%

Three growth curves were measured: a negative control where no additional nutrients were supplied to the cultivation medium, one with phosphate addition (to reach BG11 P concentration of 5.4 mg L^{-1}), and a third one where also sulphate was added to favor the growth process, at the same final concentration of BG11 ($MgSO_4 \cdot 7H_2O$ = 75 mg L^{-1}). Results are displayed in Figure 7.2.

In the first case, without any addition, *C. vulgaris* growth was much lower than the control (μ = 1.03 d^{-1}), reaching a cell concentration of barely $13 \cdot 10^6$ cells mL^{-1} because of substantial lack of P and S. When only phosphorus was added the specific growth rate was found increased, and similar to the control (μ = 1.98 d^{-1}), but due to S limitation the final biomass concentration was lower, and cells multiplication stopped at about 70 million cells mL^{-1}. On the other hand, in the case of both P and S addition, microalgal growth was comparable to the control, as all the necessary nutrients were provided in the correct amount, reaching a final concentration of about $340 \cdot 10^6$ cells mL^{-1} (see Fig. 7.2). In addition, cells grew at a rate comparable to that of the control (μ = 2.07 d^{-1}), confirming that all other micronutrients were present in the liquid digestate in a sufficient amount to guarantee algal growth in this medium. In summary, *C.*

vulgaris is able to grow in the digestate, provided that the substantial lack of fundamental macronutrients such as phosphorus and sulphur is given.

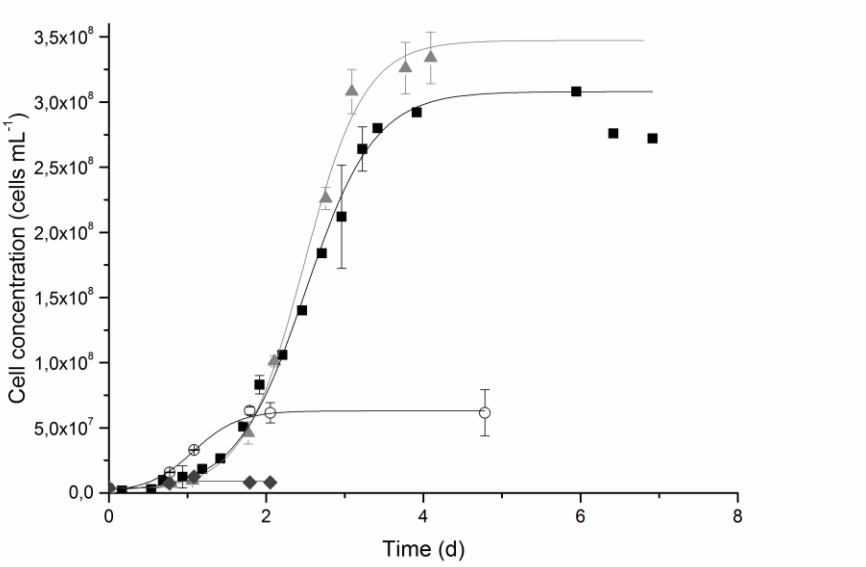

Figure 7.2 *Growth curves of C. vulgaris in BG11 medium, as a control (black squares), in the liquid digestate without any addition (gray diamonds), with phosphate addition (open circles) and with phosphate and sulfate addition (grey triangles)*

Sulphur is mostly lost as H_2S in the biogas during the anaerobic digestion operation, so little can be done to recover it in terms of chemical treatment of the digestate. Bohutskyi et al. (Bohutskyi et al., 2015), who characterized the composition of liquid digestate obtained from AD of lipid-extracted *Auxenochlorella protothecoides*, report recoveries of up to 30% of S in the liquid fraction, however this is likely available as sulfides, while microalgae are only able to uptake sulphates (Markou et al., 2014). In literature, some other solutions are reported to oxidize sulfide to sulphate during AD operation. For example, microaeration can be performed in the anaerobic digester, or the AD unit can be integrated with an external bioreactor containing a culture of sulphur-oxidizing bacteria (SOB). SOB can be present in an alkaline suspension or immobilized on various carriers to act as a biofilter (Pokorna and Zabranska, 2015). Concerning phosphorus, most of it is precipitated in the solid phase of the digestate due to the formation of insoluble phosphate salts, such as $Ca_3(PO_4)_2$, $Mg_3(PO_4)_2$, $Fe_3(PO_4)_2$ (Möller and Müller, 2012). Since P represents one of the major elements in microalgal biomass, and

its limited availability already raises a lot of concern in terms of sustainability, a number of attempts to solubilize it in the aqueous phase after digestion, and make it available as a nutrient in the cultivation medium, have been made using different techniques.

7.3.3. Phosphorus recovery

Based on stoichiometry and chemical analysis of microalgal biomass, and the concentration of inocula used for anaerobic digestion tests, it can be calculated that 1 L of mixture sludge+biomass contains approximately 35 mg of P. However, after the liquid-solid separation of digestate, only 0.88 mg L^{-1} of it remained dissolved, as a result of the precipitation phenomena described before. Thus, different treatments of the raw digestate were performed to ascertain a possible way to recover phosphate in the liquid in a bioavailable form.

7.3.3.1 Acid treatment

The raw digestate, which has a pH of 7.8, was gradually acidified by HCl addition in order to reach fixed pH values (2, 3.5, 5, 6). Phosphorus concentration obtained in the liquid phase, after centrifugation, is reported in Figure 7.3A as a function of pH, while the point at pH 7.8 represents the P concentration of the liquid digestate without any treatment. As suggested in (Mehta and Batstone, 2013), the fraction of recovered P increased during the acidification process, with an almost total solubilisation at pH = 2 (Figure 7.3A). This pH value, however, is not compatible with algal cultivation. Therefore, the centrifuged liquid was treated with NaOH to reach pH values of 7.0, 7.5 and 8, as *Chlorella vulgaris* can only live in a pH range from 7 to 9 (Xia and Murphy, 2016). On the other hand, after neutralization with sodium hydroxide, most of the soluble phosphate precipitated again as metallic (Cu, Fe, Mg, Ca) salts, as also confirmed by the dark blue/green color that was assumed by the solution. Thus, after alkaline treatment, the liquid was both centrifuged and sedimented to remove the precipitate. These centrifuged and re-suspended phases were then analysed for phosphate content confirming a low concentration of phosphorus in liquid (Figure 7.3B). It was concluded that a simple acidification step of the raw digestate is not a viable way to enhance the phosphorus recovery, and alternative methods should be assessed.

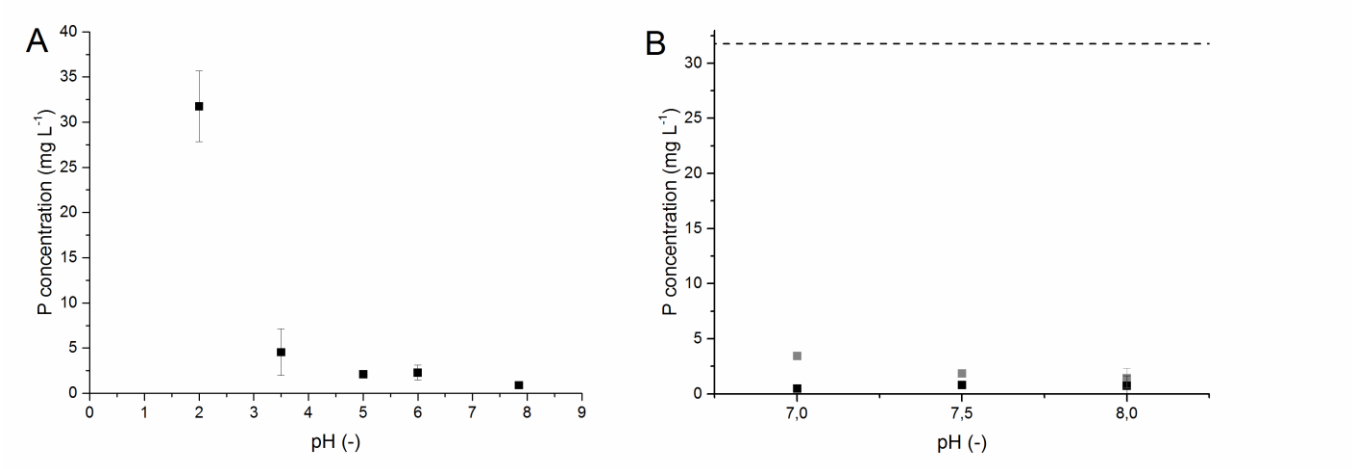

Figure 7.3 *Phosphorus concentration in the liquid phase after acidification and subsequent centrifugation at different pH set point (A). In (B) P concentration in the liquid phase after centrifugation (black squares) and sedimentation (gray squares) of an acidified mixture of solid-liquid digestate, after neutralization from pH=2 to a value of 7.0, 7.5 and 8, respectively. The initial P concentration of the acidified digestate is represented by the dashed line*

7.3.3.2 EDTA treatment

In order to overcome re-precipitation problems during neutralization, EDTA (ethylendiaminetetraacetic acid) was added after filtration of the solid particulate. EDTA is able to capture metallic ions that would instead precipitate as insoluble phosphates. This sequestration allows the phosphate ion PO_4^{3-} to be dissolved in the aqueous phase and to be available as a nutrient source for microalgae cultivation. The mixture was left to react for about 15 minutes, then NaOH was added for neutralization, centrifugation was performed and the phosphate content was measured. As reported in Figure 7.4, it is clear that the more EDTA is added, the more phosphorus is dissolved in the liquid phase. However, to reach significant concentrations of P, more than 3 g L^{-1} of EDTA must be added to the digestate. This fact definitely hinds the economical sustainability of phosphorus recovery from the digestate by EDTA addition.

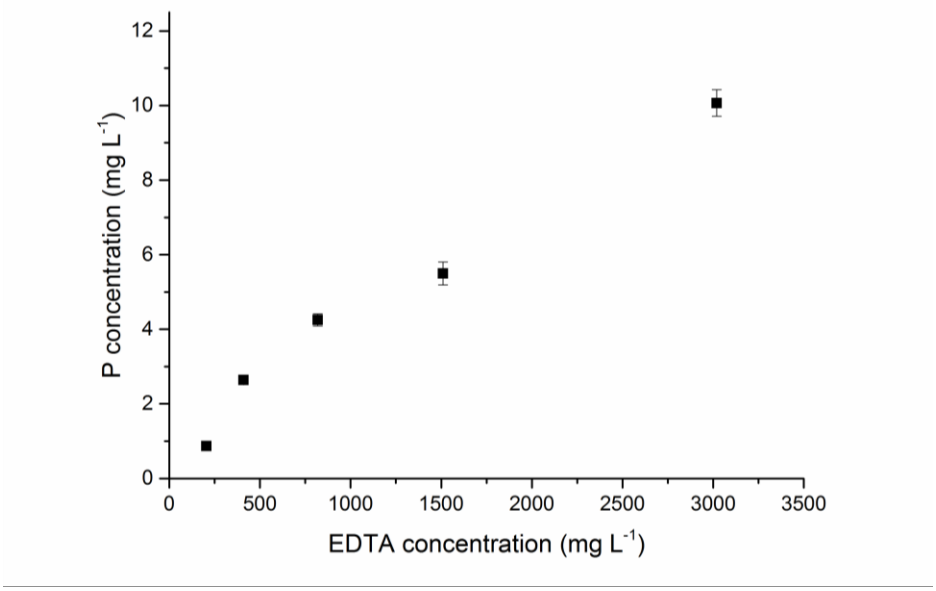

Figure 7.4 *Phosphorus concentration in the liquid phase after centrifugation at different EDTA concentrations*

7.3.3.3 Bicarbonate treatment

A procedure called "Olsen method" (Horta and Torrent, 2007), normally used to extract and determine phosphorus in soils, was tested to extract phosphorus from the solid part of the digestate into the liquid one. This method involves the use of an inexpensive and non-toxic compound such as sodium bicarbonate ($NaHCO_3$). The presence in solution of bicarbonate ions (HCO_3^-) reduces the availability of metallic ions such as calcium Ca^{2+} and aluminum Al^{3+}, thus increasing phosphate solubility. Accordingly, the raw digestate was mixed with different amounts of $NaHCO_3$, then NaOH was added to reach a mixture pH equal to 8.5, as required by the Olsen method. After the incubation, two techniques of solid-liquid separation were tested: centrifugation and sedimentation. The P content was measured in the liquid phases obtained and the results are shown in Figure 7.5. The percent of solubilized phosphorus in the liquid digestate increased with bicarbonate concentration, confirming the suitability of the Olsen method to recover P in the liquid phase. The centrifugation step, however, usually lowered the presence of P in solution, if compared to the sole sedimentation. A simple sedimentation step allowed to recover more P in solution, up to about 41% of the total P in the case of 0.5 M $NaHCO_3$.

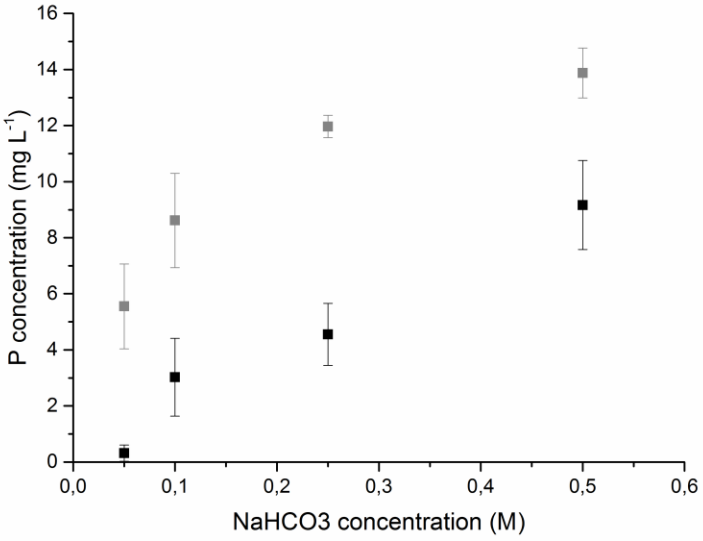

Figure 7.5 *Phosphorus concentration in the liquid digestate after centrifugation (black squares) and sedimentation (grey squares), as a function of $NaHCO_3$ concentration*

On the other hand, the turbidity of the sedimented phase was higher that the centrifuged one and this has to be considered when cultivating phototrophic organisms. This method, anyway, seems to be promising for phosphorus recovery, since the P concentration is significantly higher than in the case of untreated digestate, and would be sufficient to sustain a microalgal cultivation.

7.3.4. Growth in treated digestate

Based on the results obtained above, the raw digestate was treated with $NaHCO_3$ 0.1 M and 0.5 M respectively and, after sedimentation of the solid fraction, the corresponding liquids were used for further microalgal cultivation. The two liquid fractions were analysed with respect to ammonium and phosphate contents to evaluate the dilution to be applied prior to using these treated digestates as cultivation media. The ammonium-nitrogen concentration resulted to be about 538 mg L^{-1} N, unaffected by the treatment, while the concentration of phosphorus was about 7 and 12.5 mg L^{-1} for the 0.1 M and 0.5 M sodium bicarbonate treatment respectively. *C. vulgaris* was cultivated in the diluted liquid phase of the two treated digestates, at the same experimental conditions of the previous cultures. Sulphur was added in both cases

in the same amount as standard BG11, while no additional phosphorus nor micronutrients were supplied. The corresponding growth curves are shown in Figure 7.6, compared to that obtained in the untreated digestate with P and S addition (§7.3.2). Due to the presence of bicarbonate, the pH was adjusted during the growth curve and controlled to 7.8 value.

The growth behavior of microalgae in digestate treated with 0.1 M sodium bicarbonate followed the one of the untreated digestate control with a specific growth rate of 1.45 ± 0.27 d^{-1} up to a certain point, but the cellular concentration reached a plateau at about $160 \cdot 10^6$ cells mL^{-1}. The lower final cell concentration is reflected also in the OD_{750} (Fig. 7.6B) and in the biomass concentration (1.47 ± 0.01 g L^{-1}), which also have a lower value. This can be attributed to P limitation in the medium as, after dilution, the initial concentration was measured to be 3.0 ± 0.12 mg L^{-1} P.

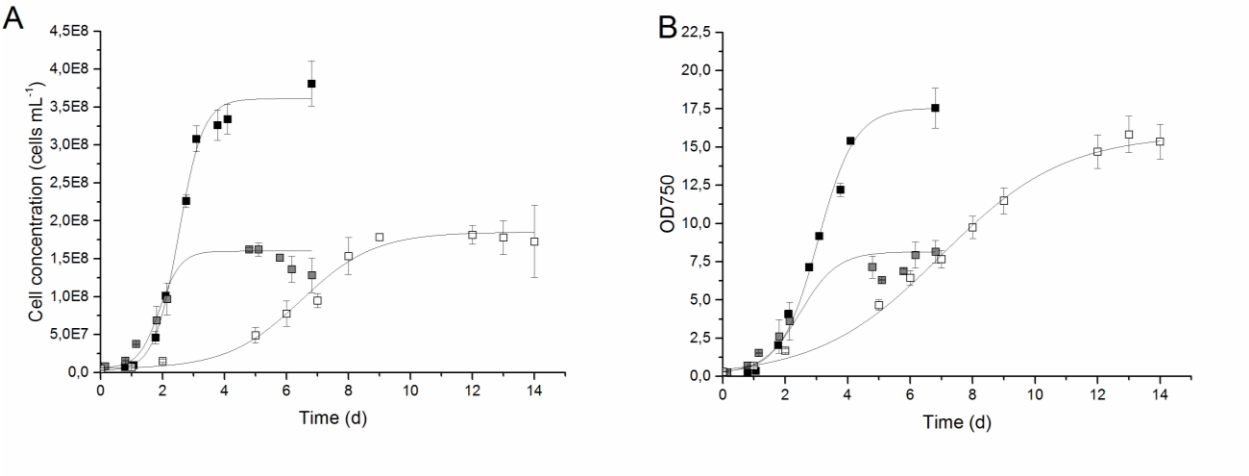

Figure 7.6 *Growth curve of C. vulgaris in digestate treated with $NaHCO_3$ 0.1 M (grey squares) and 0.5 M (empty squares), compared to untreated digestate with P and S addition (black squares). In Fig. 7.6A the cell concentration is reported, while in Fig. 7.6B the optical density at 750 nm is shown.*

On the other hand, when a 0.5 M $NaHCO_3$ concentration was used (i.e., more phosphorus is solubilized in the medium, with an initial concentration of 5.27 ± 0.26 mg L^{-1} after dilution), the growth rate was hindered (μ = 0.86 d^{-1}) because of the high bicarbonate concentration, according also to what reported in Gris et al. (Gris et al., 2014). In addition, a lower specific growth rate could be explained by considering the increased turbidity of the medium after treatment, thus affecting the light availability for phototrophic growth. However, in this case,

even though the growth rate was slower and cell multiplication stopped at a concentration of about $170 \cdot 10^6$ cells mL^{-1} (Fig. 7.6A), the final biomass concentration achieved was equal to 2.29 g L^{-1}, which is even higher than the control, as a result of higher carbon available in solution, due to the presence of bicarbonate (Gris et al., 2014). This, together with the trend of OD_{750} which reaches a final value similar to the untreated medium (Fig. 7.6B), suggests that the effect of the high bicarbonate concentration caused an osmotic stress to algal cells possibly increasing their size, as also widely reported in the literature (Gardner et al., 2013, 2012). Table 7.4 summarizes the growth rate, final biomass concentration and nutrient consumption in the treated digestates in comparison to control in untreated digestate with P and S addition.

Table 7.4 *Specific growth rate, final biomass concentration, phosphorus consumption (absolute and percentage) in digestate treated with different concentrations of $NaHCO_3$, and untreated digestate. Statistically significant results of growth rate and final biomass concentration with respect to the untreated digestate growth curve are marked with an asterisk.*

Medium	**Untreated digestate +P +S**	**Treated digestate (0.1 M $NaHCO_3$) +S**	**Treated digestate (0.5 M $NaHCO_3$) +S**
μ (d^{-1})	2.07 ± 0.02	1.45 ± 0.27	0.86 ± 0.04*
C_x (g L^{-1})	1.99 ± 0.16	1.47 ± 0.01*	2.29 ± 0.04*
ΔP (mg L^{-1})	3.90 ± 0.18	3.0 ± 0.12	5.27 ± 0.26
Y_P%	88%	100%	100%

In summary, the results obtained show that microalgal growth in the liquid digestate is possible, requiring only the addition of sulphate as external nutrients supply, after an appropriate treatment is carried out to solubilize phosphorus. However, an optimum value should be found for the concentration of $NaHCO_3$, so to reach a trade-off between fast growth with lower biomass production (due to low P available) and high final concentrations at slower growth rates (because of bicarbonate inhibition).

7.4. Final remarks

The possible exploitation of the liquid phase recycled from anaerobic digestion of lipid-extracted microalgal biomass to cultivate the same species was assessed in this chapter, in view of the development of a closed-loop process. The digestion of lipid-extracted biomass showed a good BMP confirming microalgal biomass as a valuable substrate for anaerobic digestion. The liquid digestate was tested as a culture medium, and re-growth experiments were carried out. All macro and micronutrients were found to be non-limiting, except for sulphur, which is lost mainly as H_2S during the digestion process, and phoshorus, which is in fact re-mineralized, but is lost during the liquid-solid separation. Different protocols to re-suspend precipitated phosphorus were assessed, and the exploitation of sodium bicarbonate following the Olsen method appeared as the most promising. The presence of bicarbonate in solution, on the other hand, should be properly optimized, in order to avoid increased osmotic pressure during re-growth experiments.

Chapter 8

Nutrient recycling for large-scale microalgal production: mass and energy analysis of different recovery strategies

Nutrient supply for large-scale microalgal cultivation has emerged as one of the key limiting factors of renewable biofuels production: considering the impacts that nutrients requirement has on the environmental and economic sustainability of the process, their recovery and recycle is of paramount importance. In this context, different technologies have been recently proposed and tested from the experimental point of view, but less information are available on the actual nutrient recovery yields and on the energy balance of the closed-loop process. In this chapter, two different technologies for simultaneous biofuels production and nutrient recycling, namely anaerobic digestion (AD) and flash hydrolysis (FH), are investigated by means of process simulation. The performances of the two process alternatives are compared in terms of both nutrients recovery and of energy efficiency (EROEI), to evaluate their feasibility at industrial scale. To this aim, a photobioreactor model with Monod kinetics and Elec-NRTL thermodynamics was implemented, and laboratory experimental data on AD and FH respectively were used to implement the model. From the results obtained, FH appears to perform better in terms of nutrients recycling, with up to 70% and 60% of phosphorus and nitrogen recovered in bio-available forms, respectively. In the case of AD, the incomplete biodegradability of the biomass residues limits the extent of nutrients recovery. On the other hand, the latter requires much lower energy inputs, achieving EROEI values always favourable, while the high thermal requirements of FH, even with proper heat integration, highlights the need of further improvements of the operating conditions to reduce the energetic burden of this process.

8.1. Introduction

The increasing world energy demand and the concerns raised by environmental impacts related to the consumption of fossil fuels sources has driven, in the latest years, intense research efforts towards the development of alternative, renewable energy sources. Microalgae have received lot of emphasis as one of the most promising biomass feedstocks for the production of transportation fuels for medium-term replacement of petroleum-derived ones. Using microalgae for the production of renewable energy has several advantages: photosynthetic efficiency and growth rates higher than terrestrial energy crops together with high oil yields, which correspond also to lower environmental footprints, as less surface area is required. In addition, microalgae do not compete with food production for agricultural land. Production of algal oil has been achieved in various pilot scale facilities, but whether algal fuels can be sustainably and economically produced in sufficient quantity to meaningfully displace petroleum fuels is still a matter of debate. Significant obstacles still need to be overcome before microalgae–based biofuels production becomes cost-effective and can impact the world's supply of transport fuels (Chisti, 2013).

One of the factors recently emerged as a crucial environmental limitation to mass production of algal fuels is that microalgae cultivation is associated with a high demand of nutrients, especially nitrogen and phosphorus. In fact, the production of 1 ton of algal biomass (dry weight basis) requires ranges of 60-90 kg of nitrogen and 0.3-1.5 kg of phosphorus (Canter et al., 2015; Pate et al., 2011), depending on the cultivation conditions for microalgae. Hence, the supply of nutrients severely limits the extent to which the production of biofuels from microalgae can be sustainably expanded. In fact, nitrogen is produced from fossil sources through highly energy-intense processes, i.e. the Haber-Bosch one, (Peccia et al., 2013), while phosphorus is a mined nutrient derived from phosphate rocks, which are expected to be depleted soon (Cordell et al., 2009). A possible way to reduce the amount of nutrients required is the use of wastewaters (Ras et al., 2011; Sforza et al., 2014b) but, even though microalgae have shown to efficiently exploit this nutrient source, the amounts involved in wastewaters are not sufficient for an extensive production (Shurtz et al., 2017). However, considering that N and P are not components of the fuel precursors, the fresh nutrients demand can be reduced if they are recovered from the residual biomass and reused for further algae cultivation, in a

closed-loop process. In the recent years, many works have focused on this hot issue, mostly from the experimental (Biller et al., 2012; Bohutskyi et al., 2015; López Barreiro et al., 2015; Prajapati et al., 2014) and a few from the materials/energy modeling (Rösch et al., 2012; Yuan et al., 2015; Zhang et al., 2014) points of view. Among the various technologies available, anaerobic digestion (AD) of microalgae residue after lipids extraction and hydrothermal treatments on whole wet biomass have been commonly recognized as the most promising alternatives to achieve this goal. Anaerobic digestion is a well-developed technology, widely used also at industrial level for the treatment of various organic wastes. AD carried out on microalgae residues allows to produce biogas as an additional fuel, while nutrients are re-mineralized into the aqueous phase, which has been shown to be a good substrate for growth (Ward et al., 2014).

In the area of hydrothermal treatments, HTL (hydrothermal liquefaction) is by far the most investigated technology. Recently, also flash hydrolysis (FH), a type of rapid HTL treatment characterized by very short residence times (<10 s) has emerged as a viable way to fractionate the wet biomass into a solid fraction in which the majority of the lipids are retained (biofuels intermediate), and a liquid phase rich in N, P and other micronutrients (hydrolysate), suitable for recycling (Garcia-Moscoso et al., 2013). Such a process has several advantages compared to conventional HTL, among which the fact that lipids are preserved in the solid fraction for further biofuels production, along with the much lower concentration of toxic compounds (e.g. phenols) in the aqueous phase that is to be recycled (Garcia-Moscoso et al., 2015).

In the previous chapters, an extensive experimental activity on both anaerobic digestion and flash hydrolysis was discussed, with the aim of assessing the nutrients recovery and subsequent recycling potential of these two processes. Both of them showed promising results in terms of nutrients recovered, as well as recycling potential. In particular, in the case of the hydrolysate recovered from FH, biomass production was even enhanced thanks to mixotrophic growth, due to the high carbon content of this substrate. However, from an industrial perspective, it is necessary to evaluate material and energy balances by accurate process simulation, so to understand the actual feasibility and the impact of the technology chosen in terms of environmental, energetic and, ultimately, economic sustainability. At present, little information can be found in the literature in this regard. Rösch et al. (Rösch et al., 2012) analyzed the materials flow of anaerobic digestion and hydrothermal gasification of algae

residue after lipid extraction, focusing on the nutrients recycling aspects, while Zhang et al. (Zhang et al., 2014) compared AD with HTL also from the energy recovery point of view, concluding that the first one appears to perform better. However, the effect of nutrients concentration in the medium on algal growth kinetics and especially their bioavailability and speciation depending on pH was not considered in these works. In addition, FH presents different characteristics compared to HTL. In this chapter, the experimental results previously obtained were hence exploited, together with some literature data, to develop systematic process simulations with a detailed representation of the chemical equilibrium inside the photobioreactor, with the aim of quantitatively investigating and comparing the feasibility of the technologies considered in view of large-scale applications, focusing on nutrients as well as energy related aspects.

8.2. Model development

The model was based on previous experimental data obtained with the microalgal species *Chlorella vulgaris*. This alga was chosen as a good candidate because of its high growth rates and productivities, together with its robustness and capability of growing in non-sterile media, such as wastewaters or digestates (Ahmad et al., 2013; Lowrey et al., 2016; Ras et al., 2011). The elemental composition of the biomass, which was determined analytically, was equal to 46.45% C, 6.77% H, 7.36% N, 38.03%, 1.39% P (wt%), with an oil content of 6% (on dry weight basis). The process flowsheet is schematically represented in Fig. 8.1, and is divided into two sections, i.e. the biomass cultivation system (PBR) and the downstream process for biofuels production and nutrients recycling (AD and FH respectively). The thermodynamic model chosen for the simulations is Elec-NRTL (Electrolyte Non-Random Two Liquid), in order to accurately take into account the chemical equilibrium and ionic distribution of the nutrients involved, considering that they need to be in bio-available forms for algae to up-take them (i.e., CO_2, NH_4^+ and orthophosphates for C, N and P respectively), as well as the pH inside the PBR. For simplicity, other micronutrients necessary for algal growth have been neglected in these simulations. All other considerations and assumptions used to implement the simulation model developed with the process simulator Aspen Plus™ v.9 are summarized in the following sections.

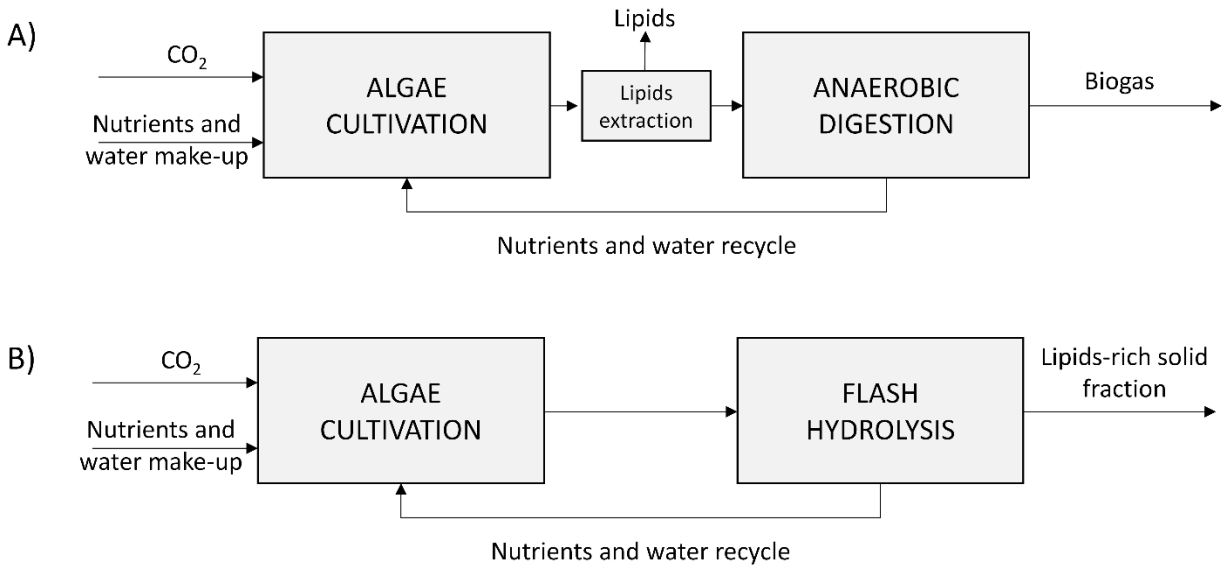

Figure 8.1 *Block-flow diagram for anaerobic digestion (A) and flash hydrolysis (B)*

8.2.1. Cultivation system

The microalgal biomass production system (highlighted in both Figure 8.2 and 8.3) is modeled as a Plug-Flow Photobioreactor (PBR) which, compared to a perfectly mixed reactor (CSTR), better represents the behavior of a large-scale application, with an increasing microalgae concentration developing along the reactor length. The kinetics of the microalgal production reaction was expressed with a Monod-like equation, taking into account multiple limiting substrates, i.e. C (CO_2), N (NH_4^+) and P. The sum of $H_2PO_4^-$ and HPO_4^{2-} was taken as representative of orthophosphates, as these are the main ionic species present, in almost equal concentrations, within the pH range considered. Thus, the reaction kinetics are expressed by:

$$R_x = \mu_{\max} \cdot c_x \cdot \prod_{i=C,N,P} \frac{c_i}{K_i + c_i} \qquad \text{(Eq. 8.1)}$$

where R_x is the growth rate in [kg m^3 d^{-1}], μ_{max} is the maximum specific growth rate [d$^-$], c_x the biomass concentration [kg m^{-3}], c_i is the concentration of substrate i [kg m^{-3}], and K_i is the corresponding half-saturation constant [kg m^{-3}]. The values of K_i were obtained from literature data for *C. vulgaris* (Concas et al., 2012), while μ_{max} was measured experimentally in the lab: in particular, it resulted equal to 1.5 d^{-1} for autotrophic growth (as in the digestate from AD), and 1.8 d^{-1} under mixotrophic conditions (as in the case of the hydrolysate from FH), at 28°C.

A total liquid flow-rate of 10000 kg h^{-1} (with non-limiting N and P concentrations) is set as calculation basis for the PBR inlet. A PBR surface area of 1 ha and a residence time of 1 d were considered as a basis for the photoautotrophic growth. In order to make the evaluation of the two evaluated downstream processes consistent, the PBR length (i.e., the residence time) was adjusted for mixotrophic growth so to obtain the same biomass production. CO_2, assumed to be available from flue gases (15% v/v) is supplied by means of a fan in non-limiting amount. After the reactor, a flash unit eliminates the gaseous products. The liquid/solid stream is sent to a gravity settler (*SEP-1*), where the biomass is concentrated fivefold, so 80% of the mixture water + residual nutrients is recycled back to the cultivation system. Part of the concentrated biomass is also sent back to the reactor in order to ensure an inlet concentration of 0.2 g L^{-1} (necessary to avoid wash-out), as well as to recycle another share of water and nutrients. In the make-up stream nutrients are supplied, together with water, in the form of K_2HPO_4 and NH_4Cl.

8.2.2. Anaerobic digestion (AD)

The complete flowsheet of the anaerobic digestion pathway is shown in Figure 8.2.
The pre-concentrated algae stream from the gravity settler is sent to a filter-press unit (*SEP-2*) for further concentration up to 20% solids content, a reasonable value for the subsequent wet oil extraction process (Sathish and Sims, 2012; Zhang et al., 2014), as well as for the following AD unit. The nutrients-rich water recovered is mostly sent back to the reactor to minimize the make-up requirement, while a small fraction (2%) is purged to account for losses in real process operation. An efficiency of 67% of oil extraction was assumed based on experimental measurements, considering that, in order not to hinder anaerobic bacteria during the digestion process, less efficient solvents have to be used. After oil extraction (*EXTR-01*), the residual biomass is heated up and sent to the digester, which operates at 35°C (mesophilic digestion).

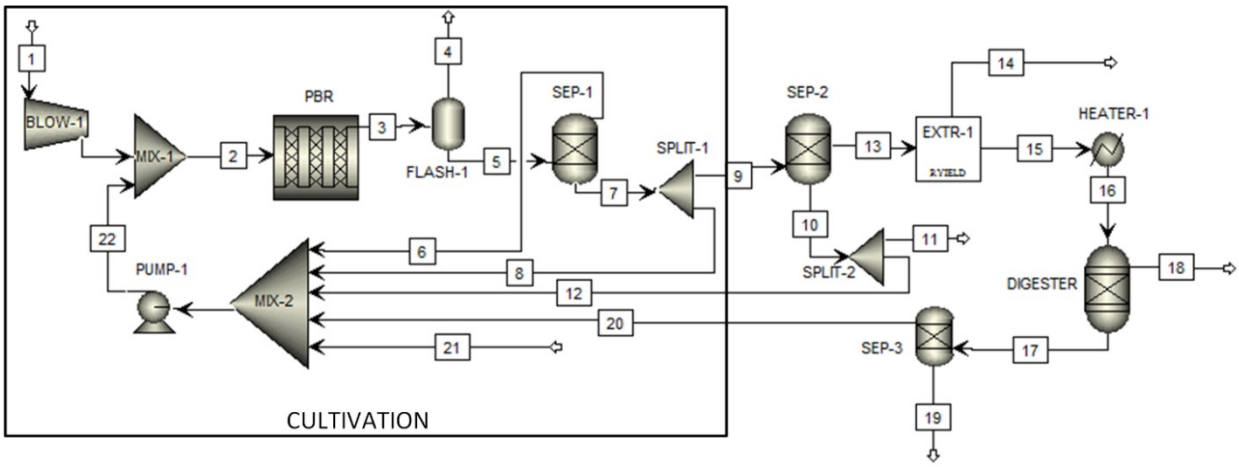

Figure 8.2 *Flowsheet diagram for the anaerobic digestion pathway*

The AD unit is simulated with a *RYield* reactor, which decomposes the biomass into the digestion products, according to a modified Buswell equation (Bruno Sialve et al., 2009). For a general algal biomass with known molar composition, the reaction is:

$$C_c H_h N_n O_o P_p + \left(-\frac{h}{4} + \frac{11p}{4} - \frac{o}{2} + c - \frac{3n}{4}\right) H_2O \rightarrow$$

$$\left(\frac{h}{8} + \frac{5p}{8} - \frac{o}{4} + \frac{c}{2} - \frac{3n}{8}\right) CH_4 + \left(-\frac{h}{8} - \frac{5p}{8} + \frac{o}{4} + \frac{c}{2} + \frac{3n}{8}\right) CO_2 + nNH_3 + pH_3PO_4 \qquad \text{(Eq 8.2)}$$

where c, h, n, o, p are the molar fractions in the biomass residue of the elements C, H, N, O, P, respectively, calculated based on the composition of the starting biomass and the amount of oil extracted. A fraction of algal biomass remains undigested and maintains its original composition, and a partial biodegradability (BD) equal to 0.54 was used according to experimental values. The effluent from the AD unit is sent to a liquid/solid separator (*SEP-3*): the solid product contains the undigested algal biomass together with a fraction of the mineralized phosphorus, as it was ascertained that phosphate ions tend to precipitate during the digestion process, forming insoluble salts together with metallic cations (Lin et al., 2015; Möller and Müller, 2012). In particular, based on the experimental data discussed in chapter 7, 41% of the P is recovered in the aqueous medium, while the rest is retained in the solids. The liquid digestate, rich in recovered nutrients, is hence recycled back to the cultivation system, reducing the amount of fresh fertilizers to be supplied as make-up.

8.2.3. Flash hydrolysis (FH)

The process scheme of the Flash Hydrolysis pathway is shown in Figure 8.3.

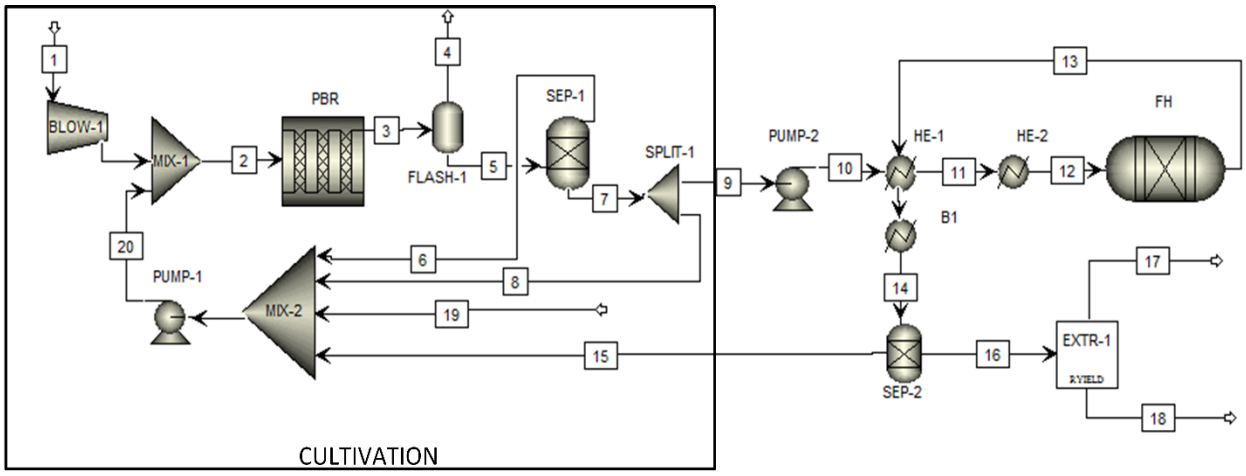

Figure 8.3 *Flowsheet diagram for the flash hydrolysis pathway*

After sedimentation, the concentrated biomass (10 g L^{-1}, according to the experimental set-up described Garcia-Moscoso et al., (2013), is directly fed to the FH reactor. The optimum operating conditions, based on experimental data, were found to be 280°C and 9 s of residence time (Garcia-Moscoso et al., 2015). The algal slurry has therefore to be pressurized up to a value greater than the vapor pressure of water at the reaction temperature (~70 bar), maintaining sub-critical liquid water conditions. The hot products from flash hydrolysis are used to pre-heat the inlet stream, in order to optimize the process energy duties. Then, a second heat exchanger (*HE-2*) increases the feed temperature to the desired value.

The FH reactor is modeled as a *RYield* unit which, according to the experimental results obtained in the lab with different algal species (Garcia-Moscoso et al., 2015; Teymouri et al., 2016), allows recovering 47% w/w of the initial biomass in the solid fraction (biofuels intermediate), in which 92% of the lipids are retained. In the aqueous hydrolysate, 71% of P in the form of orthophosphates and 61% of N are extracted, the latter being available mainly in simple organic forms (amino acids and oligopeptides), with only 10% of inorganic ammonium. For simplification, glycine was used as representative of the organic nitrogen fraction. The capability of up-taking simple organic forms is highly dependent on the species investigated (Markou et al., 2014): though this aspect was verified in Chapter 5 with the alga *Scenedesmus obliquus*, there is evidence in the literature that *C. vulgaris* can indeed utilize an array of

essential amino acids (Lowrey et al., 2016). Clearly, the reaction kinetics in the photobioreactor were slightly modified to keep into account the assimilation of organic nitrogen. After cooling down, the flash hydrolysis products are sent to a liquid-solid separation unit (*SEP-2*): the solid biofuels intermediate (20% solids content) goes to an extraction unit for the recovery of the oil, while the nutrients-rich liquid hydrolysate is recycled to the cultivation system.

The two process alternatives were compared in terms of reduction of N and P make-up due to recycling from AD or FH respectively, as well as considering their energetic profitability in terms of Energy Return on Energy Investment (EROEI). The latter is calculated, according to Ramos Tercero et al. (2013), by taking into account both the direct (i.e. heat and electricity) energy flows, *ED* [kW], as well as the indirect inputs/outputs associated with raw materials (fertilizers) and products (fuels) flowrates $\dot{m}$ [kg s^{-1}], through their energy equivalent EE [MJ kg^{-1}]:

$$EROEI = \frac{\sum_{i}(ED_{i,out} + \dot{m}_{i,out} \cdot EE_i)}{\sum_{j}(ED_{j,in} + \dot{m}_{j,in} \cdot EE_j)} \quad \text{(Eq. 8.3)}$$

8.3. Results and discussion

8.3.1. Anaerobic digestion

With the given input values (see §8.2.1), a production of 8.2 kg h^{-1} of algal biomass is obtained in the PBR, with an outlet concentration of 1.02 g L^{-1}. Considering a PBR surface of 1 ha, at middle latitudes, this production corresponds to a photosynthetic efficiency of 3.8%, which is a realistic value, and a corresponding areal productivity of 19.61 g m^{-2} d^{-1}. Based on the elemental composition of *C. vulgaris*, and the consequent reaction stoichiometry, 73.6 g of N and 13.9 g of P are required to produce 1 kg of algae, resulting in a net consumption of 0.602 kg h^{-1} and 0.114 kg h^{-1}, respectively. In order to avoid nutrients limitations and keep a high growth rate in the reactor, N and P have however to be supplied to the cultivation system in large excess (§8.2.1).

From Figure 8.3A it can be seen how the majority of nutrients and water is recovered from the separation units (*SEP-1* and *SEP-2*). Concerning nutrients however, these internal

recirculations simply handle the excess amounts that are not up-taken by the algae, but serve to maintain a high concentration in the medium (high Monod coefficients).

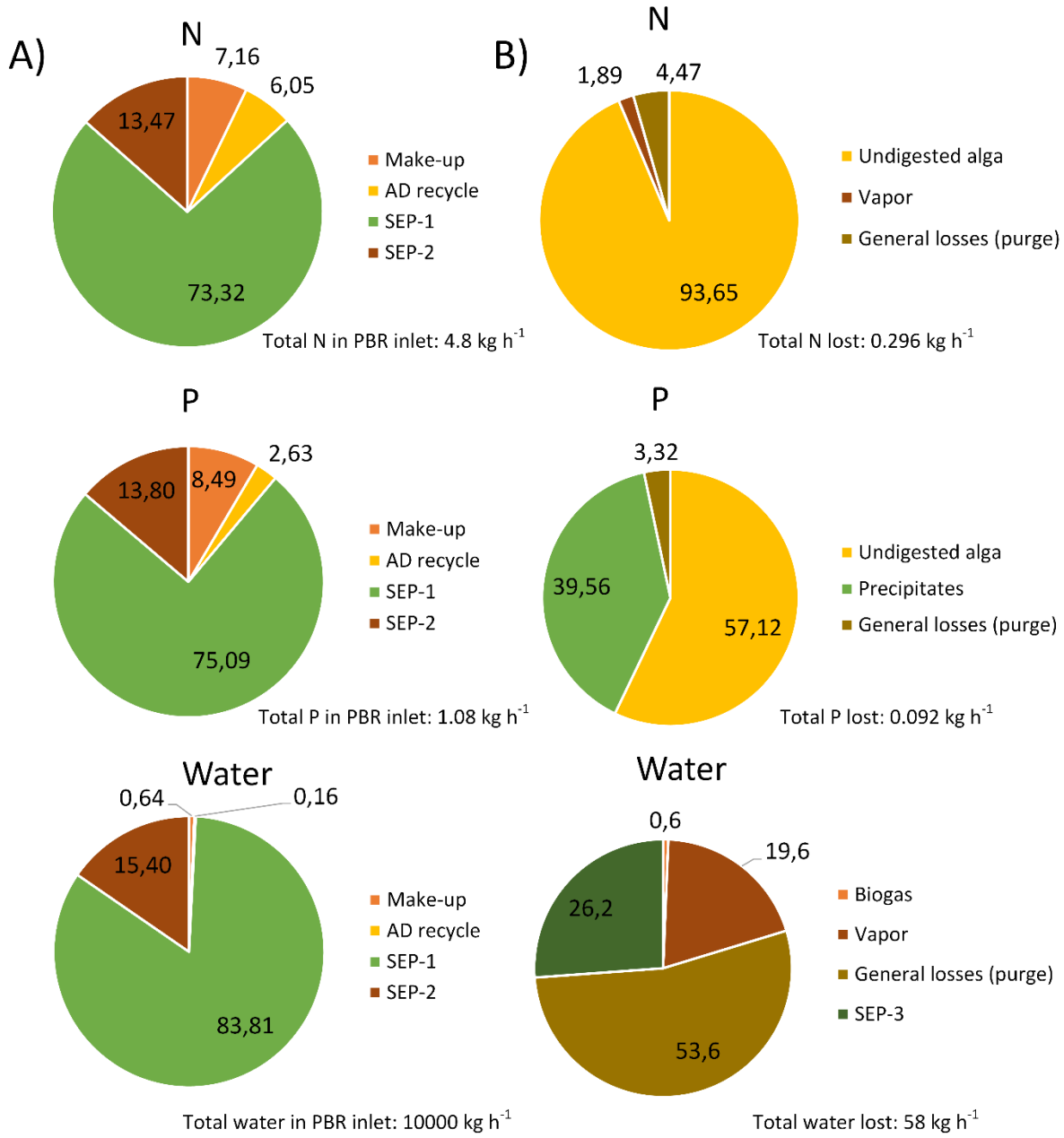

Figure 8.3 *Nutrients (N and P) and water contributions to the PBR inlet (A) and losses (B) in the AD process*

The nitrogen and phosphorus assimilated into the biomass are instead recovered from the AD process: in particular, the fresh make-up of N and P fertilizers required is reduced by 52.3% and 21.6 % respectively thanks to the recycle of the digestate, compared to the case in which

the residual biomass would be used in a different way (e.g. simply discarded or directly combusted), hence with no recovery of nutrients . Specific nutrients losses account for 36 g of N and 11.2 g of P for each kg of algae produced, meaning that almost half of the nitrogen and 80% of the phosphorus required are lost due to process inefficiency. The nutrients and water losses distribution is reported in Figure 8.3B: it can be seen that the major contribution to N and P inefficient recovery is due to the incomplete digestion of the biomass in the AD unit. A large amount of phosphorus is in addition lost due to precipitation as insoluble salts. A little amount of N is lost in the vapor phase of the cultivation system, while the ammonia contained in the biogas is assumed to be easily recovered through an absorption unit with the main water recycle stream used as solvent. Regarding water, the main loss is due to the purge, while the second major contribution is related to the separation of the solid fraction following anaerobic digestion (*SEP-3*), for which a solids content of 20% was assumed. However, the total water loss accounts for only 0.6% of the amount required by the PBR.

Finally, the overall biofuels production is equal to 0.33 kg h^{-1} of oil and 4.5 kg h^{-1} of biogas with 30% w/w methane concentration (i.e., 54% v/v). The process EROEI, whose various contributions are summarized in Table 8.1, under the conditions investigated, is equal to 2.25. Energy contributions were evaluated from literature data (Ramos Tercero et al., 2013; Yuan et al., 2015) or technical manuals ("Sereco S.r.l.," n.d.), together with results from process simulations. A value of EROEI greater than 1 means that the primary energy input to the process is favorably used for the production of energy-carrier products. The value obtained is in the range of other works reported in the literature (Ramos Tercero et al., 2013; Vasudevan et al., 2012), even though still much lower compared to those related to conventional petroleum production. It should be noted that these simulations rely on wet lipids extraction: if the algal biomass had to be dried in order to extract the oil, additional 19 kW of heat would be required, leading to an EROEI value lower than 1.

In addition to the base case simulation presented above, the effect of the lipids content in the algal biomass and that of the biodegradability in the anaerobic digestion unit on the process performances were individually investigated. In fact, an oil content of 6% is definitely low when the aim is the production of liquid fuels, while values between 20-30% are commonly reported for *C. vulgaris* (Feng et al., 2011). Hence, in the first case, oil contents of 30% and 45% (dry weight) were considered while, for BD, values of 0.65 and 0.75 were used, based on

literature data (Zhao et al., 2014). The results obtained, in terms of reduction of N and P make-up required and of EROEI, are reported in Table 8.2. A higher oil content in the algal biomass does not affect the nutrients make-up, as their recovery depends on the performances of the anaerobic digestion process only.

Table 8.1 *Direct and indirect energy contributions for EROEI calculation of the AD pathway*

Total input			**9.275**
	Flow-rate [kg h^{-1}]	**EE [MJ kg^{-1}]**	**Energy [kW]**
Material flows			
Process water	63.1	$1.33 \cdot 10^{-3}$	0.023
NH_4Cl	1.13	11.79	3.7
K_2HPO_4	0.51	12.28	1.75
Electricity			
CO_2 blower			0.691
PBR mixing			1.97
Recirculation pump			0.701
SEP-2 (Filter-press)			0.068
SEP-3 (Filter-press)			0.001
Cochlea for sludge			0.016
Digester			0.55
Heat			
Digester HE			0.282
Total output			**21.9**
	Flow-rate [kg h^{-1}]	**EE [MJ kg^{-1}]**	**Energy [kW]**
Material flows			
Oil	0.33	36	3.27
Biogas	4.47	15	18.63

The EROEI value instead increases together with the amount of lipids, as the energy density (i.e. the lower heating value) of the oil product is considerably superior to that of the starting biomass and of the biogas. It has to be noted however that not only the amount, but also the quality of the biogas obtained decreases when more oil is produced, as the residual biomass sent to the anaerobic digestion has lower C and H content. On the other hand, an increase in the biodegradability of the biomass inside the digester has a positive effect both in terms of nutrients recovery/recycling and of energy profitability. The latter is substantially improved as a direct consequence of enhanced biogas production, but also because the indirect energy

inputs associated with N and P fertilizers (which are produced through energy-intense processes) is reduced thanks to their higher recovery and recycling rate.

Table 8.2 *Effect of lipids content and biomass biodegradability on the performances of AD process*

Parameter	Lipids content (BD = 0.54)			Biodegradability (Lipids = 6%)		
	6%	**30%**	**45%**	**0.54**	**0.65**	**0.75**
N make-up reduction	52.3	52.3	52.3	52.3	63	72.7
P make-up reduction	21.6	21.6	21.6	21.6	26	30
EROEI	2.25	2.8	3.16	2.36	2.9	**3.64**

In a scenario with BD = 0.75 and 45% lipids content in the biomass, the EROEI value would be equal to 4.91. Clearly, biodegradability emerges a key factor in determining the performances of the anaerobic digestion pathway both from the material and energy points of view, and hence work should be focused on improving this step.

Finally, in all the cases considered, the possibility of exploiting the undigested biomass for further energy production (e.g., through combustion) was evaluated. However, the thermal input that would be required for drying the solids makes this choice unfavorable in terms of EROEI, so that it would be preferable to use this product as a possible soil amendment/biofertilizer.

8.3.2. Flash hydrolysis

Due to the higher growth rate achieved under mixotrophic conditions, the residence time required to reach an equal biomass production of 8.2 kg h^{-1} is reduced in this case to 0.95 d, which corresponds also to a lower PBR surface area (reduced by 14% with respect to the previous case), as a consequence of the higher areal productivity (22.6 g m^{-2} d^{-1}). The nutrients distribution in the PBR inlet is displayed in Figure 8.4A. Even in this case, the majority of nutrients (i.e., the large excess not assimilated by microalgal biomass) are recycled after the first concentration step (*SEP-1*). On the other hand, the FH process allows recovering 44.3 g

N and 9.7 g of P per kg of algae produced, reducing the make-up requirements by 59% and 69% respectively.

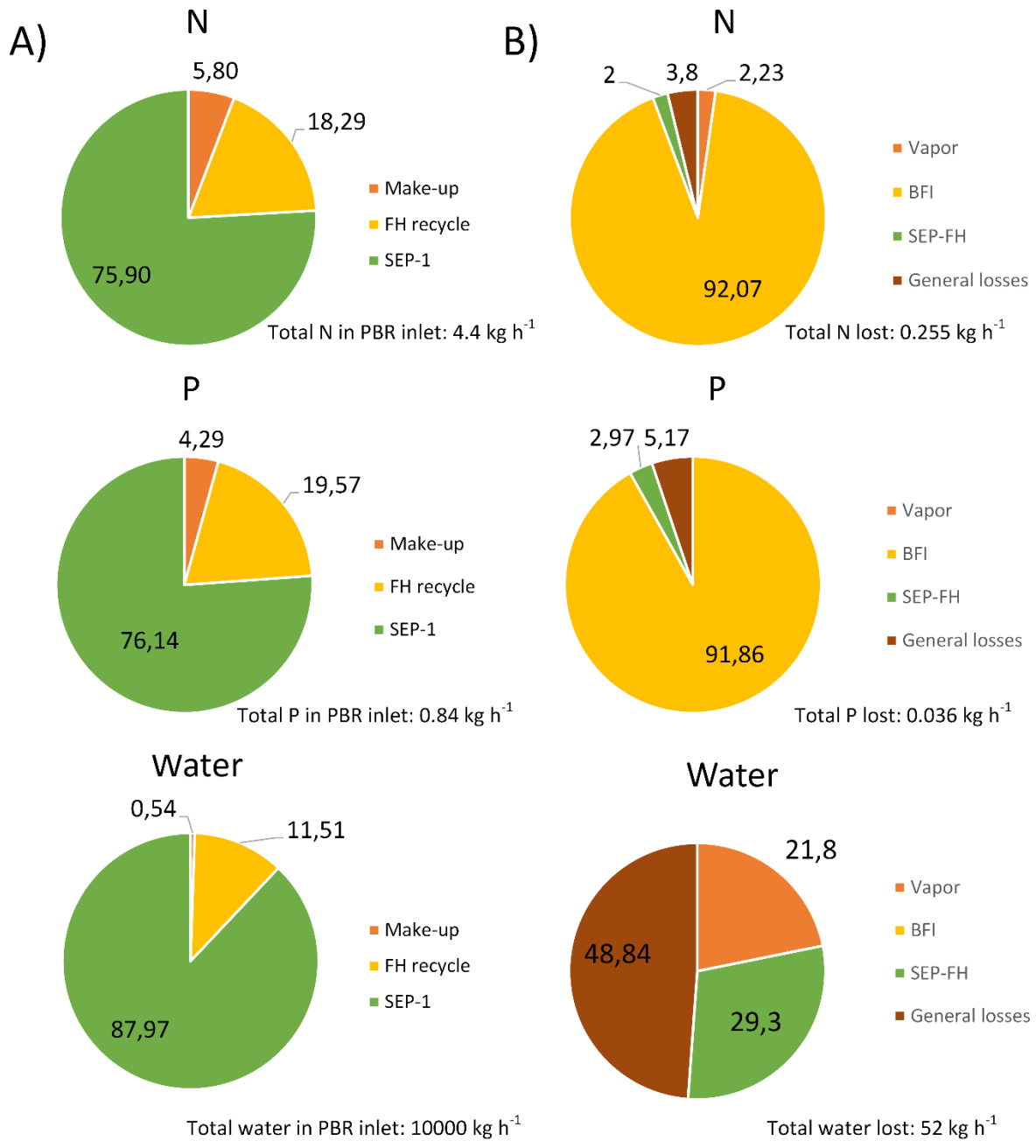

Figure 8.4 *Nutrients (N and P) and water contributions to the PBR inlet (A) and losses (B) in the FH process*

The main losses (Figure 8.4B) are related to the P and N still retained in the solid biofuel intermediates, while smaller amounts are lost in the hydrolysate fraction ending up with the

solid products after separation in *SEP-2* (even in this case, a separation efficiency with 20% solids content in the solid products was considered), and in the purge. Some nitrogen is also lost in the vapor phase from the PBR. Concerning water, similarly to the AD case the major loss contribution is due to the purge, followed by similar amounts of water lost in the vapor phase of the cultivation system and in the solid-liquid separation after the flash hydrolysis process. The energy input and output contributions of the various process steps are summarized in Table 8.3.

Table 8.3 *Direct and indirect energy contributions for EROEI calculation of the FH pathway*

Total input			**37.3**
	Flow-rate [kg h^{-1}]	**EE [MJ kg^{-1}]**	**Energy [kW]**
Material flows			
Process water	53.88	$1.33 \cdot 10^{-3}$	0.02
NH_4Cl	0.97	11.79	3.19
K_2HPO_4	0.20	12.28	0.69
Electricity			
CO_2 blower			0.691
PBR mixing			1.709
Recirculation pump			0.705
High pressure pump			2.82
SEP-2 (Filter-press)			0.05
Heat			
Flash hydrolysis HE			16.7
Drying residual solids			10.75
Total output			**28.32**
	Flow-rate [kg h^{-1}]	**EE [MJ kg^{-1}]**	**Energy [kW]**
Material flows			
Oil	0.295	36	3.27
Residual solids	3.55	25.8	25.37

The resulting EROEI is equal to 0.759. It is noteworthy that in this case the energetic contribution of the residual solids (i.e. the biofuels intermediate residues after lipids extraction) is fundamental to increase the EROEI value, which would otherwise be unacceptably low (~ 0.1), due to the small oil production (0.295 kg h^{-1}). However, even with this contribution, the energy return on investment ratio is not acceptable, indicating that more energy is consumed than produced within the process itself. By looking at Table 8.3, it is clear that the thermal duty

required to heat the algal slurry up to the operating temperature of the FH reactor represents a significant energetic burden, accounting for more than half of the energy produced. This is true even when considering proper heat integration (it is assumed that the hot products pre-heat the slurry to a temperature T = 270°C). However, it has to be considered that the operating conditions of this base case are not the most suitable for the process investigated, because of the low lipid content of the biomass, together with the diluted concentration of the algal slurry fed to the FH reactor (roughly 1% solids content, as constrained by the continuous-flow lab-scale experimental apparatus used in the study). Hence, even in this case higher oil contents (30% and 45% respectively) in the biomass were considered for a sensitivity study. In addition, higher solids contents in the algal slurry (5% and 10% respectively) were investigated, assuming that the nutrients recovery yields are unvaried (this aspect should of course be verified through experimental data). The results obtained in terms of EROEI are summarized in Table 8.4.

Table 8.4 *Effect of lipids content and slurry solids content on the EROEI of the FH process*

Parameter	Lipids content (slurry solids = 1%)			Slurry solids content (Lipids = 6%)		
	6%	30%	45%	1%	5%	10%
EROEI	0.759	0.759	0.833	0.759	1.257	1.380

An increase in lipids content up to 30% does not result in an improved EROEI value for the process, as under these conditions the exploitation of the residual solids for producing additional energy (even accounting for the thermal duty required for their drying operation) is still more favorable than considering the sole contribution of the extracted oil (EROEI = 0.56). Hence, even though the production of oil is higher, the sum of output energy contributions is the same. On the other hand, when the biomass contains 45% lipids, the trend is reversed, as the energy content of the residual solids becomes lower than their drying duty requirement, so that considering the energy output from the oil produced (22 kW for 2.2 kg h^{-1} of oil) allows reaching an EROEI of 0.833. Therefore, it is preferable to select microalgal species with high lipids content when applying the FH process. However, a high lipid content is not sufficient to obtain a positive result in terms of energy profitability. The concentration of solids in the slurry fed to the FH reactor, on the other hand, has a strong influence in this regard. In fact, within

the range considered, if the flowrate of water to be heated up to the operating temperature of 280°C is less, the thermal duty required in the *HE-2* unit decreases significantly. Unfortunately, in a continuous-flow operation, the slurry concentration should not be too high, as this would negatively affect the pumping and heat-exchanging operation and performances.

In a scenario with 45% lipids content and 10% solids in the slurry (instead of 6% and 1% respectively), the EROEI value would be equal to 2.4. This value is acceptable, and somehow comparable with other values reported in the literature: for instance, Delrue et al. (2013) finds an average value of 1.99 GJ produced/GJ consumed for a case of biodiesel from HTL carried out at 330-370 °C with 20-30% solids content in the slurry, even though they asssumed that the energy consumption of the process was due only to heating the slurry. Hence, acceptable values of EROEI can be obtained with FH, provided that the process operation is carefully designed.

8.3.3. Discussion

In this chapter, two different technologies for the production of liquid fuels from microalgae with closed-loop nutrients recycling are investigated and compared in terms of material and energy balances. They differ in the fact that AD is a biological process, which in this case is to be carried out on the biomass residues following lipids extraction, while flash hydrolysis is a hydrothermal treatment which takes advantage of the properties of subcritical water to fractionate the whole wet biomass. In particular, the short residence time (<10 s) exploits the difference in de-polymerization kinetics among lipids, carbohydrates and proteins, to extract the latter in the liquid phase, while preserving most of the lipids in the solids. Although many studies have investigated energy-related aspects of microalgal-based fuels production pathways (e.g., Davis et al. (2016); Delrue et al. (2012); Ramos Tercero et al. (2013)) and a few evaluated material balances for nutrients recycling (Rösch et al., 2012), both of these issues should be considered together.

From the analysis carried out, it clearly emerges that in terms of nutrients recovery and recycling rates, FH performs significantly better than AD, especially with respect to P. In fact, while for N the recovery values obtained in this study with the AD process (50-70%) are comparable to those reported in other works of the kind (Yuan et al., 2015; Zhang et al., 2014), consistently also with the average biodegradability of microalgal biomass, much higher values

are generally reported in the literature for P recovery (up to 90%). Nonetheless, Yuan et al. (2015), specify that the high value used in their study is an assumption, as phosphorus recovery from AD of microalgae has been rarely addressed. The same authors also report that a value of 90% is significantly higher than what has generally been found from AD of other materials (e.g. manure), where 60-80% of the P actually remained in the solid fraction of the digestate (Zhang et al., 2014). As a matter of fact, the results from AD of lipid-extracted *Chlorella vulgaris* reported in Chapter 7 show that most of the P indeed precipitates together with metallic ions as insoluble salts, and this behavior was hence considered in the present simulations. Due to the concerns related to phosphorus limited availability from phosphate mines (Cordell et al., 2009), the percent recovery (and corresponding reduction in fertilizers required in the make-up) of 70% achieved through FH is certainly a great advantage compared with the 30% obtained with AD when assuming a biomass biodegradability of 75%.

On the other hand, regarding the energy profitability of the process, AD certainly looks more favorable, achieving always EROEI values >1, while FH is strongly penalized by the high pressure and temperature involved, with the thermal duty required to heat the algal slurry being a huge energetic burden, even applying proper heat integration. Clearly, the operating conditions considered in the base case, reproducing the experimental laboratory conditions with ~1% solids in the algal slurry fed to FH, are not feasible on a large-scale, as also with a high lipid content the energy input contributions overcome the outputs in this case (EROEI <1). Nonetheless, the study shows that the performances could be markedly improved by optimizing said operating conditions, as a solid content of 5% appears to return an EROEI >1 even with low oil contents in the biomass. In this regard, the results obtained are in agreement with the work of Delrue et al. (2013), who also report that the total energetic balance is in favor of AD when compared to HTL, as the latter, has much higher energy consumption in spite of producing more biofuel energy.

Overall, the results of this study allow to draw some quantitative considerations comparing two conceptually different technologies from the material (nutrients) and energetic standpoints. Certainly, even though energy and fertilizers represent important parts also in the overall cost of the process, ultimately only a detailed techno-economic analysis would discriminate between the two pathways investigated. Even though it is outside the scope of this chapter, some qualitative considerations can be made in this regard. On the one hand, anaerobic

digestion is a somehow mature technology, already widely used even at industrial scale, that is likely to have a low technology cost compared to hydrothermal treatments, which are still under development and require high-pressure equipment (Zhang et al., 2014). However, the time-scale of the two processes is extremely different, as AD requires 20-40 days of HRT (Hydraulic Retention Time), while FH is much faster, which is reflected in a much reduced reactor volume (even compared to conventional HTL). Moreover, given the higher growth rate and productivity achieved under mixotrophic conditions, the surface area required for algal cultivation is reduced (§8.3.2), together with the associated land and cultivation system construction costs. One last consideration is related to the consumption of solvent for oil extraction which, even though not specifically modelled in this study, is likely to be lower in the FH case, as the lipid-rich solid fraction is already partially disrupted by the hydrothermal treatment (Garcia-Moscoso et al., 2013).

8.4. Final remarks

Two different pathways of closed-loop nutrients recycling in microalgal cultivation for large-scale liquid fuels production process (i.e., anaerobic digestion and flash hydrolysis) are studied in this chapter and compared in terms of material and energy balances by means of process simulation techniques. Microalgal growth in the cultivation system is accurately modelled taking into account pH, nutrients concentration, and their availability for up-take by algal cells according to the chemical equilibrium in the liquid medium. Thanks to mixotrophic growth in the hydrolysate produced by FH, the areal productivity is higher compared to that in the digestate from AD (i.e., lower residence time to achieve the same production).

In terms of nutrients recycling FH performs better than AD, especially for phosphorus, a very critical nutrient which in the latter case tends to be lost in the solid fraction of the digestate due to precipitation. On the other hand, when considering the energetic profitability of the process, AD is generally more favorable compared to FH, whose high thermal energy duty necessary to achieve the temperatures involved can lead to EROEI values <1, if the operating conditions are not properly optimized.

Overall, this study provides a method to quantitatively compare AD and FH from the standpoints of nutrients recycling and of energetic return, highlighting the strengths and

drawbacks of both processes. However, only a detailed economic analysis will ultimately allow selecting the most suitable nutrients recycling technology with a better confidence.

Conclusions

The production of renewable fuels from microalgal biomass has certainly the potential to become a feasible technology to displace petroleum-derived ones and simultaneously reduce overall carbon dioxide emissions. However, despite several advantages offered by microalgae, a number of factors are currently preventing the commercialization of algae-to-fuels technologies.

This Ph. D. thesis has been focused on studying possible solutions to improve the energetic and environmental efficiency of microalgal cultivation, with the prospect of moving towards large-scale applications. In particular, aspects related to light utilization efficiency and recycling of nutrients to increase the sustainability of the process were addressed.

Microalgal growth in continuous flat-plate photobioreactors was studied by both experiments and modeling, in order to understand the effect of key parameters such as light intensity, residence time and degree of mixing in the photobioreactor. The existence of an optimum residence time, which is correlated to the light profile along the reactor depth, allowing a maximum productivity and light conversion efficiency, was identified under all the conditions investigated.

The possibility of integrating photovoltaic (PV) technologies with microalgal cultivation in photobioreactors was investigated as a practical solution to increase the solar photons utilization per unit area. In particular, two different PV technologies were used: i) standard silicon solar panels, covering a portion of the reactor irradiated surface and ii) semitransparent orange dye-sensitized solar cells (DSC) applied on the entire surface. In both cases, it was demonstrated that, when the impinging irradiance is limiting, the reduction in light intensity received by the culture caused by the PV cover is reflected in decreased biomass productivity. However, under high values of irradiance, this light attenuation resulted to be beneficial for the microalgae culture, by reducing photosaturation and photoinhibition phenomena. Most importantly, under day-night irradiation regime, the biomass productivity was unaffected by the presence of PV, while on the other hand the overall photon conversion efficiency is greatly enhanced, as the solar cells produce electricity that can be used directly within the process for

power supply. On a large-scale, this concept could be applied by placing the cultivation system inside a greenhouse with the roof partially covered by commercial silicon PV panels. From an energetic and economic case study analysis carried out for two locations in Italy (Veneto in the North, and Sicily in the South) it was seen that, despite the larger capital investment due to photovoltaic installation, the break-even market price of the biomass produced is lower when using the PV integrated system, for both the locations considered. Moreover, overall sunlight conversion efficiency is greatly increased, and the electricity produced by PV could be exploited to energetically self-sustain the process. The Southern location appeared to be a better option, as the higher average irradiances and temperatures allow reaching higher productivities throughout the year, with a final market price 38% lower compared to Northern latitudes. Overall, the results achieved, even though on a preliminary level, highlight a tremendous potential for PV integration with microalgae cultivation systems. Certainly, much work is still needed in this regard. For instance, when considering the mature Si-PV technology, the performances of the PV-greenhouse should be optimized by accurately evaluating the number and disposition of solar panels that most suites the environmental conditions considered in each case. On the other hand, as novel alternative PV technologies are emerging, with foreseeable improvements in terms of stability and efficiency, their application should move from the lab-scale proof-of-concept, to outdoor facilities aimed at verifying the integrated PV-PBR system performances under full solar spectrum.

About nutrients recovery and recycling, this thesis investigated two possible process pathways: flash hydrolysis (FH) and anaerobic digestion (AD). Flash hydrolysis on wet algal biomass allowed recovering more than 60% of N and 80% of P in the aqueous phase. The hydrolysate obtained proved to be a good substrate for microalgal cultivation, which can be even enhanced thanks to mixotrophic growth exploiting the organic carbon available in the medium. However, the capability of up-taking the organic carbon and nitrogen was found to be highly species-dependent, so that while the freshwater *Scenedesmus obliquus* grew well in the hydrolysate in both batch and continuous PBRs, the marine species *Nannochloropsis gaditana* did not, being able to only uptake inorganic ammonium from the medium.

In addition to direct recycling of the liquid hydrolysate, the possibility of precipitating the nutrients in the form of stable fertilizers, for subsequent recycling, was also investigated. This would allow the additional recovery of other high-value molecules preserved in the

hydrolysate. Ammonium and phosphates could be precipitated from the medium in the form of Magnesium Ammonium Phosphate (MAP), which proved to be a good source of nutrients for algal cultivation. The lower N:P ratio of MAP with respect to the stoichiometric composition of algal biomass allowed replacing 100% of P from the control medium, while additional nitrogen was necessary. However, microalgal growth and productivities equal to those obtained in standard medium were achieved in either batch and continuous cultivation.
Satisfactory biogas production was obtained by anaerobic digestion of lipid-extracted microalgal biomass. The liquid digestate was collected and used as a cultivation medium for the same microalgal species. The digestate was found to have good amounts of ammonium nitrogen, however phosphates and sulfates needed to be externally supplied as they are lost in the solid phase (due to precipitation) and in the biogas products, respectively. Given the criticality of phosphorus as a scarcely available mined nutrient, different treatments were investigated to improve its resolubilization and recovery in the liquid digestate. The use of sodium bicarbonate proved to be the most efficient in this regard.
Finally, in order to quantitatively compare the two process alternatives investigated, in terms of mass and energy balances, the results obtained were implemented in the process simulator Aspen Plus^{TM}, highlighting that, while FH performs better than AD in terms of nutrients recycling, the energy consumption is considerably higher, and the process needs be designed very carefully. All the data obtained allow drawing comprehensive conclusions about the technologies investigated. However, even though energy is an important part of the whole cost of a process, ultimately a detailed economic analysis needs to be carried out to assess the actual feasibility on industrial scale.

The results obtained may be useful to provide some technological cues to improve the sustainability of microalgal production, moving towards larger scale applications and commercialization. Even though more work has to be done in this regard, and industries are currently seeking for other high-value applications of microalgae biotechnology, there is much potential for technical breakthroughs in the biofuels field. It is clear that this ultimately requires targeted efforts at a global level, by both governmental and institutional policies, in order to make microalgae production a new renewable alternative to face the threats posed by climate change and fuel supply limitations.

Bibliography

Acién Fernández, F.G., González-López, C. V, Fernández Sevilla, J.M., Molina Grima, E., 2012. Conversion of CO2 into biomass by microalgae: how realistic a contribution may it be to significant CO2 removal? Appl. Microbiol. Biotechnol. 96, 577–86. doi:10.1007/s00253-012-4362-z

Ahmad, F., Khan, A.U., Yasar, A., 2013. The potential of chlorella vulgaris for wastewater treatment and biodiesel production. Pakistan J. Bot. 45, 461–465.

Alzate, M.E., Muñoz, R., Rogalla, F., Fdz-Polanco, F., Pérez-Elvira, S.I., 2014. Biochemical methane potential of microalgae biomass after lipid extraction. Chem. Eng. J. 243, 405–410. doi:10.1016/j.cej.2013.07.076

Bauer, N., Mouratiadou, I., Luderer, G., Baumstark, L., Brecha, R.J., Edenhofer, O., Kriegler, E., 2016. Global fossil energy markets and climate change mitigation – an analysis with REMIND. Clim. Change 136, 69–82. doi:10.1007/s10584-013-0901-6

Bernard, O., Bechet, Q., Mairet, F., Poncet, C., Suay, R., Fatnassi, H., Mangin, A., Edmé, F., Boubekri, R., Neirac, F.-P., Gatt, P., Combe, C., Laviale, M., Pruvost, E., Talec, A., Vasseur, C., Rabouille, S., Sciandra, A., 2015. Combining photovoltaic panels and microalgae: how to deflect the excess of solar energy to ensure optimal conditions of light and temperature for growth.

Bernard, O., Rémond, B., 2012. Validation of a simple model accounting for light and temperature effect on microalgal growth. Bioresour. Technol. 123, 520–7. doi:10.1016/j.biortech.2012.07.022

Bertucco, A., Beraldi, M., Sforza, E., 2014. Continuous microalgal cultivation in a laboratory-scale photobioreactor under seasonal day-night irradiation: experiments and simulation. Bioprocess Biosyst. Eng. 1–8. doi:10.1007/s00449-014-1125-5

Bhuiyan, M.I.H., Mavinic, D.S., Koch, F. a., 2008. Thermal decomposition of struvite and its phase transition. Chemosphere 70, 1347–1356. doi:10.1016/j.chemosphere.2007.09.056

Bilad, M.R., Arafat, H. a., Vankelecom, I.F.J., 2014. Membrane technology in microalgae cultivation and harvesting: A review. Biotechnol. Adv. 32, 1283–1300. doi:10.1016/j.biotechadv.2014.07.008

Biller, P., Ross, a. B., Skill, S.C., Lea-Langton, a., Balasundaram, B., Hall, C., Riley, R., Llewellyn, C. a., 2012. Nutrient recycling of aqueous phase for microalgae cultivation from the hydrothermal liquefaction process. Algal Res. 1, 70–76. doi:10.1016/j.algal.2012.02.002

Bjornsson, W.J., Nicol, R.W., Dickinson, K.E., McGinn, P.J., 2013. Anaerobic digestates are useful nutrient sources for microalgae cultivation: Functional coupling of energy and biomass production. J. Appl. Phycol. 25, 1523–1528. doi:10.1007/s10811-012-9968-0

Blankenship, R.E., Tiede, D.M., Barber, J., Brudvig, G.W., Fleming, G., Ghirardi, M., Gunner, M.R., Junge, W., Kramer, D.M., Melis, A., Moore, T.A., Moser, C.C., Nocera, D.G., Nozik, A.J., Ort,

D.R., Parson, W.W., Prince, R.C., Sayre, R.T., 2011. Comparing Photosynthetic and Photovoltaic Efficiencies and Recognizing the Potential for Improvement. Science (80-.). 332, 805–810.

Bohutskyi, P., Ketter, B., Chow, S., Adams, K.J., Betenbaugh, M.J., Allnutt, F.C.T., Bouwer, E.J., 2015. Anaerobic digestion of lipid-extracted Auxenochlorella protothecoides biomass for methane generation and nutrient recovery. Bioresour. Technol. 183, 229–239. doi:10.1016/j.biortech.2015.02.012

Bonvincini, G., Venturin, A., Facco, L., Mordini, C., Rentocchini, P., 2015. Algae Bioenergy Siting, Commercial Deployment and Development Analysis; Final Report.

Borowitzka, M., Moheimani, N., 2012. Algae for biofuels and energy.

Bridger, G.L., Salutsky, M.L., Starostka, R.W., 1962. Micronutrient Sources, Metal Ammonium Phosphates as Fertilizers. J. Agric. Food Chem. 10, 181–188. doi:10.1021/jf60121a006

Cai, T., Park, S.Y., Racharaks, R., Li, Y., 2013. Cultivation of Nannochloropsis salina using anaerobic digestion effluent as a nutrient source for biofuel production. Appl. Energy 108, 486–492. doi:10.1016/j.apenergy.2013.03.056

Cannavale, A., Eperon, G.E., Cossari, P., Abate, A., Snaith, H.J., Gigli, G., 2015. Perovskite photovoltachromic cells for building integration. Energy Environ. Sci. 8, 1578–1584. doi:10.1039/C5EE00896D

Canter, C.E., Blowers, P., Handler, R.M., Shonnard, D.R., 2015. Implications of widespread algal biofuels production on macronutrient fertilizer supplies: Nutrient demand and evaluation of potential alternate nutrient sources. Appl. Energy 143, 71–80. doi:10.1016/j.apenergy.2014.12.065

Carvalho, A.P., Silva, S.O., Baptista, J.M., Malcata, F.X., 2011. Light requirements in microalgal photobioreactors: An overview of biophotonic aspects. Appl. Microbiol. Biotechnol. 89, 1275–1288. doi:10.1007/s00253-010-3047-8

Chiaramonti, D., Prussi, M., Casini, D., Tredici, M.R., Rodolfi, L., Bassi, N., Zittelli, G.C., Bondioli, P., 2013. Review of energy balance in raceway ponds for microalgae cultivation: Re-thinking a traditional system is possible. Appl. Energy 102, 101–111. doi:10.1016/j.apenergy.2012.07.040

Chisti, Y., 2007. Biodiesel from microalgae. Biotechnol. Adv. 25, 294–306. doi:10.1016/biotechadv.2007.02.001

Chisti, Y., 2013. Constraints to commercialization of algal fuels. J. Biotechnol. 167, 201–214. doi:10.1016/j.jbiotec.2013.07.020

Chisti, Y., Yan, J., 2011. Energy from algae: Current status and future trends. Appl. Energy 88, 3277–3279. doi:10.1016/j.apenergy.2011.04.038

Circ.18-12-2014, law 09-01-1991 n10, Ministero dello Sviluppo Economico, Italy, 2014.

Concas, A., Lutzu, G.A., Pisu, M., Cao, G., 2012. Experimental analysis and novel modeling of semi-batch photobioreactors operated with Chlorella vulgaris and fed with 100% (v/v) CO2. Chem. Eng. J. 213, 203–213. doi:10.1016/j.cej.2012.09.119

Cordell, D., Drangert, J.O., White, S., 2009. The story of phosphorus: Global food security and food for thought. Glob. Environ. Chang. 19, 292–305. doi:10.1016/j.gloenvcha.2008.10.009

Cossu, M., Murgia, L., Ledda, L., Deligios, P. a., Sirigu, A., Chessa, F., Pazzona, A., 2014. Solar radiation distribution inside a greenhouse with south-oriented photovoltaic roofs and effects on crop productivity. Appl. Energy 133, 89–100. doi:10.1016/j.apenergy.2014.07.070

Cuaresma, M., Janssen, M., van den End, E.J., Vílchez, C., Wijffels, R.H., 2011. Luminostat operation: A tool to maximize microalgae photosynthetic efficiency in photobioreactors during the daily light cycle? Bioresour. Technol. 102, 7871–7878. doi:10.1016/j.biortech.2011.05.076

Cuaresma, M., Janssen, M., Vílchez, C., Wijffels, R.H., 2009. Productivity of Chlorella sorokiniana in a short light-path (SLP) panel photobioreactor under high irradiance. Biotechnol. Bioeng. 104, 352–359. doi:10.1002/bit.22394

Davis, R., Markham, J., Kinchin, C., Grundl, N., Tan, E.C.D., Humbird, D., Davis, R., Markham, J., Kinchin, C., Grundl, N., Tan, E.C.D., Humbird, D., 2016. Process Design and Economics for the Production of Algal Biomass : Algal Biomass Production in Open Pond Systems and Processing Through Dewatering for Downstream Conversion Process Design and Economics for the Production of Algal Biomass : Algal Biomass P.

Davis, R.W., Siccardi, A.J., Huysman, N.D., Wyatt, N.B., Hewson, J.C., Lane, T.W., 2015. Growth of mono- and mixed cultures of Nannochloropsis salina and Phaeodactylum tricornutum on struvite as a nutrient source. Bioresour. Technol. 198, 577–585. doi:10.1016/j.biortech.2015.09.070

De Farias Silva, C.E., Bertucco, A., 2015. Bioethanol from microalgae and cyanobacteria: A review and technological outlook. Process Biochem. 1–10. doi:10.1016/j.procbio.2016.02.016

Delrue, F., Li-Beisson, Y., Setier, P.-A., Sahut, C., Roubaud, A., Froment, A.-K., Peltier, G., 2013. Comparison of various microalgae liquid biofuel production pathways based on energetic, economic and environmental criteria. Bioresour. Technol. 136, 205–212. doi:10.1016/j.biortech.2013.02.091

Delrue, F., Setier, P.-A., Sahut, C., Cournac, L., Roubaud, A., Peltier, G., Froment, A.-K., 2012. An economic, sustainability, and energetic model of biodiesel production from microalgae. Bioresour. Technol. 111, 191–200. doi:10.1016/j.biortech.2012.02.020

Demmig-Adams, B., Adams, W.W., Barker, D.H., Logan, B.A., Bowling, D.R., Verhoeven, A.S., 1996. Using chlorophyll fluorescence to assess the fraction of absorbed light allocated to thermal dissipation of excess excitation. Physiol. Plant. 98, 253–264.

Detweiler, A.M., Mioni, C.E., Hellier, K.L., Allen, J.J., Carter, S. a., Bebout, B.M., Fleming, E.E., Corrado, C., Prufert-Bebout, L.E., 2015. Evaluation of wavelength selective photovoltaic panels on microalgae growth and photosynthetic efficiency. Algal Res. 9, 170–177. doi:10.1016/j.algal.2015.03.003

Doucha, J., Livansky, K., 2014. High density Outdoor Microalgal Culture, in: Algal Biorefineries V1: Cultivation of Cells and Products. Springer Dordrecht Heidelberg London New York, p. 147.

Douglas, J., 1988. Conceptual design of chemical processes. McGraw-Hill, New York.

Doyle, J.D., Parsons, S.A., 2002. Struvite formation, control and recovery. Water Res. 36, 3925–3940. doi:10.1016/S0043-1354(02)00126-4

Driver, T., Bajhaiya, A., Pittman, J.K., 2014. Potential of Bioenergy Production from Microalgae. Curr. Sustain. Energy Reports 1, 94–103. doi:10.1007/s40518-014-0011-8

Du, Z., Hu, B., Shi, A., Ma, X., Cheng, Y., Chen, P., Liu, Y., Lin, X., Ruan, R., 2012. Cultivation of a microalga Chlorella vulgaris using recycled aqueous phase nutrients from hydrothermal carbonization process. Bioresour. Technol. 126, 354–357. doi:10.1016/j.biortech.2012.09.062

Dussap, C., 2009. A Simple and Reliable Formula for Assessment of Maximum Volumetric Productivities in Photobioreactors. doi:10.1021/bp.138

Ehimen, E. a, Connaughton, S., Sun, Z.F., Carrington, G.C., 2009. Energy recovery from lipid extracted, transesterified and glycerol codigested microalgae biomass. Glob. Chang. Biol. Bioenergy 1, 371–381. doi:DOI 10.1111/j.1757-1707.2009.01029.x

Ehimen, E.A., Sun, Z.F., Carrington, C.G., Birch, E.J., Eaton-Rye, J.J., 2011. Anaerobic digestion of microalgae residues resulting from the biodiesel production process. Appl. Energy 88, 3454–3463. doi:10.1016/j.apenergy.2010.10.020

Elliott, D.C., 2016. Review of recent reports on process technology for thermochemical conversion of whole algae to liquid fuels. Algal Res. 13, 255–263. doi:10.1016/j.algal.2015.12.002

Feng, Y., Li, C., Zhang, D., 2011. Lipid production of Chlorella vulgaris cultured in artificial wastewater medium. Bioresour. Technol. 102, 101–105. doi:10.1016/j.biortech.2010.06.016

Fernandes, B.D., Mota, A., Ferreira, A., Dragone, G., Teixeira, J. a., Vicente, A. a., 2014. Characterization of split cylinder airlift photobioreactors for efficient microalgae cultivation. Chem. Eng. Sci. 117, 445–454. doi:10.1016/j.ces.2014.06.043

Garcia Alba, L., Torri, C., Fabbri, D., Kersten, S.R. a., (Wim) Brilman, D.W.F., 2013. Microalgae growth on the aqueous phase from Hydrothermal Liquefaction of the same microalgae. Chem. Eng. J. 228, 214–223. doi:10.1016/j.cej.2013.04.097

Garcia-Moscoso, J.L., Obeid, W., Kumar, S., Hatcher, P.G., 2013. Flash hydrolysis of microalgae (Scenedesmus sp.) for protein extraction and production of biofuels intermediates. J. Supercrit. Fluids 82, 183–190. doi:10.1016/j.supflu.2013.07.012

Garcia-Moscoso, J.L., Teymouri, A., Kumar, S., 2015. Kinetics of Peptides and Arginine Production from Microalgae (*Scenedesmus sp* .) by Flash Hydrolysis. Ind. Eng. Chem. Res. 54, 2048–2058. doi:10.1021/ie5047279

Gardner, R.D., Cooksey, K.E., Mus, F., Macur, R., Moll, K., Eustance, E., Carlson, R.P., Gerlach, R., Fields, M.W., Peyton, B.M., 2012. Use of sodium bicarbonate to stimulate triacylglycerol accumulation in the chlorophyte Scenedesmus sp. and the diatom Phaeodactylum tricornutum. J. Appl. Phycol. 24, 1311–1320. doi:10.1007/s10811-011-9782-0

Gardner, R.D., Lohman, E.J., Cooksey, K.E., Gerlach, R., Peyton, B.M., 2013. Cellular cycling, carbon utilization, and photosynthetic oxygen production during bicarbonate-induced triacylglycerol accumulation in a Scenedesmus sp. Energies 6, 6060–607. doi:10.3390/en6116060

Ghasemi Naghdi, F., González González, L.M., Chan, W., Schenk, P.M., 2016. Progress on lipid extraction from wet algal biomass for biodiesel production. Microb. Biotechnol. doi:10.1111/1751-7915.12360

Gifford, M., Liu, J., Rittmann, B.E., Vannela, R., Westerhoff, P., 2015. Phosphorus recovery from microbial biofuel residual using microwave peroxide digestion and anion exchange. Water Res. 70, 130–137. doi:10.1016/j.watres.2014.11.052

Giordano, F., Guidobaldi, A., Petrolati, E., Vesce, L., Riccitelli, R., Reale, A., Brown, T.M., Di Carlo, A., 2013. Realization of high performance large area Z-series-interconnected opaque dye solar cell modules. Prog. Photovoltaics Res. Appl. 21, 1653–1658. doi:10.1002/pip.2228

Gons, H.J., Mur, L.R., 1980. Energy Requirements for growth and maintenance of Scenedesmus protuberans Fritsch in light-limited continuous cultures. Arch. Microbiol. 125, 9–17. doi:10.1007/BF00403192

Gonzalez-Fernandez, C., Sialve, B., Molinuevo-Salces, B., 2015. Anaerobic digestion of microalgal biomass: Challenges, opportunities and research needs. Bioresour. Technol. 198, 896–906. doi:10.1016/j.biortech.2015.09.095

Green, M.A., Emery, K., Hishikawa, Y., Warta, W., Dunlop, E.D., 2012. Solar cell efficiency tables (version 39). Prog. Photovoltaics Res. Appl. 20, 12–20. doi:10.1002/pip.2163

Gris, B., Morosinotto, T., Giacometti, G.M., Bertucco, A., Sforza, E., 2013. Cultivation of Scenedesmus obliquus in Photobioreactors: Effects of Light Intensities and Light-Dark Cycles on Growth, Productivity, and Biochemical Composition. Appl. Biochem. Biotechnol. 172, 1–13. doi:10.1007/s12010-013-0679-z

Gris, B., Sforza, E., Vecchiato, L., Bertucco, A., 2014. Development of a Process for an Efficient Exploitation of CO 2 Captured from Flue Gases as Liquid Carbonates for Chlorella protothecoides Cultivation. Ind. Eng. Chem. Res. 53, 16678–16688. doi:10.1021/ie502336d

Grobbelaar, J.U., 2006. Photosynthetic Response and Acclimation of Microalgae to Light Fluctuations, in: Algal Cultures, Analogues of Blooms and Applications. Science Publishers, pp. 671–683.

Gu, H., Nagle, N., Pienkos, P.T., Posewitz, M.C., 2015. Nitrogen recycling from fuel-extracted algal biomass: residuals as the sole nitrogen source for culturing Scenedesmus acutus. Bioresour. Technol. 184, 153–60. doi:10.1016/j.biortech.2014.11.095

Gutierrez-Wing, M.T., Benson, B.C., Rusch, K. a., 2012. Impact of light quality and quantity on growth rate kinetics of Selenastrum capricornutum. Eng. Life Sci. 12, 79–88. doi:10.1002/elsc.201000217

Halim, R., Danquah, M.K., Webley, P. a., 2012. Extraction of oil from microalgae for biodiesel production: A review. Biotechnol. Adv. 30, 709–732. doi:10.1016/j.biotechadv.2012.01.001

Han, S.-F., Jin, W.-B., Tu, R.-J., Wu, W.-M., 2015. Biofuel production from microalgae as feedstock: current status and potential. Crit. Rev. Biotechnol. 35, 255–268. doi:10.3109/07388551.2013.835301

Heilmann, S.M., Jader, L.R., Harned, L. a., Sadowsky, M.J., Schendel, F.J., Lefebvre, P. a., von Keitz, M.G., Valentas, K.J., 2011. Hydrothermal carbonization of microalgae II. Fatty acid, char, and algal nutrient products. Appl. Energy 88, 3286–3290. doi:10.1016/j.apenergy.2010.12.041

Horta, M.D.C., Torrent, J., 2007. The Olsen P method as an agronomic and environmental test for predicting phosphate release from acid soils. Nutr. Cycl. Agroecosystems 77, 283–292. doi:10.1007/s10705-006-9066-2

http://www.agenziaentrate.gov.it/ [WWW Document], n.d.

IEA, I.E.A., 2015. World Energy Outlook. doi:http://www.iea.org/publications/freepublications/publication/WEB_WorldEnergyOutlook2015ExecutiveSummaryEnglishFinal.pdf

IEC 60904-3 (Ed. 2), Photovoltaic devices - Part 3: Measurement principles for terrestrial photovoltaic (PV) solar devices with reference spectral irradiance data., 2008. doi:10.5594/J09750

InflationData, 2016. No Title [WWW Document]. URL www.InflationData.com, Uodated 10/06/2016

Istituto nazionale di Statistica, 2013. Il carico fiscale e contributivo sul lavoro e sulle famiglie. Rome, Italy.

Jena, U., Vaidyanathan, N., Chinnasamy, S., Das, K.C., 2011. Evaluation of microalgae cultivation using recovered aqueous co-product from thermochemical liquefaction of algal biomass. Bioresour. Technol. 102, 3380–3387. doi:10.1016/j.biortech.2010.09.111

John, E.H., Flynn, K.J., 2000. Modelling phosphate transport and assimilation in microalgae; how much complexity is warranted? Ecol. Modell. 125, 145–157. doi:10.1016/S0304-3800(99)00178-7

Kaewkannetra, P., Enmak, P., Chiu, T., 2012. The effect of CO2 and salinity on the cultivation of scenedesmus obliquus for biodiesel production. Biotechnol. Bioprocess Eng. 17, 591–597. doi:10.1007/s12257-011-0533-5

Kim, C.W., Sung, M.G., Nam, K., Moon, M., Kwon, J.H., Yang, J.W., 2014. Effect of monochromatic illumination on lipid accumulation of Nannochloropsis gaditana under continuous cultivation. Bioresour. Technol. 159, 30–35. doi:10.1016/j.biortech.2014.02.024

Kim, D., Ryu, H.-D., Kim, M.-S., Kim, J., Lee, S.-I., 2007. Enhancing struvite precipitation potential for ammonia nitrogen removal in municipal landfill leachate. J. Hazard. Mater. 146, 81–85. doi:10.1016/j.jhazmat.2006.11.054

Kumar, S., Hablot, E., Moscoso, J.L.G., Obeid, W., Hatcher, P.G., DuQuette, B.M., Graiver, D., Narayan, R., Balan, V., 2014. Polyurethanes preparation using proteins obtained from microalgae. J. Mater. Sci. 49, 7824–7833. doi:10.1007/s10853-014-8493-8

Lee, R.E., 1989. Phycology, Second Edi. ed. Cambridge University Press.

Levenspiel, O., 1996. The Chemical Reactor Omnibook.

Levine, R.B., Sambolin Sierra, C.O., Hockstad, R., Obeid, W., Hatcher, P.G., Savage, P.E., 2013. The Use of Hydrothermal Carbonization to Recycle Nutrients in Algal Biofuel Production. Environ. Prog. Sustain. Energy 32, 962–975. doi:10.1002/ep.11812

Liao, Q., Li, L., Chen, R., Zhu, X., 2014. A novel photobioreactor generating the light/dark cycle to improve microalgae cultivation. Bioresour. Technol. 161, 186–91. doi:10.1016/j.biortech.2014.02.119

Lin, H., Gan, J., Rajendran, A., Reis, C.E.R., Hu, B., 2015. Phosphorus Removal and Recovery from Digestate after Biogas Production. Biofuels - Status Perspect. doi:10.5772/60474

López Barreiro, D., Bauer, M., Hornung, U., Posten, C., Kruse, A., Prins, W., 2015. Cultivation of microalgae with recovered nutrients after hydrothermal liquefaction. Algal Res. 9, 99–106. doi:10.1016/j.algal.2015.03.007

López Barreiro, D., Prins, W., Ronsse, F., Brilman, W., 2013. Hydrothermal liquefaction (HTL) of microalgae for biofuel production: State of the art review and future prospects. Biomass and Bioenergy 53, 113–127. doi:10.1016/j.biombioe.2012.12.029

Lowrey, J., Armenta, R.E., Brooks, M.S., 2016. Nutrient and media recycling in heterotrophic microalgae cultures. Appl. Microbiol. Biotechnol. 100, 1061–1075. doi:10.1007/s00253-015-7138-4

Markou, G., Vandamme, D., Muylaert, K., 2014. Microalgal and cyanobacterial cultivation: The supply of nutrients. Water Res. 65, 186–202. doi:10.1016/j.watres.2014.07.025

Marrou, H., Wery, J., Dufour, L., Dupraz, C., 2013. Productivity and radiation use efficiency of lettuces grown in the partial shade of photovoltaic panels. Eur. J. Agron. 44, 54–66. doi:10.1016/j.eja.2012.08.003

Marti, N., Pastor, L., Bouzas, A., Ferrer, J., Seco, A., 2010. Phosphorus recovery by struvite crystallization in WWTPs: Influence of the sludge treatment line operation. Water Res. 44, 2371–2379. doi:10.1016/j.watres.2009.12.043

Mata, T.M., Martins, A.A., Caetano, N.S., 2010. Microalgae for biodiesel production and other applications: A review. Renew. Sustain. Energy Rev. 14, 217–232. doi:10.1016/j.rser.2009.07.020

Maugeri, L., 2013. The Shale Oil Boom: a US Phenomenon, Harvard University, Geopolitics of Energy Project, Belfer Center for Science and International Affairs, Discussion Paper.

Maxwell, K., Johnson, G.N., 2000. Chlorophyll fluorescence — a practical guide. J. Exp. Bot. 51, 659–668.

McCree, K.J., 1972. The action spectrum, absorptance and quantum yield of photosynthesis in crop plants. Agric. Meteorol. 9, 191–216.

Mehta, C.M., Batstone, D.J., 2013. Nutrient solubilization and its avaiiability foiiowing anaerobic digestion. doi:10.2165/wst.2012.622

Milano, J., Ong, H.C., Masjuki, H.H., Chong, W.T., Lam, M.K., Loh, P.K., Vellayan, V., 2016. Microalgae biofuels as an alternative to fossil fuel for power generation. Renew. Sustain. Energy Rev. 58, 180–197. doi:10.1016/j.rser.2015.12.150

Milledge, J.J., 2010. Commercial application of microalgae other than as biofuels: a brief review. Rev. Environ. Sci. Bio/Technology 10, 31–41. doi:10.1007/s11157-010-9214-7

Moed, N.M., Lee, D.J., Chang, J.S., 2015. Struvite as alternative nutrient source for cultivation of microalgae Chlorella vulgaris. J. Taiwan Inst. Chem. Eng. 56, 73–76. doi:10.1016/j.jtice.2015.04.027

Mohsenpour, S.F., Willoughby, N., 2013. Luminescent photobioreactor design for improved algal growth and photosynthetic pigment production through spectral conversion of light. Bioresour. Technol. 142, 147–53. doi:10.1016/j.biortech.2013.05.024

Molin, G., 1983. Measurement of the maximum specific growth rate in chemostat of Pseudomonas spp. with different abilities for biofilm formation. Eur. J. Appl. Microbiol. Biotechnol. 18, 303–307. doi:10.1007/BF00500496

Möller, K., Müller, T., 2012. Effects of anaerobic digestion on digestate nutrient availability and crop growth: A review. Eng. Life Sci. 12, 242–257. doi:10.1002/elsc.201100085

Muller, P., Li, X., Niyogi, K.K., 2001. Non-Photochemical Quenching . A Response to Excess Light Energy 1 125, 1558–1566.

Muñoz-Tamayo, R., Mairet, F., Bernard, O., 2013. Optimizing microalgal production in raceway systems. Biotechnol. Prog. 29, 543–552. doi:10.1002/btpr.1699

Munoz-Tamayo, R., Martinon, P., Bougaran, G., Mairet, F., Bernard, O., Cedex, S., 2013. Design of optimal experiments for parameter estimation of microalgae growth models. Comput. Appl. to Biotechnol. hal–00856749. doi:10.3182/20131216-3-IN-2044.00043

Pandey, A., Lee, D.J., Chisti, Y., Soccol, C.R., 2014. Biofuels from Algae, Elsevier. doi:10.1016/S1471-0846(06)70577-7

Parlevliet, D., Moheimani, N., 2014. Efficient conversion of solar energy to biomass and electricity. Aquat. Biosyst. 10, 4. doi:10.1186/2046-9063-10-4

Pate, R., Klise, G., Wu, B., 2011. Resource demand implications for US algae biofuels production scale-up. Appl. Energy 88, 3377–3388. doi:10.1016/j.apenergy.2011.04.023

Patel, B., Guo, M., Izadpanah, A., Shah, N., Hellgardt, K., 2016. A review on hydrothermal pre-treatment technologies and environmental profiles of algal biomass processing. Bioresour. Technol. 199, 288–299. doi:10.1016/j.biortech.2015.09.064

Peccia, J., Haznedaroglu, B., Gutierrez, J., Zimmerman, J.B., 2013. Nitrogen supply is an important driver of sustainable microalgae biofuel production. Trends Biotechnol. 31, 134–138. doi:10.1016/j.tibtech.2013.01.010

Pokorna, D., Zabranska, J., 2015. Sulfur-oxidizing bacteria in environmental technology. Biotechnol. Adv. 33, 1246–1259. doi:10.1016/j.biotechadv.2015.02.007

Posten, C., 2009. Design principles of photo-bioreactors for cultivation of microalgae. Eng. Life Sci. 9, 165–177. doi:10.1002/elsc.200900003

Pottier, L., Pruvost, J., Deremetz, J., Cornet, J.F., Legrand, J., Dussap, C.G., 2005. A fully predictive model for one-dimensional light attenuation by Chlamydomonas reinhardtii in a torus photobioreactor. Biotechnol. Bioeng. 91, 569–582. doi:10.1002/bit.20475

Powell, N., Shilton, A., Chisti, Y., Pratt, S., 2009. Towards a luxury uptake process via microalgae – Defining the polyphosphate dynamics. Water Res. 43, 4207–4213. doi:10.1016/j.watres.2009.06.011

Prajapati, S.K., Kumar, P., Malik, A., Vijay, V.K., 2014. Bioconversion of algae to methane and subsequent utilization of digestate for algae cultivation: A closed loop bioenergy generation process. Bioresour. Technol. 158, 174–180. doi:10.1016/j.biortech.2014.02.023

Pruvost, J., Cornet, J.F., Goetz, V., Legrand, J., 2011a. Modeling Dynamic Functioning of Rectangular Photobioreactors in Solar Conditions. AIChe J. 57, 1947–1960. doi:10.1002/aic

Pruvost, J., Van Vooren, G., Le Gouic, B., Couzinet-Mossion, a., Legrand, J., 2011b. Systematic investigation of biomass and lipid productivity by microalgae in photobioreactors for biodiesel application. Bioresour. Technol. 102, 150–158. doi:10.1016/j.biortech.2010.06.153

Quinn, J.C., Catton, K., Wagner, N., Bradley, T.H., 2011. Current Large-Scale US Biofuel Potential from Microalgae Cultivated in Photobioreactors. BioEnergy Res. 5, 49–60. doi:10.1007/s12155-011-9165-z

Quinn, J.C., Davis, R., 2015. The potentials and challenges of algae based biofuels: A review of the techno-economic, life cycle, and resource assessment modeling. Bioresour. Technol. 184, 444–452. doi:10.1016/j.biortech.2014.10.075

Rahman, M.M., Salleh, M.A.M., Rashid, U., Ahsan, A., Hossain, M.M., Ra, C.S., 2014. Production of slow release crystal fertilizer from wastewaters through struvite crystallization - A review. Arab. J. Chem. 7, 139–155. doi:10.1016/j.arabjc.2013.10.007

Ramos Tercero, E.A., Domenicali, G., Bertucco, A., 2014. Autotrophic production of biodiesel from microalgae: An updated process and economic analysis. Energy 76, 807–815. doi:10.1016/j.energy.2014.08.077

Ramos Tercero, E.A., Sforza, E., Bertucco, A., 2013. Energy profitability analysis for microalgal biocrude production. Energy 60, 373–379. doi:10.1016/j.energy.2013.08.003

Ramos-Suárez, J.L., Carreras, N., 2014. Use of microalgae residues for biogas production. Chem. Eng. J. 242, 86–95. doi:10.1016/j.cej.2013.12.053

Ras, M., Lardon, L., Bruno, S., Bernet, N., Steyer, J.P., 2011. Experimental study on a coupled process of production and anaerobic digestion of Chlorella vulgaris. Bioresour. Technol. 102, 200–206. doi:10.1016/j.biortech.2010.06.146

Redfield, A.C., 1934. On the Proportions of Organic Derivatives in Sea Water and Their Relation to the Composition of Plankton, in: University Press of Liverpool. pp. 176–192.

Ribeiro, L.A., da Silva, P.P., Mata, T.M., Martins, A.A., 2015. Prospects of using microalgae for biofuels production: Results of a Delphi study. Renew. Energy 75, 799–804. doi:10.1016/j.renene.2014.10.065

Ringsmuth, A.K., Landsberg, M.J., Hankamer, B., 2016. Can photosynthesis enable a global transition from fossil fuels to solar fuels, to mitigate climate change and fuel-supply limitations? Renew. Sustain. Energy Rev. 62, 134–163. doi:10.1016/j.rser.2016.04.016

Rodolfi, L., Chini Zittelli, G., Bassi, N., Padovani, G., Biondi, N., Bonini, G., Tredici, M.R., 2009. Microalgae for oil: strain selection, induction of lipid synthesis and outdoor mass cultivation in a low-cost photobioreactor. Biotechnol. Bioeng. 102, 100–12. doi:10.1002/bit.22033

Rodriguez, C., Alaswad, A., Mooney, J., Prescott, T., Olabi, A.G., 2015. Pre-treatment techniques used for anaerobic digestion of algae. Fuel Process. Technol. 138, 765–779. doi:10.1016/j.fuproc.2015.06.027

Rösch, C., Skarka, J., Wegerer, N., 2012. Materials flow modeling of nutrient recycling in biodiesel production from microalgae. Bioresour. Technol. 107, 191–9. doi:10.1016/j.biortech.2011.12.016

Ruiz, J., Olivieri, G., de Vree, J., Bosma, R., Willems, P., Reith, J.H., Eppink, M.H.M., Kleinegris, D.M.M., Wijffels, R.H., Barbosa, M.J., 2016. Towards industrial products from microalgae. Energy Environ. Sci. 24, 405–413. doi:10.1039/C6EE01493C

Sathish, A., Sims, R.C., 2012. Biodiesel from mixed culture algae via a wet lipid extraction procedure. Bioresour. Technol. 118, 643–647. doi:10.1016/j.biortech.2012.05.118

Sereco S.r.l. [WWW Document], n.d.

Sforza, E., Cipriani, R., Morosinotto, T., Bertucco, A., Giacometti, G.M., 2012a. Excess CO2 supply inhibits mixotrophic growth of Chlorella protothecoides and Nannochloropsis salina. Bioresour. Technol. 104, 523–529. doi:10.1016/j.biortech.2011.10.025

Sforza, E., Enzo, M., Bertucco, A., 2014a. Design of microalgal biomass production in a continuous photobioreactor: An integrated experimental and modeling approach. Chem. Eng. Res. Des. 92, 1153–1162. doi:10.1016/j.cherd.2013.08.017

Sforza, E., Ramos-Tercero, E.A., Gris, B., Bettin, F., Milani, A., Bertucco, A., 2014b. Integration of Chlorella protothecoides production in wastewater treatment plant: From lab measurements to process design. Algal Res. 6, 223–233. doi:10.1016/j.algal.2014.06.002

Sforza, E., Simionato, D., Giacometti, G.M., Bertucco, A., Morosinotto, T., 2012b. Adjusted light and dark cycles can optimize photosynthetic efficiency in algae growing in photobioreactors. PLoS One 7, e38975. doi:10.1371/journal.pone.0038975

Sforza, E., Urbani, S., Bertucco, A., 2014c. Evaluation of maintenance energy requirements in the cultivation of Scenedesmus obliquus: effect of light intensity and regime. J. Appl. Phycol. 27, 1453–1462. doi:10.1007/s10811-014-0460-x

Shurtz, B.K., Wood, B., Quinn, J.C., 2017. Nutrient resource requirements for large-scale microalgae biofuel production: Multi-pathway evaluation. Sustain. Energy Technol. Assessments 19, 51–58. doi:10.1016/j.seta.2016.11.003

Sialve, B., Bernet, N., Bernard, O., 2009. Anaerobic digestion of microalgae as a necessary step to make microalgal biodiesel sustainable. Biotechnol. Adv. 27, 409–416. doi:10.1016/j.biotechadv.2009.03.001

Stephenson, P.G., Moore, C.M., Terry, M.J., Zubkov, M. V., Bibby, T.S., 2011. Improving photosynthesis for algal biofuels: Toward a green revolution. Trends Biotechnol. 29, 615–623. doi:10.1016/j.tibtech.2011.06.005

Tagliaferro, R., Colonna, D., Brown, T.M., Reale, A., Di Carlo, A., 2013. Interplay between transparency and efficiency in dye sensitized solar cells. Opt. Express 21, 3235–42. doi:10.1364/OE.21.003235

Takache, H., Christophe, G., Cornet, J.F., Pruvost, J., 2010. Experimental and theoretical assessment of maximum productivities for the microalgae Chlamydomonas reinhardtii in two different geometries of photobioreactors. Biotechnol. Prog. 26, 431–440. doi:10.1002/btpr.356

Takache, H., Pruvost, J., Cornet, J.F., 2012. Kinetic modeling of the photosynthetic growth of Chlamydomonas reinhardtii in a photobioreactor. Biotechnol. Prog. 28, 681–692. doi:10.1002/btpr.1545

Talbot, C., Garcia-Moscoso, J., Drake, H., Stuart, B.J., Kumar, S., 2016. Cultivation of microalgae using flash hydrolysis nutrient recycle. Algal Res. 18, 191–197. doi:10.1016/j.algal.2016.06.021

Tang, D., Han, W., Li, P., Miao, X., Zhong, J., 2011. CO2 biofixation and fatty acid composition of Scenedesmus obliquus and Chlorella pyrenoidosa in response to different CO2 levels. Bioresour. Technol. 102, 3071–3076. doi:10.1016/j.biortech.2010.10.047

Tercero, E.A.R., Alibardi, L., Cossu, R., Bertucco, A., 2014. Anaerobic digestion of microalgal residues to enhance the energetic profit of biocrude production. Chem. Eng. Trans. 37, 793–798. doi:10.3303/CET1437133

Tredici, M.R., Rodolfi, L., Biondi, N., Bassi, N., Sampietro, G., 2016. Techno-economic analysis of microalgal biomass production in a 1-ha Green Wall Panel (GWP®) plant. Algal Res. 19, 253–263. doi:10.1016/j.algal.2016.09.005

U.S. Congress, 2007. Energy independence and security act of 2007. Public Law 1–311. doi:papers2://publication/uuid/364DB882-E966-450B-959F-AEAD6E702F42

U.S. DOE, 2016. 2016 Billion-Ton Report I, 411.

Uggetti, E., Sialve, B., Latrille, E., Steyer, J.P., 2014. Anaerobic digestate as substrate for microalgae culture: The role of ammonium concentration on the microalgae productivity. Bioresour. Technol. 152, 437–443. doi:10.1016/j.biortech.2013.11.036

Ullah, K., Ahmad, M., Sofia, Sharma, V.K., Lu, P., Harvey, A., Zafar, M., Sultana, S., 2015. Assessing the potential of algal biomass opportunities for bioenergy industry: A review. Fuel 143, 414–423. doi:10.1016/j.fuel.2014.10.064

Valiela, I., 1995. Marine Ecological Processes. Springer New York. doi:10.1007/978-1-4757-4125-4

Van Ginkel, S.W., Oh, S.E., Logan, B.E., 2005. Biohydrogen gas production from food processing and domestic wastewaters. Int. J. Hydrogen Energy 30, 1535–1542. doi:10.1016/j.ijhydene.2004.09.017

Vasudevan, V., Stratton, R.W., Pearlson, M.N., Jersey, G.R., Beyene, A.G., Weissman, J.C., Rubino, M., Hileman, J.I., 2012. Environmental performance of algal biofuel technology options. Environ. Sci. Technol. 46, 2451–2459. doi:10.1021/es2026399

Vejrazka, C., Janssen, M., Streefland, M., Wijffels, R.H., 2012. Photosynthetic efficiency of Chlamydomonas reinhardtii in attenuated, flashing light. Biotechnol. Bioeng. 109, 2567–74. doi:10.1002/bit.24525

Vonshak, A., Abeliovich, A., Boussiba, S., Arad, S., Richmond, A., 1982. Production of spirulina biomass: Effects of environmental factors and population density. Biomass 2, 175–185. doi:10.1016/0144-4565(82)90028-2

Wang, L., Li, Y., Chen, P., Min, M., Chen, Y., Zhu, J., Ruan, R.R., 2010. Anaerobic digested dairy manure as a nutrient supplement for cultivation of oil-rich green microalgae Chlorella sp. Bioresour. Technol. 101, 2623–2628. doi:10.1016/j.biortech.2009.10.062

Ward, a. J., Lewis, D.M., Green, F.B., 2014. Anaerobic digestion of algae biomass: A review. Algal Res. 5, 204–214. doi:10.1016/j.algal.2014.02.001

Wellburn, A.R., 1994. The spectral determination of chlorophylls a and b, as well as total carotenoids, using various solvents with spectrophotometers of different resolution. J. Plant Physiol. 144, 307–313.

Wondraczek, L., Batentschuk, M., Schmidt, M. a, Borchardt, R., Scheiner, S., Seemann, B., Schweizer, P., Brabec, C.J., 2013. Solar spectral conversion for improving the photosynthetic activity in algae reactors. Nat. Commun. 4, 2047. doi:10.1038/ncomms3047

www.fao.org/3/a-az386e.pdf [WWW Document], n.d.

Xia, A., Murphy, J.D., 2016. Microalgal Cultivation in Treating Liquid Digestate from Biogas Systems. Trends Biotechnol. 34, 264–275. doi:10.1016/j.tibtech.2015.12.010

Xin, L., Hong-ying, H., Ke, G., Ying-xue, S., 2010. Effects of different nitrogen and phosphorus concentrations on the growth, nutrient uptake, and lipid accumulation of a freshwater microalga Scenedesmus sp. Bioresour. Technol. 101, 5494–5500. doi:10.1016/j.biortech.2010.02.016

Yang, Y., Wu, Q., Wang, M., Long, J., Mao, Z., Chen, X., 2014. Hydrothermal Synthesis of Hydroxyapatite with Di ff erent Morphologies : In fl uence of Supersaturation of the Reaction System.

Yano, a., Kadowaki, M., Furue, a., Tamaki, N., Tanaka, T., Hiraki, E., Kato, Y., Ishizu, F., Noda, S., 2010. Shading and electrical features of a photovoltaic array mounted inside the roof of an east–west oriented greenhouse. Biosyst. Eng. 106, 367–377. doi:10.1016/j.biosystemseng.2010.04.007

Yuan, J., Kendall, A., Zhang, Y., 2015. Mass balance and life cycle assessment of biodiesel from microalgae incorporated with nutrient recycling options and technology uncertainties. GCB Bioenergy 7, 1245–1259. doi:10.1111/gcbb.12229

Zelibor, J.L., Romankiw, L., Hatcher, P.G., Colwell, R.R., 1988. Comparative analysis of the chemical composition of mixed and pure cultures of green algae and their decomposed residues by C nuclear magnetic resonance spectroscopy. Appl. Environ. Microbiol. 54, 1051–1060.

Zhang, Y., Kendall, A., Yuan, J., 2014. A comparison of on-site nutrient and energy recycling technologies in algal oil production. Resour. Conserv. Recycl. 88, 13–20. doi:10.1016/j.resconrec.2014.04.011

Zhao, B., Ma, J., Zhao, Q., Laurens, L., Jarvis, E., Chen, S., Frear, C., 2014. Efficient anaerobic digestion of whole microalgae and lipid-extracted microalgae residues for methane energy production. Bioresour. Technol. 161, 423–430. doi:10.1016/j.biortech.2014.03.079

Zhu, L., 2015. Biorefinery as a promising approach to promote microalgae industry: An innovative framework. Renew. Sustain. Energy Rev. 41, 1376–1384. doi:10.1016/j.rser.2014.09.040

Zhu, X.G., Long, S.P., Ort, D.R., 2008. What is the maximum efficiency with which photosynthesis can convert solar energy into biomass? Curr. Opin. Biotechnol. 19, 153–159. doi:10.1016/j.copbio.2008.02.004